30 Fortschritte der chemischen Forschung
Topics in Current Chemistry

Nuclear Quadrupole Resonance

Springer-Verlag
Berlin Heidelberg New York 1972

ISBN 3-540-05781-1 Springer-Verlag Berlin Heidelberg New York
ISBN 0-387-05781-1 Springer-Verlag New York Heidelberg Berlin

Contents

Crystal Field Effects in Nuclear Quadrupole Resonance

Prof. Dr. Alarich Weiss
Institut für Physikalische Chemie der Universität Münster, Münster

Contents

I. Introduction

Nuclear quadrupole resonance spectroscopy (NQR) is a very direct and experimentally quite simple method for studying the interaction between the electric quadrupole moment of a nucleus and the electric field gradient at its site. Since the discovery of the method by Dehmelt and Krüger [3,6] in 1950, a large amount of experimental material has been collected, most of which has been interpreted within the frame of semiempirical theories.

As in any other branch of spectroscopy with electromagnetic waves, the quantities accessible to experiment are:

a) *Frequencies* of spectral lines or spectral bands, connected with energy transitions within the system under investigation by $\nu = \frac{\Delta E}{h}$.

b) *Intensities*, connected with transition probabilities, life-times of energy states within the system, and concentrations of the particles influenced by the applied electromagnetic radiation (i.e. nuclei in NQR).

The vast majority of NQR investigations deals with the study of resonance frequencies. Intensity measurements are very seldom found in the literature and, because of experimental and theoretical difficulties, their interpretation is more or less qualitative. In this article we are concerned only with the discussion of frequency measurements.

Considering the state of the matter, NQR is a branch of solid state spectroscopy. Consequently, the NQR frequencies are due to transitions between different energy levels in the solid.

The spacing of the different energy levels studied by NQR is due to the interaction of the nuclear quadrupole moment and the electric field gradient at the site of the nucleus considered. Usually the *electric quadrupole moment* of the nucleus is written eQ, where e is the *elementary charge; Q* has the dimension of *an area and is of the order of* 10^{-24} *cm*^{2}. More exactly, the electric quadrupole moment of the nucleus is described by a second order tensor. However, because of its symmetry and the validity of the Laplace equation, the scalar quantity eQ is sufficient to describe this tensor.

The *electric field gradient*, EFG, at the site of the nucleus can also be described by a second order tensor. The components of the EFG tensor in the principal axes system (x,y,z) are

$$eq_{xx},\ eq_{yy} \text{ and } eq_{zz}.$$

Here again, e is the elementary charge and the q_{ij} are given by

$$eq_{ij} = \frac{-\partial E_i}{\partial j} = \frac{\partial^2 U}{\partial i \partial j}, \quad i, j = x, y, z. \tag{I.1}$$

E_i is the i-component of the electric field at the site of the nucleus and U is the electrostatic potential at this site. The Laplace equation gives the relation

$$eq_{xx} + eq_{yy} + eq_{zz} = 0. \tag{I.2}$$

Per definitionem the Cartesian coordinate system of the EFG tensor is chosen in such a way, that

$$|eq_{xx}| \leqslant |eq_{yy}| \leqslant |eq_{zz}| \tag{I.3}$$

holds. From the Eqs. (I.2) and (I.3) the *asymmetry parameter* is deduced as

$$0 \leqslant \eta \equiv \frac{q_{xx} - q_{yy}}{q_{zz}} \leqslant 1. \tag{I.4}$$

The interaction energy can be described by the two parameters [45]

$$\frac{eq_{zz} \cdot eQ}{h} = \frac{e^2qQ}{h}, \text{ and } \eta. \tag{I.5}$$

$\frac{e^2qQ}{h}$ is called the *quadrupole coupling constant* and is normally given in frequency units. From NQR spectroscopy on single crystals combined with the study of Zeeman splitting the orientation of the EFG-tensor with respect to the crystal axes x', y', z' can be deduced, i.e. the directional cosines $\cos(x, x')$, $\cos(y, y')$, and $\cos(z, z')$ are available.

Besides NQR spectroscopy and the study of nuclear quadrupole interaction effects in broad-line NMR spectroscopy, paramagnetic electron resonance [60], Mössbauer spectroscopy, and the study of perturbed angular correlation of γ-rays, are suitable methods for studying nuclear quadrupole interactions in solids. Indirect methods are also available for acquiring information about the nuclear quadrupole coupling constant from the liquid state (particularly NMR spectroscopy in liquids and in liquid crystals in some cases gives information about this constant). By microwave spectroscopy, the nuclear quadrupole interaction may be studied in the gaseous phase (see the paper by Zeil). We shall deal here only with the aspect of NQR spectroscopy in solids since this method has the broadest applicability to chemical problems in comparison with the other methods mentioned.

The *chemical usefulness* of the NQR method can be seen from Fig. I.1 which shows in the scheme of the periodic system all the elements which contain stable nuclei or very long-living unstable nuclei with a nuclear quadrupole moment $eQ \neq 0$. An observable quadrupole moment is connected with a *nuclear spin* $I \geqslant 1$. Many nuclei with $I = 0$ or $I = 1/2$ have excited states with $I \geqslant 1$. Therefore methods which rely on excited states, such as Mössbauer spectroscopy and the study of γ-ray correlation, allow the study of nuclear qua-

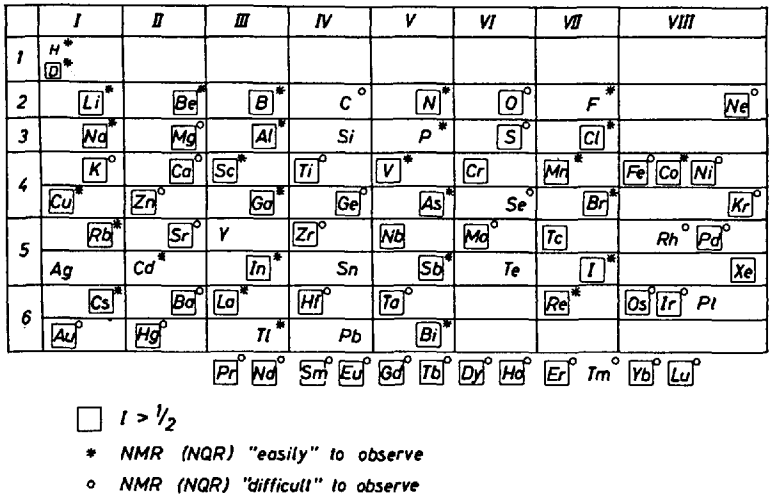

Fig. I.1. Periodic system of elements with stable nuclei or long living unstable nuclei, $I \neq 0$. The marks ○ and * distinguish between elements with nuclei difficult accesible (○) to NMR (NQR) experiments, and elements easy accesible (*) to the NMR(NQR) experiments. This distinction depends from many parameters such as the concentration of the isotope with $I \neq 0$, the chemical bond in the lattice, the experience of the experimentator,....

drupole interactions in chemical systems with such nuclei. A combination of these methods renders the majority of elements in the periodic system open to the study of nuclear quadrupole interactions. The exceptions, very unfortunately for chemistry, are the elements carbon and silicon, to which none of these methods can be applied. A recent comprehensive paper on Mössbauer spectroscopy in chemistry has been written by Greenwood [154], who discusses also the study of nuclear quadrupole interactions in solids by this method. Information on the interdependence of studies of perturbed angular correlations of γ-rays and nuclear quadrupole interactions is given in [89,96,108].

II. Nuclear Quadrupole Interactions in Solids

1. Several Aspects of the Study of NQR in Solids

The interaction energy of the nucleus with its surroundings, as observed by NQR spectroscopy, generally contains two important terms

$$E_{\text{total}} = E_{\text{magnetic}} + E_{\text{quadrupole}} . \qquad \text{(II.1)}$$

a) Magnetic Interactions

The first term in Eq. (II.1) is due to the effect of internal magnetic fields at the site of the nucleus in the crystalline substance under investigation. The coupling between magnetic fields and the nucleus is always present since a magnetic moment is intrinsically connected with the spin I of the nucleus.

However, in NQR spectroscopy, internal noncooperative magnetic fields are negligible in most cases. The diamagnetic fields and the paramagnetic fields at the site of the nucleus considered, as will appear from a study of the Zeeman splitting of NQR spectra, may be corrected for quite easily. This effect is equivalent to the well known chemical shifts in NMR. In the study of the *Zeeman splitting of NQR spectra* the material under investigation (mostly a single crystal) is exposed to an external magnetic field, thereby removing the degeneracy of energy levels in pure NQR spectroscopy. Cooperative magnetic effects on NQR spectra have been observed and studied in a few cases. The nuclear spin-spin interaction, appearing in NMR as magnetic dipole-dipole interaction and as electron coupled spin-spin interaction, may be observed in NQR in very favourable cases. Since the effect is quite small, normally the line width in NQR prohibits such observations. A magnetic dipole-dipole interaction was observed by Livingstone and Zeldes [38] as a line splitting in the NQR spectrum of ^{127}I in HIO_3.

Appreciable magnetic fields are observed in crystals which exhibit antiferromagnetism. In such crystals below the Neel point splittings of the NQR lines have been found, and from these splittings the orientation and magnitude of the internal magnetic Zeeman field can be evaluated. Important conclusions about the magnetic structure of such substances may be drawn from NQR experiments ($MnCl_2 \cdot 2H_2O$) [160]. Such Zeeman splittings should be also observable in ferromagnetic substances. Here we shall not further discuss crystal field effects of magnetic origin.

b) Electric Interactions

The second term in Eq. (II.1) is the crucial one in discussing NQR investigations in the frame of chemical bonding in the solid state. In a general form, we may write the nuclear quadrupole interaction energy as

$$E_{\text{quadrupole}} = f\left(\frac{e^2qQ}{h}, \eta, I, m\right). \tag{II.2}$$

An investigation of the complete NQR spectrum using single-crystal Zeeman spectroscopy results in the knowledge of

a) the nuclear quadrupole coupling constant e^2qQ/h;

b) the asymmetry parameter η, that is, the knowledge of the principal components of the electric field gradient tensor;

c) the orientation of the electric field gradient tensor at the nuclear site with respect to the crystal axes;
d) the spin of the nucleus considered;
e) structural information about the site symmetry of the nuclei considered.

A comprehensive review of the theoretical and experimental background needed to determine these parameters is given by Das and Hahn [45] and by Reif and Cohen [40]. More recent treatments of the whole subject may be found in the monograph by Lucken [143] and the review article by Schempp and Bray [159]. A review on studies of nuclear quadrupole interactions for the period 1960 and 1966 is given by Weiss [125] and experimental data up to 1966 have been compiled by Biryukov *et al.* [139].

The vast majority of NQR experiments was performed using polycrystalline materials or powder samples, so that the information gained from the experiment is restricted to items a), b), d), and e). Any information on directional dependence of the interaction is lost by the averaging process due to the random orientation of the single crystals. A further restriction is introduced in the case of experiments with nuclei with $I = 3/2$. Here the information on the asymmetry parameter η is lost due to the degeneracy of the energy levels. This can be seen from Table II.1, where the NQR frequencies for different spins I are given as a function of the coupling constant $e^2 qQ/h$ and the asymmetry parameter η. In very favourable cases, also for $I = 3/2$, η may be determined by Zeeman spectroscopy on powder specimens [72].

Let us assume that we have found from NQR experiment the quadrupole coupling constant and the asymmetry parameter η.

What conclusion about the nature of chemical bond in the solid can be drawn from this information?

c) Accuracy of NQR Measurements

Before discussing NQR results, first we must realise that the *experimental accuracy is very high.* The transition frequencies may be determined to ±5 kHz provided the line width is ⩽ 5–15 kHz. In most NQR spectra the line width is below 15 kHz. The NQR frequencies range between a few kHz and 1000 MHz. Below 1 MHz the experimental measurement of NQR frequencies by pure quadrupole resonance is not successful. Therefore the main frequency range in NQR spectroscopy is 1 MHz $\leqslant \nu \leqslant$ 1000 MHz and the accuracy is

$$10^{-2} \geqslant \frac{\Delta \nu}{\nu} \geqslant 10^{-6}.$$

Also, for determination of η, the error is mostly below 2 %. A theoretical calculation of $\frac{e^2 qQ}{h}$ and of η from first principles with an accuracy comparable to the accuracy of the experiment cannot be achieved to-day. However, semi-

Table II.1. *Transition frequencies* $\frac{1}{h}\{E[\pm m] - E[\pm(m+1)]\} = \frac{\Delta E}{h} = \nu[\pm m \rightleftarrows \pm(m+1)]$.
The condition for the approximation (η up to the order η^4 is considered) is:
$0 \leqslant \eta < 0.30$ *for* $I > \frac{3}{2}$

$I = 1$ (^{2}D, ^{14}N)

$$\nu_+ = \nu(0 \rightleftarrows +1) = \frac{3}{4}\left(\frac{e^2qQ}{h}\right)\left(1 + \frac{1}{3}\eta\right)$$

$$\nu_- = \nu(0 \rightleftarrows -1) = \frac{3}{4}\left(\frac{e^2qQ}{h}\right)\left(1 - \frac{1}{3}\eta\right)$$

$I = \frac{3}{2}$ (^{7}Li, ^{9}Be, ^{23}Na, ^{33}S, ^{35}Cl, ^{37}Cl, ^{69}Ga, ^{71}Ga, ^{75}As, ^{79}Br, ^{81}Br, ^{87}Rb, ^{125}Ba, ^{197}Au, ^{201}Hg)

$$\nu\left(\pm\frac{1}{2} \rightleftarrows \pm\frac{3}{2}\right) = \frac{1}{2}\left(\frac{e^2qQ}{h}\right)\left(1 + \frac{\eta^2}{3}\right)^{1/2}$$

$I = \frac{5}{2}$ (^{17}O, ^{27}Al, ^{47}Ti, ^{55}Mn, ^{85}Rb, ^{121}Sb, ^{127}J, ^{185}Re, ^{187}Re)

$$\nu_1 = \nu\left(\pm\frac{1}{2} \rightleftarrows \pm\frac{3}{2}\right) = \frac{3}{20}\left(\frac{e^2qQ}{h}\right)(1 + 1.0926\,\eta^2 - 0.6340\,\eta^4 + \ldots)$$

$$\nu_2 = \nu\left(\pm\frac{3}{2} \rightleftarrows \pm\frac{5}{2}\right) = \frac{6}{20}\left(\frac{e^2qQ}{h}\right)(1 - 0.2037\,\eta^2 + 0.1622\,\eta^4 + \ldots)$$

$I = \frac{7}{2}$ (^{45}Sc, ^{51}V, ^{59}Co, ^{123}Sb, ^{133}Cs, ^{139}La, ^{181}Ta)

$$\nu_1 = \nu\left(\pm\frac{1}{2} \rightleftarrows \pm\frac{3}{2}\right) = \frac{1}{14}\left(\frac{e^2qQ}{h}\right)(1 + 3.6833\,\eta^2 - 7.2607\,\eta^4 + \ldots)$$

$$\nu_2 = \nu\left(\pm\frac{3}{2} \rightleftarrows \pm\frac{5}{2}\right) = \frac{2}{14}\left(\frac{e^2qQ}{h}\right)(1 - 0.5667\,\eta^2 + 1.8595\,\eta^4 + \ldots)$$

$$\nu_3 = \nu\left(\pm\frac{5}{2} \rightleftarrows \pm\frac{7}{2}\right) = \frac{3}{14}\left(\frac{e^2qQ}{h}\right)(1 - 0.1000\,\eta^2 - 0.0180\,\eta^4 + \ldots)$$

$I = \frac{9}{2}$ (^{73}Ge, ^{83}Kr, ^{93}Nb, ^{113}In, ^{115}In, ^{209}Bi)

$$\nu_1 = \nu\left(\pm\frac{1}{2} \rightleftarrows \pm\frac{3}{2}\right) = \frac{1}{24}\left(\frac{e^2qQ}{h}\right)(1 + 9.0333\,\eta^2 - 45.691\,\eta^4 + \ldots)$$

$$\nu_2 = \nu\left(\pm\frac{3}{2} \rightleftarrows \pm\frac{5}{2}\right) = \frac{2}{24}\left(\frac{e^2qQ}{h}\right)(1 - 1.3381\,\eta^2 + 11.722\,\eta^4 + \ldots)$$

$$\nu_3 = \nu\left(\pm\frac{5}{2} \rightleftarrows \pm\frac{7}{2}\right) = \frac{3}{24}\left(\frac{e^2qQ}{h}\right)(1 - 0.1875\,\eta^2 - 0.1233\,\eta^4 + \ldots)$$

$$\nu_4 = \nu\left(\pm\frac{7}{2} \rightleftarrows \pm\frac{9}{2}\right) = \frac{4}{24}\left(\frac{e^2qQ}{h}\right)(1 - 0.0809\,\eta^2 - 0.0043\,\eta^4 + \ldots)$$

---

empirical treatments of NQR results on a relative scale from the viewpoint of the chemical bonding in solids may be accurate to a few percent.

d) The Nuclear Quadrupole Coupling Constant

Table II.1 shows that the quadrupole coupling constant and η may be deduced from the transition frequencies. The main application of NQR in chemistry is in the interpretation of

$$\frac{e^2qQ}{h} \qquad \text{and } \eta$$

in terms of the chemical bonding.

For chemists, the important factor in the nuclear quadrupole coupling constant $\frac{e^2qQ}{h}$ is the electric field gradient eq. Here the difficulty is to separate the two terms eq and eQ. The nuclear quadrupole moments are not known very accurately. Therefore an error may be introduced in the determination of eq by splitting the factor eQ from the product $\frac{e^2qQ}{h}$ measured. Relative comparisons of the quadrupole coupling constant $\frac{e^2qQ}{h}$ or of the resonance frequencies ν are quite often used in chemistry. Considering experimental NQR frequencies of the same nucleus in different chemical environments, for instance, in two substances "I" and "II", the nuclear quadrupole moment is of no importance. As an example, we choose ^{35}Cl ($I = 3/2$) in two different chemical environments "I" and "II". Then the ratio of the frequencies is given by

$$\frac{\nu_I}{\nu_{II}} = \frac{\left[\left(\frac{1}{2}\frac{e^2qQ}{h}\right)\left(1+\frac{\eta^2}{3}\right)^{1/2}\right]_I}{\left[\left(\frac{1}{2}\frac{e^2qQ}{h}\right)\left(1+\frac{\eta^2}{3}\right)^{1/2}\right]_{II}} = \frac{eq_I\left(1+\frac{\eta_I^2}{3}\right)^{1/2}}{eq_{II}\left(1+\frac{\eta_{II}^2}{3}\right)^{1/2}} . \qquad \text{(II.2a)}$$

For $0 \leqslant \eta \lesssim 0.1$

$$\frac{\nu_I}{\nu_{II}} = \frac{eq_I}{eq_{II}} \qquad \text{(II.2b)}$$

follows in good approximation.

For $I \neq 3/2$, eq and η can be separated (see Table II.1).

Similar relations can be used in comparing two isotopes of the same element. By observation of the same transition frequency of the two isotopic nuclei in one compound, one can assume a constant electric field gradient (that is, no measurable influence of the nuclear mass and the nuclear charge distribution on the core electrons).

$$\frac{\nu_1(Q_\mathrm{I})}{\nu_2(Q_\mathrm{II})} = \frac{\left\{\left(\frac{e^2qQ}{h}\right)f(\eta)\right\}_\mathrm{I}}{\left\{\left(\frac{e^2qQ}{h}\right)f(\eta)\right\}_\mathrm{II}} = \frac{Q_\mathrm{I}}{Q_\mathrm{II}} = \text{constans.} \qquad \text{(II.3)}$$

The situation is more complicated in cases where one wishes to compare the electric field gradients at the sites of different nuclei A and B (belonging to different chemical elements). Here the only reliable way to discuss and compare electric field gradients measured in different substances at the sites of different nuclei supposes an independent knowledge of $Q_\mathrm{A}/Q_\mathrm{B}$ from theory or experiment.

e) The Electric Field Gradient eq; Point Charge Model

The electric field gradient eq at the site of the nucleus under investigation (the "resonating" nucleus) can be obtained from NQR experiments. This quantity is of crucial importance to chemists and solid state physicists. Crystals are built up from atomic nuclei and electrons in an arrangement periodic in the three dimensions of the space. Thus the charge distribution within the crystal is periodic in space. We shall call the coordinate system of the crystal x', y', z'. The charge within the unit volume $dx'\,dy'\,dz' = d\tau'$ is given by $\rho(x'y'z')\,d\tau'$. The nucleus considered (with the quadrupole moment eQ) is located at the origin of the coordinate system x', y', z'. Then the z' component of the electric field gradient at the site of the nucleus is given by

$$eq_{z'z'} = \int_\tau \left\{ \frac{3z'^2\rho(x'y'z')d\tau'}{(r(x'y'z'))^5} - \frac{\rho(x'y'z')d\tau'}{(r(x'y'z'))^3} \right\}. \qquad \text{(II.4)}$$

From the components eq_{ij}, of the electric field gradient tensor with respect to the system of the crystal axes, the coupling constant, $eq_{zz} \equiv eq$, and η can be calculated by transformation of the tensor to its principal axes.

For application, Eq. (II.4) has to be considerably simplified. The simplest model is the assumption of point charges. We take the crystal lattice as composed from the point charges $\pm n_i e$, where e is the elementary charge. The index i, $o \leqslant i \leqslant k$, distinguishes the different kinds of charged points (particles) within the lattice. Assuming the system of crystal axes already transformed to the principal axes system of the tensor, we calculate the coupling constant from

$$eq_{zz} = \sum_{i=o}^{k} n_i e \sum_{j=1}^{\infty} \left\{ \frac{3z_{ij}^2}{r_{ij}^5} - \frac{1}{r_{ij}^3} \right\}. \qquad \text{(II.5)}$$

The summation over the index j takes into consideration all particles of the charge number n_i. Similar equations can be written for eq_{yy} and eq_{xx} and then η can be be calculated. There is no doubt about the crudeness of this model.

f) Quadrupole Polarizability and Antishielding Factor

A first improvement of the simple point charge model is the consideration of the core polarization of the atom (ion) to which the "resonating" nucleus belongs. We assume that for the free particle (ion) the core is spherically symmetric, and therefore no electric field gradient is created by this core at the site of the nucleus. A quadrupole moment is induced in the core by the point charges outside the ion. This moment is proportional to the quadrupole polarizability of the core. The induced moment produces at the site of the nucleus an electric field gradient, which amplifies or weakens the field gradient created by the external charges. To take the core quadrupole polarization into account, Sternheimer introduced the antishielding factor in 1950. The total electric field gradient at the site of the nucleus is given by

$$\begin{aligned} eq_{\text{total}} &= eq_{\text{external}} + eq_{\text{core}} \\ &= eq_{\text{external}} - \gamma_\infty eq_{\text{external}} \\ &= eq_{\text{external}}\,(1-\gamma_\infty) \end{aligned} \qquad \text{(II.6)}$$

γ_∞ is the *antishielding factor* or *Sternheimer factor*.

For ions, γ_∞ is between +1 and ~ (−200). Negative values of γ_∞ lead to an amplification of the external field gradients. There are numerous published calculations of γ_∞ for ions and atoms [4,10,12,15,22,34,40,41,77,85-87,97,106,120].

There is some experimental evidence that the Sternheimer factors γ_∞ calculated for the free ions by the Hartree-Fock, or Thomas-Fermi method are too large. The incorporation of the ions into the crystal lattice changes the orbitals of the ions. This results in antishielding factors which are different from the factors calculated for the free ions. This crystal field effect was discussed empirically by Barnes *et al.* [75] and Brill and Hugus [151] and theoretically by Burns and Wikner [66] and by Paschalis and Weiss [145]. In Table II.2 antishielding factors of some ions are given. From the magnitude of these factors it is quite clear that a good knowledge of $(1-\gamma_\infty)$ is very important for conclusions about the charge distribution in crystals.

g) The Multipole Model of Ionic Crystals

The point charge model of ionic crystals, first applied by Bersohn [44] in calculating e^2qQ/h (^{27}Al) in Al_2O_3, and e^2qQ/h (^{63}Cu) in Cu_2O, is quite inadequate to describe the nuclear interactions in ionic solids. This was shown first by Burns [50] for the alkali halide gases and by Brun and Hafner [81] for the ionic crystals Al_2O_3 and $MgAl_2O_4$. These authors pointed out that dipole moments are induced in the core of the ions through the electric fields within the crystal and through the polarizability of the ions. These induced dipole moments of the ions in reverse produce electric field gradients at the site of the "resonating"

Table II.2. *Antishielding factors γ_∞ for some closed shell ions.* □ *Calculated for the free ion;* * *Calculated for the "crystal" ion, the ion in the solid*

Ion	γ_∞	Ref.
Li^+	0.257 □	106)
	0.271 *	145)
Be^{2+}	0.186 □	106)
	0.190 *	145)
O^{2-}	- 429 □	106)
	- 28 bis - 34 *	66)
	- 10.6 *	145)
Na^+	- 4.51 □	106)
	- 4.75 *	145)
Cl^-	- 66.6 □	106)
	- 27.0 *	66)
	- 37.9 *	145)
Rb^+	- 70.7 □	34)
Cs^+	- 143.5 □	34)

nucleus, in addition to the electric field gradients produced by the monopoles. Furthermore, electric quadrupole moments of ions are not caused solely by the field gradient from the monopoles but also by the field gradient from the dipoles. For a complete calculation of the electric field gradient at the nuclear site considered, therefore, a self-consistent treatment of the multipole model has to be performed to gain reliable results. The *mathematical procedure* for calculating the EFG in the frame of the multipole model is as follows:

α) We suppose a determination of the crystal structure of very high accuracy. This supposition is a very basic one for any quantitative discussion of crystal field effects independent of the particular nature of chemical bond.

β) We assume a certain charge distribution in the solid.

γ) From α) and β) the electric field at any lattice point is calculated. Then with the known dipole polarizabilities of the ions the induced dipole moments are calculated.

δ) From α), β) and γ) new resulting electric fields at any lattice point are evaluated; new induced dipole moments are obtained; cycle δ) is repeated until convergence is reached.

ϵ) From the monopole and dipole distribution in the lattice the resulting elec-

tric field gradients are calculated, thus allowing the determination of the induced core quadrupole moments. This step too, can be done in a self-consistent way.

ζ) From the resulting final distribution of electric monopoles, electric dipoles, and electric quadrupoles, the final electric field gradient at the site of the nucleus considered is obtained by including the appropriate antishielding factor γ_∞.

By varying the charge distribution according to β) and applying the self-consistent calculation of the multipole field gradient, a charge distribution consistent with the NQR results can be calculated. Such calculations have been done for α-Al_2O_3 by Hafner and Raymond [129] and for $NaNO_2$ by Schmidt [147]. The convergence of the lattice sum for the calculation of the monopole contribution to the EFG is fairly slow (see Eq. (II.5)). Methods to calculate the lattice sums have been worked out by De Wette *et al.* [46,51,67,101] and by Coogan *et al.* [100,124].

Summarizing the use of NQR spectroscopy in the determination of chemical bonding and of charge distribution in ionic solids one can say:

Under the assumption of the existence of ideal ionic crystals, built up from point charges and point multipoles, the NQR spectrum is completely determined by the crystal field of the electric multipoles. The experimental results of NQR can be explained within the frame of this model. Refinements of the model, such as the dependence of multipole polarizabilities upon the crystal field or the influence of overlapping of the electron clouds, are not yet understood quantitatively.

h) NQR in Nonionic Crystals

The main application of NQR is to study the electric field gradients in crystals where the intramolecular bonds are mainly nonionic. Suppose the crystal under consideration is a solid, built up from neutral molecules. Then to a first approximation there is no electric field gradient created by external charges at the sites of the nuclei considered. Even gradients from external dipole moments may be very small where the molecules are highly symmetric. Rewriting Eq. (II.5) for a single electron (charge = $-e$) at distance r from the nucleus, the potential at the nuclear site is

$$V_{zz}(r) = -e\,\frac{3\cos^2\vartheta - 1}{r^3}\,, \tag{II.7}$$

where ϑ is the angle between $\vec{r}$ and the angular momentum vector $\vec{I}$ of the nucleus. Taking the quantum mechanical behaviour of the electron into account, the electric field gradient eq_{zz} is given by

$$eq_{zz} \equiv \langle V_{zz}\rangle = -\int_\tau \psi^*\,\frac{3\cos^2\vartheta - 1}{r^3}\,\psi\,d\tau. \tag{II.8}$$

If the electron in question has pure *s*-character with respect to the nucleus, eq_{zz} will be zero.

Any deviation from *s*-symmetry, however, will produce quite a strong field gradient at the site of the nucleus. A *p*-electron, in particular, is very effective in building up an electric field gradient. Such high electric field gradients are found in molecules where the atom considered (the atom with the "resonating" nucleus) is bound by directed (covalent) bonds to its neighbouring atoms.

A simple semiempirical theory for the interpretation of nuclear quadrupole coupling constants in terms of chemical bonding was developed by Townes and Dailey [2,24]. This theory is treated in many summary papers on NQR, e.g. [39,45,94,143,159]. An extension of the Townes-Dailey treatment was given by Cotton and Harris [113,123]. Besides these simple model theories, a variety of more elaborate calculations have been done on the influence of intramolecular bonding on NQR spectra (see the discussion in [143,159]).

Since *the Townes-Dailey model* is the basis of most interpretations, we shall discuss here the results of this theory. For simplicity, we consider a single bond between an element and a halogen atom.

The covalency of the bond is calculated from Townes-Dailey theory by the relation

$$\left(\frac{e^2qQ}{h}\right)_{exp} = (1-i)\,(1-s)\left(\frac{e^2qQ}{h}\right)_{at}. \tag{II.9}$$

Here i is the ionic character of the bond and therefore $(1-i)$·the covalent character of this bond. s is the extent of the *s*-character in the bonding orbital of the halogen and $(e^2qQ/h)_{at}$ the atomic quadrupole coupling constant. From Eq. (II.9) it follows:

$$(1-i) = \frac{\left(\frac{e^2qQ}{h}\right)_{exp}}{\left(\frac{e^2qQ}{h}\right)_{at}} \cdot \frac{1}{1-s}. \tag{II.10}$$

Following Townes and Dailey, we assume that the atomic orbital of the halogen has 15 % *s*-character when the halogen atom is bonded to an element which is more electropositive than the halogen atom by at least 0.25 in Pauling's electronegativity scale.

The unfortunate situation is that this model interprets NQR results in terms of the intramolecular chemical bond only. *The influences of the crystal field on the NQR frequencies are neglected.*

2. Classification of the Crystal Field Effects

Chemists want to learn from NQR experiments about the chemical bond within the molecule. Let us consider *an example:*

NQR frequencies for ^{35}Cl at 77 °K in *ortho-*, *meta-* and *para*-dichlorobenzene are given in Table II.3. The interpretation of the results runs into difficulties because of the crystal field effects. These influences are very difficult to evaluate. They certainly change from substance to substance. Qualitatively, we can characterize the crystal field effect in the following way [76].

1. Electrostatic forces between the molecules. These forces may be composed of:
   a) monopole-monopole interactions in crystals composed of molecular ions (such as A_2BCl_6, A = K, NH_4, Rb . . , B = Pt, Pd . .);
   b) dipole-dipole interactions, as in 1,2-dichlorobenzene, 1,3-dichlorobenzene etc., and multipole forces;
2. dispersion forces;
3. intermolecular bonding;
4. short-range repulsion forces.

Table II.3. *^{35}Cl-NQR-frequencies of the three dichlorobenzenes at T = 77 °K. The chemical equivalence of the two Cl-atoms disappears in the solid state for 1,2-dichlorobenzene and 1,3-dichlorobenzene. The crystal field effect $|\Delta|$ is $\lesssim 400$ kHz ($\lesssim 1.2\,\%$). Data taken from* [139]

Compound	$\nu(^{35}Cl)$ (77 °K) / MHz	$\bar{\nu}$ / MHz	Δ / MHz $= \bar{\nu} - \nu$ / MHz
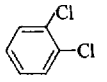	35.824 35.775 35.755 35.580	35.735	$+0.155 \geqslant \Delta \geqslant -0.089$
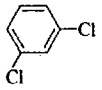	35.030 35.030 34.875 34.809	34.938	$+0.129 \geqslant \Delta \geqslant -0.092$
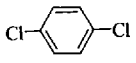	34.775 (α-phase) 34.760 (β-phase) 35.208 (γ-phase)	34.914	$+0.139 \geqslant \Delta \geqslant -0.294$

A quantitative treatment of these effects on NQR is outside the scope of today's solid state theory. Therefore a qualitative estimation of the crystal field effect seems to be necessary. This justifies classifying the crystal field

effects according to their effect on the NQR spectra. We can divide the crystal field effects up into different classes.

A. The condensation of the molecules into the solid state taken as a rigid, ordered arrangement of molecules.
B. The dynamical behaviour of the lattice, that is, the lattice vibrations.
C. The lattice defects, such as dislocations, impurities, etc.

Also, external parameters influencing the crystal field effects (besides the temperature-dependent dynamical behaviour) such as pressure or external electric fields have to be taken into account.

Within this framework we consider the bonding electrons as the main source of the EFG. For the crystal field, effects A) and B) are most important. Lattice defects seem to play a minor role in molecular crystals. The influence of the external parameters on NQR is quite important since, with external fields, the crystal field may be influenced experimentally. However, very little work has been done in this field.

3. Quantitative Approaches in Estimating Crystal Field Effects

Of the two main parts A) and B) of crystal field effects, effect B, the influence of lattice dynamics on NQR, can be excluded, at least to a large extent, by an appropriate experimental method, that is, by determining the nuclear quadrupole coupling parameters $\frac{e^2qQ}{h}$, η and $\cos(x,x')$, $\cos(y,y')$, $\cos(z,z')$ at a very low temperature (below 4 °K). The calculation of the change of NQR parameters through the condensation of gaseous molecules into the solid is therefore the main problem.

In case of NQR in ionic crystals, particularly in crystals with approximately spherical ions, the determination of the crystal field is discussed above. For molecular crystals very little work has been done.

Bersohn [76] has calculated the crystal field created by the molecular dipoles in the lattice of CH_3Cl. The static dipole moment of the molecules induces through the polarizability of the molecules an additional dipole moment which increases the dipole moment of the free molecule by a factor of about 1.05. This in turn means that the C–Cl bond has increased in ionic character under the influence of the intermolecular electric fields and therefore (see Eq. (II.9)) the quadrupole coupling constant will be lower relative to the gaseous state. Besides the dipole moment induced in the direction of the static dipole, a perpendicular partial moment should be induced, too. Therefore the axial symmetry of the C–Cl bond will be disturbed and the asymmetry parameter η may become unequal zero. A small asymmetry parameter $\eta = 0.028$ has been observed for the nuclear quadrupole interaction in solid CH_3I. Bersohn also calculated from the known crystal structure of 1,3,5-trichlorobenzene the induced

dipole moments at each of the three C–Cl bonds. He found that the electrostatic crystal field effect should raise the solid state nuclear quadrupole coupling constant in comparison to the gaseous state. The relative splitting of the NQR frequencies in the solid into a triplet is adequately explained by Bersohn's model. The comparison with the isostructural 1,3,5-tribromobenzene is also satisfactory.

For an absolute agreement between the observed and calculated crystal field effects in such dipolar crystal lattices, the zero point vibrations have to be considered, as Bersohn pointed out. Furthermore, we think that the part of the solid state shift is due to the contribution of the quadrupole polarization (anti-shielding factor). The inner shell electrons of the atom considered experience an induced quadrupole moment under the influence of the external fields. This

Table II.4. *The influence of the condensation of the molecules into the crystal lattice on NQR. The formation of hydrogen bonds in solid NH_3 shows up in the very strong "crystal field effect" (> 22 %)*

Compound	Nucleus	$\frac{e^2qQ}{h \cdot MHz}$ (Gas)	$\frac{e^2qQ}{h \cdot MHz}$ (Solid, 77 °K)	Δ[a] (in %)
CH_3Cl	^{35}Cl	74.77	68.04	+ 9.0009
CF_3Cl	^{35}Cl	77.93	77.58	+ 0.4491
$(CH_3)_3CCl$	^{35}Cl	66.9	62.12	+ 7.1450
C_6H_5Cl	^{35}Cl	72.6	69.14	+ 4.7658
CH_3Br	^{79}Br	577.15	528.9	+ 8.3600
CF_3Br	^{79}Br	619	604.0	+ 2.4233
$(CH_3)_3CBr$	^{79}Br	511.6	467.0	+ 8.7177
C_6H_5Br	^{79}Br	567.0	537.0	+ 5.2910
CH_3J	^{127}J	1929	1767.3	+ 8.3826
CF_3J	^{127}J	2143.8	2069.2	+ 3.4798
NF_3	^{14}N	7.07	7.07 (0 °K)	0
$(CH_3)_3N$	^{14}N	5.47	5.19	+ 5.1188
NH_3	^{14}N	4.084	3.161	+ 22.6004
C_5H_5N	^{14}N	4.88	4.60	+ 5.7377
N-methylpyrrole[b]	^{14}N	$< \nu$ (Solid)	$> \nu$ (Gas)	Negative!

a) $$\Delta = \frac{\frac{e^2qQ}{h}\,(\text{Gas}) - \frac{e^2qQ}{h}\,(\text{Solid})}{\frac{e^2qQ}{h}\,(\text{Gas})}$$

b) Ref. [159]

should affect the crystal field. Inner shell Sternheimer factors will become more important with increasing atomic number of the atom considered (for instance, in NQR experiments with bromine or iodine).

A calculation of the crystal field effect on the NQR spectrum of ^{35}Cl in the molecular ion $[PtCl_6]^{2-}$ was done by Smith and Stoessiger [148]. A self-consistent procedure was used for the determination of the electric field gradients produced by the monopoles and dipoles in the lattice at the site of the resonating nucleus. The results show a considerable improvement in comparison to the simple monopole model. However, no complete agreement with the experiment was reached. The electrostatic crystal field effects are quite remarkable for the two substances investigated ($\nu(^{35}Cl)$ in K_2PtCl_6 and Cs_2PtCl_6).

For a series of hexachlorostannates A_2SnCl_6, A = K, Rb, Cs, NH_4, CH_3NH_3, $(CH_3)_3NH$, $(CH_3)_4N$ and $BSnCl_6$, B = $Mg(H_2O)_6$, $Co(H_2O)_6$, $Ni(H_2O)_6$, Brill *et al.* [152] investigated the ^{35}Cl(NQR) spectrum and used the point charge model to calculate the EFG.Semiempirical LCAO-MO calculations have also been used. An empirical Sternheimer factor of −10 for chlorine was used to explain the crystal field effects which amount to 10 % for $\nu(^{35}Cl)$ in $[SnCl_6]^{2-}$.

In many molecular crystals, intermolecular bonding may play the most important part in the crystal field effects. Here hydrogen bonds in particular are important, as O'Konski *et al.* [107,140,141] and others pointed out. In such cases the condensation from the gaseous state into the solid state may alter the quadrupole coupling constant by up to 20 % and more. The shifts of e^2qQ/h between the gaseous and the solid state are shown for a number of compounds in Table II.4. The data are taken from Lucken [143].

III. Symmetry of Crystal Fields and NQR

The simplest and most easily recognized crystal field effect is the influence of the symmetry of the crystal on the NQR spectrum. Starting from the molecular field, the NQR spectrum is determined by the isolated molecules. The crystal field then produces a fine structure of the spectrum which can be used to explore the site symmetry of the nuclei considered.

1. Asymmetric Unit; Crystallographic Equivalence and Physical Equivalence of Lattice Sites

The unit cell of the crystal contains the asymmetric unit, which may be composed of one or more atoms. The electric field gradient within the asymmetric unit differs from site to site. The asymmetric unit is multiplied by the symmetry elements of the crystal to build up the unit cell. The macroscopic crys-

tal lattice follows by the appropriate translations of the unit cell. Neither the translational operations nor the inversion influence the NQR spectrum (simply because the electric field gradient is a tensor of second order). Therefore the NQR spectrum reveals the Laue group of the crystal.

In molecular crystals, the *asymmetric unit* of the unit cell may be composed of a part of the chemical unit, of the chemical unit itself, or even of more than one chemical unit. The chemical unit is understood as the single molecule or the formula unit of the substance. For the free molecule (or formula unit) we can define *"chemically equivalent" sites* within the molecule.

Two positions at a molecule are termed "chemically equivalent" if they are not distinguishable in the free molecule, assuming free rotation about single bonds. These positions can become "crystallographically inequivalent" in the solid state if the atoms are now at crystallographically different sites. Therefore, the components of the principal field gradient tensors at the respective sites then become different in magnitude and direction due to interactions between neighbouring molecules ("crystal field effect"). The term *"physical inequivalence"* is applied to nuclei on lattice sites which differ only in the direction, and not in the magnitude, of the respective principal components of the field gradient tensor. Physically inequivalent atoms, therefore, can only be distinguished by Zeeman splitting of the single-crystal NQR spectrum.

As *an example*, consider the molecule 1,3,5-trichlorobenzene. In the free molecule we term the three Cl atoms chemically equivalent. Another example is 2,4,6-trichloro-1-nitrobenzene: in the free molecule the Cl atoms in positions 2 and 6 are chemically equivalent and the Cl atoms in position 4 is chemically inequivalent with respect to the other two Cl atoms.

For an atom at the general point position, Table III.1 [94] gives the number of sites distinguishable by studying the Zeeman splitting in NQR spectroscopy. This number is identical with the number of nuclei of the same kind which show the same frequency, nuclear quadrupole coupling constant and asymmetry parameter. Only the orientation of the field gradient tensors with respect to the crystal axes is different. The number of the corresponding crystallographically equivalent lattice sites is generally higher but does not show up in the NQR spectrum because of the insensitivity of the method to symmetry operations such as inversion or the Bravais translations.

Experimental knowledge of the directional cosines of the electric field gradient tensor at one lattice site with respect to the crystal axes, together with a knowledge of the crystal structure, is sufficient to calculate the orientation of all other electric field gradient tensors belonging to the same crystallographic point position.

The number of different orientations of the EFG tensor due to the symmetry operations of the Laue group is lower if the nuclei occupy special crystallographic sites (special point positions). Information about such special sites of nuclei can be found from NQR single-crystal Zeeman spectroscopy. This is

Table III.1. *Crystal class, Laue symmetry, and number of possible different orientations of the electric field gradient tensor for the nuclei at the general point position in the crystal lattice*

Crystal class	Laue symmetry	Number of different orientations of the EFG tensor for the general point position
Triclinic	$\bar{1}$; C_i	1
Monoclinic	2/m; (C_{2h})	2
Orthorhombic	m m m; (D_{2h})	4
Tetragonal	4/m; (C_{4h})	4
Tetragonal	4/m m m; (D_{4h})	8
Rhombohedral	$\bar{3}$; (C_{3i})	3
Rhombohedral	$\bar{3}$ m; (D_{3d})	6
Hexagonal	6/m; (C_{6h})	6
Hexagonal	6/m m m; (D_{6h})	12
Cubic	m 3; (T_h)	12
Cubic	m 3 m; (O_h)	24

very helpful in crystal structure determinations [94]. For the further discussion on crystal symmetry and NQR spectroscopy, see also [42].

Concerning the two examples discussed here, we know only the crystal structure of 1,3,5-trichlorobenzene. There are four molecules in the unit cell. One molecule is identical with the asymmetric unit [76]. This means that in the solid, due to the crystal field effects, the three chlorine atoms are crystallographically inequivalent:

$$\left(\frac{e^2qQ}{h}\right)_{Cl(1)} \neq \left(\frac{e^2qQ}{h}\right)_{Cl(3)} \neq \left(\frac{e^2qQ}{h}\right)_{Cl(5)}.$$

For 2,4,6-trichloro-1-nitrobenzene two solid state modifications exist [126]. The crystal structures of these modifications are not known. However, the NQR spectra show that in each modification the Cl atoms in positions 2 and 6 are crystallographically equivalent. Single-crystal NQR investigations would reveal the nature of the symmetry operations which connect Cl(2) and Cl(6). The chemical inequivalence of Cl(2,6) and Cl(4) shows up as a crystallographic inequivalence in the solid state.

Generally, the crystal field lowers the symmetry of the free molecule. Chemical equivalence in the free molecule may occasionally be preserved as crystallographic equivalence in the solid. Chemical inequivalence in the free molecule cannot be reconciled with crystallographic equivalence in the solid by crystal field effects.

Table III.2. *Crystal field effect, $\Delta\nu = \nu' - \nu''$, of $\nu(^{35}Cl)$, $\nu(^{79}Br)$, and $\nu(^{127}I)$ in benzene derivatives. The solid phases listed contain more than one molecule in the asymmetric crystallographic unit. $\Delta\nu$ is the splitting NQR frequencies due to the crystallographic inequivalence of two or more molecules in the unit cell. $|\Delta|$ is $\lessapprox$ 500 kHz for $\nu(^{35}Cl)$ and $\lessapprox$ 4 500 kHz for $\nu(^{79}Br)$*

Substance	$\frac{\nu(^{35}Cl)}{MHz}$ at 77 °K	Assignment	Number of molecules in the asymmetric unit	$\frac{\Delta\nu/MHz = \nu' - \nu''}{MHz}$	Ref.
1,2-Dichlorobenzene	35.824 35.755 35.755 35.580	1,3	2	$0 \leqslant \Delta \leqslant 0.244$	11)
1,3-Dichlorobenzene	35.030 35.030 34.875 34.809	1,3	2	$0 \leqslant \Delta \leqslant 0.221$	11)
3-Chlorophenol	34.825 34.766	3	2	0.059	35)
4-Chlorobenzol	34.945 34.700	4	2	0.245	11)
4-Chlorophenyl-ω-chloroacetate[a] $4\text{-}ClC_6H_4OCOCH_2Cl$ I	36.792 36.372 35.412 35.162	ω 4	2	0.420 (ω) 0.250 (4)	126)
II	36.396 35.848 35.017 34.733	ω 4	2	0.548 (ω) 0.284 (4)	

Table III.2 (continued)

Substance	$\nu(^{35}Cl)$ at 77 °K / MHz	Assignment	Number of molecules in the asymmetric unit	$\Delta\nu$/MHz = $\nu' - \nu''$ / MHz	Ref.
1,2,3-Trichlorobenzene	37.031	2	2	0.058	28,35)
	36.973				
	36.523	1,3		$0.024 \leqslant \Delta \leqslant 0.309$	
	36.268				
	36.238				
	36.214				
1,2,4-Trichlorobenzene	36.623	2	2	0.223	21)
	36.400				
	36.380	1		0.207	
	36.173				
	35.617	4		0.428	
	35.189				
3,4-Dichloro-1-jodobenzene	36.512	3	2	0.212	126)
	36.300				
	36.012	4		0.050	
	35.942				
2,4-Dichloro-3,5-dimethylphenetole	36.038				
$2,4\text{–}Cl_2\text{–}3,5\text{–}(CH_3)_2C_6HOC_2H_5$	35.625	2	3	$\leqslant 0.471$	126)
	35.567				
	34.752				
	34.354	4			
	34.322			$\leqslant 0.430$	

2,4,5-Trichloro-1-nitrobenzene	38.441	2		0.153	
	38.288				
	37.435	5	2	0.097	136)
	37.338				
	36.717	4		0.132	
	36.585				
2,3,5,6-Tetrachloro-1-nitrobenzene	38.672	2,6		$0.052 \leqslant \Delta \leqslant 0.207$	
	38.566				
	38.507				
	38.465		2		136)
	38.066	3,5		$0.119 \leqslant \Delta \leqslant 0.461$	
	37.947				
	37.814				
	37.605				
2,4,5-Trichloro-benzenediazoniumtetrafluoborate	38.859	2		$0.084 \leqslant \Delta \leqslant 0.287$	
	38.775				
$2,4,5\text{-}Cl_3C_6H_2N_2^{\oplus}BF_4^{\ominus}$	38.572				
	37.980	5	3	$0.037 \leqslant \Delta \leqslant 0.320$	146)
	37.943				
	37.660				
	37.274	4		$0.030 \leqslant \Delta \leqslant 0.083$	
	37.244				
	37.191				

Table III.2 (continued)

Substance	$\frac{\nu(^{35}Cl)}{MHz}$ at 77 °K	Assignment	Number of molecules in the asymmetric unit	$\frac{\Delta\nu/MHz = \nu' - \nu''}{MHz}$	Ref.
3,4,5-Trichloro-1-nitrobenzene	37.832	4		0.120	
	37.712				
	37.460	3,5	2	$0.008 \leqslant \Delta \leqslant 0.222$	146)
	37.360				
	37.352				
	37.238				
1,2,3,5-Trichlorobenzene	37.567	2		0.174	
	37.483				
	37.289	1,3	2	$0.056 \leqslant \Delta \leqslant 0.473$	28)
	37.020				
	36.872				
	36.816				
	36.386	5		0.201	
	36.185				
4-Chlorobenzenediazoniumtetrafluoborate $4\text{-}ClC_6H_4N_2^{\oplus}BF_4^{\ominus}$	35.441	4	2	0.245	149)
	35.686				
3-Chloro-1-bromobenzene	34.992	3	2	0.144	137)
	34.848				

3-Chloro-1-fluoro-benzene	35.052 34.968	3	2	0.084	137)
4-Chloro-1-fluorobenzene	35.285 35.223 34.815	4	3	0.470	126)
	(35.286) (35.226) (34.818)				137)
	$\nu(^{79}Br)$/MHz				
4-Bromophenylsulfonylchloride 4-$BrC_6H_4SO_2Cl$	236.665 236.642	4	2	0.023	139)
4-Bromo-1-fluorobenzene	275.741 275.234 271.077	4	3	$0.507 \leqslant \Delta \leqslant 4.664$	139)
2,4-Dibromophenol	281.025 278.212 277.302	2	3	$0.910 \leqslant \Delta \leqslant 3.723$	139)
	275.722 275.688 274.122	4		$0.034 \leqslant \Delta \leqslant 1.600$	
3-Bromophenol	272.745 271.420	3	2	1.325	139)

Table III.2 (continued)

Substance	$\frac{\nu(^{79}Br)}{MHz}$ at 77 °K	Assignment	Number of Molecules in the asymmetric unit	$\frac{\Delta\nu/MHz = \nu' - \nu''}{MHz}$	Ref.
4-Bromophenol[a]	I 274.795 271.500	4	2	3.295	139)
	II 269.830 268.378	4	2	1.452	
	$\nu(^{127}J)(m = \pm\frac{1}{2} \rightleftarrows m = \pm\frac{3}{2})/MHz$				
1,2-Dijodobenzene	285.173 284.406 284.047 282.260	1,2	2	$0.359 \leqslant \Delta \leqslant 2.913$	139)
Na-salt of 4-jodo-benzoic acid	283.25 280.82 277.59 (at 295.7 °K)	4	3	$\leqslant 4.66$	139)

[a] The substance crystallizes in two modifications (I and II).

NQR spectroscopy also gives some hint about the numer of molecules in the asymmetric unit of the crystal. Let us consider 2,4-dichloro-3,5-dimethylphenetole (see Table III.2). At 77 °K six ^{35}Cl NQR lines have been found [126] and it therefore follows that there are three formula units in the asymmetric crystallographic unit.

From the knowledge of NQR frequencies of nuclei at chemically equivalent but crystallographically inequivalent sites of the molecule it is possible to estimate the crystal field effect. In Table III.2 the ^{35}Cl, ^{79}Br and ^{127}I NQR frequencies of some Cl, Br, I-substituted aromatic compounds are given. In these compounds more than one molecule belongs to the asymmetric crystallographic unit. The differences in resonance frequencies of nuclei at the same position within the molecule but at different crystallographic sites in the unit cell are $\leqslant 500$ kHz for ^{35}Cl and $\leqslant 5$ MHz for ^{79}Br.

2. Polymorphism and Crystal Field Effects

In molecular crystals we assume to a first approximation that the molecules are not changed in their structure and chemical bond properties. Therefore the differences in NQR frequencies must be due to the crystal field effect. The following forces may be responsible for the stability of different crystal modifications at different temperatures or pressures:

a) Electrostatic multipole forces (Van der Waals forces) and London forces between the molecules;
b) intermolecular hydrogen bonds in competition with intramolecular hydrogen bonds or with thermal motions of the molecules in the solid state;
c) steric effects in competition with the thermodynamic parameters T and p.

Only the forces a) are truly intermolecular. In the cases b) and c) intramolecular forces are involved. It is very difficult to draw definite conclusions from NQR spectra about such interactions as hydrogen bonds or steric effects so long as the NQR frequency shifts are within the limits of the crystal field effect. Table III.3 shows the NQR frequencies at 77 °K of compounds which exhibit polymorphism. In the aromatic compounds 1,4-dichlorobenzene, 2,4,6-trichloro-1-nitrobenzene, and 2,4,6-trichlorobenzenediazoniumfluoborate, the crystal field effect is probably due solely to intermolecular multipole forces and to London forces. For these substances the polymorphic shifts are $|\Delta\nu| \leqslant 0.9$ MHz. Also, for dichlorodinitromethane the polymorphic shift is $\leqslant 0.7$ MHz. Considering now the other ^{35}Cl resonances of Table III.3, 4-chlorophenyl-ω-chloroacetate with $|\Delta_{I,II}(\text{para})| \leqslant 0{:}68$ MHz and 2,4,6-trichlorophenylacetate, with $|\Delta_{I,II}| \leqslant 0.7$ MHz, it is seen that possible intramolecular polymorphism (conformation polymorphism) cannot be distinguished from the intermolecular forces by NQR powder spectroscopy. NQR work on iodine compounds which show polymorphism (or NQR spectroscopy with other nuclei $I \neq 3/2$)

Table III.3 *Crystal field effect of $\nu(^{35}Cl)$ due to the appearence of different modifications of the solid. $|\Delta\nu|$ between different modifications is $\lessapprox 900$ kHz for the Cl-atoms bound to the benzene ring. $|\Delta\nu| = |\nu$ (Modification A) $- \nu$ (Modification B)$| \equiv \Delta$*

Substance	Modification	ν/MHz (77 °K)	Assignment	Characterization of modification	Crystal field effect $\lvert\Delta\rvert$/MHz	Remarks	Ref.
1,4-Dichlorobenzene	I	34.775	1,4		$\lvert\Delta_{I,II}\rvert = 0.015$		
	II	34.760	1,4		$\lvert\Delta_{II,III}\rvert = 0.448$		139)
	III	35.208	1,4		$\lvert\Delta_{I,III}\rvert = 0.423$		
4-Chlorophenyl-ω-chloroacetate 4-$ClC_6H_4OCOCH_2Cl$	I	36.792	ω		$\lvert\Delta_{I,II}(\omega)\rvert \geqslant 0.024$ $\leqslant 0.944$		126)
		36.372	ω				
		35.412	4		$\lvert\Delta_{I,II}(4)\rvert \geqslant 0.145$ $\leqslant 0.679$		
		35.162	4				
	II	36.396	ω				126)
		35.848	ω				
		35.017	4				
		34.733	4				
2,4,6-Trichloro-1-nitro-benzene	I	37.517	2,6	Instable form (from the melt)	$\lvert\Delta_{I,II}(2,6)\rvert = 0.219$		126)
		36.783	4				
	II	37.736	2,6	Stable form (from alcohol)	$\lvert\Delta_{I,II}(4)\rvert = 0.534$		
		36.249	4				
2,4,6-Trichlorophenyl-acetate 2,4,6-$Cl_3C_6H_2OCOCH_3$	I	36.787	2,6	After destillation	$\geqslant 0.001$		126)
		36.748	2,6		$\lvert\Delta_{I,II}(2,6)\rvert$		
		36.648	2,6		$\leqslant 0.152$		
		36.636	2,6				
		36.150	4				
		35.650	4		$\lvert\Delta_{I,II}(4)\rvert \geqslant 0.188$		
	II	36.788	2,6	From the melt	$\leqslant 0.688$		
		36.781	2,6				
		36.338	4				

2,4,6-Trichloro-benzamide $2,4,6\text{-}Cl_3C_6H_2CONH_2$	I	36.948 36.834 36.649 36.276 36.181 36.105	2,6 2,6 2,6 2,6 2,6 (uncertain) 2,6	From ethanol	$\lvert\Delta_{I,II}(2,6)\rvert \begin{matrix}\geqslant 0.177\\ \leqslant 1.054\end{matrix}$		126)
		35.824 35.636 35.582	4 4 4 (uncertain)		$\lvert\Delta_{I,II}(4)\rvert \begin{matrix}\geqslant 0.129\\ \leqslant 0.183\end{matrix}$		
	II	36.427 35.894 35.765	2,6 2,6 4	From the melt			126)
2,4,6-Trichlorobenzene-diazoniumtetrafluoborate $2,4,6\text{-}Cl_3C_6H_2N_2^{\oplus}BF_4^{\ominus}$	I	38.587 38.546 36.910	2,6 2,6 4	Crystallized from water	$\lvert\Delta_{I,II}(2,6)\rvert$ $\geqslant 0.285$ $\leqslant 0.386$	The very high crystal field induced difference $\lvert\Delta_{I,II}(4)\rvert$ is probably due to the strong monopole forces between the molecular ions.	126) 146)
	II	38.932 38.872 35.991	2,6 2,6 4	Crystallized from CH_3CN	$\lvert\Delta_{I,II}(4)\rvert$ $= 0.919$		146)
$(NO_2)_2CCl_2$	I	42.287 42.133			$\lvert\Delta_{I,II}\rvert \begin{matrix}\geqslant 0.224\\ \leqslant 0.378\end{matrix}$		109) 121)
	II	41.909			$\lvert\Delta_{I,III}\rvert \begin{matrix}\geqslant 0.532\\ \leqslant 0.686\end{matrix}$		98)
	III	41.601			$\lvert\Delta_{II,III}\rvert = 0.308$		139)

Table III.3 (continued)

Substance	Modification	ν/MHz (77 °K)	Assignment	Characterization of modification	Crystal field effect $\lvert\Delta\rvert$/MHz	Remarks	Ref.
$CH_2ClCOOH$	I	36.429 36.131			$\lvert\Delta_{I,II}\rvert \geqslant 0.02$ $\leqslant 0.32$	Intermolecular hydrogen bonds are probably important for the existence of the modifications	139)
	II	36.45			$\lvert\Delta_{I,III}\rvert \geqslant 0.01$ $\leqslant 0.29$		
	III	36.14			$\lvert\Delta_{II,III}\rvert = 0.31$		
CH_2Br_2	I	282.072 (^{79}Br)		Low temperature phase	$\lvert\Delta_{I,II}\rvert \geqslant 0.973$ $\leqslant 1.173$		19) 16)
	II	281.099 (^{79}Br) 280.899		High temperature phase			139) 121)
4-Bromophenol	I	274.795 (^{79}Br) 271.500			$\lvert\Delta_{I,II}\rvert \geqslant 1.670$ $\leqslant 6.417$	Probably very strong influence of intermolecular hydrogen bond	17) 48) 74) 78) 121) 33) 139) 19)
	II	269.830 (^{79}Br) 268.378					
CH_3CN	I	2.8078 (^{14}N) 2.7992 $\eta = 0.0046$	ν_+ ν_-		$\lvert\Delta_{I,II}(\nu_+)\rvert = 0.0030$		139)
	II	2.8108 2.7954 $\eta = 0.0082$	ν_+ ν_-		$\lvert\Delta_{I,II}(\nu_-)\rvert = 0.0038$		

would shed some light on this question through the knowledge of the asymmetry parameter η. Clearly, single-crystal investigations of the structure of different modifications by NQR and X-ray work are needed for further advances.

3. The Site Effect

From the viewpoint of the crystal symmetry, the crystal field effect may be divided into two parts:

a) the appearance of more than one asymmetric unit;
b) occupation of different point positions of chemically equivalent atomes within one molecule and/or one asymmetric unit.

Today, we do not know the physical reason why there may be more than one asymmetric unit in the unit cell, nor do we have definite answer to the question: When is the symmetry of the free molecule reduced by the condensation into a solid and when is this symmetry preserved? Typical examples are the substituted 2,4,6-trichloro-1-X-benzenes. The symmetry of the gaseous molecule is preserved in the solid in so far as the Cl atoms in positions 2 and 6 are crystallographically equivalent for X = NO_2 and X = Br. Sites 2 and 6 of the molecule, however, are inequivalent in the solid for X = I, Cl, OH, and all other compounds for which the NQR spectrum is known. In the vast majority of molecules, the symmetry is reduced by condensation. We shall take the frequency splitting of NQR resonances due to this breakdown of symmetry as a qualitative measure of the crystal field effect.

Table III.4. *Crystal field effect of $\nu(^{35}Cl)$, $\nu(^{79}Br)$ and $\nu(^{127}I)$ for chemically equivalent atoms in subsituted benzene derivatives.* $|\Delta\nu(^{35}Cl)| \lessapprox 500$ *kHz;* $|\Delta\nu(^{79}Br)| \lessapprox 3$ *MHz*

Substance	$\nu(^{35}Cl)$ / MHz [a]	Assignment	$\bar{\nu}$	$\frac{\Delta}{\text{MHz}} = \frac{\bar{\nu}-\nu}{\text{MHz}}$
1,3,5-Trichlorobenzene	36.115 35.894 35.545	1,2,3	35.851	+ 0.306 to −0.264
2,6-Dichlorotoluene	34.788 34.755	2,6	34.772	± 0.016
2,6-Dichlorophenol	35.819 35.306	2,6	35.563	± 0.257
1,2,3,4-Tetrachlorobenzene	37.577 37.455	2,3	37.506	± 0.051

[a] $T = 77\ ^{\circ}K$.

Table III.4 (continued)

Substance	$\frac{\nu(^{35}Cl)}{MHz}$ [a]	Assignment	$\bar{\nu}$	$\frac{\Delta}{MHz} = \frac{\bar{\nu} - \nu}{MHz}$
1,2,3,4-Tetrachlorobenzene	37.013 37.013	1,4	37.013	± 0.000
1,2,4,5-Tetrachlorobenzene	36.905 36.843 36.738 36.702	1,2,4,5	36.797	+ 0.095 to -0.208
2,4,6-Trichloro-1-jodobenzene	37.034 36.356 35.807	2,6 4	36.695	± 0.399
2,6-Dichloro-4-nitroaniline	35.924 35.524	2,6	35.724	± 0.200
2,6-Dichloro-4-nitrophenol	37.364 36.263	2,6	36.814	± 0.551
2,4,6-Trichlorophenetole $2,4,6\text{-}Cl_3C_6H_4OC_2H_5$	36.542 36.158 35.736	2,6 4	36.350	± 0.192
Hexachlorobenzene	38.493 38.452 38.381		38.442	+ 0.061 to -0.041

Substance	$\frac{\nu(^{79}Br)}{MHz}$ [a]	$\bar{\nu}$	$\frac{\Delta}{MHz} = \frac{\bar{\nu} - \nu}{MHz}$
1,2,4,5-Tetrabromobenzene	290.572 289.675	290.124	± 0.448
1,3,5-Tribromobenzene	280.834 280.210 279.214	280.129	+ 0.915 to -0.705
1,2-Dibromobenzene	282.574 282.455	282.515	± 0.059
2,6-Dibromoaniline	272.012 270.606	271.309	± 0.703

[a] $T = 77\ ^{\circ}K$.

Table III.4 (continued)

Substance	$\frac{\nu(^{79}Br)}{MHz}$ a)	$\bar{\nu}$	$\frac{\Delta}{MHz} = \frac{\bar{\nu}-\nu}{MHz}$
3,5-Dibromoaniline	275.692 273.658	274.675	± 1.017
1,4-Difluoro-2,3,5,6-Tetrabromobenzene	309.894 303.959	306.927	± 2.968
Hexabromobenzene	305.880 305.298 305.200	305.459	+ 0.259 to -0.421

Substance	$\frac{\nu(^{127}I)\ (m = \pm\frac{1}{2} \rightleftarrows m = \pm\frac{3}{2})}{MHz}$ a)	$\bar{\nu}$	$\frac{\Delta}{MHz} = \frac{\bar{\nu}-\nu}{MHz}$
1,3,5-Trijodobenzene	286.111 285.734 280.478	284.081	+ 3.603 to -2.030
Hexajodobenzene	312.642 311.678 309.063	311.128	+ 2.065 to -1.514

a) $T = 77\ ^{\circ}K$.

We have already considered the multiplicity of asymmetric units and shall now discuss the positioning of chemically equivalent atoms at different point positions. Table III.4 shows the splitting of the ^{35}Cl NQR frequencies at 77 °K in benzene derivatives [126]. Only substances with one asymmetric unit in the unit cell are considered. One recognizes the spread of the frequencies for "chemically" equivalent chlorine atoms. The crystal field effect $|\Delta\nu|$ is within the limit of $\Delta\nu \lessapprox 500$ kHz.

In Fig. III.1 a distribution function of $\Delta\nu$ (^{35}Cl) is drawn for a number of aromatic compounds. A mean crystal field effect of about 300 kHz shows up in this graph (more than one asymmetric unit, different point positions within one asymmetric unit, and different modifications are considered).

The ratio

$$\frac{\nu(^{79}Br)}{\nu(^{35}Cl)}$$

is about 7.8 in comparable compounds. For instance

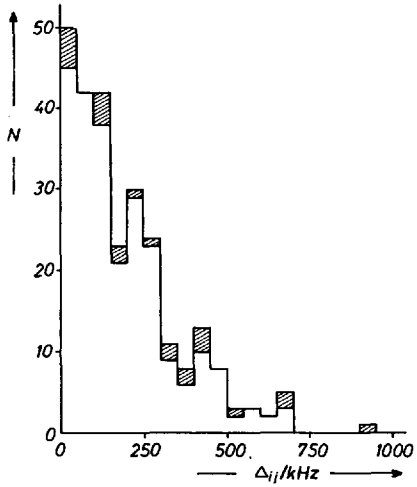

Fig. III.1. Distribution of ^{35}Cl–NQR frequency differences $|\Delta_{ij}| = |\nu_i - \nu_j|$ for chemically equivalent and crystallographically inequivalent Cl-atoms bound to the benzene ring. Only measurements with an unique assignement "frequency↔position of Cl-atom in the molecule" have been used. Substances with more than one formula unit in the asymmetry cell and substances with different modifications are included. Out of 265 frequencies observed (Σ N = 265), 211 Δ_{ij} -values (79.62 %) are in the range between 0–300 kHz. 251 Δ_{ij}-values (94.72 %) are in the range between 0–500 kHz, and 257 Δ_{ij}-values (96.98 %) are in the range between 0–600 kHz. The step width Δ in the graph is 50 kHz. The hatched areas reflect Δ_{ij} from different modifications

$$\frac{\nu(C_6H_5Br)}{\nu(C_6H_5Cl)}, \frac{\bar{\nu}\,(1,2\text{-dibromobenzene})}{\bar{\nu}\,(1,2\text{-dichlorobenzene})},$$

and others follow this rule. For the crystal field effect we expect in first approximation: $\Delta\nu(^{35}Cl) \cdot 7.8 = \Delta\nu(^{79}Br)$. Table III.4 shows that this rule of thumb is roughly correct, since $|\Delta\nu(^{79}Br)|$ in aromatic compounds goes up to 6 MHz. The very few values of $\Delta\nu(^{127}I)$ do not allow a comparison with $\Delta\nu(^{35}Cl)$. However, from the increasing order of polarizability $\alpha(Cl) < \alpha(Br) < \alpha(I)$, a relative crystal field effect $\frac{|\Delta\nu|}{\bar{\nu}}$ is expected which increases with the polarizability. For ^{14}N NQR such simple evaluations and comparisons of the crystal field effect are not possible.

IV. The Temperature Dependence of NQR Spectra

In NMR spectroscopy of nuclei with spin $I = 1/2$ certain features of the spectrum change with temperature. It is mainly the line width and the fine stru-

ture of the spectrum which are influenced and in most cases changes of frequency with temperature are negligible. This is due to the temperature independence of the diamagnetism. Strong changes of NMR frequencies with temperature are due to paramagnetic (or cooperative magnetic) effects in matter.

Quite a different situation is experienced in NQR spectroscopy. Dehmelt and Krüger (1950/1951) [3,6] found that the temperature dependence of NQR frequencies in organic materials is considerable. For instance, the temperature coefficient of $\nu(^{35}Cl)$ for chlorine bonded to carbon atoms is found to be in the range

$$1 \cdot 10^{-5} < \bar{\alpha} = \frac{1}{\bar{\nu}} \cdot \frac{\Delta\nu}{\Delta T} < 5 \cdot 10^{-4}$$

at room temperature. In ionic crystals, this temperature coefficient may cover an even larger range.

Near the solid state transformation points the isobaric temperature coefficients can reach very high values. An example of such behaviour is the temper-

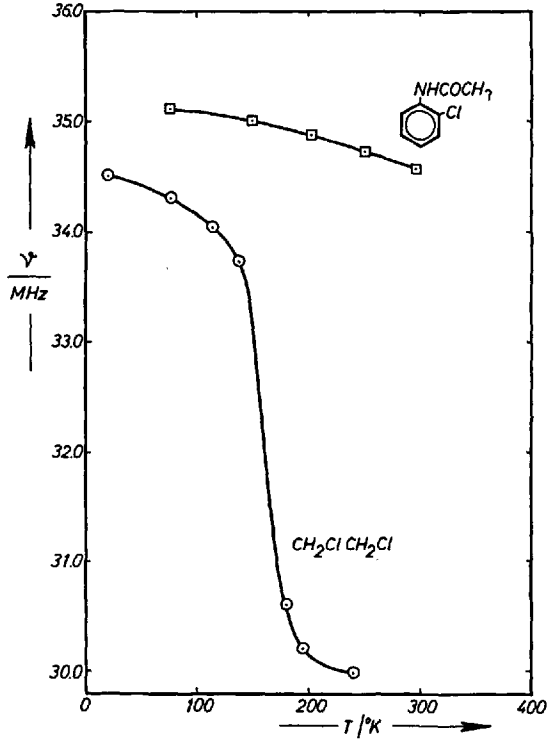

Fig. IV.1. $\nu(^{35}Cl)$ in 1,2-dichloroethane and in 2-chloroacetanilide as a function of temperature

ature dependence of $\nu(^{35}Cl)$ in 1,2-dichloroethane, $ClCH_2-CH_2Cl$, where $\bar{\alpha}$ is about $2 \cdot 10^{-3}$ degree^{-1} in the temperature range $130\,°K < T < 180\,°K$[30].

In Fig. IV.1 typical examples of the temperature dependence of $\nu(^{35}Cl)$ are shown. The solid transformation in 1,2-dichloroethane, due to the excitation of the free rotation of the whole molecule along the "long" axis of the molecule, is easily recognized. The usual temperature dependence of ^{35}Cl NQR frequencies in organic molecules is shown up in the curve $\nu(^{35}Cl) = f(T)$ in 2-chloroacetanilide, where $\bar{\alpha}$ is about $2 \cdot 10^{-5}$ degree^{-1}.

1. General Aspects of NQR and Temperature

In the discussion of NQR results in the frame of the Townes-Dailey theory, the influence of temperature on NQR frequencies is normally ignored. The temperature dependence of NQR spectra is considered here as a crystal field effect and in the following we shall discuss some of its aspects.

Most of the NQR spectra have been investigated at 77 °K. There are many reasons for choosing this particular temperature as the standard temperature in this branch of spectroscopy. (The standard pressure is 1 atm).

1. NQR is intrinsically a solid state experiment. At 77 °K all except a very few elements and compounds are in the solid state and therefore accessible to NQR experiments as long as the substance incorporates nuclei with $I > 1/2$.
2. The spin-lattice relaxation of nuclei with $I > 1/2$ is mainly due to nuclear quadrupole relaxation and the relaxation time at a temperature of 77 °K is still fairly short (of the order of milliseconds for many nuclei of interest to chemists). Therefore the experimental methods usually applied do not involve relaxation problems. The full RF fields available – for instance, with a superregenerative NQR spectrometer – may be applied successfully, resulting in an improved signal-to-noise ratio for the resonance at 77 °K as compared with room temperature. There are exceptions to this rule (e.g. ^{14}N NQR spectroscopy where saturation problems come into play at 77 °K).
3. At 77 °K many thermal motions of the molecules in the solid, still excited at room temperature, are frozen in. The amplitudes of the vibrations are small and the temperature coefficient $\bar{\alpha}$ is quite often found to be smaller than at room temperature (see Fig. IV.1).
4. The boiling point of liquid nitrogen (77 °K) is a very convenient fix point in the temperature scale.
5. Liquid nitrogen is a coolant which is available in most chemical laboratories and safe for work with organic substances.

The physical reason for the strong temperature dependence of NQR frequencies was first explained qualitatively by Dehmelt and Krüger [3,6], and then

quantitatively discussed by H. Bayer in his thesis [5]. Dehmelt and Krüger and Bayer assume that the librational motions of the molecules in the lattice or the motions of certain groups within the molecules are responsible for the coefficient

$$\bar{\alpha} = \frac{1}{\bar{\nu}} \cdot \frac{\Delta \nu}{\Delta T} .$$

The librational frequencies are much higher than the NQR frequencies:

$$\frac{\nu_{OSC}}{\nu_{NQR}} \gtrapprox 10^2 .$$

Therefore, the NQR transitions experience an electric field gradient which is averaged by the librational motions.

From such a simple argument one would expect a negative quotient:

$$\frac{\Delta \nu (NQR)}{\Delta T} = \frac{\nu(T_A) - \nu(T_B)}{T_A - T_B} < 0; T_A > T_B .$$

This behaviour is qualitatively found in all NQR investigations on ^{35}Cl in organic molecules. A positive temperature coefficient was found in some transition metal compounds such as K_2WCl_6 [153], K_2ReBr_6, K_2ReCl_6 [105], $TiBr_4$ [31,43], $ThCl_4$ [73], but also in alums [55].

Table IV.1. *$\nu(^{35}Cl)$ and $\nu(^{79}Br)$ in complex salts $K_2[XY_6]$ at $T = 20\ ^\circ C$. The mean temperature coefficient at $p = 1$ atm, $\bar{\alpha} = (\frac{1}{\bar{\nu}} \cdot \frac{\Delta \nu}{\Delta T})_p$ is between $-0.4 \cdot 10^{-4}$ degree^{-1} and $+0.4 \cdot 10^{-4}$ degree^{-1}. Data taken from Ref.* [101,167]

Substance	$\frac{\nu(20\ ^\circ C)}{MHz}$	$\bar{\alpha} = \frac{\left(\frac{1}{\bar{\nu}} \frac{d\nu}{dT}\right)_p}{degree}$	Temp. range/°C
K_2PtCl_6	25.82	$-0.3873 \cdot 10^{-4}$	−75.0 to 23.5
K_2IrCl_6	20.73	$-0.2605 \cdot 10^{-4}$	−69.0 to 24.2
K_2OsCl_6	16.84	$-0.1306 \cdot 10^{-4}$	−70.0 to 26.0
K_2ReCl_6	13.89	$+0.0936 \cdot 10^{-4}$	−76.0 to 21.2
K_2WCl_6	10.22	$+0.4305 \cdot 10^{-4}$	10.5 to 35.0
K_2ReBr_6	112.71	$+0.2484 \cdot 10^{-4}$	− 3.0 to 181.0

In Table IV.1 the temperature coefficients $\bar{\alpha}$ are given for a number of complexes $K_2[XY_6]$, X = Pt, Ir, Os, Re, W; Y = Cl,Br. The temperature coefficients of ν(NQR) show the appearance of a positive $\bar{\alpha}$ in some $[XY_6]^{2-}$ions, due to the chemical bond within the complex ion. A quantitative interpreta-

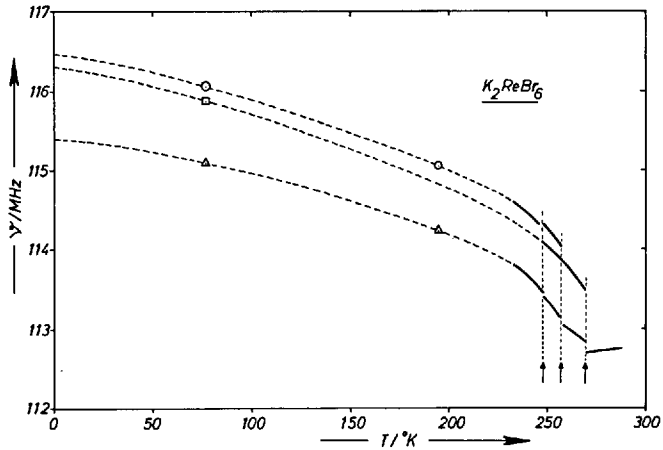

Fig. IV.2. Temperature dependence $\nu(^{79}Br)$ in K_2ReBr_6. The three solid state phase transitions in the temperature range between 240 °K $\leqslant T \leqslant$ 280 °K are clearly recognized

Table IV.2 *Mean temperature coefficient of halogen-NQR in hexahalogenocomplexes with K_2PtCl_6-type crystal structure; $-0.2 \cdot 10^{-4} \leqslant \alpha \cdot$ degree $\leqslant -1.9 \cdot 10^{-4}$; p = 1 atm. Data taken from Refs.* [61,84,95]

Substance	T_1/°K	ν_1/MHz	T_2/°K	ν_2/MHz	$\bar{\alpha} = \frac{\left(\frac{1}{\bar{\nu}} \frac{\Delta\nu}{\Delta T}\right)_p}{\text{degree}}$
K_2SeCl_6	294.7	20.431	77	20.576	$-0.3248 \cdot 10^{-4}$
$(NH_4)_2SeCl_6$	295.8	20.693	77	20.877	$-0.4046 \cdot 10^{-4}$
K_2PtCl_6	296.7	25.813	77	26.021	$-0.3653 \cdot 10^{-4}$
$(NH_4)_2PtCl_6$	299.2	26.065	77	26.282	$-0.3731 \cdot 10^{-4}$
Rb_2PtCl_6	298.2	26.29	77	26.44	$-0.2572 \cdot 10^{-4}$
Cs_2PtCl_6	298.3	26.60	77	26.70	$-0.1696 \cdot 10^{-4}$
$(NH_4)_2SeBr_6$	293.2	171.357	77	172.623	$-0.3405 \cdot 10^{-4}$
Cs_2SeBr_6	292.2	176.61	77	177.44	$-0.2179 \cdot 10^{-4}$
K_2PtBr_6 [a]	299.5	200.18	201.2	200.74	$-0.2842 \cdot 10^{-4}$
$(NH_4)_2PtBr_6$	295.0	202.524	77	203.983	$-0.3293 \cdot 10^{-4}$
Rb_2PtBr_6	295.0	204.37	77	205.63	$-0.2819 \cdot 10^{-4}$
Cs_2PtBr_6	296.3	207.19	77	208.32	$-0.2480 \cdot 10^{-4}$
$(NH_4)_2PtJ_6$ [b]	295.2	199.84	196.2	203.54	$-1.8530 \cdot 10^{-4}$
Rb_2PtJ_6	295.2	203.40	77	205.33	$-0.4328 \cdot 10^{-4}$

[a] Phase transformation: K_2PtCl_6-type → X-type (unknown) in the temperature range 201 °K > T > 77 °K.

[b] Phase transformation: K_2PtCl_6-type → Y-type (unknown) in the temperature range 196 °K > T > 77 °K.

tion of the positive temperature coefficient in terms of intramolecular bond in the $[XY_6]$ complex ion is difficult, since the resulting $\bar{\alpha}$ is composed of the normal (negative) Bayer term and a positive term.

The temperature dependence of $\nu(^{79}Br)$ in K_2ReBr_6 can be seen from Fig. IV.2. The change in sign of $\bar{\alpha}$ and three phase transitions in the compound are clearly revealed. Table (IV.2) gives the range of temperature coefficients $\bar{\alpha}$ found in complex salts with the K_2PtCl_6 type crystal structure. For a theoretical discussion of positive temperature coefficients $\bar{\alpha}$(NQR) see [104,105,153].

Temperature coefficients of the central atoms in complex ions have been investigated too. Fig. IV.3 gives the temperature dependence of $\nu(^{185}Re)$ ($m = \pm 1/2 \rightleftarrows m = \pm 3/2$) and $\nu(^{187}Re)$ ($m = \pm 1/2 \rightleftarrows m = \pm 3/2$) in $KReO_4$ (Rogers and Rama Rao [135]).

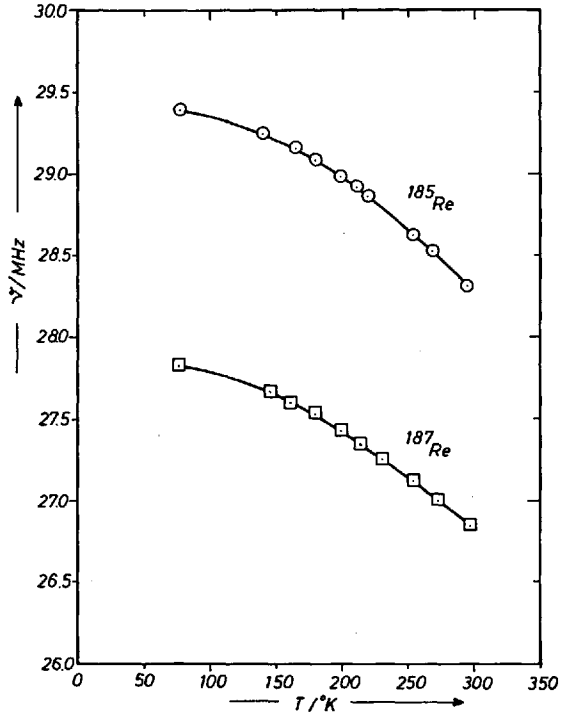

Fig. IV.3. Temperature dependence of $\nu(^{185}\text{Re})$ ($m = \pm\frac{1}{2} \rightleftarrows m = \pm\frac{3}{2}$) and $\nu(^{187}\text{Re})$ ($m = \pm\frac{1}{2} \rightleftarrows m = \pm\frac{3}{2}$) in $KReO_4$

To a first approximation one may assume [5] that the molecule in the lattice experiences only torsional vibrations around one axis, that is, the vibrations are limited to one plane within the molecule. This assumption simply takes account of the fact that at room temperature and below only the torsion-

al motions are excited (besides the zero point vibrations). Therefore one normal mode may be dominant. Furthermore, it is assumed that the electric field gradient at the site of the nucleus considered is axially symmetric, that is, $\eta = 0$.

The main part of the electric field gradient is determined by the chemical bond. For ^{35}Cl NQR in organic molecules, this would be the C–Cl bond. No temperature influence on this bond is assumed. The main influence of temperature on the quadrupole coupling constant, therefore, is due to the fast motion of the molecule considered, and to the motions of certain groups of the molecule. A certain part of the temperature dependence of the NQR frequencies is due the motion of the nucleus within the electric field gradient created at the site of the nucleus.

With these assumptions, the temperature dependence of ν(NQR) is given by

$$\nu(T) = \nu(0)\left\{1 - \frac{3}{2}\frac{\hbar}{I\omega}\left[\frac{1}{2} + \frac{1}{\exp\left(\frac{\hbar\omega}{kT}\right) - 1}\right]\right\}, \qquad \text{(IV.1)}$$

where I is the moment of inertia of the torsional oscillator considered, ω is the torsional frequency, T is the temperature of the crystal and $\hbar$ and k are Planck's constant and Boltzmann's constant, respectively. Introducing the characteristic temperature

$$\Theta = \frac{\hbar\omega}{k}$$

we can write Eq. (IV.1) in the form

$$\nu(T) = \nu(0)\left\{1 - \frac{3}{2}\frac{\hbar^2}{k\Theta I}\left[\frac{1}{2} + \frac{1}{\exp\left(\frac{\Theta}{T}\right) - 1}\right]\right\}. \qquad \text{(IV.2)}$$

At temperatures above 77 °K, one can assume that $\frac{\hbar\omega}{kT} \ll 1$ and with

$$\frac{1}{2} + \frac{1}{\exp\left(\frac{\hbar\omega}{kT}\right) - 1} \approx \frac{kT}{\hbar\omega} + \frac{1}{12}\frac{\hbar\omega}{kT} + \ldots,$$

it follows that

$$\nu(T) = \nu(0)\left\{1 - \frac{3}{2}\frac{\hbar}{I\omega}\left[\frac{kT}{\hbar\omega} + \frac{1}{12}\frac{\hbar\omega}{kT}\right]\right\}$$

and in an abbreviated form

$$\nu(T) = \nu(0)\left\{1 + bT + cT^{-1}\right\}. \qquad \text{(IV.3)}$$

Another way of writing the Bayer equation is:

$$\nu(T) = \nu(0)\left\{1 - \frac{\beta}{4}\frac{\hbar^2}{I\Theta k}\,\mathrm{ctgh}\,\frac{\Theta}{2T}\right\} \qquad \text{(IV.4)}$$

using the identity

$$\frac{1}{2} + \frac{1}{e^x - 1} \equiv \frac{1}{2}\,\mathrm{ctgh}\,\frac{x}{2}.$$

In the literature the Bayer equation is often used in the form

$$\nu(T) = \nu(0)\left\{\alpha + \frac{\beta}{\exp\left(\frac{\Theta}{T}\right) - 1}\right\}. \qquad \text{(IV.5)}$$

The first generalization of Bayer's theory would be the introduction of more than one vibrational mode into the theory and the consideration of deviations from the rotational symmetry of the electric field gradient tensor, that is, $\eta \neq 0$. Then the coefficients b and c in Eq. (IV.3) are given by

$$b = -\frac{3}{2}k\sum_n \frac{A_n}{\omega_n^2};\quad c = -\frac{\hbar^2}{8k}\sum_n A_n.$$

Here the coefficients A_n depend upon the moments of inertia of the molecule and the asymmetry parameter η. Further generalizations of Bayer's theory (consideration of stretching vibrations, introduction of the lattice expansion with temperature) have been introduced by Kushida *et al.* [26,32], by Wang [27] and by Lotfullin and Semin [132].

Applying Eq. (IV. 3–5) to the experimental data, good agreement can be found between the measurements and the theory. However, difficulties arise in interpreting the constants b and c, and in most cases a quantitative calculation of the torsional modes of the molecules from a measurement of ν(NQR) = $f(T)$ is not possible. In Figs. IV.4 and IV.5 the temperature dependence of $\nu(^{35}\mathrm{Cl})$ and $\nu(^{79}\mathrm{Br})$ is shown for a number of hexahalogeno complexes which all crystallize with the K_2PtCl_6 type in the temperature range investigated. The qualitative agreement between the measurement and Bayer's theory is quite good, but there is no quantitative agreement. In Table IV.3 the moments of inertia are given for the $[XCl_6]$ ions $[PtCl_6]^{2-}$ and $[IrCl_6]^{2-}$, calculated from very careful measurements of $\nu(^{35}\mathrm{Cl}) = f(T)$. One would expect almost no difference between $I([IrCl_6]^{2-})$ and $I([PtCl_6]^{2-})$ since there is only a negligible mass difference and a very small difference in the distance X–Cl between the two ions. However, the moment of inertia calculated from NQR data (Eq. (IV.4)) turns out to be higher for $[IrCl_6]^{2-}$ than for $[PtCl_6]^{2-}$ by a factor of about ten [155]. The excellent agreement between experiment and Eq. (IV.4) in the tem-

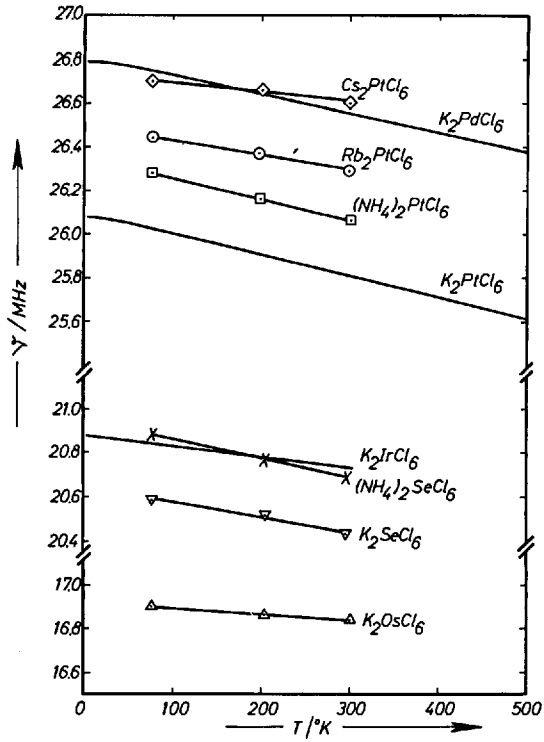

Fig. IV.4. Temperature dependence of $\nu(^{35}Cl)$ in salts A_2XCl_6 with K_2PtCl_6-type structure

perature range 4.2 °K $\leqslant T \leqslant$ 500 °K and 3 °K $\leqslant T \leqslant$ 300 °K for K_2PtCl_6 and K_2IrCl_6, respectively, is probably due to the simple geometry of the $[XCl_6]^{2-}$ ion.

Some workers in the field of NQR spectroscopy have preferred a modification of Eq. (IV.3), considering the constant b in the term $(\nu_0 b \cdot T)$ as a function of temperature. The reasoning for this assumption is the volume dependence of the different ω_n. In molecular crystals the temperature dependence of the modes ω_n,

$$\omega_n = \omega_n^0 (1 - g_n \vartheta)$$

should cover most of the temperature-dependent volume effects, as Brown [54] pointed out. In the above relation, ϑ is the temperature of the crystal measured from any arbitrary zero point, ω_n^0 are the librational modes in the frequency spectrum at temperature $\vartheta = 0$, and g_n are parameters varying with n, that is, for each lattice mode a separate g_n is used. The superiority of Brown's treatment of the temperature dependence of NQR over the simple Bayer theory was

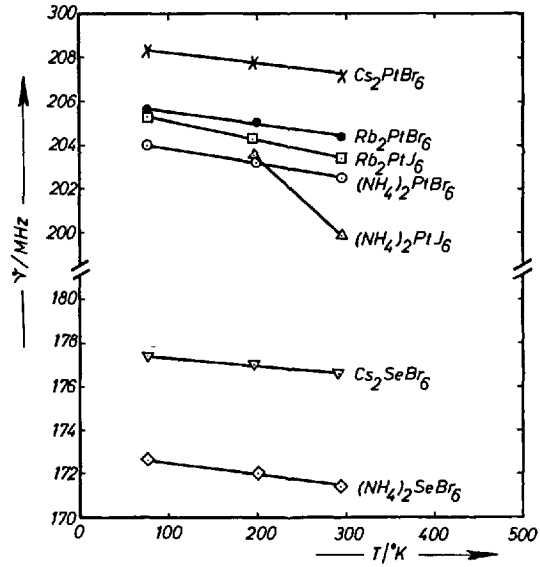

Fig. IV.5 Temperature dependence of $\nu(^{79}\mathrm{Br})$ and $\nu(^{127}\mathrm{I})$ ($m = \pm\frac{1}{2} \rightleftarrows m = \pm\frac{3}{2}$) in K_2PtCl_6-type compounds

Table IV.3 *Moment of inertia I, and characteristic temperature* $\Theta = \frac{\hbar\omega}{k}$ *according to the Bayer-theory for* K_2PtCl_6, K_2PdCl_6 *and* K_6IrCl_6. *I and* Θ *are gained from measurements* $\nu(^{35}Co) = f(T)$. *Data taken from Refs.* [130,138,150,155])

Substance	ν_0/MHz	Θ/°K	$\frac{I \cdot 10^{37}}{g \cdot m^2}$
K_2PtCl_6	26.102	55 ($\triangleq$ 38 cm^{-1})	1.1
K_2PdCl_6	26.819	28 ($\triangleq$ 41 cm^{-1})	
K_2IrCl_6	20.884	20 ($\triangleq$ 14 cm^{-1})	12.5

shown by Dinesh and Narasimhan for the ^{35}Cl NQR spectrum of $HgCl_2$ [114], by Kantimati [142] ($\nu(^{35}Cl) = f(T)$ in 2,4-dichloroaniline, in 2,6-dichloroaniline, in 4-fluoro-3-chloroaniline and in p-chlorophenoxyacetic acid) and by Matzkanin *et al.* [118] ($\nu(^{14}N) = f(T)$ in hexamethylenetetramine). The improvement given by Brown's treatment is not surprising since additional parameters are used in Eq. (IV.3).

2. Temperature Dependence of NQR Frequencies and Bond Parameters

The question of primary interest here is the effect of the temperature dependence of NQR spectra on the determination of the charge distribution within the

molecules or molecular ions by the NQR data. Therefore we shall now consider the influence of temperature on ν(NQR) in the application of the Townes-Dailey model. As an example, we take from Fig. IV.4 the temperature dependence of $\nu(^{35}Cl)$ in the salts K_2PtCl_6, K_2PdCl_6 and K_2IrCl_6, where the measurements are very carefully done and cover the temperature range down to $\sim 4\ ^\circ K$ [130,138,150,155]. The temperature coefficients for all the substances shown in Fig. IV.4 and listed in Table IV.2 are of the same order of magnitude.

From the Townes-Dailey theory (Eq. (II.9)) different values of $(1-i)$ will be calculated when frequencies measured at different temperatures are used. Comparing temperatures T_1 and T_2, the relation for the covalent character is

$$\frac{(1-i)_{T_1}}{(1-i)_{T_2}} = \frac{[(e^2qQ/h)_{exp}]_{T_1}}{[(e^2qQ/h)_{exp}]_{T_2}} \quad . \tag{IV.6}$$

Since for the K_2PtCl_6-type structure $\eta = 0$ it follows that

$$\frac{(1-i)_{T_1}}{(1-i)_{T_2}} = \frac{[\nu(\mathrm{NQR})]_{T_1}}{[\nu(\mathrm{NQR})]_{T_2}} \quad . \tag{IV.7}$$

From Table IV.2 we see that the temperature coefficients $|\bar{\alpha}|$ are between $0.1 \cdot 10^{-4}$ degree^{-1} and $0.5 \cdot 10^{-4}$ degree^{-1}. Therefore, in the calculation of $1-i$ or of i, the error introduced through neglect of the vibrational motions of the molecules is not more than 1 % for the whole temperature range usually explored in NQR spectroscopy. This error is certainly well within the limits of the model of Townes and Dailey, and a comparison of the parameter $1-i$ calculated from measurements at different temperatures is justified so long as the crystal structure does not change with T. This assumption is probably also valid in comparing the covalent character of two different, isostructural substances A and B using $\nu(\mathrm{A})_{T_1}$ and $\nu(\mathrm{B})_{T_2}$, since the temperature coefficients of substances with the same crystal structure lie within a small range of values (Table IV.2).

The situation is quite different when the Townes-Dailey Equation (IV.6) is applied to substances which change the crystal structure at certain transformation points within the usual range of measurements. Such an example is shown in Fig. IV.2. The effective temperature coefficient $|\bar{\alpha}|$ is fairly high and differs considerably from modification to modification. The consequence is a difference of up to 5 per cent in the calculation of the covalent character from NQR measurements at different temperatures.

The Townes-Dailey approach is also often used in evaluating the covalent character of carbon-halogen bonds in organic molecules. Again the temperature coefficients $\bar{\alpha} = \frac{1}{\bar{\nu}} \frac{\Delta\nu}{\Delta T}$ are mostly of the same order of magnitude as the $|\bar{\alpha}|$ values in Table IV.2. In Table IV.4 some temperature coefficients of $\nu(^{35}Cl)$ are given, measured on the chlorine bound to carbon in aromatic systems. A

Table IV.4 *Mean Temperature coefficient of $\nu(^{35}Cl)$, $\bar{\alpha}$, for chloroacetanilides at p = 1 atm: $-0.5 \cdot 10^{-4} < \bar{\alpha} \cdot \text{degree} < -0.9 \cdot 10^{-4}$. Data taken from Ref.* [162]

Substance	$\frac{\nu_1}{\text{MHz}}\left(\frac{T}{^\circ\text{K}}\right)$	$\frac{\nu_2}{\text{MHz}}\left(\frac{T}{^\circ\text{K}}\right)$	$\bar{\alpha} = \frac{\left(\frac{1}{\bar{\nu}} \cdot \frac{\Delta\nu}{\Delta T}\right)_p}{\text{degree}}$	Assignment
$2\text{-ClC}_6\text{H}_4\text{NHCOCH}_3$	35.153(77)	34.576(295)	$-0.7592 \cdot 10^{-4}$	o
$2,3\text{-Cl}_2\text{C}_6\text{H}_3\text{NHCOCH}_3$	36.366(77)	35.924(295)	$-0.5609 \cdot 10^{-4}$	o
$2,3\text{-Cl}_2\text{C}_6\text{H}_3\text{NHCOCH}_3$	36.199(77)	35.658(295)	$-0.6907 \cdot 10^{-4}$	m
$2,6\text{-Cl}_2\text{C}_6\text{H}_3\text{NHCOCH}_3$	36.020(77)	35.304(295)	$-0.9210 \cdot 10^{-4}$	o
$2,6\text{-Cl}_2\text{C}_6\text{H}_3\text{NHCOCH}_3$	35.866(77)	35.183(295)	$-0.8819 \cdot 10^{-4}$	o
$3,5\text{-Cl}_2\text{C}_6\text{H}_3\text{NHCOCH}_3$	35.926(77)	35.854(114)	$-0.5422 \cdot 10^{-4}$	m
$3,5\text{-Cl}_2\text{C}_6\text{H}_3\text{NHCOCH}_3$	35.926(77)	35.843(114)	$-0.6251 \cdot 10^{-4}$	m
$3,5\text{-Cl}_2\text{C}_6\text{H}_3\text{NHCOCH}_3$	35.578(77)	35.506(114)	$-0.5475 \cdot 10^{-4}$	m
$3,5\text{-Cl}_2\text{C}_6\text{H}_3\text{NHCOCH}_3$	35.472(77)	35.404(114)	$-0.5186 \cdot 10^{-4}$	m
$2,4,6\text{-Cl}_3\text{C}_6\text{H}_2\text{NHCOCH}_3$	36.738(77)	36.127(295)	$-0.7693 \cdot 10^{-4}$	o
$2,4,6\text{-Cl}_3\text{C}_6\text{H}_2\text{NHCOCH}_3$	36.412(77)	35.832(295)	$-0.7365 \cdot 10^{-4}$	o
$2,4,6\text{-Cl}_3\text{C}_6\text{H}_2\text{NHCOCH}_3$	36.035(77)	35.442(295)	$-0.7611 \cdot 10^{-4}$	p

Table IV.5 *Mean temperature coefficient $\bar{\alpha}$ (^{35}Cl) for aliphatic chlorocompounds at p = 1 atm: $-1 \cdot 10^{-4} < \bar{\alpha} \cdot \text{degree} < -8.6 \cdot 10^{-4}$. Data taken from Ref.* [139]

Substance	$\frac{\nu_1}{\text{MHz}}\left(\frac{T}{^\circ\text{K}}\right)$	$\frac{\nu_2}{\text{MHz}}\left(\frac{T}{^\circ\text{K}}\right)$	$\bar{\alpha} = \left(\frac{1}{\bar{\nu}} \cdot \frac{\Delta\nu}{\Delta T}\right)_p$ /degree
$CHCl_3$	38.308 (77)	37.577 (202)	$-1.5413 \cdot 10^{-4}$
	38.254 (77)	37.346 (202)	$-1.9217 \cdot 10^{-4}$
CH_2Cl_2	35.991 (77)	34.895 (174)	$-3.1879 \cdot 10^{-4}$
$[ClCH_2COO]^-Na^+$	34.794 (77)	33.943 (295)	$-1.1358 \cdot 10^{-4}$
$ClCH_2COCH_2Cl$	35.943 (77)	34.902 (295)	$-1.3481 \cdot 10^{-4}$
CH_3COCH_2Cl	35.485 (77)	34.461 (196)	$-2.4605 \cdot 10^{-4}$
	35.071 (77)	34.452 (196)	$-1.4964 \cdot 10^{-4}$
$ClCH_2CH_2Cl$	34.361 (77)	29.92 (238)	$-8.5823 \cdot 10^{-4}$

calculation of the covalent character of a C–Cl bond from Eq. (II.9) results in differences of 2 % in $(1-i)$ when $\nu(^{35}Cl)_{77\,^\circ K}$ and $\nu(^{35}Cl)_{293\,^\circ K}$ are used respectively.

The parameterization of the NQR spectra is a common method for comparing the "bond character" of carbon-halogen bonds in organic systems. Following the idea of Meal [11], the NQR frequencies of halogens in aromatic systems are given by

$$\nu = \nu_0 + k \sum_i \sigma_i . \qquad \text{(IV.8)}$$

ν_0 is a constant which depends on the nucleus investigated ($\nu_0 \approx 34.7$ MHz for ^{35}Cl). The σ_i are the well-known σ values introduced by Hammett [1]. The index i distinguishes substituent groups and their position with respect to the Cl nucleus considered. k is a constant, with a value near 1 MHz for ^{35}Cl, and is comparable with the reaction parameter ρ in the Hammett equation. In considering a fairly large number of aromatic compounds with C–Cl bonds at the benzene ring the relation

$$\nu = \nu_0 + \sum_i \kappa_i \qquad \text{(IV.9)}$$

was used by Biedenkapp and Weiss [126] and by Pies, Rager and Weiss [162] to compare the influence of aromatic substitutions on the C–Cl bond. A similar linear relation holds for NQR frequencies on aliphatic C-halogen bonds and Tafts σ^* values [99,122].

With the help of Eq. (II.9), the NQR subsituent parameters κ_i can be interpreted as a measure of the changes effected in the covalent bond character by the substitution considered.

$$\Delta(1-i) = \frac{1}{1-s} \cdot \frac{\kappa_i}{\left(\frac{1}{2}\frac{e^2qQ}{h}\right)_{at}} . \qquad \text{(IV.10)}$$

In the first approximation of the Townes-Dailey theory, changes of the s-character of the bonding orbital of chlorine and also changes in the double bond character causing a different η are neglected.

The parameterization of the NQR spectra requires the assignment of NQR frequencies of the spectrum to certain chlorine atoms in the molecule. This procedure has been discussed at length [126,146,162]. Here it should be emphasized that the frequencies to be assigned in multichlorosubstituted compounds have to be measured at the same temperature. To demonstrate this, we will consider the NQR spectrum of ω,2,3-trichloroacetanilide, $2,3\text{-}Cl_2C_6H_3NHCOCH_2Cl$ (Fig. IV.6). From the preliminary calculations with unique assignment, it follows for the $-NHCOCH_2Cl$ group that $\kappa_o > \kappa_m > \kappa_p$. Thus ν(2–Cl) should be higher than ν(3–Cl). Taking one frequency, $\nu = 36.140$ MHz (△ in Fig. IV.6) at 77 °K and the other one, $\nu = 36.019$ MHz, (● in Fig. IV.6) at 295 °K, the assignment would be inverted as against that done at the same temperature.

From Fig. IV.6 a second requirement is obvious. Chlorine atoms in aliphatic compounds or in aliphatic side chains of aromatic compounds exhibit a temperature coefficient, $|\overline{\alpha}|$, which is higher by about a factor of two than that of chlorine atoms bound to aromatic systems. This can be seen by comparing Tables IV.4 and IV.5. Therefore the temperature dependence of the NQR spectrum has to be measured when there are C–Cl bonds of both kinds within a molecule,

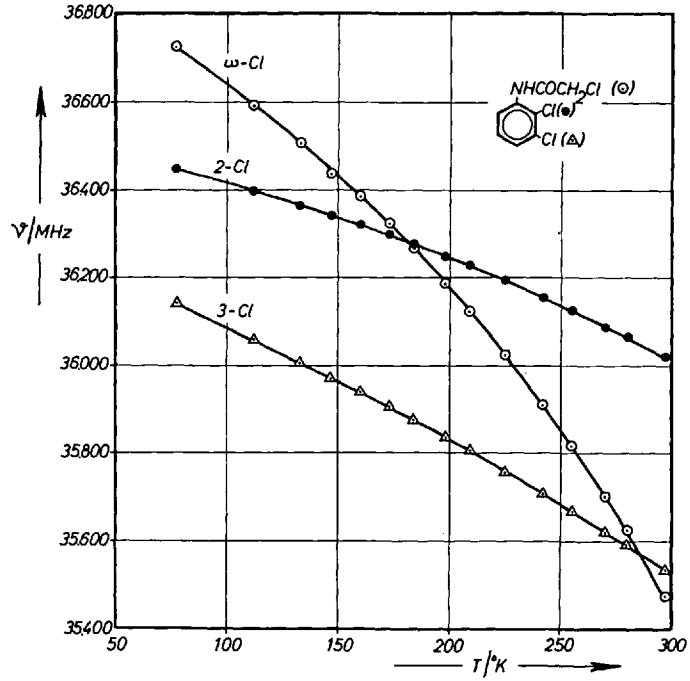

Fig. IV.6. Temperature dependence of the ^{35}Cl-NQR spectrum of ω,2,3-trichloroacetanilide, 2,3-$Cl_2C_6H_3NHCOCH_2Cl$; ⊙: ω-Cl; ●: 2-Cl; △: 3-Cl

e.g. aromatic derivatives of monochloroacetic acid, $ClCH_2 \cdot CO-R_{arom.}$. Selected examples are shown in Table IV.6. The large crystal field effect at 77 °K of the *(ω-Cl)NQR*, $|\bar{\nu} - \nu| \lessapprox 500$ kHz, is to a great extent due to the large $|\bar{\alpha}|$.

The differences in the temperature coefficient of aliphatically and aromatically bound chlorine can be easily understood. The mean square amplitudes of the thermal vibrations of singly bonded $-CH_{3-x}Cl_x$ groups are much higher than the thermal vibrations of the chlorine-substituted aromatic ring. Even at fairly low temperatures (below room temperature) the hindered rotations around a C–C bond are excited and free rotation (or almost free rotation) is possible, as shown by the measurements on 1,2-dichloroethane (Fig. IV.1). In many cases, the ^{35}Cl NQR frequencies of the side chain atoms and of aliphatic chlorine atoms disappear at temperatures below the melting point of the substances (fading-out phenomenon [57]).

The relation between the κ_i and the NQR frequencies shows deviations from the regression line. These deviations may be due to:

a) failure of the additivity assumed in Eq. (IV.9),
b) crystal field effect.

Table IV.6 *Mean temperature coefficient* $\bar{\alpha} = \left(\frac{1}{\bar{\nu}} \cdot \frac{\Delta\nu}{\Delta T}\right)_p$ *of chlorine atoms bound to carbon of the benzene ring and to the side chain respectively. The ratio* $\bar{\alpha}$*(ring)/*$\bar{\alpha}$*(side chain) is in the order of 2–3. Data taken from Refs.* [126,162]

Substance	$\nu(^{35}Cl)$ MHz ($T = 77$ °K)	$\nu(^{35}Cl)$ MHz (T/°K)	Assignment	$\bar{\alpha} = \frac{1}{\bar{\nu}} \cdot \frac{\Delta\nu}{\Delta T}$/degree
2,4-Dichlorophenyl-ω-chloroacetate	36.561	35.954 (268)	2	$-0.877 \cdot 10^{-4}$
	35.213	34.803 (268)	4	$-0.613 \cdot 10^{-4}$
	36.602	34.989 (268)	ω	$-2.359 \cdot 10^{-4}$
2,4,6-Trichlorophenyl-ω-chloroacetate	37.327	36.629 (296)	2,6	$-0.862 \cdot 10^{-4}$
	37.278	36.691 (296)		$-0.725 \cdot 10^{-4}$
	36.017	35.500 (296)	4	$-0.660 \cdot 10^{-4}$
	36.858	35.102 (296)	ω	$-2.229 \cdot 10^{-4}$
ω,2-Dichloroacetanilide	35.351	35.329 (89)	2	$-0.519 \cdot 10^{-4}$
	36.278	36.117 (89)	ω	$-3.707 \cdot 10^{-4}$
ω,4-Dichloroacetanilide	34.962	34.748 (197)	4	$-0.512 \cdot 10^{-4}$
	35.745	35.541 (114)	ω	$-1.547 \cdot 10^{-4}$
ω,2,3-Trichloroacetanilide	36.447	36.019 (295)	2	$-0.542 \cdot 10^{-4}$
	36.140	35.532 (295)	3	$-0.778 \cdot 10^{-4}$
	36.725	35.474 (295)	ω	$-1.590 \cdot 10^{-4}$
ω,2,5-Trichloroacetaniiide	35.506	35.074 (295)	2	$-0.562 \cdot 10^{-4}$
	35.402	34.918 (295)	5	$-0.632 \cdot 10^{-4}$
	35.584	34.774 (295)	ω	$-1.056 \cdot 10^{-4}$
ω,2,6-Trichloroacetanilide	36.180	35.558 (295)	2,6	$-0.796 \cdot 10^{-4}$
	35.754	35.106 (295)		$-0.839 \cdot 10^{-4}$
	36.674	35.530 (192)	ω	$-2.756 \cdot 10^{-4}$
ω,3,4-Trichloroacetanilide	36.344	36.118 (193)	3	$-0.538 \cdot 10^{-4}$
	36.209	35.921 (193)	4	$-0.688 \cdot 10^{-4}$
	36.589	36.432 (113)	ω	$-1.195 \cdot 10^{-4}$
ω,2,4,5-Tetrachloro-acetanilide	36.424	36.234 (199)	2	$-0.429 \cdot 10^{-4}$
	36.530	36.289 (199)	5	$-0.543 \cdot 10^{-4}$
	36.989	36.770 (199)	4	$-0.487 \cdot 10^{-4}$
	36.730	35.827 (199)	ω	$-2.040 \cdot 10^{-4}$

Wrong assignment may be caused by a) or b). However, both would enlarge the deviations from the regression line. In Fig. IV.7 such a correlation is shown for chloroacetanilides, $Cl_xC_6H_{5-x}NHCOCH_{3-y}Cl_y$ [162]. From this graph it follows that the crystal field effect is of the order of ± 500 kHz.

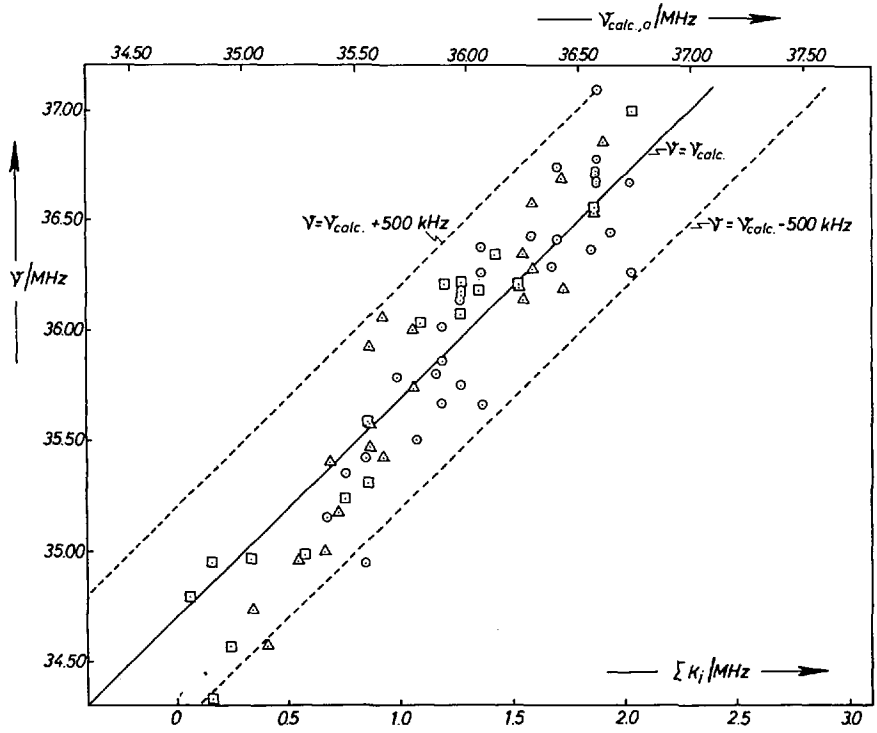

Fig. IV.7. Correlation between the observed ^{35}Cl-frequencies, ν, of chloroacetanilides, $Cl_xC_6H_{5-x}NHCOCH_{3-y}Cl_y$ and the NQR-substituent parameters, κ_i. *Distinct* κ_i-values are used for the different groups $-NHCOCH_3$, $-NHCOCH_2Cl$, $-NHCOCHCl_2$, and $-NHCOCCl_3$. The frequencies $\nu_{calc,a}$ are related to $\Sigma\,\kappa_i$ by Eq. (IV.9)
⊙ = ortho, △ = meta, ⊡ = para

V. Nuclear Quadrupole Resonance on Molecular Compounds

Extensive NQR work has been done on molecular compounds (≡ molecular addition compounds), particularly in the last ten years. The first NQR experiment on such compounds was performed by Dehmelt, who investigated the ^{35}Cl NQR in nitrobenzene. $SnCl_4$ and $AlCl_3 \cdot O(C_6H_5)_2$ [13]. In $C_6H_5NO_2 \cdot SnCl_4$ Dehmelt observed a considerable decrease of $\nu(^{35}Cl)$ in the molecular compound with respect to pure $SnCl_4$.

The direct connection between nuclear quadrupole coupling constant and charge distribution leads to the expectation that NQR should be a sensitive device for the study of intermolecular charge transfer in the solid state. The nu-

Table V.1 *NQR-data of molecular compounds with highly symmetric partner A (Br_2,CBr_4, CCl_4, chloranil). The mean crystal field shifts are* $|\Delta| \lesssim 2.6$ *MHz* (^{81}Br) *and* $|\Delta| \lesssim 0.30$ *MHz* (^{35}Cl)

Component A	Component B	ν/MHz (77 °K)	$\bar{\nu}$/MHz	$\Delta = \{\bar{\nu}(A) - \bar{\nu}(A_xB_y)\}$/MHz	Ref.
Br_2	--	319.539 (^{81}Br)	319.539		93) 6) 20) 37)
Br_2	Paraxylene	321.83 (^{81}Br)	321.83	- 2.29	93)
CBr_4	--	^{79}Br			93)
		322.79			58)
		322.57			23)
		322.47	$\bar{\nu}(^{79}Br)$=		74)
		322.26	320.66 MHz		111)
		321.44			121)
		321.18			
		320.88	$\bar{\nu}(^{81}Br)$=		
		320.88	267.99 MHz		
		319.98	(calculated)		
		319.60			
		319.42			
		319.22			
		318.48			
		318.01			
		^{79}Br ^{81}Br			
CBr_4	Paraxylene	322.09 269.18	^{79}Br: 319.55		93)
		317.00 264.95	^{81}Br: 267.07	+ 0.97 (^{81}Br)	128)
CCl_4		^{35}Cl			14)
		40.817			23)
		40.797			57)
		40.782			8)
		40.721			69)
		40.696			93)
		40.655			
		40.643			
		40.639	40.633		
		40.607			
		40.587			
		40.576			

Table V.1 (continued)

Component A	Component B	ν/MHz (77 °K)	$\bar{\nu}$/MHz	$\Delta = \{\bar{\nu}(A) - \bar{\nu}(A_xB_y)\}$/MHz	Ref.
		40.549 40.540 40.540 40.521 40.465			
CCl_4	Paraxylene	40.689, 40.472 (^{35}Cl)	40.581	+ 0.052	93)
CCl_4 1 :	Benzene 1	40.400, 40.368, 40.288 (^{35}Cl)	40.352	+ 0.281	103)
CCl_4 2 :	Benzene 1	40.904, 40.576, 40.280 (^{35}Cl)	40.587	+ 0.046	103)
CCl_4 3 :	Benzene 1	40.800, 40.648, 40.496, 40.306 (^{35}Cl)	40.563	+ 0.070	103)
CBr_4	Benzene	268.63, 266.57 (^{81}Br)	267.60	+ 0.39	128)
CBr_4	Orthoxylene	269.42, 268.86, 268.35 (^{81}Br)	268.88	- 0.89	128)
CBr_4	Mesithylene	268.57, 267.92, 266.77 (^{81}Br)	267.75	+ 0.24	128)
CBr_4	Durene	269.35, 267.65 (^{81}Br)	268.50	- 0.51	128)
CBr_4	2,6-Lutidine	269.38, 266.92 (^{81}Br)	268.15	- 0.16	128)
CBr_4	2,4,6-Collidine	266.26, 265.26, 264.62 (^{81}Br)	265.38	+ 2.61	128)

Table V.1 (continued)

Component A	Component B	ν/MHz (77 °K)	$\bar{\nu}$/MHz	$\Delta = \{\bar{\nu}(A) - \bar{\nu}(A_xB_y)\}$/MHz	Ref.
Chloranil 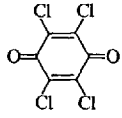	—	37.585 37.515 37.470 37.442 (^{35}Cl)	37.503		56)
Chloranil 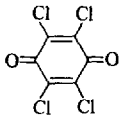	Hexamethylbenzene	37.716 37.504 (^{35}Cl)	37.610	- 0.107	56)
Chloranil 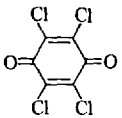	Mesithylene	37.646 37.639 37.387 (^{35}Cl)	37.557	- 0.054	103)

merous investigations of charge transfer complexes in solution are of considerable interest to the theory of chemical bonding. The experimental results are well understood within the frame of current theory [65,157].

The class of intermolecular compounds most suitable for NQR studies are the charge transfer complexes, where the individual molecules of the compound are highly symmetric and no monopole-monopole, monopole-dipole, or dipole-dipole interaction should mask the charge transfer effect on the NQR spectra. In Table V.1 such molecular complexs are listed with their NQR frequencies and the NQR frequencies of the individual compounds. Generally a small downward shift of the frequencies $\nu(^{35}Cl, ^{81,79}Br)$ is observed, caused by the formation of the complex. However, the differences $\Delta = |\bar{\nu}(A) - \bar{\nu}(A_xB_y)|$ are comparable to the line splittings in the pure compounds A. In the compound Br_2·paraxylene, an upward shift of 2.29 MHz is observed in comparison to pure Br_2. It seems that for these compounds no conclusions about charge transfer can be drawn from the NQR results. The supposition of Hooper [93] that the formation of the complex molecules in the lattice is not due to charge transfer but to van der Waals-type forces seems to be justified.

The chance of finding molecular complexes in the solid state seems quite high if one or both of the partner molecules already carry a permanent dipole moment in the gaseous state. A number of such molecular complexes was investigated by NQR. Table V.2 gives the NQR results on molecular compounds,

Table V.2 *Crystal field shifts $\Delta\nu$ for molecular compounds with dipolar components (CH_3Cl, ..)$|\Delta(^{35}Cl)| \lessapprox 0.7$ MHz for molecular compounds without nitrogen; $|\Delta(^{35}Cl)| \lessapprox 1.2$ MHz for nitrogen containing compounds*

Component A	Component B	$\nu(^{35}Cl)$ a) MHz	$\bar{\nu}$ MHz	$\Delta = \{\bar{\nu}(A) - \bar{\nu}(A_xB_y)\}$ MHz	Ref.
$CHCl_3$		38.308 38.254	38.281		9) 57) 156)
$CHCl_3$	$(CH_3)_2CO$	37.752 37.650 37.310	37.571	+0.710	103)
$CHCl_3$	$(C_2H_5)_2O$	37.896 37.896 37.627	37.806	+0.475	103)
$CHCl_3$	2 $(C_2H_5)_2O$	38.160 37.874 37.608 37.272	37.739	+0.542	103)
$CHCl_3$	3 $(C_2H_5)_2O$	38.169 37.946 37.274	37.796	+0.485	103)
2 $CHCl_3$	$(C_2H_5)_2O$	37.842 37.704 37.420 37.170	37.534	+0.747	103)
$CHCl_3$	Orthoxylene	37.842 37.814	37.828	+0.453	103)
$CHCl_3$	Mesitylene	37.938 37.938 37.578	37.818	+0.363	103)
$CHCl_3$	Methanol	38.290 37.968 37.804 37.507	37.892	+0.389	103)
Picrylchloride	–	39.367			35) 70)

a) $T = 77\ ^\circ K$.

Table V.2 (continued)

Component A	Component B	$\nu(^{35}Cl)$ a) / MHz	$\bar{\nu}$ / MHz	$\Delta = \{\bar{\nu}(A) - \bar{\nu}(A_xB_y)\}$ / MHz	Ref.
Picrylchloride	Naphtalene	39.932		- 0.565	70) 139)
Pentafluoro-chlorobenzene 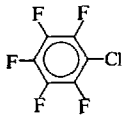	–	39.410			110)
Pentafluoro-chlorobenzene	Benzene	38.717		+ 0.693	110)
–	Chlorobenzene	34.622			14)
Pentafluoro-chlorobenzene	Chlorobenzene	39.36		+ 0.05 ($C_6F_5\underline{Cl}$)	110)
		34.68		- 0.06 ($C_6H_5\underline{\underline{Cl}}$)	110)
Pentafluoro-chlorobenzene	Toluene	39.16		+ 0.25	110)
Pentafluoro-chlorobenzene	Mesitylene	38.68		+ 0.73	110)
Pentafluoro-chlorobenzene	$(C_2H_5)_3N$	39.284		+ 0.126	110)
Pentafluoro-chlorobenzene	Aniline	38.64		+ 0.77	110)
1,3,5-Trichloro-2,4,6-trifluoro-benzene 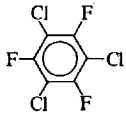	–	39.312			110)
1,3,5-Trichloro-2,4,6-trifluoro-benzene	Mesitylene	38.850		+ 0.462	110)

a) $T = 77\ ^\circ K$.

Table V.2 (continued)

Component A	Component B	$\nu(^{35}Cl)$ [a] / MHz	$\bar{\nu}$ / MHz	$\Delta = \bar{\nu}(A) - \bar{\nu}(A_xB_y)$ / MHz	Ref.
1,3,5-Trichloro-2,4,6-trifluoro-benzene	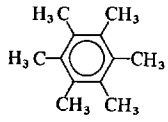	38.830		+ 0.482	110)
$CHCl_3$	Pyridine	37.761 37.678 37.242	37.764	+ 0.517	156)
$CHCl_3$	4-Pyroline Phase I	37.761 37.678 37.242	37.560	+ 0.721	156)
	Phase II	37.404 37.059 36.944	37.136	+ 1.145	
$CHCl_3$	3,5-Lutidine	37.296 37.273 36.983	37.184	+ 1.095	156)
$CHCl_3$	Piperidine Phase I	37.425 37.371 37.147	37.314	+ 0.967	156)
	Phase II	37.427 37.419 37.969	37.272	+ 1.009	
$CHCl_3$	Piperazine	37.509 37.349 37.315	37.391	+ 0.890	156)
$CHCl_3$	Triethylamine	37.166 37.131 37.003	37.100	+ 1.181	156)
$CHCl_3$	Triethylenediamine	37.955 37.853 37.666	37.824	+ 0.457	156)
$CHCl_3$	$(C_2H_5)_2HN$	37.447 37.156 36.908	37.170	+ 1.111	156)

[a] $T = 77\ ^{\circ}K$.

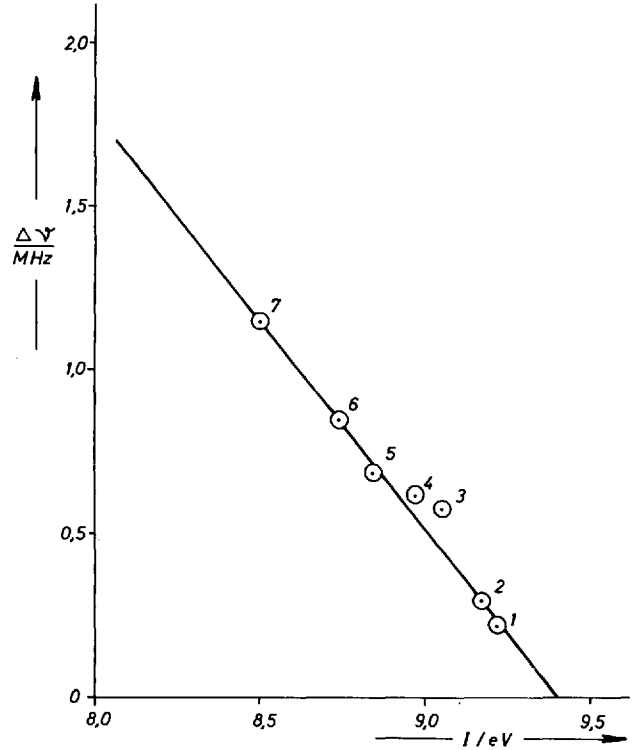

Fig. V.1. Frequency shift $\Delta = \nu(^{35}Cl)_A - \nu(^{35}Cl)_{A_xB_y}$ at 77 °K in charge transfer complexes as a function of the ionisation potential I. A = picrylchloride, $C_6H_2(NO_2)_3Cl$; $x = y = 1$. The number at the points measured note the substance B in the complex AB. (1) Benzene; (2) fluobenzene; (3) chlorobenzene; (4) bromobenzene; (5) toluene; (6) iodobenzene; (7) phenol

particularly those having chloroform as one component. From the results in Table V.2 it is seen that generally the formation of the molecular compound causes a downward shift of $\nu(^{35}Cl)$. These shifts are in the range $0.2\ MHz \leqslant \Delta \equiv |\nu(A) - \nu(A_xB_y)| \leqslant 1.1\ MHz$. Lucas and Guibé [156] have concluded from their results on molecular compounds $CHCl_3 \cdot X$ (X = nitrogen-containing molecule) that there is a charge transfer from the molecule X to the chloroform of the order of 0.02 electrons/molecule. This hypothesis is supported by the ^{35}Cl NQR results of Semin *et al.* [110] on $C_6F_5Cl \cdot C_6H_5Cl$. Certainly, any conclusion about a charge transfer taken from NQR results is only qualitative. The calculation of the amount of charge transfer from the NQR data is influenced by the crystal field effect, particularly by multipole interactions, as can be seen from a comparison of Tables V.1 and V.2.

An interesting discussion of charge transfer and NQR is given by Maksyutin *et al.* [144]. These authors investigated the ^{35}Cl NQR at 77 °K for 20 molecular compounds of picrylchloride with substituted aromatic molecules. Generally, an upward shift of $\nu(^{35}Cl)$ is found, which is between 0.1 and 1.1 MHz. The shift is explained by assuming charge transfer and geometrical factors. In Fig. V.1 the linear relationship between the shift $\Delta\nu$ and the donor ionization potential is shown. With polysubstituted benzenes, no such linear relationship was found.

1. NQR in Molecular Compounds and Intramolecular Rearrangement

In molecular compounds, where the individual components (or one of the components) have a fairly high ionic character of the bonds, the NQR frequency shifts due to the formation of molecular complexes are quite high. Numerous NQR investigations have been published, particularly on ^{35}Cl NQR and $^{123,121}Sb$ NQR. The favoured class of such compounds is the group of complexes of $SbCl_3$, $SbBr_3$, and $AsCl_3$ with aromatic molecules. Table V.3 lists a selected number of compounds of group-V halides with aromatic molecules together with $\nu(^{35}Cl)$, $\nu(^{79}Br)$, $\nu(^{121}Sb)$ and $\nu(^{123}Sb)$. More information on molecular compounds of this type is found in [139]. The molecular compounds with $SbCl_3$ and $SbBr_3$ show statistical scattering of Cl, Br, and Sb NQR frequencies where the NQR powder data are concerned. The single crystal investigations of Okuda *et al.* [134,158] are, however, very promising for further investigations of complexes of the Mentschukin type. Crystal structure determinations on Mentschukin-complexes have been done recently by Hulme *et al.* [163-165].

The determination of the asymmetry parameters and the direction cosines, together with x-ray investigations of the crystal structure, will shed some light on the crystal field effect in solids. NQR powder spectra can only permit very rough and qualitative conclusions on the intermolecular forces. The results on the Mentschukin complexes with $AsCl_3$ show that the metal-chlorine bond is virtually unaffected by the formation of molecular compounds. From single-crystal NQR spectroscopy, particularly on the As nucleus, some geometrical information about the molecular compounds can be expected.

The answers concerning the interaction between the molecules in molecular compounds become more certain with increasing ionic character of the compounds. This is qualitatively seen from the complexes with $SnCl_4$, $POCl_3$, and $HgCl_2$ (see Table V.3). Increase of ionic character produces a more effective antishielding factor of the valence shell and therefore a stronger influence of multipole fields on the electric field gradient at the site of the nucleus. The results of NQR spectroscopy in the molecular compounds of $POCl_3$ with $SnCl_4$ and of $HgCl_2$ with dioxane are in agreement with the known crystal structure

Table V.3 *Crystal field effect in molecular compounds of the Mentschutkin-type ($SbCl_3 \cdot X$), ($AsCl_3 \cdot X$), ($SbBr_3 \cdot X$) and of some molecular compounds with $SnCl_4$, $POCl_3$ and $HgCl_2$*

Substance	$\nu(^{35}Cl)$ (77 °K) MHz	^{121}Sb		^{123}Sb		Ref.
		$\nu(\pm 1/2 \rightleftarrows \pm 3/2)$	$\nu(\pm 3/2 \rightleftarrows \pm 5/2)$	$\nu(\pm 1/2 \rightleftarrows \pm 3/2)$	$\nu(\pm 3/2 \rightleftarrows \pm 5/2)$	
$SbCl_3$	20.9077	59.709 (83 °K)	114.300	39.094		27)
	19.3047					139)
	19.3047					
$2\,SbCl_3 \cdot C_6H_6$	20.509	59.774 (133 °K)	117.595	38.566		88)
	20.459	59.602	116.239	37.177		134)
	20.349					91)
	20.068					115)
	18.749					116)
	18.655					
$2\,SbCl_3 \cdot C_{10}H_8$	20.810	59.462	118.903	36.100	72.151	88)
	19.893					127)
	19.187					115) 116)
$2\,SbCl_3 \cdot C_6H_5C_6H_5$	20.671	58.384		36.358		88)
	20.378	55.598		36.253		115)
	19.667					116)
	19.229					127)
	19.160					
	18.873					
$SbCl_3 \cdot 1,4\text{-}(CH_3)_2C_6H_4$	20.956					
	20.402					115)
	18.500					
$2\,SbCl_3 \cdot 1,4\text{-}(CH_3)_2C_6H_4$	20.631	58.268	111.867	37.990		88)
	19.609					115)
	18.631					116) 127)

Substance	$\nu(^{81}Br)$ (77 °K) MHz	^{121}Sb $\nu(\pm 1/2 \rightleftarrows \pm 3/2)$	^{121}Sb $\nu(\pm 3/2 \rightleftarrows \pm 5/2)$	^{123}Sb $\nu(\pm 1/2 \rightleftarrows \pm 3/2)$	^{123}Sb $\nu(\pm 3/2 \rightleftarrows \pm 5/2)$	Ref.
$SbBr_3$	143.324	50.273	99.215	31.186	60.107	47)
Phase I	137.630					27)
	137.403					14)
	142.622	49.061 (304 °K)	94.160 (304 °K)	31.990 (304 °K)	56.544 (304 °K)	158)
Phase II	141.923					119)
	135.499					
$2SbBr_3 \cdot C_6H_6$	142.794	50.717		33.568		158)
	142.177					91)
	133.533					115)
$2SbBr_3 \cdot C_{10}H_8$	146.832	50.301		30.654		83)
	139.480					92)
	137.376					
						117)
$2SbBr_3 \cdot C_6H_5C_6H_5$	164.762 (^{79}Br)	47.207		28.717		83) 92) 115) 119)
$2SbBr_3 \cdot 1,4\text{-}(CH_3)_2C_6H_4$	149.648	49.963		33.238		83)
	145.682	48.798		30.493		92)
	136.310					116)
	132.821					
	132.510					
	128.428					

Table V.3 (continued)

Substance	$\nu(^{35}Cl)$ (77 °K) / MHz	$\bar{\nu}$ / MHz	$\Delta = (\bar{\nu}(A) - \bar{\nu}(A_xB_y))$ / MHz	Ref.
$AsCl_3$	25.406			14)
	25.058	25.141	–	
	24.960			127)
$2AsCl_3 \cdot C_6H_6$	25.634			
	25.560			
	25.406	25.167	- 0.026	127)
	25.261			
	24.765			
	24.378			
$2AsCl_3 \cdot C_{10}H_8$	25.805			
	25.350	25.292	- 0.151	127)
	24.720			
$2AsCl_3 \cdot (C_6H_5)_2CH_2$	25.388			
	24.858	24.982	+ 0.159	127)
	24.701			
$2AsCl_3 \cdot 1,4\text{-}(CH_3)_2C_6H_4$	25.535			
	25.169	24.915	+ 0.226	127)
	24.040			
$2AsCl_3 \cdot C_6H_5C_2H_5$	25.321			
	25.238			
	25.174	25.041	+ 0.020	127)
	25.135			
	25.059			
	24.309			

Table V.3 (continued)

Substance	$\frac{\nu(^{35}Cl)}{MHz}$ (77 °K)	$\frac{\bar{\nu}}{MHz}$	$\Delta=(\frac{\bar{\nu}(A)-\bar{\nu}(A_xB_y)}{MHz})$	Ref.
$SnCl_4$	24.294 24.226 24.140 23.719	24.095		14)
$POCl_3$	28.984 28.938	28.961		14)
$2POCl_3 \cdot SnCl_4$	30.213 30.117	30.165	- 1.204	
	21.146 19.807 19.035	19.996	+ 4.099	88)
$POCl_3 \cdot AsCl_3$	29.208 29.168 29.154	29.177	- 0.216	88)
	25.481 25.125 24.799	25.135	+ 0.006	
$SnCl_4 \cdot 2(C_2H_5)_2O$	19.473 19.435	19.459	+ 4.636	88)
$HgCl_2$	22.873 22.521	22.697		18) 88) 29)
$HgCl_2 \cdot$ Dioxane	21.196	21.196	+ 1.501	88) 166)

Table V.4 *Crystal field shift of $\nu(^{81}Br)$ in molecular compounds $AlBr_3 \cdot X$. The mean shift referred to $AlBr_3$ is $\Delta(^{81}Br) \lessapprox 9.5$ MHz*

Substance	$\frac{\nu(^{79}Br)}{MHz}$(77 °K)	$\frac{\nu(^{81}Br)}{MHz}$ (77 °K)	$\frac{\bar{\nu}}{MHz}$ (^{81}Br)	$\frac{\Delta\nu}{MHz} = \left\{\frac{\bar{\nu}(A) - \bar{\nu}(A_xB_y)}{MHz}\right\}$	Ref.
Al_2Br_6	115.450	96.426	91.099		
	113.790	95.055			
	97.945	81.815			
$AlBr_3 \cdot (C_2H_5)_2O$	101.016	84.44			
	100.512	84.00	83.49	+ 7.61	133)
	98.192	82.04			
$AlBr_3 \cdot (C_2H_5)O(C_6H_5)$	106.688	89.160			
	103.972	86.858	85.734	+ 5.365	133)
	97.257	81.185			
$AlBr_3 \cdot (C_6H_5)_2O$	105.948	88.570			
	103.72	86.932	86.335	+ 4.764	133)
	99.92	83.504			
$AlBr_3 \cdot (CH_3)_2S$	99.376	83.025	81.553	+ 9.546	133)
	95.920	80.080			
$AlBr_3 \cdot C_5H_5N$	99.484	83.16			
	98.401	82.18	82.22	+ 8.88	133)
	97.318	81.313			

of these compounds. Also the strong increase of $\nu(^{35}Cl)$ of $POCl_3$ and the decrease of $\nu(^{35}Cl)$ of $SnCl_4$ in $SnCl_4 \cdot 2POCl_3$ is in qualitative accordance with the rearrangement of the tetrahedral configuration of $SnCl_4$ in pure $SnCl_4$ and with an octahedral coordination of Sn in $SnCl_4 \cdot 2POCl_3$. For other molecular complexes $SnCl_4 \cdot X$, see [131].

Similar decreases of $\nu(^{79,81}Br)$ are found in molecular compounds of $AlBr_3 \cdot X$ [133]. In these compounds the ionic character is increased by the breakdown of the bridge structure

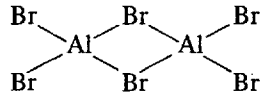

to the tetrahedral structure $AlBr_3 \cdot X$. Single-crystal Zeeman NQR spectra would be particularly valuable for compounds of this type. Table V.4 shows the strong influence of the rearrangement on the NQR spectra.

For a large number of molecular compounds of trichloric acetic acid (TCA) with aldehydes, ketones, acids, esters, alcohols, phenols and ethers, Biedenkapp and Weiss [112] have measured the ^{35}Cl NQR frequencies at 77 °K. In Table V.5 a selection of these measurements is given. A slight overall shift of $\nu(^{35}Cl)$ is caused by the formation of the complex molecule $CCl_3COOH \cdot X$. Fig. V.2 is a histogram showing the spread of $\nu(^{35}Cl)$ for the CCl_3 group in $CCl_3COOH \cdot X$ and derivatives of the $CH_{3-y}Cl_y$ group in derivatives of chloro-acetanilides, $Cl_xC_6H_{5-x}NHCOCH_{3-y}Cl_y$ [162]. All distributions of the frequencies around the respective average frequency, $\overline{\nu}$, of each group have been added up in Fig. V.2 to show the overall distribution of $\omega - Cl$ NQR frequencies in the molecular compounds with TCA and in the chloro-acetanilides. Of the total number of 212 values, 33 (= 15,5 %) are beyond the ± 500 kHz mark and 13 (= 6 %) are beyond the ± 600 kHz mark. From these investigations (and other ^{35}Cl NQR measurements in chloroacetanilides) the crystal field effect was estimated to be about ± (500 – 600) kHz. Here, too, single crystal NQR and x-ray investigations will be very useful in exploring the crystal field effect more specifically. In particular, the fact that in all of the compounds $CCl_3COOH \cdot X$ and $CCl_3CO–R$ the three Cl atoms are crystallographically inequivalent needs further experimental work.

One point seems to be quite important in discussing NQR results on molecular compounds with regard to intermolecular interactions, like charge transfer etc. The modes of thermal vibrations of the individual molecules may be influenced considerably by intermolecular interactions. This is equivalent to assuming that the Debye temperature is changed by the change in the geometrical arrangement of the molecules within the lattice and by specific intermolecular interactions. Therefore, to take 77 °K as the reduced temperature seems to

Table V.5 *Crystal field effect in molecular compounds of trichloroacetic acid with ethers, aldehydes etc. and of some salts of the trichloroacetic acid.* $|\Delta(^{35}Cl)| \leqslant 0.7$ *MHz in the compounds TCA·X;* $|\Delta(^{35}Cl)| \leqslant 1.6$ *MHz in the salts*

Substance	$\nu(^{35}Cl)$ MHz [a]	$\bar{\nu}$ MHz	Δ MHz $= \{\bar{\nu}(TCA) - \bar{\nu}(TCA \cdot X)\}$ MHz
Cl_3CCOOH (≡TCA)	40.240 40.165 39.967	40.12	
TCA · benzaldehyde	40.357 39.599 39.438	39.80	+ 0.32
TCA · H_3CO–C$_6$H$_3$–CHO	39.793 39.766 39.766	39.78	+ 0.34
TCA · HO–C$_6$H$_3$(–CHO)–H_3CO	40.230 40.122 40.098 39.781 39.353	39.92	+ 0.20
TCA · phenol	40.413 39.818 39.770	40.00	+ 0.12
TCA · 4-methylphenol	40.236 40.176 39.687	40.03	+ 0.09
TCA · 4-chlorophenol	40.620 40.370 40.102 40.015 39.709 39.533	40.06	+ 0.06
	34.903 34.874	34.89	− 0.07 ($\bar{\nu}(^{35}Cl)$ in Parachlorophenol : 34.82 MHz)
TCA · 2,4-chlorophenol	40.357 40.063 39.930	40.12	0
	36.006 35.458	35.72	− 0.35 ($\bar{\nu}(^{35}Cl)$ in 2,4-dichlorophenol : 35.373 MHz (T = 77 °K))

[a] T = 77 °K.

Table V.5 (continued)

Substance	$\frac{\nu(^{35}Cl)}{MHz}$ [a]	$\frac{\bar{\nu}}{MHz}$	$\frac{\Delta}{MHz}=\left\{\frac{\bar{\nu}(TCA)-\bar{\nu}(TCA\cdot X)}{MHz}\right\}$
$TCA\cdot(CH_3)_2CO$	40.085 39.983 39.776 39.644 39.610 39.565	39.78	+ 0.34
$TCA\cdot C_6H_5COCH_3$	40.148 39.729 39.373	39.75	+ 0.37
$TCA\cdot C_6H_5-CH_2-O-CH_2-C_6H_5$	39.855 39.715 39.702 39.462 39.380 39.348	39.58	+ 0.54
$TCA\cdot C_6H_5-COOH$	40.488 40.274 40.214 39.716 39.645 39.268	39.93	+ 0.19
$TCA\cdot CH_3COOC_2H_5$	40.227 39.911 39.789 39.744 39.710 39.640	39.83	+ 0.29
CCl_3COONa	39.443 38.892 38.329	38.89	+ 1.23
$(CCl_3COO)_2Co\cdot 4H_2O$	40.071 39.862 39.489 39.404 38.476 38.197	39.25	+ 0.87

[a] $T = 77\ ^{\circ}K$.

Table V.5 (continued)

Substance	$\frac{\nu(^{35}Cl)}{MHz}$ a)	$\frac{\bar{\nu}}{MHz}$	$\frac{\Delta}{MHz} = \frac{\bar{\nu}(TCA) - \bar{\nu}(TCA \cdot X)}{MHz}$
$(CCl_3COO)_2Co \cdot 4$ pyridine	38.817		
	38.400	38.50	+ 1.62
	38.275		
$(CCl_3COO)_2HK$	39.747		
	39.147	39.34	+ 0.78
	39.113		
$(CCl_3COO)_2HRb$	40.187		
	39.226	39.51	+ 0.61
	39.121		

a) $T = 77\ ^\circ K$.

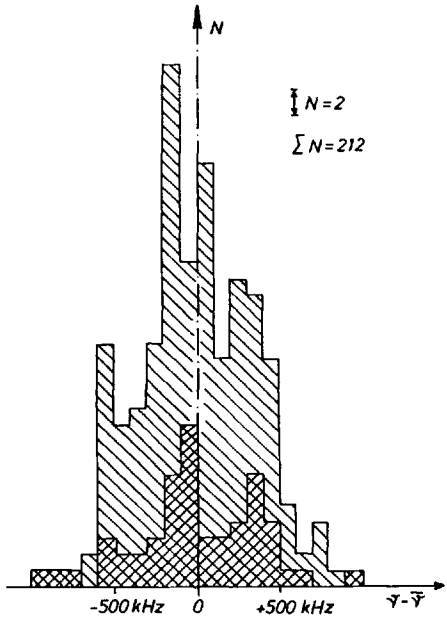

Fig. V.2. Histogram showing the distribution of the ω-^{35}Cl-NQR frequencies, ν, around the average frequency, $\bar{\nu}$, of all chloroacetyl groups a) in chloroacetanilides, $Cl_xC_6H_{5-x}$ $NHCOCH_{3-y}Cl_y$ (lower distribution: ▨), b) in chloroacetanilides, $Cl_xC_6H_{5-x}NHCOCH_{3-y}Cl_y$, and in trichloroacetic acid (TCA) derivatives from Ref. [112] (overall distribution: ▧)
$\Delta\nu$ is choosen as 100 kHz

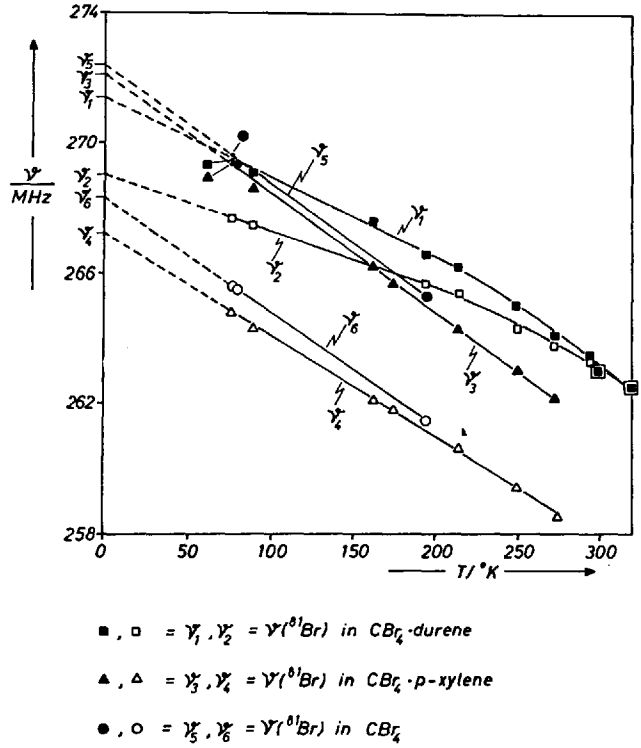

Fig. V.3. Temperature dependence of $\nu(^{81}\mathrm{Br})$ in the molecular compounds CBr_4·durene, CBr_4·paraxylene, and in CBr_4

be a somewhat doubtful procedure. The investigation of Gilson and O'Konski [128] on compounds $CBr_4 \cdot X$ shows quite clearly the necessity to extrapolate, or better, to measure down to 4 °K, before discussing the charge transfer effect on NQR. In Fig. V.3 the temperature dependence of $\nu(^{81}\mathrm{Br})$ in CBr_4 is shown together with the temperature dependence of $\nu(^{81}\mathrm{Br})$ in molecular compounds $CBr_4 \cdot X$. An extrapolation of $\nu = f(T)$ to $T = 0$ °K results in a splitting of the ^{81}Br NQR spectra into two groups of NQR lines. No significant influence of the molecule X in $CBr_4 \cdot X$ on the NQR spectrum of ^{81}Br can be found at 0 °K.

VI. Study of the Crystal Field Effect by Continuous Variation of Crystal Field Parameters

At first sight, experiments in which the influence of external parameters on the NQR spectrum is continuously varied seem very promising in elucidating the character of the crystal field effect.

Such variable parameters are:

1. temperature;
2. pressure;
3. external electric fields;
4. intermolecular forces created by point defects or dislocations within the crystal to change continuously the matrix around the molecule considered. A much larger variation of the matrix may be effected by preparing mixed crystals.

1. The Pressure Dependence of NQR Spectra

In chapter IV we have discussed the influence of temperature on NQR spectra. As already shown by Kushida *et al.* [32], the investigation of the pressure dependence of NQR spectra is a necessary completion of such work. A combination of measurements $\nu(\mathrm{NQR}) = f(T, p)$ reveals the quadrupole interaction at constant volume. Unfortunately, very little work has been done in this field. In ionic crystals, for example, $NaBrO_3$, Gutowsky *et al.* [36,53], investigated the pressure dependence of $\nu(^{23}\mathrm{Na})$. The experimental and theoretical work in this field up to 1962 is summarized by Benedek [79]. In molecular crystals, studies of $\nu(\mathrm{NQR}) = f(p)$ have been carried out by Fuke [68,82]. An extensive investigation of $\nu(^{14}\mathrm{N}) = f(T,p)$ in hexamethylenetetramine was done by Matzkamin *et al.* [118]. The main effect of pressure on NQR is the increase of $\nu(\mathrm{NQR})$ with increasing pressure. We expect such pressure behaviour of $\nu(\mathrm{NQR})$ in a first approximation. With increasing pressure, the overall Debye temperature of the lattice increases and therefore the lattice may become more rigid. The decrease of the intermolecular distances with increasing pressure may act in two ways, as Bersohn pointed out for 1,3,5-trichlorobenzene and CH_3Cl [76].

2. The Influence of an External Electric Field on NQR Spectra

The application of an external electric field to the crystal during the NQR experiment is very important. Such experiments have been done by Bloembergen *et al.* [62,63], and by Kushida and Saiki [71]. The subject is treated extensively by Bloembergen [80] an by Dixon [90,102]. The external electric fields usable in such experiments are limited by the electric breakdown in the substance. Electric fields of the order of $(10^4 - 10^5)$ V/cm are the upper limit for most solids. On the other hand, the internal electric fields are of the order of 10^9 V/cm (the electric field of a point charge e at a distance of one Å). In molecular crystals, Bloembergen and Dixon [64,90] studied the electric field induced frequency shifts. The overall crystal field splitting of $\nu(^{35}\mathrm{Cl})$ in 1,3,5-trichloro-

benzene ($\Delta\nu \approx 500$ kHz) is in agreement with the effect of the external field on $\nu(^{35}Cl)$ in this substance [76]. The experimental difficulties and the small usable external electric fields have inhibited extensive work in this field.

Table VI.1 *The influence of external electric fields on ^{35}Cl-NQR frequencies. $\Delta\nu$ = frequency shift*

Substance	$\frac{\Delta\nu(^{35}Cl)\cdot Volt}{kHz\cdot cm}$
1,4-Dichlorobenzene	$\sim 0.590\cdot 10^{-4}$
1,3,5-Trichlorobenzene	$\sim 1.0\cdot 10^{-4}$
CH_3Cl	$0.035\cdot 10^{-4}$

3. NQR and Matrix Effects

Usually pure compounds are used in NQR spectroscopy. The matrix around a molecule is composed of molecules of the same kind. It appears quite interesting to change the matrix by incorporating the molecule studied into a matrix which can be varied. The crystal field effect can thereby be changed in a continuous way. An experimental method is to measure the NQR spectrum of a molecule B in mixed crystals A_xB_{1-x} in the range $0 \leqslant x < 1$. A wide range of miscibility is desirable. For small concentrations x, we can consider the molecules of type A as point defects in the lattice of B. Since these point defects are statistically distributed within the lattice, the crystal field effect at the sites of the molecules B will vary in a random way if the intermolecular interaction between A and B is different from the interaction between B and B. A statistical distribution of NQR frequencies follows and only at very small concentrations of point defects the NQR lines will be observable. The effect of impurities on the NQR spectrum is:

a) an increase in the line width, and
b) a shift of the line center.

Imaeda [59] investigated the chlorine and the bromine NQR in alkali chlorates and alkali bromates at 0 °C as a function of impurity concentration. Bromates, chlorates, and nitrates served as impurities. The results of Imaeda's investigation are given in Table VI.2. There is a considerable frequency shift, which is mostly negative (decrease in frequency) if the impurity ions are larger in size than the host ions. In cases where the impurity is smaller than the host ion, the frequency increases. Imaeda assumes that the distortion of the electronic wave functions about the impurities is responsible for the frequency shift. Temperature effects are ruled out since the impurity shift in the bromates

Table VI.2 *Impurity shifts of $\nu(^{35}Cl)$ and $\nu(Br)$ in chlorates and bromates (The isotope of Br is not stated in Ref.* [59])

Host material	Impurity	Impurity content (mole %)	Frequency shift $\Delta\bar{\nu}$ / Hz	Half width Δb / Hz
$KClO_3$	$NaClO_3$	0.9 ± 0.1	+ 1100 ± 200	2280 ± 200
$KClO_3$	$AgClO_3$	0.97 ± 0.05	+ 630 ± 30	1450 ± 100
$KClO_3$	$LiClO_3$		0 ± 50	1100 ± 100
$KClO_3$	$Ba(ClO_3)_2$	0.13 ± 0.03	0 ± 40	1350 ± 100
$KClO_3$	$Ni(ClO_3)_2$	0.16 ± 0.03	0 ± 30	1100 ± 100
$KClO_3$	KNO_3	0.44 ± 0.03	+ 135 ± 45	1600 ± 150
$KClO_3$	$KBrO_3$	0.39 ± 0.03	− 250 ± 45	1880 ± 100
$NaClO_3$	$KClO_3$	7.2 ± 0.1	− 760 ± 30	1800 ± 100
$NaClO_3$	$AgClO_3$	1.3 ± 0.15	− 1320 ± 40	2100 ± 100
$NaClO_3$	$NaBrO_3$	0.48 ± 0.03	− 1015 ± 70	2100 ± 100
$NaClO_3$	$NaNO_3$	2.23 ± 0.03	+ 90 ± 30	1650 ± 100
$KBrO_3$	$NaBrO_3$		0 ± 500	10000 ± 500
$KBrO_3$	$KClO_3$		+ 3000 ± 300	9700 ± 500
$NaBrO_3$	$KBrO_3$		− 2700 ± 300	13000 ± 500
$NaBrO_3$	$NaClO_3$		+ 3300 ± 150	8300 ± 500
$NaBrO_3$	$NaJO_3$		− 2000 ± 200	7000 ± 500
$NaBrO_3$	$LiBrO_3$		0 ± 200	8000 ± 500

was found to be independent of temperature. This second statement of Imaeda seems somewhat questionable. In the cases investigated, the larger-size impurities are also the heavier ones, and the increases in mass should result in a decrease of the Debye temperature. Therefore the NQR frequency should decrease at constant temperature. The temperature coefficient $\bar{\alpha} = \frac{1}{\bar{\nu}} \cdot \frac{\Delta\nu}{\Delta T}$ seems to be influenced by such effects only in second order.

Investigations of the influence of lattice defects on NMR and the accompanying nuclear quadrupole effects have been studied in many papers (see references [125,161]).

An extensive study of the line width of $\nu(^{35}Cl)$ in paradichlorobenzene containing various impurities was done by Kojima *et al.* [25]. The results are interpreted as an effect of the volume difference $V_A - V_B$ and of the stresses and strains induced by the impurities. No overall frequency shift was reported by these authors.

Very remarkable frequency shifts of $\nu(^{35}Cl)$ in paradichlorobenzene, dissolved in a small amount (3.5 Mole %) in various host lattices have been observed by Baer and Dean [49]. The results of the investigation are shown in Table VI.3a. Within the matrix *p*-xylene Baer and Dean observed the dependence of $\nu(^{35}Cl)$

Table VI.3a *NQR-frequency shift of $\nu(^{35}Cl)$ in paradichlorobenzene dissolved in different host lattices*

Host material	$\frac{\Delta\nu(^{35}Cl)}{kHz}$ ($T = 0\ ^\circ C$)	$\frac{\Delta\nu(^{35}Cl)}{kHz}$ ($T = -78\ ^\circ C$)
Quinone	−35 ± 12	−20 ± 5
Paradibromobenzene	+11 ± 4	+14 ± 5
Phenylenediamine	−26 ± 5	−23 ± 5
Terephthalic acid	+15 ± 10	−12 ± 5
Terephthalonitrile	0 ± 5	−13 ± 7
Hydroquinone[a)]	–	+ 5 ± 5

[a)] Probably intermolecular compounds are formed in the system hydroquinone-paradichlorobenzene. No frequency shift, within the limit of errors was observed for the following host materials: dimethoxybenzene, paradinitrobenzene, dimethylterephthalate, diethoxybenzene.

Table VI.3b *NQR frequency shift of $\nu(^{35}Cl)$ ($T = -78\ ^\circ C$) in paradichlorobenzene dissolved in para-xylene as a function of concentration*

Concentration of paradichlorobenzene in Mole %	$\frac{\Delta\nu(^{35}Cl)}{kHz}$
13.4	−95 ± 25
37.5	−55 ± 15
47.5 − 90.9	0 ± 15[a)]
98.7	+440 ± 15

[a)] Not observable by the large line width.

(para-dichlorobenzene) upon concentration. A considerable frequency shift was found (Table VI.3b). An interesting example of the matrix effect is the study of $\nu(^{14}N)$ in β-quinol chlathrates by Meyer and Scott [52)]. An extensive study of the temperature dependence of ν(NQR) of "dissolved" molecules would be very interesting for the discussion of the crystal field effect.

VII. Conclusions

A quantitative investigation of the crystal field effect is quite difficult. From the large number of NQR measurements available, the following qualitative conclusions can be drawn.

a) The crystal field effect is of the order of $\Delta\nu$ (^{35}Cl) = ± 500 kHz in Cl atoms bound to carbon.
b) With increasing ionic character of a bond Cl–X, the crystal field effects become more pronounced, because the multipole moments of the molecules in the lattice and the quadrupole polarizability of the core electrons of the ^{35}Cl nucleus increase. This second point is equivalent to an increasing antishielding factor γ_∞ for Cl.
c) Quantitative calculations of the charge transfer in molecular compounds or of the ionic character induced within a molecule through the formation of the complex are only possible if the crystal structure is known and single-crystal NQR data (including η) are available. From NQR powder data, only qualitative conclusions can be drawn.
d) The temperature dependence of NQR frequencies should be investigated carefully to correct for the crystal field effect as accurately as possible.
e) For other nuclei besides ^{35}Cl, and ^{79,81}Br, such as ^{127}I, ^{14}N, . . . , more experimental evidence is needed to clarify the connection between NQR and the specific interactions between molecules in the solid state and in molecular addition compounds.

Valuable discussions with Mr. Wolfgang Pies are gratefully acknowledged.

References

1) Hammett, L.: Physical Organic Chemistry. New York: McGraw-Hill 1943.
2) Townes, C. H., Dailey, B. P.: J. Chem. Phys. *17*, 782 (1949).
3) Dehmelt, H. G., Krüger, H.: Naturwissenschaften *37*, 111 (1950).
4) Sternheimer, R. M.: Phys. Rev. *80*, 102 (1950).
5) Bayer, H.: Z. Phys. *130*, 227 (1951).
6) Dehmelt, H. G., Krüger, H.: Z. Phys. *129*, 401 (1951).
7) – Z. Phys. *130*, 480 (1951).
8) Livingston, R.: J. Chem. Phys. *19*, 1434 (1951).
9) – Phys. Rev. *82*, 289 (1951).
10) Sternheimer, R. M.: Phys. Rev. *84*, 244 (1951).
11) Meal, H. C.: J. Am. Chem. Soc. *74*, 6121 (1952).
12) Sternheimer, R. M.: Phys. Rev. *86*, 316 (1952).
13) Dehmelt, H. G.: J. Chem. Phys. *21*, 380 (1953).
14) Livingston, R.: J. Phys. Chem. *57*, 496 (1953).
15) Sternheimer, R. M., Foley, H. M.: Phys. Rev. *92*, 1460 (1953).
16) Zeldes, H., Livingston, R.: J. Chem. Phys. *21*, 1418 (1953).
17) Bray, P. J., Barnes, R. G.: J. Chem. Phys. *22*, 2023 (1954).
18) Dehmelt, H. G., Robinson, H. G., Gordy, W.: Phys. Rev. *93*, 480 (1954).
19) Hatton, J., Rollin, R. V.: Trans. Faraday Soc. *50*, 358 (1954).
20) Kojima, S., Isukada, K., Shimauchi, A., Hinaga, Y.: J. Phys. Soc. Japan *9*, 795 (1954).
21) Monfils, A., Duchesne, J.: J. Chem. Phys. *22*, 1275 (1954).

22) Sternheimer, R. M., Foley, H. M.: Phys. Rev. *95*, 736 (1954).
23) Schawlow, A. W.: J. Chem. Phys. *22*, 1211 (1954).
24) Dailey, B. P., Townes, C. H.: J. Chem. Phys. *23*, 118 (1955).
25) Kojima, S., Ogawa, S., Minematsu, M., Tanaka, M.: J. Phys. Soc. Japan *13*, 446 (1958).
26) Kushida, T.: J. Sci. Hiroshima Univ., Ser. A, *19*, 327 (1955).
27) Wang, T. C.: Phys. Rev. *99*, 566 (1955).
28) Bray, P. J., Barnes, R. G., Bersohn, R.: J. Chem. Phys. *25*, 813 (1956).
29) Dautreppe, D., Dreyfus, B.: C. R. Acad. Sci. Paris *242*, 766 (1956).
30) Dodgen, H. W., Ragle, J. L.: J. Chem. Phys. *25*, 376 (1956).
31) Hamlen, R. P., Koski, W. S.: J. Chem. Phys. *25*, 360 (1956).
32) Kushida, T., Benedek, G. B., Bloembergen, N.: Phys. Rev. *104*, 1364 (1956).
33) Ludwig, G. W.: J. Chem. Phys. *25*, 159 (1956).
34) Sternheimer, R. M., Foley, H. M.: Phys. Rev. *102*, 731 (1956).
35) Bray, P. J., Barnes, R. G.: J. Chem. Phys. *27*, 551 (1957).
36) Gutowsky, H. S., Williams, G. A.: Phys. Rev. *105*, 464 (1957).
37) Kojima, S., Abe, Y., Minematsu, M., Tsukada, K., Shimauchi, H.: J. Phys. Soc. Japan *12*, 1225 (1957).
38) Livingston, R., Zeldes, H.: J. Chem. Phys. *26*, 351 (1957).
39) Orville-Thomas, W. J.: Quart. Rev. *11*, 62 (1957).
40) Reif, F., Cohen, M. H.: Solid State Phys. *5*, 322 (1957).
41) Sternheimer, R. M.: Phys. Rev. *105*, 158 (1957).
42) Shimomura, K.: J. Phys. Soc. Japan *12*, 652 (1957).
43) Barnes, R. G., Engardt, D.: J. Chem. Phys. *29*, 248 (1958).
44) Bersohn, R.: J. Chem. Phys. *29*, 326 (1958).
45) Das, T. P., Hahn, E. L.: Solid State Phys., Suppl. *1* (1958).
46) De Wette, F. W., Nijboer, B. R. A.: Physica *24*, 1105 (1958).
47) Ogawa, S. J.: J. Phys. Soc. Japan *13*, 618 (1958).
48) Alderdice, D. S., Brown, J. C., Iredale, T.: J. Chem. Phys. *30*, 344 (1959).
49) Baer, R., Dean, C.: J. Chem. Phys. *31*, 1690 (1959).
50) Burns, G.: Phys. Rev. *115*, 357 (1959).
51) De Wette, F. W.: Physica *25*, 1125 (1959).
52) Meyer, H., Scott, T. A.: J. Phys. Chem. Solids *11*, 215 (1959).
53) Bernheim, R. A., Gutowsky, H. S.: J. Chem. Phys. *32*, 1072 (1960).
54) Brown, R. J. C.: J. Chem. Phys. *32*, 116 (1960).
55) Burns, G.: J. Chem. Phys. *32*, 1585 (1960).
56) Douglas, D.: J. Chem. Phys. *32*, 1882 (1960).
57) Gutowsky, H. S., McCall, D. W.: J. Chem. Phys. *32*, 548 (1960).
58) Hooper, H. O., Bray, P. J.: J. Chem. Phys. *33*, 334 (1960).
59) Imaeda, Y.: J. Phys. Soc. Japan *15*, 1699 (1960).
60) Low, W.: Solid State Phys., Suppl. *2* (1960).
61) Nakamura, D., Kurita, Y., Ito, K., Kubo, M.: J. Am. Chem. Soc. *82*, 5783 (1960).
62) Armstrong, J., Bloembergen, N., Gill, D.: Phys. Rev. Letters *7*, 11 (1961).
63) Bloembergen, N.: Science *133*, 1363 (1961).
64) Bloembergen, N.: J. Chem. Phys. *35*, 1131 (1961).
65) Briegleb, G.: Elektronen-Donator-Acceptor-Komplexe. Berlin-Heidelberg-New York: Springer 1961.
66) Burns, G., Wikner, E. G.: Phys. Rev. *121*, 155 (1961).
67) De Wette, F. W.: Phys. Rev. *123*, 103 (1961).
68) Fuke, T.: J. Phys. Soc. Japan *16*, 266 (1961).
69) Gretschischkin, V. S., Svetlov, Y. G., Soifer, G. B.: Fiz. Tverd. Tela *3*, 2390 (1961).
70) Kitaigorodskii, A. I., Fedin, E. I.: Zh. Strukt. Khim. *2*, 216 (1961).

71) Kushida, T., Saiki, K.: Phys. Rev. Letters *7*, 9 (1961).
72) Morino, Y., Togana, M.: J. Chem. Phys. *35*, 1289 (1961).
73) Reddoch, A. H.: J. Chem. Phys. *35*, 1085 (1961).
74) Semin, G. K.: Zh. Strukt. Khim. *2*, 370 (1961).
75) Barnes, R. G., Segel, S. L., Jones, W. H.: J. Appl. Phys. *33*, Suppl. 1, 296 (1962).
76) Bersohn, R.: J. Appl. Phys. *33*, Suppl. 1, 286 (1962).
77) Dalgarno, A.: Advan. Phys. *11*, 281 (1962).
78) Semin, G. K.: Zh. Strukt. Khim. *3*, 292 (1962).
79) Benedek, G. B.: Nuclear magnetic resonance at high pressure. New York: J. Wiley & Sons 1963.
80) Bloembergen, N.: Proc. XIth, Colloque Ampère, p. 39. Amsterdam: North Holland Publ. Comp. 1963.
81) Brun, E., Hafner, S.: Z. Krist. *117*, 37, 63 (1963).
82) Fuke, T.: J. Phys. Soc. Japan *18*, 1154 (1963).
83) Gretschischkin, V. S., Kyuntsel, I. A.: Opt. i Spektoskopiya *15*, 832 (1963).
84) Nakamura, D., Ito, K., Kubo, M.: Inorg. Chem. *2*, 61 (1963).
85) Sternheimer, R. M.: Phys. Rev. *130*, 1423 (1963).
86) Sternheimer, R. M.: Phys. Rev. *132*, 637 (1963).
87) Watson, R. E., Freeman, A. J.: Phys. Rev. *131*, 250 (1963).
88) Biedenkapp, D., Weiss, A.: Z. Naturforsch. *19a*, 1518 (1964).
89) Bodenstedt, E., Rogers, J. D.: Perturbed angular correlations, p. 91. Amsterdam: North Holland Publ. Comp. 1964.
90) Dixon, R. W., Bloembergen, N.: J. Chem. Phys. *41*, 1720, 1731 (1964).
91) Gretschischkin, V. S., Kyuntsel, I. A.: Optika i Spektoskopiya *16*, 161 (1964).
92) Gretschischkin, V. S., Kyuntsel, I. A., Soifer, G. B.: Tr. Estestvennonauchnogo Instituta Permskogo Gosudarstvennogo Universiteta *11*, 3 (1964).
93) Hooper, H. O.: J. Chem. Phys. *41*, 599 (1964).
94) Jeffrey, G. A., Sakurai, T.: Progress in solid state chemistry (ed. H. Reiss), Vol. 1, p. 380. London: Pergamon Press 1964.
95) Nakamura, D., Kubo, M.: J. Phys. Chem. *68*, 2986 (1964).
96) Steffen, R. M., Fraunfelder, H., in: Perturbed angular correlations, p. 1. Amsterdam: North Holland Publ. Comp. 1964.
97) Watson, R. E., Freeman, A. J.: Phys. Rev. *135 A*, 1209 (1964).
98) Babushkina, T. H., Robas, V. I., Safin, I. A., Semin, G. K.: Fiz. Tverd. Tela *7*, 924 (1965).
99) Biryukov, I. P., Voronkov, M. G.: Latvijas PSR Zinatnu Akad. Vestis. Khim. Ser. *1965* (1), 115–116 (Russ.); – Chem. Abstr. *63*, 14239d (1965).
100) Campbell, I. D., Coogan, C. K.: J. Chem. Phys. *39*, 3061 (1965).
101) DeWette, F. W., Schacher, G. E.: Phys. Rev. *137*, A 78, A 92 (1965).
102) Dixon, R. W.: Proc. XIIIth Colloque Ampère, p. 213. Amsterdam: North Holland Publ. Comp. 1965.
103) Gretschischkin, V. S., Kyuntsel, I. A.: Zh. Strukt. Khim, *7*, 119 (1966).
104) Haas, T. E., Marram, E. P.: J. Chem. Phys. *43*, 3985 (1965).
105) Ikeda, R., Nakamura, D., Kubo, M.: J. Phys. Chem. *69*, 2101 (1965).
106) Langhoff, P. W., Hurst, R. P.: Phys. Rev. *139*, A 1415 (1965).
107) Lehrer, S. S., O'Konski, C. T.: J. Chem. Phys. *43*, 1941 (1965).
108) Odehnal, M., Scott, M.: Czech. J. Phys. *B15*, 307 (1965).
109) Semin, G. K.: Zh. Strukt. Khim. *6*, 292 (1965).
110) Semin, G. K., Robas, V. L., Steingans, V. D., Yakobson, S. G.: Zh. Strukt. Khim. *6*, 160 (1965).
111) Alderdice, D. S., Iredale, T.: Trans. Faraday Soc. *62*, 137 (1966).
112) Biedenkapp, D., Weiss, A.: Ber. Bunsenges. Physik. Chem. *70*, 788 (1966).

113) Cotton, F. A., Harris, C. B.: Proc. Natl. Acad. Sci. U.S. *56,* 12 (1966).
114) Dinesh, Narasimhan, P. T.: J. Chem. Phys. *45,* 2170 (1966).
115) Gretschischkin, V. S., Kyuntsel, I. A.: Tr. Estestvennonauchnogo Instituta Permskogo Gosudarstvennogo Universiteta *11,* 9 (1966).
116) Gretschischkin, V. S., Kyuntsel, I. A.: Tr. Estestvennonauchnogo Instituta Permskogo Gosurdarstvennogo Universiteta *12,* 15 (1966).
117) Gretschischkin, V. S., Gordev, A. D.: Tr. Estestvennonauchnogo Instituta Permskogo Gosudarstvennogo Universiteta *12,* 3 (1966).
118) Matzkanin, G. A., O'Neal, T. N., Scott, T. A., Haigh, D. J.: J. Chem. Phys. *44,* 4171 (1966).
119) Negita, H., Okuda, T., Kashima, M.: J. Chem. Phys. *45,* 1067 (1966).
120) Sternheimer, R. M.: Phys. Rev. *146,* 140 (1966).
121) Babushkina, T. A., Robas, V. I., Semin. G. K., in: Radiospektroskopija Tverdogo Tela [Solid State Spectroscopy, Conference Report], p. 221 (ed. Akad. Nauk SSSR, Sov. po fizike tverdogo tela. Inst. fiziki SO AN SSSR). Moskau: Atomizdat 1967.
122) Biryukov, I. P., Voronkov, M. G.: Collection Czech. Chem. Commun. *32,* 830 (1967).
123) Cotton, F. A., Harris, C. B.: Inorg. Chem. *6,* 369, 376 (1967).
124) Coogan, C. K.: Australian J. Chem. *20,* 2552 (1967).
125) Weiss, A.: Proc. XIVth Colloque Ampère, p. 1076. Amsterdam: North Holland Publ. Comp. 1967.
126) Biedenkapp, D., Weiss, A.: J. Chem. Phys. *48,* 3933 (1968).
127) Biedenkapp, D., Weiss, A.: Z. Naturforsch. *23b,* 174 (1968).
128) Gilson, D. F. R., O'Konski, C. T.: J. Chem. Phys. *48,* 2767 (1968).
129) Hafner, S., Raymond, M.: J. Chem. Phys. *49,* 3570 (1968).
130) Jeffrey, K. R., Armstrong, R. L.: Phys. Rev. *174,* 359 (1968).
131) Kravchenko, E. A., Maksyutin, Y. K., Guryanova, E. N., Semin, G. K.: Izv. Akad. Nauk. SSSR, Ser. Khim. *6,* 1271 (1968).
132) Lotfullin, R. S., Semin, G. K.: Zh. Strukt. Khim. *9,* 813 (1968).
133) Maksyutin, Y. K., Bryukhova, E. V., Semin, G. K., Guryanova, E. N.: Izv. Akad. Nauk. SSSR, Ser.Khim. *11,* 2688 (1968).
134) Okuda, T., Nakao, A., Shiroyama, M., Negita, H.: Bull. Chem. Soc. Japan *41,* 61 (1968).
135) Rogers, M. T., Rama Rao, K. V. S.: J. Chem. Phys. *49,* 1229 (1968).
136) Semin, G. K., Babushkina, T. A., Kobrina, L. S., Yakobson, G. G.: Izv. Sibirsk Otd. Akad. Nauk SSSR, Ser. Khim. Nauk *5,* 69 (1968).
137) – Kobrina, L. S., Yakobson, G. G.: Izv. Sibirsk. Otd. Akad. Nauk SSSR, Ser. Khim. Nauk *4,* 84 (1968).
138) Armstrong, R. L., Cooke, D. F.: Canad. J. Phys. *47,* 2165 (1969).
139) Biryukov, I. P., Voronkov, M. G., Safin, I. A.: Tables of NQR Frequencies, Israel Program for Scientific Translations, Jerusalem 1969.
140) Elter, S., Ha, T. K., O'Konski, C. T.: J. Chem. Phys. *51,* 1430 (1969).
141) Ha, T. K., O'Konski, C. T.: J. Chem. Phys. *51,* 460 (1969).
142) Kantimati, B.: Indian J. Pure Appl. Phys. *7,* 238 (1969).
143) Lucken, E. A. C.: Nuclear quadrupole coupling constants. New York: Academic Press 1969.
144) Maksyutin, Yu. K., Babushkina, T. A., Guryanova, Ye. N., Semin, G. K.: Theoret. Cim. Acta *14,* 48 (1969).
145) Paschalis, E., Weiss, A.: Theoret. Chim. Acta *13,* 381 (1969).
146) Pies, W., Weiss, A.: Z. Naturforsch. *24b,* 1268 (1969).
147) Schmidt, P.: Diplomarbeit, Münster 1969 .
148) Smith, P. W., Stoessiger, R.: Mol. Phys. *17,* 503 (1969).

149) Upadyskeva, A. V., Babushkina, T. A., Bryukhova, E. V., Robas, V. I., Kazitsyna, L. A., Semin, G. K.: Izv. Akad. Nauk SSSR, Ser. Khim. *9,* 2068 (1969).
150) Armstrong, R. L., Baker, G. L., Jeffrey, K. R.: Phys. Rev. (B) *1,* 2847 (1970).
151) Brill, T. B., Hugus, Z. Z., Jr.: J. Phys. Chem. *74,* 3022 (1970).
152) Brill, T. B., Hugus, Z. Z., Jr., Schreiner, A. F.: J. Phys. Chem. *74,* 2999 (1970).
153) Brown, T. L., Kent, L. G.: J. Phys. Chem. *74,* 3572 (1970).
154) Greenwood, N. N., in: Physical chemistry, An Advanced Treatise (eds. H. Eyring, D. Henderson, W. Jost), Vol. IV, p. 633. New York: Academic Press 1970.
155) Lindop, A. J.: J. Phys. (London) (C) *3,* 1984 (1970).
156) Lucas, J. P., Guibé, L.: Mol. Phys. *19,* 85 (1970).
157) Mulliken, R. S., Person, W. B., in: Physical chemistry, An Advanced Treatise (eds. H. Eyring, D. Henderson, W. Jost), Vol. III, p. 538. New York: Academic Press 1970.
158) Okuda, T., Terao, H., Ege, O., Negita, H.: Bull. Chem. Soc. Japan *43,* 2398 (1970).
159) Schempp, E., Bray, P. J., in: Physical chemistry, An Advanced Treatise (eds. H. Eyring, D. Henderson, W. Jost), Vol. IV, p. 521–632. New York: Academic Press 1970.
160) Spence, R. D., Rama Rao, K. V. S.: J. Chem. Phys. *52,* 2640 (1970).
161) Kanert, O., Mehring, M.: NMR, Basic principles and progress, Vol. 3. Berlin-Heidelberg-New York: Springer 1971.
162) Pies, W., Rager, H., Weiss, A.: Organic Magn. Res. *3,* 147 (1971).
163) Hulme, R., Scruton, J. C.: J. Chem. Soc. (A) *1968,* 2448.
164) Hulme, R., Szymanski, J. T.: Acta Cryst. *B 25,* 753 (1969).
165) Hulme, D., Mullen, D.: Acta Cryst. *A 25,* 171 (1969).
166) Brill, T. B., Hugus, Z. Z., Jr.: Inorg. Chemistry *9,* 984 (1970).
167) Ito, K., Nakamura, D., Ito, K., Kubo, M.: Inorg. Chem. *2,* 690 (1963).

Received January 25, 1971

Nitrogen Quadrupole Resonance Spectroscopy

Dr. Lucien Guibé

Institut d' Electronique Fondamentale, Université de Paris, Faculté des Sciences d'Orsay, Orsay, France

Contents

1. Introduction

Nitrogen quadrupole resonance spectroscopy has developed much more slowly than that of chlorine and far fewer resonances are known for nitrogen.

This difference ist due mainly to experimental difficulties: nitrogen resonances fall within the low-frequency range, 1 to 5 MHz, while most of the chlorine resonances, especially in covalent compounds, are located in the 30–40 MHz band.Thus the Boltzmann factor $h\nu/kT$ for nitrogen is seven times smaller and the line intensity is accordingly reduced. Moreover, the splitting of the nitrogen resonance line by the asymmetry of the electric field gradient tensor reduces the line intensity by a factor of more than 2.

As far as apparatus is concerned, chlorine resonances are more easily detected with superregenerative spectrometers in which induction phenomena yield enhanced signals. Continuous wave spectrometers, which do not have this advantage, have their effective sensitivity limited by the long relaxation times encountered in many of the compounds studied.

It is not lack of interest that has hampered the development of nitrogen quadrupole resonance studies: the spin 1 of ^{14}N means that a simple determination of the resonance frequencies is sufficient to give both the coupling constant e^2Qq and the electric-field gradient asymmetry η, without any need for Zeeman experiments on single crystals, as is the case with chlorine and bromine compounds. The polyvalency of nitrogen produces a wide variety of compounds and explains the deep interest they present for many scientists. The presence of a lone electron pair on nitrogen may be interesting, particularly when electron donator acceptor complexes are concerned.

Nitrogen quadrupole resonance studies have so far followed two major directions of investigation: on the one hand, quadrupole coupling constants are interpreted in terms of the distribution of the bonding electrons, with many attempts to use the available molecular orbitals computed from models of various degrees of sophistication; on the other hand, the effect of temperature on resonances yields information on the molecular motions and relaxation processes.

It is worth mentioning that the recent observation of resonances in various new compounds, such as 4-coordinated nitrogen derivatives [1], or polymolecular compounds, such as charge-transfer complexes [2] may open up new fields of investigation.

There are several papers and books [3–5] devoted to nuclear quadrupole resonance spectroscopy; however, we think it better to begin with a brief survey of some of the theoretical aspects of pure quadrupole resonance for a spin $I = 1$, as well as of the experimental apparatus, before dealing with the detailed study of nitrogen resonances.

II. Pure Quadrupole Resonance for a Spin $I = 1$

A. Hamiltonian, Energy Levels and Transition Frequencies

With pure quadrupole resonance experiments one observes the transitions between the energy levels of the nuclear quadrupole coupling directly. These energy levels may be obtained from the quadrupolar hamiltonian:

$$H_q = \frac{e^2 Qq}{4I(2I-1)} \left[3I_z^2 - I^2 + \frac{\eta}{2}(I_+^2 + I_-^2)\right]$$

where eQ is the nuclear quadrupole moment,
eq is the main component of the electric field gradient tensor, (along its principal z axis),
η is the asymmetry of the electric field gradient.

If η is zero, only one transition is observed:

$$\nu = 3K \qquad \text{with } K = \frac{e^2 Qq}{4}$$

between the two levels:

$$E \pm 1 = K$$

$$E_0 = -2K$$

If η is different from zero, three transitions are possible between the three non-degenerate levels:

$$E_+ = (1+\eta)K \qquad \nu_+ = (3+\eta)K$$

$$E_- = (1-\eta)K \qquad \nu_- = (3-\eta)K$$

$$E_0 = -2K \qquad \nu_0 = 2\eta K$$

When η is small, the third line occurs at a low frequency and is often unobservable, while, with higher values of η, its frequency increases and it may then be quite easily observed. For example, η reaches the value 0.8 in hydrazine [6] and 0.9 in S_4N_4 [7] and the three lines are readily observed in these two compounds.

The observation, when possible, of the third line provides a check that the observed ν_+ and ν_- lines belong to the same resonance, especially in cases where several sites are expected to be present.

Theoretically [3], the intensities of the three lines are equal; however, the Boltzmann factor, possible anisotropy of the crystalline sample and, most of all, the relaxation times can modify them to the extent that some lines remain unobserved (cf. Ref. 77 in "Five-membered heterocycles").

B. Zeeman Effect

The Zeeman effect must be mentioned in the case of nitrogen: it behaves normally when $\eta = 0$; but, in the general case of a non-zero asymmetry, the Zeeman part of the hamiltonian no longer commutes with the quadrupolar part and there appears to be no first-order Zeeman effect, The second-order treatment of the perturbation yields the following values for the transition frequencies [8]:

$$\nu'_+ = (3+\eta)K + \frac{D^2\cos^2\theta}{2\eta K} + \frac{2D^2\sin^2\theta\cos^2\varphi}{(3+\eta)K} + \frac{D^2\sin^2\theta\sin^2\varphi}{(3-\eta)K}$$

$$\nu'_- = (3-\eta)K - \frac{D^2\cos^2\theta}{2\eta K} + \frac{D^2\sin^2\theta\cos^2\varphi}{(3+\eta)K} + \frac{2D^2\sin^2\theta\sin^2\varphi}{(3-\eta)K}$$

$$\nu'_0 = 2\eta K + \frac{D^2\cos^2\theta}{2\eta K} + \frac{D^2\sin^2\theta\cos^2\varphi}{(3+\eta)K} - \frac{D^2\sin^2\theta\sin^2\varphi}{(3-\eta)K}$$

where $D = g\mu_o H_o$, while θ and ψ are the polar angles of the magnetic field H_o with respect to the axes of the electric field gradient.

From these expressions it will be seen that the sign of the shift depends upon the nature ν_+, ν_- or ν_0 of the lines, which is useful for the interpretation of a newly observed spectrum by identifying the nature of the lines.

The shift is proportional to η^{-1} and, when η is large, a strong magnetic field is needed to shift the lines appreciably, especially ν_-, for which the Zeeman effect contains terms of opposite sign; this is particularly inconvenient when Zeeman modulation is to be used.

C. Transition Probabilities

As mentioned, the line intensities are equal exept for the contribution of the Boltzmann factor, the relaxation times and the orientation of the sample crystallites relative to the radio-frequency magnetic field.They thus deserve no further mention.

III. Observation of the Resonance Lines

A. Spectrometers

Superregenerative spectrometers have been used for the observation of low-frequency resonance signals[9]; they do not seem to have been extensively used for nitrogen, though some resonances were detected with such spectrometers[a]. The reason may be either the difficulty in operating these spectrometers at low frequencies, or a lack of sensitivity due to line saturation by the strong radio-frequency burst of the superregenerative cycle.

Two types of spectrometer are used to display nitrogen resonances: the continuous wave (cw) spectrometer, which detects the absorption line or its derivative, and the pulse apparatus on which free precession decays or echo signals are observed.

The first type seems better suited to the search for new lines. the most widely used set-ups being those of Watkins [10] and Robinson [11]. Searches for new lines may be carried out at room temperature provided the sample is in a crystalline state. But many compounds are liquid at room temperature, so it is necessary to work at a lower temperature and liquid nitrogen is convenient for most cases.

Some compounds, however, display no resonance at this temperature, e. g. ICN [10] and piperazine [12] ; in the former compound, strains may explain the absence of the lines observed at higher temperatures. Operation at liquid nitrogen temperature is convenient because it enhances the Boltzmann factor and the tank coil quality factor. On the other hand, long relaxation times may reduce line intensities below observability, so that it may be better to operate at a slightly higher temperature where relaxation times are shorter while the Boltzmann factor and the coil quality are not much decreased [13].

Both Zeeman and frequency modulation are used for line observation but each has its drawbacks: frequency modulation is often accompanied by a steady drift of the recorder base line, while Zeeman modulation becomes inefficient when the electric field gradient is highly asymmetric, especially for the ν_- lines.

Pulse techniques are fairly well developed for nuclear magnetic resonances, and the experimental requirements are less restrictive for nitrogen quadrupole resonance than for standard proton resonance in solids, so we shall not describe them here.

---

a) Krause, L., Whitehead, M.A.: J. Chem. Phys. *52*, 2787 (1970). – Yim, C.T., et al.: Can. J. Chem. *46*, 3595 (1968).

B. Improvement of the S/N Ratio with Digital Memory Oscilloscopes and Computers

Signals obtained with both cw and pulse spectrometers are usually weak and their improvement is often desirable.

With cw, the increase of the recording time constant is not as efficient as expected because the low-frequency components of the noise are stronger and the reduction of the sweep speed increases line saturation. But with digital memory oscilloscopes and computers it is now possible to repeat the sweeps and average the different recordings. The improvement on a given line is obvious. The experiment is relatively easy to set up and it has been used for Stark effect studies [14]. But the stability and reproducibility needed in the search of new lines, with broader sweeps, make this technique somewhat difficult to use and no such experiment seems so far to have been reported for nitrogen.

The problem is quite different with pulse spectrometers, for which the prospects are good: free precession and echo signals are rather long as compared to those of protons in solids and they can readily be fed into a standard digital memory oscilloscope with an access time of about 40 microseconds. The gain is considerable [15, 16] provided good sample temperature and spectrometer frequency stabilizations are achieved.

IV. Study of Nitrogen Resonances

The first step in quadrupole resonance studies is the detection of lines in new compounds and the interpretation of the observed frequencies in the light of the molecular and crystalline structure of the compound. In the second step, physical studies are developed which yield informations on the temperature and pressure effects, on the isotopic shift, and on the Zeeman and Stark effects.

We first present the results of physical studies on nitrogen resonances.

A. Physical Aspects of the Resonances

1. Dependence of the Frequency on Temperature

Thermal agitation, consisting in small, fast ($\nu = 10^{12}$ Hz), oscillations of the molecules from their static position, reduces the mean electric field gradient, "seen" by the nuclei, to a value below that of the static molecule. The study

of the dependence of frequency upon temperature yields the quasi-static coupling in the resting molecule. This coupling generally differs from that at 77 °K by a negligible amount, though in the case of ammonia it reaches 9% [17].

The temperature dependence of the quadrupole coupling constant is usually interpreted in terms of the Bayer theory [18], modified and completed by Kushida [19], Kushida, Benedek and Bloembergen [20], and by Gutowsky and Williams [21].

In the Bayer theory, no account is taken of the dilatation effects in constant pressure experiments (atmospheric pressure) and the fit between the predicted curve and the experimental points worsens as the temperature increases. In hexamethylenetetramine, a great improvement was achieved by considering the temperature dependence of the frequency of the torsional vibrations, previously obtained from X-ray measurements [22]: at room temperature the discrepancy between theory and experiment was reduced from 34 kHz to 0.3 kHz, that is, less than half the line width. The more complete theory of Kushida, Benedek and Bloembergen, also gives a good approximation, though an observed temperature effect on the coefficients is neglected [22].

With NF_3 [23], the temperature range is restricted by the triple point at 66.4° K, and the application of Bayer's theory is limited to temperatures below 35° K, above this, the diagreement between theory and experiment increases towards a transition at 56.6° K. This transition might have been explained as a rotation of the molecules around their C_3 axis, but N.M.R. studies seem to show, as predicted by thermodynamic calculations, that the motions is a more general one.

The quadrupolar quasi-static coupling in NF_3 – 7.068 MHz– is very close to the value obtained from microwave measurements – 7.07 MHz –; this feature may be interpreted as a clue that intermolecular effects are negligible in this compound unless, by a fortuitous coincidence, thes intermolecular effects are cancelled by some other mechanism, such as a molecular deformation in the solid (the coupling is very sensitive to slight variations of the pyramidal angle, as discussed below).

For ammonia [17], the study of the resonance in its deuterated derivatives (NH_2D, NHD_2 and ND_3) leads to the conclusion that the difference between their respective quadrupole coupling constants arises from differences in the amplitude of the molecular motions related to the differences in the moments of inertia of each type of molecule.

The difference between the quasi-static coupling for ammonia in the solid state – 3.47 MHz – and that measured in the gas by microwave spectroscopy – 4.08 MHz – cannot be explained by the contribution of the crystalline electric field gradient alone, but must be attributed to a redistribution of the bonding electrons in the molecule under the influence of the crystalline electric field or of the intermolecular hydrogen bonds.

2. Phase Transitions

Phase transitions may be detected by the corresponding anomaly in the temperature dependence of the quadrupole coupling constant. For example, in monomethylamine a phase transition occurs at ~80 °K and a hysteresis loop has been observed in the frequency vs. temperature curve with a broadening of the lines just before the transitions [24] This transition has been confirmed by the N.M.R. study of the proton line width and by the dielectric behavior, but no precise explanation has been given.

In ethylenediamine [25] , two transitions were observed but the slight changes in the coupling constants imply that they are only small rearrangements of the molecules in the crystal.

A transition observed in the nitrogen resonance of hydrocyanic acid was related to a structural modification established by X-ray investigations [26].

Malononitrile is particularly interesting as it shows a second-order transition [27] ; no discontinuity of the pure quadrupole resonance is detected, but, over a limited temperature range, each line splits into two components, whose separation varies with temperature in a continuous manner, from zero to a maximum and then back to zero, without any hysteresis.

When no study of the temperature dependence of the quadrupole coupling constant is available, phase transitions may be detected by observing the quadrupole resonance at low-temperature on samples that have been cooled in different ways: with slow cooling, the phase transition may take place and the low-temperature phase resonance is observed, while fast cooling "freezes" the sample in its high-temperature phase. Two crystalline forms have been identified in acetonitrile [26] and some other compounds [2].

The above-mentioned transitions are accompanied by only slight modifications of the coupling constant; however, drastic changes occur above the transition temperature when strong molecular motions take place with nearly complete reorientation of the molecules: the quadrupole resonance is no longer observable, while a rapid change in the resonance frequency and a broadening of the line are seen just before the transition.

Pure quadrupole resonance has been observed in solid molecular nitrogen, in its low-temperature phase at atmospheric pressure [28] between 1.5 and 35 °K (the transition occurs at 35.5 °K); the frequency is 3.487 MHz at 4.2 °K. In the high-temperature phase, the N.M.R. of nitrogen reveals a low coupling (about 3 kHz at 62° K) which is attributed to a small anisotropy of the reorientational motions in the hexagonal crystal.

A plastic transition is known in triethylenediamine at ~80 °C and the resonance frequency shows a rapid decline as the temperature nears 80 °C. [29].

A similar disappearance of the resonance line has been observed in NF_3 at 56.6 °K [23].

3. Effects of Temperature on Relaxation

Molecular motions, besides exerting an averaging effect on the electric field gradient, induce transitions between the spin energy levels and thus contribute to relaxation.

Hexamethylenetetramine has been extensively studied in this respect [30], and it has been shown that for temperatures ranging above room temperature, reorientational motions are responsible for the strong relaxation. More exactly, hindered rotations interchange the tetrahedron apexes and the nuclei are thus subjected to a sudden reorientation of the electric field gradient. The correlation time of such motions can be derived from the observed signals and experimental results may be depicted by the relation

$$\tau^{-1} = \nu_0 \, e^{-\Delta E/kT}$$

from which the reorientation frequency at infinite temperature

$$\nu_0 = 7.6 \times 10^{12} \text{ sec}^{-1}$$

and the activation energy of the process

$$\Delta E = 15.6 \text{ kcal/mole}$$

are derived.

It is worth mentioning that these values are close to those obtained from proton N.M.R. studies [31].

In triethylenediamine, the relaxation processes are somewhat different because the reorientation of the molecules around their C_3 axis does not influence the electric field gradient acting on the nitrogen nuclei; indeed the variation of the dipolar coupling between the nitrogen nuclei and the neighboring protons is the cause of the relaxation [29], which is maximum when the molecule rotation frequency is precisely equal to the pure quadrupole resonance frequency. At the corresponding temperature, the relaxation time vs. temperature curve shows a minimum.

A more complicated but interesting situation is encountered with hydrazine: the two nitrogen atoms in the molecule have different crystalline sites and hence different resonance frequencies; the molecular reorientations ensure an interchange of these two nitrogen atoms, i. e., an interchange between two different resonant systems. It is thus possible to carry on a cross-relaxation experiment which gives information concerning the relative orientation of the principal sets of axes of the electric field gradient [32].

4. Line Width

Owing to the special form of the eigenwave functions for $\eta \neq 0$, and in accordance with the absence of first-order Zeeman effect, it may be shown that the magnetic dipolar contribution to nitrogen resonance line width is very small [33,34]. Lines are consequently narrow for many of the compounds studied, a very convenient feature when weak effects, like the Stark effect, are to be studied [35].

However, when $\eta = 0$, the dipolar contribution to the line width is not negligible and line widths of about one kilohertz are observed in hexamethylenetetramine [22] and in triethylenediamine [29], while broader lines are observed in ammonia and deuteroammonia [17].

As the temperature increases, the line width may be reduced by an averaging of the dipolar magnetic field at the nitrogen nuclei when a motion of the neighboring protons takes place [17].

Another contribution of temperature to line width is a broadening of the resonance accompanying the set-up of fast reorientational motions which change the electric field gradient orientation without modifying its module, thus shortening the life of a nitrogen nucleus in a given state. This is precisely the case of hexamethylenetetramine when the temperature rises above room temperature [36].

No systematic study seems to have been reported concerning other sources of line broadening; yet crystalline strains or impurities may explain the breadth or even the failure to observe some lines.

5. Isotopic Effect

This is a frequency change accompanying the substitution of a non-resonant atom in a molecule by an isotope of different mass. We have already mentioned that, in ammonia and deuteroammonia, molecular motions of different amplitudes were responsible for the observed differences in the resonance frequencies.

A similar phenomenon occurs with nitrogen after the substitution, in the molecule, of a ^{14}N atom by a ^{15}N atom; ^{15}N has no quadrupole moment and only the ^{14}N resonance is observed in $^{14}N-^{14}N$ and $^{14}N-^{15}N$ molecules: the resonance frequency is slightly higher in the heavier asymmetric molecule [37].

Other isotopic substitution experiments were developed on urea [38] and on 2-aminopyridine [39]. In the latter compound the NH_2 group deuteration increases the inertial moment of this group and the amplitude of the oscillation is thus reduced: the corresponding quadrupole resonance frequency is increased while the heterocyclic nitrogen atom is virtually unaffected by the resulting small relative weight increase of the entire molecule. Such an experiment affords a new clue for the interpretation of the spectrum and the attribution of one of the observed sets of resonance to the amino nitrogen atom.

In urea, deuteration was used to interpret the molecular motion as reorientation of the NH_2 group around the N–C bond direction, instead of reorientation of the molecule as a whole.

6. Stark Effect

The application of a strong static electric field modifies the quadrupole coupling constant as an effect of the sample polarization. The phenomenon has been reviewed by Lucken [5] who mentions some results concerning halogens.

These studies have been extended to nitrogen [35,40] and, while weak broadening or asymmetric deformation of the lines is observed for some compounds (such as acetonitrile, hexamethylenetetramine and triethylenediamine), the pyridine lines are split into two components as predicted from the theory.

7. Zeeman Effect

This has not been studied so extensively as for halogen resonances, some of the possible reasons being (i) for nitrogen, the quadrupole coupling constant and its asymmetry are directly derived from the resonance frequencies observed on a polycrystalline sample, while, for halogens (iodine ecepted), a Zeeman study of a single crystal is necessary; (ii) there is no first-order Zeeman effect for nitrogen when $\eta \neq 0$, which is the most frequent situation. The second-order term has an angular dependence on the square of the angle sine or cosine, and the potential resolution of the technique is thus reduced because angular diagrams have a π periodicity instead of a 2π periodicity and because, when η is large, the variation of one term in the frequency expression (cf. II.B.) is masked by the variation of another term, so that the frequency may appear to be nearly constant.

There are few published reports of experiments on the Zeeman effect in nitrogen quadrupole resonance. In her study of *p*-bromoaniline, Minematsu [41] showed that the Ox and Oy axes of the electric field gradient tensor lie in the molecule plane, with Oy being directed along the molecule axis of symmetry and Ox perpendicular to it.

In a careful study of thiourea, Smith and Cotts [42] not only determined the principal directions of the electric field gradient tensor, they also detected a small deviation in the orientation of these directions from the symmetry axes of the corresponding chemical bonds. They suggested this deviation was due to intra- and extra-molecular contributions to the electric field gradients.

B. Interpretation of the Observed Quadrupole Coupling Constants

This paragraph will be chiefly devoted to the determination of the ^{14}N quadrupole moment and of the quadrupole coupling of a "p" electron in this atom. These quantities cannot be obtained from experiments on atomic beams because the fundamental state of the nitrogen atom has no quadrupole coupling, owing to its symmetry; we therefore have to resort to the quadrupole coupling determination in a given molecule to derive the nitrogen quadrupole moment from the observed coupling constant and from a value of the electric field gradient computed from theoretical data.

Such determinations have been made, for the ^{14}N nucleus, from the microwave spectroscopy determinations of the coupling in HCN and NH_3 (cf. paragraph 6.3 in Ref. [5]), and the most probable value seems to be

$$eQ = +0.015 \text{ barns}$$

This quantity was also evaluated in quite a different way, from E.S.R. experiments on NO and a value of eQ close to the preceding one was obtained.

The determination of the coupling of a "p" electron appears to be more useful for the interpretation of the molecular couplings by means of the Townes and Dailey theory and through the computation of the "p" contribution of each molecular orbital involved in the nitrogen atom bonding[43].

The interpretation of the nitrogen coupling in NF_3 [44], NH_3 [45], and in some larger molecules like hexamethylenetetramine, pyridine[46] or heterocycles containing several nitrogen atoms [47, 48], finally leads to the following estimate of a "p" electron coupling in nitrogen:

$$e^2 Qq_0 = 9 \text{ MHz}$$

This estimate is quite generally accepted though some computations rely on slightly different, higher or lower, values.

We may take this opportunity to recall that the atomic quadrupole coupling constant is dependent upon the effective electric charge of the atom in question: if a nitrogen atom bears more than the five electrons corresponding to its neutral configuration, the interelectronic repulsion increases the average distance of a "p" electron from the nucleus, and the corresponding atomic quadrupole coupling constant is thus reduced. Conversely, a reduction of the atomic charge increases the coupling constant. A correction taking this effect into account can be introduced with a factor

$$\frac{1}{1 + i\epsilon}$$

in the expression of the atomic quadrupole coupling constant. In this factor "i" is the nitrogen atom ionicity and "ϵ" is a constant characteristic of the studied atom (i. e., nitrogen), estimated in the present case at 0.30[49].

Though this correction does not seem to have been considered, we must note that its effect is far from negligible when compounds as different as NH_3, $N(CH_3)_3$ and NF_3 are involved; in these molecules, the nitrogen "σ" bond populations are 1.33, 1.22 and 1.53, respectively according to one determination, and 1.39, 1.23 and 0.95 according to another [50]. It can readily be appreciated that the correction for the charge effect may be as high as 2 MHz.

C. Study of Nitrogen Compounds

1. Molecules with a Triply Bonded Nitrogen Atom

a) Computation of the Quadrupole Coupling Constant

The triple bond is described with a "sp" "σ" bond, plus two pure "p" "π" bonds, while the lone pair is localized in a "sp" orbital; the standard description of these orbitals is as follows:

$$\psi\sigma = -\alpha \cdot p_z + (1-\alpha^2)^{\frac{1}{2}} \cdot s \qquad b$$

$$\psi\pi 1 = p_x \qquad a$$

$$\psi\pi 2 = p_y \qquad a$$

$$\psi lp = (1-\alpha^2)^{\frac{1}{2}} \cdot p_z + \alpha \cdot s \qquad 2$$

Oz being chosen along the C≡N bond direction; the orbital populations on the nitrogen atom are shown on the right; they are dependent upon the nature of the bonded group and upon the bond polarization.

The electric field gradient component produced along Oz by a "p_z" electron is eq_0 and $-\frac{1}{2}eq_0$ along Ox and Oy. So, with the proposed orbitals and populations, the nitrogen atom quadrupole coupling constant in a C≡N group is

$$e^2Qq = [2(1-\alpha^2) - a + \alpha^2 b]\, e^2Qq_0$$

The α parameter cannot be derived from structural data, and we have to rely upon theoretical considerations and upon the experimental coupling observed in molecular nitrogen to fix its value [5]. With $\alpha^2 = \frac{1}{2}$ one gets

$$e^2Qq = [1 - \tfrac{1}{2}(2a - b]\, e^2Qq_0$$

It may then be noted that e^2Qq and e^2Qq_0 have the same sign; as the quadrupole coupling constant in HCN, determined by microwave spectroscopy, is negative, and as the electric field gradient of a "p" electron is also negative, it may be concluded that the nitrogen quadrupole moment eQ is positive.

When the molecule to which the C≡N group is attached is unsymmetrical, the cyano group loses its symmetry and the two "π" bonds become different; the coupling may then be expressed as

$$e^2Qq = [\,1 - \tfrac{1}{2}(a_1 + a_2 - b)]\, e^2Qq_0$$

with an asymmetry

$$\eta = \frac{3}{2}\ \frac{a_1 - a_2}{2 + b - a_1 - a_2}$$

b) Nitriles

Their study [51, 52] was undertaken after the observation of the nitrogen resonance in some simple terms [53, 54].

In simple aliphatic nitriles, when the length of the chain increases, the nitrogen coupling remains very close to a limit value – 3.8 MHz – obtained for the longest molecules studied.

A similar limit is obtained with dinitriles. However for the shortest of them, the presence of a second, electronegative cyano group leads to an increase of the coupling, which is maximal for cyanogen and still observable for malono- and succinonitrile.

The influence of the substituents is more easily interpreted in symmetrical compounds. If it is supposed that the substituent has only an inductive effect, the bond symmetry is expected to be conserved and the electron withdrawing (or releasing) trend of the substituent will alter both "a" and "b" in the same sense, though not to the same extent. As the coupling depends upon the difference $2a - b$, it is difficult to foresee what the effect of the substituent will be unless one supposes a greater polarizability of the "π" electrons. An electron withdrawing substituent will then be expected to increase the coupling constant.

The complexity of the relation between a substituent electronegativity and its effect on the coupling constant makes it difficult to find a simple relation between the quadrupole coupling constant and a characteristic parameter of the substituent, such as Hammett's "σ" factor.

Nevertheless, most of the observed couplings may be interpreted in the light of the known properties of the substituents: methyl is an electron donor even via hyperconjugation and this accounts for a lower coupling in acetonitrile

than in hydrocyanic acid; on the other hand, the electronegative chlorine atoms in trichloracetonitrile increase the coupling with respect to that of acetonitrile.

A substituent interesting by its conjugative power, is the benzene ring: from a comparison of the coupling asymmetry in benzonitrile and in isonicotinonitrile, it may be shown that conjugation in benzonitrile takes place with an electron charge transfer towards the cyano group. Other benzonitriles have now been studied [a].

In unsymmetrical substituted nitriles the problem is that the asymmetry sign cannot be experimentally determined (unless Zeeman experiments are developed, but the difficulties have been stressed above), so it is impossible to know from the observed coupling whether a substituent is an electron donor or acceptor. Usually, asymmetries remain small and only a few nitriles present an asymmetry higher than 0,1, but less than 0,2; these are monochloracetonitrile, methoxyacetonitrile, cyclopropylcyanide and benzonitrile [51].

c) Thiocyanates

Thiocyanates differ from nitriles in having a smaller coupling constant and a strong asymmetry, close to 0.5 [55], which is attributed to the resonating structure

$$R-\overset{+}{S}=C=N^{-}$$

with an electron charge transfer towards the nitrogen atom. From the observed coupling and asymmetry, this transfer has been estimated as 0.09 electron.

d) Metal–Cyano Complexes

Two sorts of metal–cyano complexes have been studied. The first contains an atom of zinc, cadmium, mercury or copper as the central atom, and the nitrogen quadrupole coupling is only a little higher than it is in nitriles (4.0–4.2 MHz against 3.8–4.0 MHz). In the second sort, the central atom is either platinum or cobalt and the observed couplings are markedly lower (3.47–3.68 MHz).

The difference is explained by a "$d_\pi - p_\pi$" contribution to the cyano group bonding with the central atom. Such a modification of the bond is also revealed by a reduction of the force constant as determined from infra-red spectra [56].

2. Amides and Amines

Here the nitrogen hybridization is sp^2 or sp^3 according to the planarity or non planarity of the $-NR_2$ group.

a) sp^2 Hybridization

The bonding orbitals of the nitrogen atom are described by:

[a] Calligioni, A., Ambrosetti, R., Guibé, L.: J. Chem. Phys. *54*, 2105 (1971).

$$\psi_{lp} = p_z \qquad 2c$$

$$\psi_{NC} = \alpha \cdot s - (1-\alpha^2)^{\frac{1}{2}} \cdot p_y \qquad b_{NC}$$

$$\psi_{NH} = 2^{-\frac{1}{2}}[(1-\alpha^2)^{\frac{1}{2}} \cdot s + \alpha \cdot p_y + p_x] \qquad b_{NH}$$

$$\psi_{NH'} = 2^{-\frac{1}{2}}[(1-\alpha^2)^{\frac{1}{2}} \cdot s + \alpha \cdot p_y - p_x] \qquad b_{NH'}$$

with $\alpha = \cot \gamma$
and γ being one half of angle HNH

In the simplified situation
where $\gamma = \pi/3$, we get:

$$e^2 Qq/e^2 Qq_0 = 2c - \tfrac{1}{3} b_{NC} - \tfrac{2}{3} b_{NH}$$

$$\eta \cdot e^2 Qq/e^2 Qq_0 = b_{NH} - b_{NC}$$

Applying this to the urea molecule, for which $e^2 Qq = 3.51$ MHz and $\eta = 0.32$, with $e^2 Qq_0 = 9$ MHz [41], yields 0.12 electron for the difference between the populations of the "σ" N–H and N–C bonds.

The smaller coupling observed in thiourea [42] results from a stronger conjugation of the type

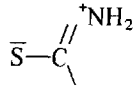

The solid state coupling of formamide – 2.3 MHz [57] – is still smaller and very different from the gas value [58] – 3.6 MHz –; the latter is close to that of urea. The difference between the solid state and gas couplings of formamide is probably due to intermolecular contributions, particularly hydrogen bonding, whose existence is established by the high boiling point and by the dielectric properties [59] of this compound. It may be seen that, if "c" is decreased, the coupling becomes smaller and the asymmetry increases, as is effectively observed.

The study of some methyl derivatives of formamide would be very helpful in determining the hydrogen bonding contribution; unfortunately, the lines are very weak and the spectra are incompletely observed [60].

The importance of intermolecular effects can be appreciated for urea and thiourea from the observation of the nitrogen resonance when these molecules are in different molecular environments, in clathrates or in complex salts, for example (see "Polymolecular systems").

Nitrates and nitrites also have a sp^2 hybridized nitrogen atom in their anion; the nitrogen resonance has been observed in several of these salts.

In nitrates [61,62] the coupling is rather small, ~1 MHz, and the nitrogen lone pair seems to be highly delocalized while most of the ion charge is located on the oxygen atoms.

In nitrites the coupling have recently been studied extensively, both experimentally[63–66] and theoretically, by computing the coupling in the NO_2^- ion [67, 68].

In ferroelectric sodium nitrite the resonance disappears when the temperature is increased to the vicinity of the ferro-paraelectric transition and the nitrite ions start to rotate. Moreover, the frequency exhibits a strong temperature dependence that cannot be explained by the Bayer theory.

b) sp^3 Hybridization

For the sp^3 hybridization encountered in the amines, the orbital expressions are somewhat more complicated; but for symmetrical compounds the coupling can be still expressed in a simple form

$$\frac{e^2Qq}{e^2Qq_0} = -\frac{3\cos\alpha}{1-\cos\alpha} \quad (2-a)$$

where "a" is the "σ" bond population and "α" the angle RNR; the lone pair is supposed to be localized on the nitrogen atom.

From this expression it is clear that an increase in "a" is followed by a decrease in the coupling constant, as experimentally illustrated by the lower coupling in ammonia (4.1 MHz in the gas) compared to trimethylamine (5.5 MHz); in the ammonia molecule, the NH bonds are more strongly polarized than the $N-CH_3$ in the trimethylamine. The coupling may also be lowered by a reduction of the lone pair population, as happens with the formation of hydrogen bonds. In solid NH_3 the coupling (3.16 MHz) is lower than in gaseous NH_3 even if the contribution of the molecular motions is excluded by calculating the coupling quasi-static value (3.47 MHz)[5, 17].

The interpretation remains essentially qualitative for asymmetric amines in which the exact orientation of the principal axes of the electric field gradient remains unknown.

Hydrazine, already mentioned for its relaxation processes, is also peculiar in its molecular structure: the presence of two identical adjacent nitrogen atoms ensures that the population of the corresponding "σ" N–N bond is exactly one on each nitrogen atom, while the N–H bonds have a population between 1.3 and 1.6. Thus it may be understood why, in hydrazine salts [1], the coupling is of the same order of magnitude as in amines. This is particularly worth mentioning as, in glycine, where the nitrogen atom is found in a 4–coordinated zwitterion structure, the coupling is low[69].

3. Six–membered Heterocycles

Six-membered conjugated heterocycles have a special importance for the determination of the coupling of a nitrogen "p" electron, as was mentioned in paragraph IV.B.

They are also convenient molecules for the study of the effect of substituents on the conjugated ring.

Owing to the presence of the molecular "π" system, the nitrogen sp^2 hybridized orbitals are not quite similar to those of amides and the following set of functions is usually employed to describe a pyridino nitrogen orbital [47]:

$$\psi_\pi = p_x \qquad a$$

$$\psi_{lp} = 3^{-\frac{1}{2}} \cdot s + (2/3)^{\frac{1}{2}} \cdot p_z \qquad 2$$

$$\psi_{\sigma 1} = 3^{-\frac{1}{2}} \cdot s + 2^{-\frac{1}{2}} \cdot p_y - 6^{-\frac{1}{2}} \cdot p_z \qquad b$$

$$\psi_{\sigma 2} = 3^{-\frac{1}{2}} \cdot s - 2^{-\frac{1}{2}} \cdot p_y - 6^{-\frac{1}{2}} \cdot p_z \qquad b$$

Oz is directed along the C_2 axis, while Ox is perpendicular to the molecular plane and Oy lies in this plane.

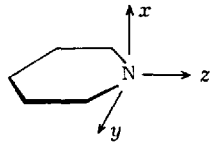

To take account of the exact values of the CNC angle which may differ from $2\pi/3$, more complete expressions of the orbitals have been proposed [47].

$$\psi_\pi = p_x \qquad a$$

$$\psi_{lp} = \cot\varphi \cdot s + (1 - \cot^2\varphi)^{\frac{1}{2}} \cdot p_z \qquad 2$$

$$\psi_{\sigma_1} = 2^{-\frac{1}{2}} \cdot [(1 - \cot^2\varphi)^{\frac{1}{2}} \cdot s + p_y - \cot\varphi \cdot p_z] \qquad b$$

$$\psi_{\sigma_2} = 2^{-\frac{1}{2}} \cdot [(1 - \cot^2\varphi)^{\frac{1}{2}} \cdot s + p_y - \cot\varphi \cdot p_z] \qquad b$$

where $2\varphi = \angle$ CNC

From these expressions the quadrupole coupling components on the three principal axes may be calculated and, for the interpretation, it appears convenient to use the following quantitites [71]:

$$\alpha\eta = \pm (3/2) \cdot (a - b)$$

$$2 - a = \alpha \cdot (1 - \cot^2\varphi)^{\frac{1}{2}} \cdot [1 \pm (2/3) \cdot \eta \cdot (\cot^2\varphi - 1/2)]$$

$$2 - b = \alpha \cdot (1 - \cot^2\varphi)^{\frac{1}{2}} \cdot (1 \pm \eta/3)$$

where α is now the ratio e^2Qq/e^2Qq_0 of the molecular coupling to the atomic "p" electron coupling.

Note that the difference a-b is obtained from the experimental value of e^2Qq and η without the intervention of the angle CNC.

The consideration of the exact value of the angle CNC was quite reasonable, both for the sake of completeness and because $2-a$ and $2-b$ are very sensitive to the value 2φ of this angle. Nevertheless, owing to the many approximations on which the Townes and Dailey theory is based, it did not always seem desirable to consider φ deviations from a 60° mean value [71].

The experimental results have made it possible:

– to ascertain the Oz orientation along the molecular C_2 axis;

– by comparing the coupling in several heterocycles [47], to choose between the two possible orientations of the Ox and Oy axes, confirming the above mentioned disposition. With the disposition adopted, the population "b" of the "σ" orbitals is, as expected from the greater polarizability of "σ" electrons, less affected by the passage from one molecule to another than the population "a" of the "π" orbitals;

– to compare the experimental results with the values calculated by several M. O. Methods of various degrees of sophistication, for the "π" electron density at the nitrogen atom. Taking the "b" population as constant, there is a good correlation between calculated and observed "a" values [70]. To extend [71, 72] the calculation to asymmetric molecules, like pyrimidine or pyridazine, the new orientation of the electric field gradient tensor must be considered. In pyridazine the two nitrogen Oz axes are rotated in a way that brings them nearer parallel and, from microwave measurements, this rotation was estimated at 9° [73]. Though it does not bring any very new result for pyridazine this extension of the calculation illustrates the general character ot the interpreting theory.

– to obtain informations on the electronic effects of various substituents by a systematic study of substituted pyridine derivatives [71, 74, 75]. Setting $2\varphi = 2\eta/3$ we get:

$$b - a = \frac{2}{3} \cdot \eta \cdot \alpha$$

$$2 - b = \frac{3}{2} \cdot \left(1 - \frac{\eta}{3}\right) \cdot \alpha$$

with which "a" and "b" may be derived from the experimental values of e^2Qq and η.

Considering, in a first step, symmetrical derivatives, we see that "a" varies, for the compounds studied, by 0.116 electron, while "b" variations are limited to a more restricted range, 0.042 electron, thus stressing the greater polarizability of "π" electrons. It is also clear that electron-releasing substituents affect the nitrogen quadrupole coupling more strongly when they are situated

in the *ortho* or *para* position, for which resonant structures, involving a charge transfer on the nitrogen atom are possible. The strong electronegativity of halogens produces a reduction of the nitrogen "σ" bond by inductive effect. The behavior of the methoxy group is characterized by an increase of the population of both "σ" and "π" nitrogen orbitals.

A simplification can be effected, for unsymmetrically subsituted derivatives, by introducing a mean value of the "σ" bonds population, namely $(1/3)(2 + b_1 + b_2)$, the results obtained for the "π"populations being quite similar to those of the symmetrically substituted derivatives

A classification of the substituents with respect to their "π" or "σ" electron-releasing ability has been proposed from these observations [75]:

"π" electron donor $\quad NH_2 > Cl > CH_3 \simeq H > CN$

"σ" electron donor $\quad NH_2 > CH_3 \simeq H > Cl > CN$

Aminopyridines are in a somewhat special situation with the very strong influence of the NH_2 group on the heterocyclic nitrogen quadrupole resonance in the *ortho* and *para* compounds; the effect is in accordance with the strong electron-releasing character of the amino group. In addition, it must be noted that the amino nitrogen resonance is virtually unaffected by the ring nitrogen atom position [76].

4. Five-membered Heterocycles

In these compounds, some of the resonances occur at low frequencies: for example, pyrrole ν_+ and ν_- line frequencies are respectively 1.685 and 1.408 MHz [77, 78]. Despite the necessary simplifications, the "π" population on the pyrrole nitrogen, as estimated from experimental data, is not very different from the theoretically computed value.

In other five-membered heterocycles, the lack of symmetry and the existence of intermolecular hydrogen bonding, for some of them, makes the discussion somewhat uncertain [77, 79].

Note: some saturated heterocycles, like piperedine or piperazine, have been studied, but the absence of a conjugated system makes them resemble amines, and they are not considered here.

5. Polymolecular Systems

In this paragraph compounds are considered in which at least two sorts of molecules are present. Hydrates are well known, but such less frequently

encountered compounds as clathrates, ammoniacates, ureates, complexes, etc., must also be mentioned.

The study of such compounds may be interesting in several respects: (i) An appreciation of the molecular effects on a given molecule, when engaged in different structures, may be obtained from the corresponding quadrupole coupling constants; furthermore, the temperature dependence of the frequency may supply indications on the strength of intermolecular forces. (ii) Charge transfer accompanying intermolecular bonding, like hydrogen bonding, can be estimated from the observed effect on the quadrucoupling constant. (iii) In special situations, as when a para-ferro-ferromagnetic-magnetic transition occurs, the resonance may be observed in both phases, and from the ferromagnetic phase resonance one may expect to obtain data concerning the local magnetic field.

Only a few such resonances have been studied so far.

a) Nitrogen Clathrates

Nitrogen clathrate in β-quinol was studied by Scott [28] in spite of many experimental difficulties. Among the findings obtained in this study, we may mention the existence of a seven-line spectrum whose intensity depends upon the preparation, history and age of the sample; a slow loss of nitrogen by the sample; the fact that the line frequencies are independent of the factors which alter line intensities and that the structure may be due to a partial filling of the β-quinol lattice holes.

b) Thiourea Inclusion Compounds

While the resonance of nitrogen in a urea clathrate containing heptane appeared to be unobservable [80], due to a fluctuation in the vicinity of urea molecules, the nitrogen resonance was recently found to be visible in thiourea-cyclohexane clathrate [81] in which a well-defined crystalline structure leads to a unique environment for each thiourea molecule. This observation needs further confirmation.

c) Hydrates

For hydrates, the question is, to what extent does the nitrogen atom lone pair contribute to hydrogen bonding in amine hydrates? Hydrogen bonding is expected to explain the difference between gaseous and solid ammonia couplings. A study [82] of ammonia hemi-hydrate, whose resonance frequencies are not very different from those of ammonia, supports the view that hydrogen bonds linking ammonia to water molecules are not very different from ammonia-to-ammonia bonds.

Some attempts to observe resonances in other amine hydrates were unsuccessful.

d) Ureates

The nitrogen resonance of urea has recently been observed, at 77 °K [83] in a complex salt containing one copper formate molecule with two water and two urea molecules. The coupling is quite close to that in pure urea, showing that the intermolecular contribution to the coupling is probably weak.

e) Charge-Transfer Complexes

These are formed by an association of two molecules, described by a wave function containing, beside the ground state wave functions of the two molecules, a contribution of excited states characterized by the transfer of one electron from the donor molecule to the acceptor molecule [84].

The special interest of pure quadrupole resonance is that it affords a means of measuring the small charge transfer in solid complexes.

In a paper recently published [2], we point out that, except for a bromine-benzene complex studied by Duchesne, the results reported in the literature do not offer any clear evidence for charge transfer. A systematic observation of both nitrogen and chlorine resonances in some complexes led us to admit the existence of a small transfer (0.05 electron) in chloroform complexes with amines and pyridine derivatives. Though the number of compounds studied is still small, the observed effects are not thought to be due to mere coincidence, and it appears very desirable to extend such experiments especially for "stronger" complexes.

V. Conclusion

After reviewing nitrogen resonance studies, we may wonder whether it is possible to increase the reliability of the data obtained. Such a question has at least two aspects. First, some imprecision is introduced by the complexity of the molecules which do not have the symmetries of a simple molecule; these symmetries reduce the number of necessary parameters, enabling them to be clearly related to the two experimentally available constants, e^2Qq and η. It seems obvious that the only solution here is to obtain some of the parameters by other means. A second, more general aspect of the question is how to refine the simple Townes and Dailey theory. Several attempts have been made to improve the fit of the experimental data by using precisely computed molecular orbitals, instead of the standard $s-p$ hybridized M.O., to obtain the electric field gradient in the molecules. Such a method has been proposed by Cotton and Harris [85], and available computed M.O. have been used to derive the quadrupole coupling constants in some heterocyclic molecules [86, 87]

and in ammonia[88]. The use of calculated M.O. may sometimes look deceptive because the values obtained for the coupling constants may differ from the experimental ones. In fact, the coupling is very sensitive to small variations of the charge distribution, especially in the vicinity of the resonant nucleus. Nevertheless, the method may be valuable if one does not pay too much attention to the actual coupling values, concentrating rather on the variations of the coupling in different molecules.

Nitrogen quadrupole resonance investigations are being developed in a steady fashion. Their interest as well as their difficulties have been stressed in the past, and the fact that papers devoted to nitrogen resonances continue to be published illustrates, if proof is needed, the vitality of this branch of spectroscopy and the diversity of the studies involved.

VI. References

1) Marino, R. A., Oja, T.: Chem. Phys. Letters *4*, 489 (1970).
2) Lucas, J. P., Guibé, L.: Molecular Physics *19*, 85 (1970).
3) Das, T.P., Hahn, E.L.: Nuclear Quadrupole Resonance Spectroscopy. Supplement 1 to Solid State Physics, New York: Academic Press 1958.
4) O'Konski, C.T.: Nuclear Quadrupole Resonance Spectroscopy. In: Determination of Organic Structure by Physical Methods (ed. F.C. Nachod, W.D. Phillips). New York: Academic Press 1962.
5) Lucken, E.A.C.: Nuclear Quadrupole Coupling Constants. New York: Academic Press 1969.
6) Abe, Y., Kamishina, Y., Kojima, S.: J. Phys. Soc. Japan *21*, 2083 (1966).
7) Guibé, L.: To be published.
8) Casabella, P.A., Bray, P. J.: J. Chem. Phys. 28, 1182 (1952).
9) Narath, A.: J. Chem. Phys. *40*, 1169 (1964).
10) Watkins, G. D.: Thesis, Harvard (1952).
11) Robinson, F. N. H.: J. Sci. Instr. *36*, 481 (1959).
12) Tzalmona, A.: Phys. Letters *20*, 478 (1966).
13) Colligiani, A., et al.: To be published.
14) Read, M., Colot, J. L.: Proceedings of the XVth Colloque Ampère, Grenoble (1968). Amsterdam: North Holland Publishing Co. 1969.
15) Zussman, A., Alexander, S.: J. Chem. Phys. *48*, 3534 (1968).
16) Péneau, A., Guibé, L.: Unpublished results.
17) Lehrer, S., O'Konski, C. T.: J. Chem. Phys. *43*, 1941 (1965).
18) Bayer, H.: Physik *130*, 227 (1951).
19) Kushida, T.: J. Sci. Hiroshima Univ., Ser. A *19*, 327 (1955).
20) – Benedek, G. B., Bloembergen, N.: Phys. Rev. *104*, 1364 (1956).
21) Gutowsky, H. S., Williams, G. A.: Phys. Rev. *105*, 464 (1957).
22) Matzkanin, G. A., O'Neal, T. N., Scott, T. A., Haigh, P. J.: J. Chem. Phys., *44*, 4171 (1966).
23) – Scott, T. A., Haigh, P. J.: J. Chem. Phys. *42*, 1646 (1965).
24) Haigh, P. J., Canepa, P. C., Matzkanin, G. A., Scott, T. A.: J. Chem. Phys. *48*, 4234 (1968).
25) Abe, Y.: J. Phys. Soc. Japan *18*, 1804 (1963).
26) Negita, H., Casabella, P. A., Bray, P. J.: J. Chem. Phys. *32*, 314 (1960).

27) Zussman, A., Alexander, S.: J. Chem. Phys. *49*, 3792 (1968).
28) Scott, T. A.: Thesis, Harvard (1959).
29) Zussman, A., Alexander, S.: Chem. Phys. *48*, 3534 (1968).
30) Alexander S., Tzalmona, A.: Phys. Rev. *138 A*, 845 (1965).
31) Smith, G. W.: J. Chem. Phys. *43*, 4325 (1965).
32) Zussman, A., Alexander, S.: J. Chem. Phys. *49*, 5179 (1968).
33) Leppelmeier, G. W., Hahn, E. L.: Phys. Rev. *141*, 724 (1966).
34) Choy, W. T. P.: J. Chem. Phys. *46*, 1678 (1967).
35) Colot, J. L.: Thesis, Université de Liège (1970);
36) Eletr, S.: To be published.
37) Haigh, P. J., Scott, T. A.: J. Chem. Phys. *38*, 117 (1963).
38) Widman, R. H.: J. Chem. Phys. *43*, 2922 (1965).
39) Ikeda, R., Onda, S., Nakamura, D., Kubo, M.: J. Phys. Chem. *72*, 2501 (1968).
40) Colot, J. L., Cornil, P.: Compt. Rend. Acad. Sci. (Paris) *265 B*, 613 (1967).
41) Minematsu, M.: J. Phys. Soc. Japan *14*, 1030 (1959).
42) Smith, D. H., Cotts, R. M.: J. Chem. Phys. *41*, 2403 (1964).
43) Townes, C. H., Dailey, B. P.: J. Chem. Phys. *17*, 782 (1949).
44) Sheridan, J., Gordy, W.: Phys. Rev. *79*, 513 (1950).
45) Kato, Y., Fukurane, U., Takeyama, H.: Bull. Chem. Soc. Japan *32*, 527 (1959).
46) Lucken, E. A. C.: Trans. Faraday Soc. *57*, 729 (1961).
47) Guibé, L., Lucken, E. A. C.: Proceedings of the XIII Colloque Ampère, Leuwen (1964). Amsterdam: North Holland Publishing Co. 1965.
48) Schempp, E., Bray, P. J.: J. Chem. Phys. *46*, 1186 (1967).
49) Townes, C. H., Schawlow, A. L.: Microwave Spectroscopy, p. 239. New York: Graw Hill Books 1955.
50) Ref.[5], p. 219.
51) Colligiani, A., Guibé, L., Lucken, E. A. C., Haigh, P.J.: Mol. Phys. *14*, 89 (1968).
52) Onda, S., Ikeda, R., Nakamura, D., Kubo, M.: Bull. Chem. Soc. Japan *42*, 1171 (1969).
53) Casabella, P. A., Bray, P.J.: J. Chem. Phys. *29*, 1105 (1958).
54) Negita, H., Bray, P. J.: J. Chem. Phys. *33*, 1876 (1960).
55) Ikeda, R., Nakamura, D., Kubo, M.: J. Phys. Chem. *70*, 3626 (1966).
56) – – – J. Phys. Chem. *72*, 2982 (1968).
57) Guibé, L., Lucken, E. A. C.: Compt. Rend. Acad. Sci. (Paris) *263*, 815 (1966).
58) Kurland, R. J., Wilson, E.B.: J. Chem. Phys. *27*, 585 (1957).
59) Smyth, C. P.: Dielectric Behavior and Structure. New York: Mc Graw Hill Books 1955.
60) Guibé, L.: Unpublished results.
61) Ray, J.D.: Quoted by R. A. Forman in a private communication.
62) Gourdji, M., Guibé, L.: Compt. Rend. Acad. Sci. (Paris) *260*, 1131 (1965).
63) Oja, T., Marino, R. A., Bray, P. J.: Phys. Letters *26 A*, 11 (1967).
64) Ikeda, R., Mikami, M., Nakamura, D., Kubo, M.: J. Magn. Resonance *1*, 211 (1969).
65) Marino, R. A., Oja, T., Bray, P. J.: Phys. Letters *27 A*, 263 (1968).
66) Oja, T., Marino, R. A., Bray, P. J.: Phys. Letters *28 A*, 16 (1968).
67) Marino, R. A., Bray, P. J.: J. Chem. Phys. *48*, 4833 (1968).
68) Betsuyaku, H.: J. Chem. Phys. *50*, 3117 (1969).
69) Andersson, L. O., Gourdji, M., Guibé, L., Proctor, W. G.: Compt. Rend. Acad. Sci. (Paris) *267 B*, 803 (1968).
70) Guibé, L., Lucken, E. A. C.: Mol. Phys. *10*, 273 (1966).
71) – – Mol. Phys. *14*, 79 (1968).
72) Schempp, E., Bray, P. J.: J. Chem. Phys. *46*, 1186 (1967).
73) Werner, W., Dreizler, H., Rudolph, H. D.: Naturforsch. *A 22*, 531 (1967).
74) Schempp, E., Bray, P. J.: J. Chem. Phys. *49*, 3450 (1968).
75) Ikeda, R., Onda, S., Nakamura, D., Kubo, M.: J. Phys. Chem. *72*, 2501 (1968).
76) Marino, R. A., Guibé, L., Bray, P. J.: J. Chem. Phys. *49*, 5104 (1968).
77) Guibé, L., Lucken, E. A. C.: Mol. Phys. *14, 73* (1968).
78) Schempp, E., Bray, P. J.: J. Chem. Phys. *48*, 2380 (1968).

79) – – Phys. Letters *25 A*, 414 (1967).
80) Guibé, L.: Ann. Phys. *7*, 1177 (1962).
81) Clément, R., Gourdji, M., Guibé, L.: Molecular Physics *21*, 247 (1971).
82) Eletr, S.: Thesis, Berkeley University (1968).
83) Guibé, L., Renard, J. P.: Unpublished results.
84) Brieglieb, G.: Elektronen-Donator-Acceptor-Komplexe. Berlin-Heidelberg-New York: Springer 1961.
85) Cotton, F. A., Harris, C. P.: Proc. Am. Acad. Sci., Serie *M 56*, 12 (1966).
86) Schempp, E., Bray, P. J.: J. Chem. Phys. *48*, 2381 (1968).
87) Eletr, S.: Mol. Phys. *18*, 119 (1970).
88) – Tae Kyu Ha, O'Konski, C. T.: J. Chem. Phys. *51*, 1430 (1969).

Received April 20, 1970

Bestimmung der Kernquadrupolkopplungskonstanten aus Mikrowellenspektren

Prof. Dr. Werner Zeil

Abteilung für Physikalische Chemie am Zentrum Chemie-Physik-Mathematik der Universität Ulm

Inhalt

Abstract

In a rotating molecule containing one quadrupolar nucleus there is an interaction between the angular momentum $\vec{J}$ of the molecule and the nuclear spin momentum $\vec{I}$. The operator of this interaction can be written as a scalar product of two irreducible tensor operators of second rank. The first tensor operator describes the nuclear quadrupole moment and the second describes the electrical field gradient at the position of the nucleus under investigation.

The interaction operator can be written

$$\hat{H} = -(\hat{V}^{(2)} \cdot \hat{Q}^{(2)})$$

where the $2q + 1$ components of each tensor operator can be written in the following manner

$$\hat{Q}_q^{(2)} = \sum_n r_n^2 e_n \hat{C}_q^{(2)}(\theta_n, \phi_n)$$

$$\hat{V}_q^{(2)} = \sum_e \frac{e_e}{r_e^3} \hat{C}_q^{(2)}(\theta_e, \phi_e)$$

$-2 \leqslant q \leqslant +2$. The spherical harmonics $C_q^{(2)}(\theta, \phi)$ are given in the notation of Racah

$$C_0^{(2)}(\theta,\phi) = \frac{1}{2}(3\cos^2\theta - 1)$$

$$C_1^{(2)}(\theta,\phi) = -\frac{\sqrt{6}}{2} e^{i\phi} \sin\theta \cos\phi$$

$$C_2^{(2)}(\theta,\phi) = \frac{\sqrt{6}}{4} e^{i2\phi} \sin^2\theta$$

$$C_{-q}^{(l)}(\theta, \phi) = (-1)^q C_q^{(l)*}(\theta,\phi)$$

Through the interaction described above, the nuclear spin momentum is coupled to the rotation of the molecule with the result that the rotational levels of the molecule are split into a number of components, giving an associated hyperfine structure to the spectra.

Neglecting this interaction, the energy levels can be described by the operator $\hat{H}_{rot}$. The matrixelements of this operator are given below for the most common case of the asymmetric rotor in the S representation.

These functions form a orthonormal set and are proportional to the Jacobian polynomials. The wanted matrix elements are given as follows

$$\langle J\,K\,M\,|\hat{H}_{rot}|\,J\,K\,M\rangle = \frac{\hbar^2}{4}\left\{\left(\frac{1}{I_x} + \frac{1}{I_y}\right)[J(J+1) - K^2] + \frac{2K^2}{I_z}\right\}$$

$$\langle J\,K\,M\,|\hat{H}_{rot}|\,J\,K+2M\rangle = \langle J\,K+2M\,|\hat{H}_{rot}|\,J\,K\,M\rangle =$$

$$= \frac{\hbar^2}{8}\left(\frac{1}{I_y} - \frac{1}{I_x}\right)[(J-K)(J-K-1)(J+K+1)(J+K+2)]^{\frac{1}{2}}$$

For calculating the matrix elements of the operator $\hat{H}_Q$ a so-called "coupled basis" is needed; the simple product function of $|JJ_Z\rangle$ and $|\,II_Z\rangle$ is not suitable because it would not be diagonal in J^2, I^2, F and M_F, where $\vec{F} = \vec{J} + \vec{I}$.

The desired coupled basis will be performed by the methods given by Racah and Wigner. Making use of the Wigner-Racah formalism and of the Wigner-Eckart theorem and observing some rules for the matrix elements of the products of tensor operators, we obtain for the matrix elements of the quadrupole interaction operator $\hat{H}_Q$

$$\langle JKIF|\hat{H}_Q|J'K'IF\rangle =$$

$$= (-1)^{I+J+J'-K+F+1}\,\frac{1}{4}\sqrt{2J'+1}\,\sqrt{2J+1}\,\begin{Bmatrix} F & I & J \\ 2 & J' & I \end{Bmatrix}\cdot\begin{pmatrix} I & 2 & I \\ -I & 0 & I \end{pmatrix}^{-1}\cdot\begin{pmatrix} J & 2 & J' \\ -K & -q & K' \end{pmatrix}\chi_q$$

$$\chi_q = e\,Q\,\chi'_q$$

$$\chi'_0 = \frac{\partial^2 V}{\partial z^2}$$

$$\chi'_{\pm 1} = \mp\sqrt{2/3}\left(\frac{\partial^2 V}{\partial x\,\partial z} \pm \frac{\partial^2 V}{\partial y\,\partial z}\right)$$

$$\chi'_{\pm 2} = \sqrt{1/6}\left(\frac{\partial^2 V}{\partial x^2} - \frac{\partial^2 V}{\partial y^2} \pm 2\mathrm{i}\,\frac{\partial^2 V}{\partial x\,\partial y}\right)$$

The matrix elements for the operator $\hat{H}_{ges} = \hat{H}_{rot} + \hat{H}_Q$, which describes the problem of a rotating molecule containing a quadrupolar nucleus, are obtained by simple addition of the matrix elements of the operators $\hat{H}_{rot}$ and $\hat{H}_Q$. This arises from the fact that $\hat{H}_{rot}$ operates only on the coordinates of the one system described by the rotational coordinates, i.e. the Euler's angles.

The allowed transitions can be calculated in a straightforward manner by constructing the matrix of the dipole moment operator $\hat{\mu}$.

The exact calculation of the rotational levels of a molecule with a quadrupolar nucleus by the method given above needs a large amount of computer storage space. In most cases, therefore, the results used are calculated by means of the perturbation theory of quantum mechanics. This gives the following equations for the perturbation energy in first order.

$$E_Q^1 = \frac{1}{2}\,\frac{e^2 Q}{I(2I-1)\,J(2J-1)}\left[\frac{3}{4}C(C+1) - I(I+1)\,J(J+1)\right]\cdot q_J$$

$$q_J = \frac{J}{2J+3}\left[D_1(J,\tau,\kappa)\left(\frac{\partial^2 V}{\partial a^2}\right) + D_2(J,\tau,\kappa)\left(\frac{\partial^2 V}{\partial b^2}\right)\right]$$

$$D_1(J,\tau,\kappa) = \frac{2}{J(J+1)}\left[E(\kappa) - \kappa\,\frac{dE(\kappa)}{d\kappa}\right]$$

$$D_2(J,\tau,\kappa) = \frac{1}{J(J+1)}\left[E(\kappa) + (3-\kappa)\,\frac{dE(\kappa)}{d\kappa}\right] - 1$$

The equation describes the perturbation energy in terms of the two independent field gradient components χ_{aa} and χ_{bb}, the so-called "reduced rotational energy" $E_\tau^J(\kappa)$ and the

value of $\frac{dE_\tau^J(\kappa)}{d\kappa}$. Both these values are tabulated or can be calculated easily by known computer programs.

The special cases of the symmetric rotor and the linear rotor can be performed by using or neglecting the appropriate quantum numbers in the general expression given above.

The case of *two* quadrupolar nuclei in a molecule, where

$$\hat{H}_{\text{ges}} = \hat{H}_{\text{rot}} + \hat{H}_{Q1} + \hat{H}_{Q2}$$

will be described in the following coupling scheme

$$\vec{I}_1 + \vec{J} = \vec{F}_1; \quad \vec{F}_1 + \vec{I}_2 = \vec{F}$$

The resulting matrix elements, calculated by the exact method using the Wigner-Racah formalism, are as follows

$$\langle I_1 J K F_1 I_2 F M_F | \hat{H}_Q | I_1 J_1' K' F_1' I_2 F M_F \rangle =$$

$$= \frac{1}{4}(-1)^{F_1'+J'+I_1+J-K+1} \delta_{F_1 F_1'} \sqrt{2J+1}\sqrt{2J'+1} \frac{\begin{pmatrix} J & 2 & J' \\ -K & -q & K' \end{pmatrix}}{\begin{pmatrix} I_1 & 2 & I_1 \\ -I_1 & 0 & I_1 \end{pmatrix}} \begin{Bmatrix} F_1' & I_1 & J' \\ 2 & J & I_1 \end{Bmatrix} \chi_{-q}^{(1)}$$

$$+ \frac{1}{4}(-1)^{F+F_1+F_1'+I_1+I_2-K+1} \sqrt{2J+1}\ \sqrt{2J'+1}$$

$$\sqrt{2F_1+1}\ \sqrt{2F_1'+1} \frac{\begin{pmatrix} J & 2 & J' \\ -K & -q & K' \end{pmatrix}}{\begin{pmatrix} I_2 & 2 & I_2 \\ -I_2 & 0 & I_2 \end{pmatrix}} \begin{Bmatrix} F & I_2 & F_1' \\ 2 & F_1 & I_2 \end{Bmatrix} \begin{Bmatrix} I_1 & J' & F_1' \\ 2 & F_1 & J \end{Bmatrix} \chi_{-q}^{(2)}$$

These matrix elements, too, can be reduced to the case of the symmetric rotor or the linear molecule in a straightforward manner. If the assignment and interpretation of a measured microwave spectrum have been done only with first-order perturbation theory, then it is impossible to obtain all the information needed for calculating the complete field gradient tensor. On the other hand, if measurements have been done on *two* isotopic species of a molecule under investigation, then it is possible to work out the components of the field gradient tensor in its main axis system. This requires the following equation, which must be solved by a graphical method.

$$\chi_{aa}(2) = \frac{\alpha x^2 - \beta x \cdot \sqrt{1-x^2} + \gamma}{1-2x^2}$$

$\alpha = c - (c+2a)(u^2 - v^2)$ $\quad x = \sin\theta(1)$ $\quad u = \cos\vartheta$

$\beta = 2(c+2a)\,u\,v$ $\quad a = \chi_{aa}(1)$ $\quad v = \sin\vartheta$

$\gamma = a - v^2(c+2a)$ $\quad c = \chi_{cc}(1)$ $\quad \vartheta = \theta(2) - \theta(1) = \varphi(2) - \varphi(1)$

For the meaning of the different angles, see Fig. 4.

1. Einleitung

An Molekülen im gasförmigen Zustand kann mit Hilfe der Mikrowellenspektroskopie (Rotationsspektroskopie) die *Kernquadrupolkopplungskonstante* oder – besser – der ihr zugrunde liegende *Feldgradiententensor* aus der Feinstruktur von Rotationslinien bestimmt werden. Die dabei erhaltenen Komponenten des Feldgradiententensors werden ausschließlich durch die *Ladungsverteilung im Molekül,* im wesentlichen durch die Bindungselektronen am Quadrupolatom, erzeugt.

Die Mikrowellenspektroskopie ist dabei prinzipiell in der Lage, die Komponenten des Feldgradiententensors in dessen Hauptachsensystem zu bestimmen. Bei bekannter Molekülstruktur lassen sich dann Aussagen über *Vorzugsrichtung und Symmetrie der Ladungsverteilung* in bezug auf die chemische Bindung, an der das Quadrupolatom beteiligt ist, gewinnen. Weiterhin können die erhaltenen Tensorkomponenten dazu dienen, molekulare Wellen-Funktionen für die Elektronenverteilung, die mit quantenchemischen *Ab-Initio*-Rechnungen ermittelt wurden, auf ihre Verläßlichkeit zu prüfen.

Die Aufspaltung der Rotationsenergieniveaus, als deren Folge die Feinstruktur der Absorptionslinien entsteht, wird durch die *Kopplung des Drehimpulses des Moleküls* mit dem *Drehimpuls (Spin) eines oder mehrerer Atomkerne,* die ein Quadrupolmoment besitzen, hervorgerufen. Diese Kopplung geschieht über die Wechselwirkung des molekularen elektrischen Feldgradienten am Kernort mit dem elektrischen Quadrupolmoment des betreffenden Atomkerns.

Den *Gesamt-Hamilton-Operator* für ein *rotierendes* Molekül mit Quadrupolkopplung schreibt man folgendermaßen

$$\hat{H}_{\text{ges}} = \hat{H}_{\text{rot}} + \hat{H}_Q \tag{1}$$

Dabei ist $\hat{H}_{\text{rot}}$ der Operator der Rotationsenergie des Moleküls ohne Wechselwirkung mit dem Quadrupolkern.

$\hat{H}_Q$ ist der Operator für die Wechselwirkungsenergie der elektrischen Ladungen des Moleküls mit dem elektrischen Quadrupolmoment des Atomkerns.

Die Einführung eines Wechselwirkungsoperators $\hat{H}_{\text{rot}Q}$ ist nicht notwendig, da der elektrische Feldgradient am Kernort in hoher Näherung unabhängig vom Rotationszustand ist, obwohl über die Zentrifugalverzerrungseffekte ein solcher Effekt möglich wäre.

Eine exakte Berechnung der Energieniveaus eines rotierenden Moleküls mit Quadrupolkernen setzt, wie Gleichung (1) zeigt, die Kenntnis der Rotationsenergieniveaus dieses Moleküls ohne Wechselwirkung zwischen Drehimpuls des Moleküls und Spin des Quadrupolkerns voraus.

2. Matrixelemente und Eigenfunktionen des Operators $\hat{H}_{rot}$ in der Näherung des starren Rotators

In diesem Abschnitt sollen die Grundbeziehungen zur Berechnung von Rotationsenergieniveaus von Molekülen ohne Quadrupolkern bzw. ohne Wechselwirkung mit demselben sowie die Auswahlregeln für Absorptionsübergänge und die Eigenfunktionen eines rotierenden Moleküls angegeben werden. Es wird dabei von der Näherung des starren Rotators Gebrauch gemacht, d.h. alle angegebenen Beziehungen gelten nur für den Schwingungsgrundzustand unter Vernachlässigung der Zentrifugalverzerrungeffekte. Eine Erweiterung, die diesen Effekt berücksichtigt, ist möglich [1], überschreitet aber den Rahmen dieses Berichtes.

2.1. Asymmetrische Kreiselmoleküle

Den allgemeinsten Fall stellt das *asymmetrische Kreiselmolekül* dar. Für diesen Molekültyp gibt es für die Eigenfunktionen des Rotationsenergieoperators keinen geschlossenen Ausdruck. Die Energie-Eigenwerte müssen dadurch gewonnen werden, daß man die dem Hamilton-Operator $\hat{H}_{rot}$, der das reine Rotationsverhalten des Moleküls beschreibt, entsprechende Matrix numerisch diagonalisiert.

Der Operator lautet [2a,b]

$$\hat{H}_{rot} = \frac{\hat{P}_x^2}{2I_x} + \frac{\hat{P}_y^2}{2I_y} + \frac{\hat{P}_z^2}{2I_z} \tag{2}$$

Dabei bedeuten:

$\hat{P}_g$ $(g = x, y, z)$ die *Drehimpulsoperatoren* um die Hauptträgheitsachsen des Moleküls

I_g $(g = x, y, z)$ die *Hauptträgheitsmomente* (Diagonalelemente des auf Hauptachsen transformierten Trägheitstensors)

Die Matrixelemente dieses Operators werden in der sogenannten *S*-Darstellung angegeben. Es werden hierbei als Basis die Eigenfunktionen des symmetrischen Kreiselmoleküls, die in geschlossener Form geschrieben werden können, verwandt. Diese stellen ein vollständiges, orthonormiertes System dar. Sie werden bei der Behandlung des symmetrischen Kreiselmoleküls – Abschnitt 2.2 – aufgeführt. In dieser Form ist die Darstellung nichtdiagonal, denn in der *S*-Darstellung lauten die nicht verschwindenden Matrixelemente des Operators $\hat{H}_{rot}$ [3]:

$$\langle J\,K\,M \mid \hat{H}_{rot} \mid J\,K\,M\rangle = \frac{\hbar^2}{4}\left[\left(\frac{1}{I_x} + \frac{1}{I_y}\right)[J(J+1) - K^2] + \frac{2K^2}{I_z}\right] \tag{3a}$$

$$\langle J\,K\,M \mid \hat{H}_{rot} \mid J\,K+2\,M\rangle = \langle J\,K+2\,M \mid \hat{H}_{rot} \mid J\,K\,M\rangle =$$

$$= \frac{\hbar^2}{8}\left(\frac{1}{I_y} - \frac{1}{I_x}\right)[(J-K)\,(J-K-1)\,(J+K+1)\,(J+K+2)]^{1/2} \tag{3b}$$

J = die Drehimpulsquantenzahl der Molekülrotation
K = die Projektionsquantenzahl des Drehimpulses auf die Figurenachse des Moleküls
M = die Projektionsquantenzahl des Drehimpulses auf eine raumfeste Achse Z, z.B. auf die Richtung eines äußeren elektrischen Feldes.

Die Achsen x, y, z werden, je nachdem ob der asymmetrische Kreisel sich mehr der gestreckten oder mehr der abgeplatteten Form annähert, auf verschiedene Weise mit den Hauptträgheitsachsen a, b, c verknüpft, wobei stets die Reihenfolge $I_a \leqslant I_b \leqslant I_c$ eingehalten wird.

Bei Molekülen, die dem Grenzfall des gestreckten Kreisels entsprechen, wird folgende Zuordnung – die sogenannte I^r-Darstellung [4] – gewählt:

$$x \to b \quad y \to c \quad z \to a$$

Für die Moleküle, die dem Grenzfall des abgeplatteten Kreisels entsprechen, ist die III^r-Darstellung [4] zweckmäßig:

$$x \to a \quad y \to b \quad z \to c$$

Dementsprechend können die *Rotationskonstanten* bzw. die *Trägheitsmomente*

$$A = \frac{h}{8\pi^2 I_a} \quad B = \frac{h}{8\pi^2 I_b} \quad C = \frac{h}{8\pi^2 I_c} \tag{4}$$

zu den x, y, z zugeordnet werden. In dieser Form werden die Rotationskonstanten in MHz angegeben.

Aus der Form der Matrixelemente [Gleichung (3a u. 3b)] ersieht man, daß die Darstellung in J diagonal ist. Es findet aber eine Verknüpfung der Energieniveaus innerhalb eines J-Blocks durch die Außerdiagonalelemente zwischen K und $K \pm 2$ statt.

Wenn keine Störung vorliegt, ist also J eine „gute Quantenzahl". Aber auch, wenn die Störenergie sehr klein gegen die Energiedifferenz der Rotationsniveaus ist, kann man J noch als „gute Quantenzahl" ansehen. Im störungsfreien Fall ist es immer möglich, durch eine von Wang [5] angegebene Transformation den Rang der Matrizen zu reduzieren. Man erhält folgende Formel für die *Rotationsenergieniveaus des asymmetrischen Kreiselmoleküls* [6]:

$$E_{\text{rot}} = \frac{A+C}{2} J(J+1) + \frac{A-C}{2} E_\tau^J(\kappa) \tag{5}$$

E_{rot} wird hier und im weiteren, der Konvention folgend, in MHz angegeben, d.h. die Rotationskonstanten entsprechen Gleichung (4). $E_\tau^J(\kappa)$ bedeutet die sogenannte *Reduzierte Energie*, die in tabellierter Form in Abhängigkeit von

der Rotationsquantenzahl J, dem Asymmetrieparameter $\kappa = \frac{2B-A-C}{A-C}$ und der Pseudoquantenzahl τ vorliegt [7]. Letztere beziffert die Subniveaus für jede Hauptquantenzahl J in aufsteigender Reihenfolge der Energie und läuft von $-J$ bis $+J$.

Die Intensitäten der Rotationslinien und damit die Auswahlregeln hängen jeweils von einer der im Molekül vorhandenen Dipolmomentkomponenten in Richtung der drei Hauptträgheitsachsen und vom Asymmetrieparameter κ ab. Jeder endlichen Dipolmomentkomponente entspricht sozusagen ein eigenes Spektrum. Außerdem sind die Intensitäten abhängig von J und τ. Sie können Spezialtabellen entnommen werden [8]. Auf ihre Berechnung kann hier nicht eingegangen werden.

Die Rotationseigenfunktionen eines asymmetrischen Kreiselmoleküls werden auf numerischem Wege bei der Diagonalisierung der Energiematrix als Linearkombination der Eigenfunktionen des symmetrischen Kreiselmoleküls erhalten. Die Spaltenvektoren der Transformationsmatrix, die die Diagonalisierung gemäß der Gleichung

$$(E_{\text{Diag}}) = V^{\dagger}\,(H_{\text{rot}})\,V \tag{6}$$

bewirkt, liefern die Gewichte der gesuchten Linearkombination.

2.2. Symmetrische Kreiselmoleküle

Im symmetrischen Kreiselmolekül sind per definitionem zwei Hauptträgheitsmomente und damit auch zwei Rotationskonstanten gleich. Dieser Molekültyp besitzt mindestens C_3-Symmetrie. Die Energieniveaus erhält man aus den für den asymmetrischen Kreisel angegebenen Matrixelementen, wenn man $I_x = I_y$ setzt.

Dabei verschwinden die Matrixelemente nichtdiagonal in K. Für die Energieniveaus des gestreckten symmetrischen Kreisels ($I_a < I_b = I_c$) ergibt sich

$$E_{\text{rot}} = B\,J(J+1) + (A-B)\,K^2 \tag{7a}$$

und für den abgeplatteten symmetrischen Kreisel ($I_a = I_b < I_c$) gilt

$$E_{\text{rot}} = B\,J(J+1) + (C-B)\,K^2. \tag{7b}$$

Es gelten die Auswahlregeln $\Delta J = 0 \pm 1$, $\Delta K = 0$. $\Delta J = 0$ tritt nur dann auf, wenn ein Inversionsspektrum [9] vorliegt.

Die Eigenfunktionen des symmetrischen Kreisels, die die Basis der oben angeführten S-Darstellung liefern, lauten [10]:

$$|\psi(\alpha,\beta,\gamma)> = N_{JKM}\, e^{i(M\alpha+K\gamma)} t^{d/2}\, (1-t)^{s/2} w(s,p,d,t) \qquad (8)$$

$$t = \frac{1}{2}(1-\cos\beta)$$

$$(1-t) = \frac{1}{2}(1+\cos\beta)$$

$$d = |M-K|$$

$$s = |M+K|$$

$$w(s,p,d,t) = \sum_{r=0}^{p} (-1)^r \binom{p}{r} \frac{(d+s+p+r)!\,d}{(d+s+p)!(d+r)!}\, t^r$$

$$p = J - \mathrm{Max}\,(|M|, |K|)$$

N_{JKM} = Normierungsfaktor

Über den Zusammenhang der Funktion $w(s, p, d, t)$ mit dem Jakobischen Polynom und den Matrixelementen der Gruppe der endlichen Drehungen – diese werden später benötigt – sei auf den Anhang verwiesen. Die in den Eigenfunktionen auftretenden Winkel α,β und γ entsprechen den Eulerschen Winkeln, deren Bedeutung aus Abb. 1 hervorgeht.

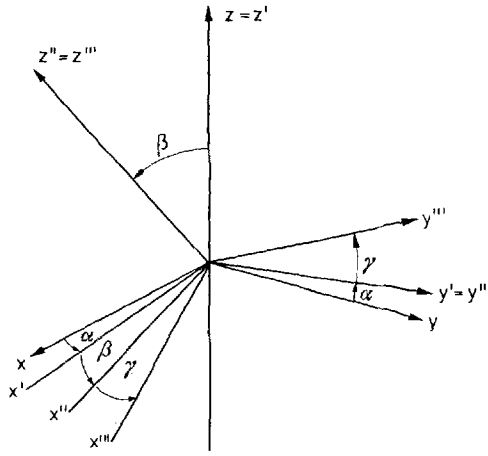

Abb. 1

Eine beliebige Drehung, beschrieben durch den Operator $\hat{D}(\alpha,\beta,\gamma) = \hat{D}(\omega)$ entspricht folgenden Einzeldrehungen:

1. Drehung um die Achse z um den Winkel α
2. Drehung um die Achse y' um den Winkel β
3. Drehung um die Achse z'' um den Winkel γ

2.3. Lineare Kreiselmoleküle

Das lineare Kreiselmolekül ist ein Spezialfall des symmetrischen Kreisels, bei dem kein Drehimpuls um die Molekülachse auftreten kann, d.h. $K = 0$ ist.

Damit lauten die Beziehungen für die Energieniveaus:

$$E_{rot} = B\,J(J+1) \tag{9a}$$

Für die Auswahlregel gilt $\Delta J = \pm 1$.

Für die Eigenfunktionen ergibt sich jetzt:

$$\psi_J = N_{JM}\, e^{iM\alpha}\, P_J^M\ (\cos\beta) \tag{9b}$$

Auf die experimentellen Grundlagen und Möglichkeiten der Mikrowellenspektroskopie kann hier nicht eingegangen werden; es sei auf die Literatur [11] verwiesen.

Es soll lediglich festgestellt werden, daß zur Bestimmung der durch die Kernquadrupolkopplung bedingten Feinstruktur von Rotationslinien bei Kernen mit kleinem Quadrupolmoment oder wenn Bindungen mit „hohem Ionencharakter" das Atom mit Quadrupolkern binden, Mikrowellenspektrometer mit sehr hohem Auflösungsvermögen erforderlich sind [12].

3. Matrixelemente des Wechselwirkungs-Operators $\hat{H}_Q$ und des Dipolmoment-Operators $\hat{\mu}$

3.1. Exakte Behandlung für einen Quadrupolkern im Molekül

Nachdem im Abschnitt 2 der erste Teil von $\hat{H}_{ges}$ [Gleichung (1)], d.h. die Matrixelemente des Operators $\hat{H}_{rot}$ behandelt wurden, soll in diesem Abschnitt die Bestimmung der Matrixelemente des Operators $\hat{H}_Q$, der die Wechselwirkung des Quadrupolkernes mit dem Molekülrumpf vermittelt, beschrieben werden.

3.1.1. Die Multipolentwicklung der elektrostatischen Wechselwirkung

Die genannte Wechselwirkung soll zunächst klassisch berechnet werden durch die sogenannte Multipol-Entwicklung [13], um dann auf die quantenmechanische Formulierung übergehen zu können. Es soll ein vereinfachter Fall, bestehend aus zwei Ladungsbereichen, behandelt werden. Im Bereich 1 befinden sich nur die positiven Ladungen des Atomkerns. Außerhalb dieses Bereiches – im Bereich 2 – befinden sich die negativen Ladungen der Elektronen. Die endliche Ausdehnung der Ladungsträger, wie sie die Quantenmechanik fordert, ist vernachlässigt. Es zeigen die Vektoren $r_{n\alpha}$ vom Ursprung eines beliebigen Koordinatensystems zu einer positiven Ladung $e_{n\alpha}$. Die Vektoren $r_{e\beta}$ gehen vom Ursprung

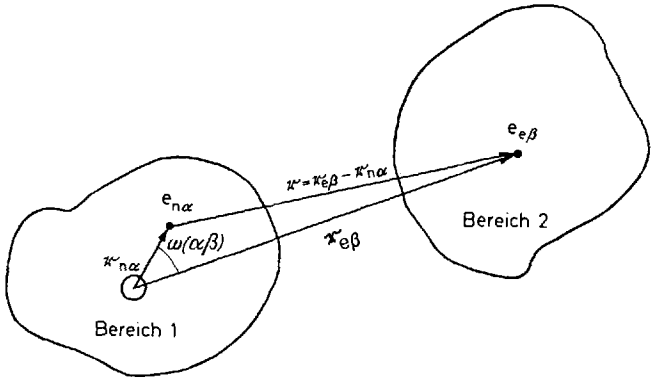

Abb. 2
$e_{n\alpha}$ = Punktladung α im Bereich B_1 (positive Ladung)
$e_{e\beta}$ = Punktladung β im Bereich B_2 (negative Ladung)
$r_{n\alpha}$ = Ortsvektor von $e_{n\alpha}$
$r_{e\beta}$ = Ortsvektor von $e_{e\beta}$

des Koordinatensystems zu den negativen Ladungen $e_{e\beta}$. Die Differenz dieser beiden Vektoren

$$r = r_{e\beta} - r_{n\alpha}$$

bedeutet damit den Abstand zweier verschiedener Ladungen. Die Wechselwirkung der Ladungen in den beiden Bereichen wird jetzt beschrieben durch

$$H = e\,V = -\sum_{\alpha\beta} \frac{e_{n\alpha} e_{e\beta}}{|r_{e\beta} - r_{n\alpha}|} \tag{10}$$

Diese Gleichung läßt sich schreiben:

$$H = -\sum_{\alpha\beta} \frac{1}{r_{e\beta}} \frac{e_{n\alpha}\, e_{e\beta}}{\left[1 - \dfrac{2r_{n\alpha}}{r_{e\beta}} \cos\omega_{\alpha\beta} + \left(\dfrac{r_{n\alpha}}{r_{e\beta}}\right)^2\right]^{1/2}} \tag{11a}$$

wobei der Winkel $\omega_{\alpha\beta}$ die in Abb. 2 angegebene Bedeutung hat. Man kann nun den Ausdruck (11a) nach Legendreschen Polynomen entwickeln, da

$$\frac{1}{(1 - 2xy + y^2)^{1/2}} = \sum_{l=0}^{\infty} P_l(x)\, y^l \tag{11b}$$

gilt, wobei $x = \cos\omega_{\alpha\beta}$ und $y = \dfrac{r_{n\alpha}}{r_{e\beta}}$ gesetzt wird.

Man erhält so die sogenannte *Multipolentwicklung* der Wechselwirkung von Ladungsverteilungen nach Legendreschen Polynomen:

$$H = -\sum_{l=0}^{\infty} \sum_{\alpha\beta} e_{n\alpha} e_{e\beta} \frac{r_{n\alpha}^{l}}{r_{e\beta}^{(l+1)}} P_l(\cos \omega_{\alpha\beta}) \tag{12}$$

Das Glied $l = 0$ bedeutet die Coulomb-Energie, das Glied $l = 1$ die Dipolenergie. Für das hier behandelte Problem ist nur das Glied $l = 2$, das den Quadrupolanteil der Wechselwirkungsenergie enthält, von Interesse. Dieser Anteil entspricht klassisch dem Produkt des Quadrupolmoment-Tensors mal dem Feldgradienten-Tensor, wie im folgenden gezeigt wird. Das Additionstheorem für Kugelfunktionen [14] erlaubt es, Legendresche Polynome als Summe von Produkten jeweils zweier Kugelfunktionen zu schreiben:

$$P_l(\cos \omega) = \sum_{q=-l}^{+l} (-1)^q C_q^{(l)}(\theta_1 \phi_1) C_{-q}^{(l)}(\theta_2 \phi_2) \tag{13}$$

Dabei ist ω der Winkel zwischen zwei Vektoren, deren Richtung durch die Polarkoordinaten $\theta_1 \phi_1$ und $\theta_2 \phi_2$ gegeben wird. Die Kugelfunktionen selbst sind in der obigen Beziehung – einem Vorschlag von Racah entsprechend [15] – besonders normiert. Sie können in dieser Form als *irreduzible Tensoroperatoren* l-ter Stufe aufgefaßt werden, da für diese gefordert wird, daß sie sich so wie die Kugelfunktionen transformieren [16]. Die uns allein interessierenden Funktionen mit $l = 2$ lauten:

$$C_0^{(2)}(\theta\phi) = \frac{1}{2}(3\cos^2\theta - 1)$$

$$C_1^{(2)}(\theta\phi) = -\frac{\sqrt{6}}{2} e^{i\phi} \sin\theta \cos\phi$$

$$C_2^{(2)}(\theta\phi) = \frac{\sqrt{6}}{4} e^{i2\phi} \sin^2\theta$$

wobei noch folgende Symmetriebedingung gilt:

$$C_{-q}^{(l)}(\theta\phi) = (-1)^q C_q^{(l)*}(\theta\phi)$$

Wir drücken jetzt den Quadrupolanteil der Wechselwirkungsenergie unseres Ladungssystems (Abb. 2) folgendermaßen als Funktion von Kugelfunktionen aus:

$$H = -\sum_{q=-2}^{+2} (-1)^q \sum_e \frac{e_e}{r_e^3} C_q^{(2)}(\theta_e \phi_e) \sum_n r_n^2 e_n C_{-q}^{(2)}(\theta_n \phi_n) \tag{14a}$$

Diesen Ausdruck können wir nun als Skalarprodukt zweier irreduzibler Tensoren 2. Stufe ansehen (Reduktion auf die Stufe Null):

$$H = -(\underset{\sim}{V}^{(2)} \cdot \underset{\sim}{Q}^{(2)})$$

Jeder dieser irreduziblen Tensoren 2. Stufe hat $2q + 1 = 5$ Komponenten, die sich folgendermaßen schreiben:

$$Q_q^{(2)} = \sum_n r_n^2 e_n C_q^{(2)}(\theta_n \phi_n) \tag{14b}$$

$$V_q^{(2)} = \sum_e \frac{e_e}{r_e^3} C_q^{(2)}(\theta_e \phi_e) \tag{14c}$$

Wie ersichtlich, sind die Tensoren in der sphärischen Basis geschrieben, in der sie im Gegensatz zur kartesischen Basis irreduzibel sind. Zwischen den sphärischen Komponenten und den kartesischen Tensorkomponenten besteht folgender Zusammenhang:

$$\begin{aligned} T_0 &= T_{zz} \\ T_{\pm 1} &= \mp \sqrt{\frac{2}{3}} (T_{xz} \pm i\, T_{yz}) \\ T_{\pm 2} &= \sqrt{\frac{1}{6}} (T_{xx} - T_{yy} \pm 2\, i\, T_{xy}) \end{aligned} \tag{15}$$

Man sieht aus (14b) und (14c), daß der Tensor $\underset{\sim}{Q}$ nur von den Größen aus dem Bereich B_1 und der Tensor $\underset{\sim}{V}$ nur von Größen aus dem Bereich B_2 abhängig ist.

Geht man jetzt von der klassischen zur quantenmechanischen Darstellung über, so werden alle Tensoren durch Tensor-Operatoren ersetzt, $\underset{\sim}{T} \to \hat{T}$. Gemäß dem oben Ausgeführten werden die Kugelfunktionen $C_q^{(2)}$ nun als irreduzible Tensor-Operatoren 2. Stufe betrachtet.

Welche Bedeutung haben nun diese *Tensor-Operatoren?*

Hierzu sei zunächst die Nullkomponente des Q-Tensor-Operators betrachtet. Sie schreibt sich

$$\hat{Q}_0^{(2)} = \sum_n r_n^2\, e_n \hat{C}_0^{(2)}(\theta_n, \phi_n) = \frac{1}{2} \sum_n e_n (3 z_n^2 - r_n^2) \tag{16}$$

Daraus ist ersichtlich, daß dieser Ausdruck proportional dem in der Elektrizitätslehre formulierten *klassischen Quadrupolmoment* ist, das für eine Ladungsverteilung $\rho(x,y,z)$ folgendermaßen angegeben wird:

$$Q^{(\text{klassisch})} = e \int (3z^2 - r^2)\, \rho\,(x,y,z)\, dx\, dy\, dz$$

Diese Analogie berechtigt, den $\underset{\sim}{Q}$-Tensor, bzw. den ihm entsprechenden Operator als Quadrupolmoment-Tensor-Operator zu bezeichnen. Er besteht aus einem Satz von fünf linear unabhängigen Komponenten $Q_q^{(2)}$, wobei

$$q = -2, -1, 0, 1, 2.$$

Die Nullkomponente des $\hat{V}$-Tensoroperators läßt sich folgendermaßen schreiben:

$$\hat{V}_0^{(2)} = \sum_e \frac{e_e}{r_e^3} \hat{C}_0^{(2)}(\theta_e, \phi_e) = \sum_e \hat{\partial}_0^2 (r_e, \theta_e, \phi_e) \frac{e_e}{r_e} \tag{17}$$

wobei $\hat{\partial}_0^2\ (r_e, \theta_e, \phi_e)$ als irreduzibler Differentialoperator in Polarkoordinaten aufzufassen ist. Aus dieser Schreibweise erkennt man, daß der V-Tensor durch die zweite Ableitung des elektrostatischen Potentials am Ort des Atomkerns verstanden werden kann, da

$$\frac{\partial^2 V}{\partial r_e^2} \sim \frac{1}{r^3} \tag{18}$$

Er entspricht also dem Gradienten des elektrischen Feldes und kann damit Feldgradiententensor genannt werden, wie oben bereits getan. Auch er besteht aus fünf linear unabhängigen Komponenten $\hat{V}_q^{(2)}$ wobei wiederum

$$q = -2, -1, 0, 1, 2.$$

3.1.2. Die „gekoppelte Darstellung" und das Wigner-Eckart-Theorem

Der Operator $\hat{H}_Q$ kann – wie in Gleichung (14) gezeigt wurde – als Skalarprodukt zweier irreduzibler Tensoroperatoren 2. Stufe dargestellt werden

$$\hat{H}_Q = -(\hat{V} \cdot \hat{Q}) .$$

Zur Berechnung der Matrixelemente von $\hat{H}_Q$ müssen die Eigenfunktionen $|\psi\rangle$ des Systems bekannt sein. Dieses System besteht bei dem hier zunächst betrachteten Fall eines Moleküls mit *einem* Quadrupolkern aus zwei miteinander gekoppelten Drehimpulsen $\vec{j}_1$ und $\vec{j}_2$, dem Drehimpuls des Moleküls und dem Drehimpuls des Quadrupolkerns. Für die beiden Drehimpulse gelten zunächst folgende Beziehungen:

$$\hat{J}_1^2 |j_1 m_1\rangle = j_1(j_1+1)|j_1 m_1\rangle;\ \hat{J}_2^2 |j_2 m_2\rangle = j_2(j_2+1)|j_2 m_2\rangle \tag{19a}$$

$$\hat{J}_{z_1} |j_1 m_1\rangle = m_1 |j_1 m_1\rangle ; \qquad \hat{J}_{z_2} |j_2 m_2\rangle = m_2 |j_2 m_2\rangle \tag{19b}$$

Die beiden Drehimpulsoperatoren wirken dabei auf verschiedene Räume (1) bzw. (2). Das Produkt der beiden Eigenfunktionen

$$|j_1 m_1\rangle \cdot |j_2 m_2\rangle$$

bezeichnet man als *ungekoppelte Darstellung*. In dieser Darstellung sind $\hat{J}_1^2$, $\hat{J}_{z_1}$ und $\hat{J}_2^2$, $\hat{J}_{z_2}$ diagonal. Der Gesamtdrehimpulsoperator $\hat{J}$ ist definiert durch

$$\hat{J} = \hat{J}_3 = \hat{J}_1 + \hat{J}_2 .$$

Gesucht wird jetzt eine Darstellung, in der $\hat{J}_3^2$ und $\hat{J}_3$ ebenso wie $\hat{J}_1^2$ und $\hat{J}_2^2$ diagonal sind, wobei für $\hat{J}_3^2$ und $\hat{J}_{z_3}$ die Eigenwerte $J_3(J_3+1)$ und m_3 sein sollen. Eine solche Darstellung, die *gekoppelte Darstellung* genannt wird, erhält man aus der ungekoppelten Darstellung durch eine unitäre Transformation [17]

$$|j_1 j_2 j_3 m_3\rangle = \sum_{m_1 m_2} C(j_1 j_2 j_3; m_1 m_2 m_3) \cdot |j_1 m_1\rangle \cdot |j_2 m_2\rangle \qquad (20a)$$

Die Koeffizienten $C(j_1 j_2 j_3; m_1 m_2 m_3)$ dieser Transformation sind die sogenannten Clebsch-Gordan-Koeffizienten. Sie sind eng verknüpft mit den Wignerschen *3j*-Symbolen [18], siehe Anhang D.

Gleichung (20a) lautet in *3j*-Symbolen:

$$|j_1 j_2 j_3 m_3\rangle = (-1)^{j_2 - j_1 - m_3} (2j_3 + 1)^{1/2} \sum_{m_1 m_2} \begin{pmatrix} j_1 & j_2 & j_3 \\ m_1 & m_2 & -m_3 \end{pmatrix} |j_1 m_1\rangle \cdot |j_2 m_2\rangle \qquad (20b)$$

Dabei muß gelten $m_1 + m_2 = m_3$ und $|j_1 - j_2| \leqslant j_3 \leqslant |j_1 + j_2|$.

Die Clebsch-Gordan-Koeffizienten bzw. die *3j*-Symbole, die wir im folgenden verwenden, liegen in tabellierter Form für die jeweilige Kombination von Drehimpulsen bzw. Spinquantenzahlen und den entsprechenden Projektionsquantenzahlen vor [18]. Über Schreibweise und Eigenschaften der *3j*-Symbole siehe Anhang D.

Die Matrixelemente eines irreduziblen Tensoroperators k-ter Stufe lassen sich nun durch die *3j*-Symbole und ein sogenanntes *„Reduziertes Matrixelement"* des betreffenden Tensoroperators darstellen. Dieser Zusammenhang ist durch das *Wigner-Eckart-Theorem* gegeben [19]:

$$\langle J M | \hat{T}_q^{(k)} | J' M' \rangle = (-1)^{J-M} \begin{pmatrix} J & k & J' \\ -M & q & M' \end{pmatrix} \langle J \| \hat{T}^{(k)} \| J' \rangle \qquad (21)$$

Dieses Theorem kann folgendermaßen interpretiert werden:

Die Matrixelemente jeder Komponente q eines irreduziblen Tensoroperators k-ter Stufe können in der Darstellung der Drehimpulse aufgespalten werden in ein Produkt aus einem *3j*-Symbol, das die geometrische Situation durch die Quantenzahlen des quantenmechanischen Systems und deren Projektionsquantenzahlen beschreibt, und eine Größe, die für alle Komponenten des Tensors gleich ist und nicht von der räumlichen Quantisierung abhängt, d.h. lediglich die physikalische Natur des Systems beinhaltet. Diese Größe heißt *Reduziertes Matrixelement (double bar element)* des Tensors und wird geschrieben

$$\langle J \| \hat{T} \| J' \rangle .$$

Dies bedeutet gleichfalls, daß die Matrixelemente für alle irreduziblen Tensoroperatoren einer gegebenen Stufe nur durch einen Skalenfaktor voneinander verschieden sind, nämlich um die Reduzierten Matrixelemente. Diese lassen sich im allgemeinen leicht ermitteln.

3.1.3. Die Matrixelemente von $\hat{H}_Q$ für Moleküle mit einem Quadrupolkern

Zur Lösung unseres Problems benötigen wir aber die Matrixelemente *eines Skalarproduktes von zwei Tensoroperatoren.* Dabei wirken diese Operatoren

auf verschiedene Teilsysteme (Räume): Der $\hat{Q}$-Tensoroperator wirkt nur auf die Koordinaten des Kerns und der $\hat{V}$-Tensoroperator nur auf die Koordinaten der Elektronen.

Ein Reduziertes Matrixelement des Produktes zweier Tensoroperatoren kann in der gekoppelten Basis allgemein folgendermaßen dargestellt werden, wobei $\hat{X}^{(G)}$ ein Tensoroperator G-ter Stufe des Produktes der Operatoren $\hat{T}^{(k_1)}$ und $\hat{U}^{(k_2)}$ bedeutet [20)*]:

$$\langle \gamma j_1 j_2 j_3 \| \hat{X}^{(G)} \| \gamma' j_1' j_2' j_3' \rangle = \sum_{\gamma''} \langle \gamma j_1 \| \hat{T}^{(k_1)} \| \gamma'' j_1' \rangle \langle \gamma'' j_2 \| \hat{U}^{(k_2)} \| \gamma' j_2' \rangle \cdot$$

$$\cdot [(2j_3+1)(2j_3'+1)(2G+1)]^{\frac{1}{2}} \begin{Bmatrix} j_1 & j_1' & k_1 \\ j_2 & j_2' & k_2 \\ j_3 & j_3' & G \end{Bmatrix} \qquad (22)$$

Der Wert in { } ist in diesem Fall ein *9j*-Symbol [21)*], das als Summe von Produkten von *3j*-Symbolen dargestellt werden kann. γ steht symbolisch für alle Quantenzahlen des Systems, auf die der betreffende Operator *nicht* wirkt. Das Matrixelement enthält die Reduzierten Matrixelemente der beiden, an der Produktbildung beteiligten Tensoroperatoren. Im speziellen Fall der Reduktion auf die Stufe Null ($G = 0$) bei der Produktbildung, d.h. wenn ein Skalarprodukt gesucht ist wie in dem vorliegenden Fall, wo ein Energiewert berechnet werden soll, reduziert sich das *9j*-Symbol auf ein *6j*-Symbol, das ebenfalls als Produkt von *3j*-Symbolen dargestellt werden kann [22)]. Es resultiert folgende Beziehung für die Matrixelemente des Skalarproduktes von zwei vertauschbaren irreduziblen Tensoroperatoren gleicher Stufe [20)] (die Operatoren sind in unserem Fall vertauschbar, da sie auf verschiedene Räume wirken):

$$\langle \gamma j_1 j_2 j_3 m_3 \mid \hat{T}^{(k)} \hat{U}^{(k)} \mid \gamma' j_1' j_2' j_3' m_3' \rangle =$$

$$= (-1)^{j_1'+j_2+j_3} \delta_{j_3 j_3'} \delta_{m_3 m_3'} \begin{Bmatrix} j_3 & j_2 & j_1 \\ k & j_1' & j_2' \end{Bmatrix} \cdot \sum_{\gamma'} \langle \gamma'' j_1 \| \hat{T}^{(k)} \| \gamma' j_1' \rangle \langle \gamma' j_2 \| \hat{U}^{(k)} \| \gamma'' j_2' \rangle \qquad (23)$$

Man entnimmt der Beziehung, daß die Darstellung in j_3 und m_3 diagonal ist. Für den gegebenen speziellen Fall der Kopplung des Drehimpulses des Moleküls mit dem Spin eines Quadrupols wählt man eine gekoppelte Darstellung, bestehend aus einer Linearkombination von Produkten der Eigenfunktion des symmetrischen Kreiselmoleküls (*S*-Darstellung) und den Spin-Eigenfunktionen des quadrupol-behafteten Atomkerns. Die Matrixelemente des gesuchten Skalarproduktes lauten dann:

$$\langle J\, K\, I\, F\, M_F | -\hat{V}^{(2)} \hat{Q}^{(2)} | J'\, K'\, I\, F'\, M_F' \rangle = \langle J\, K\, I\, F\, M_F | \hat{H}_Q | J'\, K'\, I\, F'\, M_F' \rangle =$$

$$= (-1)^{I+J'+F+1} \cdot \delta_{FF'} \delta_{M_F M_F'} \begin{Bmatrix} F & I & J \\ 2 & J' & I \end{Bmatrix} \langle J\, K \| \hat{V} \| J' K' \rangle \langle I \| \hat{Q} \| I \rangle \qquad (24)$$

* Siehe auch Anhang F.

Hier und im folgenden wird von der Voraussetzung ausgegangen, daß sich I nicht ändert, da die dazu erforderliche Energie sehr hoch ist gegenüber der Rotationsenergie. Das bedeutet, daß die Darstellung als diagonal in I angesehen werden kann. Sie ist stets in F und M_F diagonal, d.h. F und M_F sind „gute Quantenzahlen".

Zur Aufstellung der Matrix, die die Wechselwirkungsenergie zwischen Rotator und Quadrupolkern beschreibt, benötigt man also die Kenntnis von *6j*-Symbolen, die tabelliert sind [22], der reduzierten Matrixelemente des Feldgradiententensors in der *S*-Darstellung (Eigenfunktion in der Darstellung des symmetrischen Kreisels) und des Quadrupolmoment-Tensors in der Spindarstellung.

Zur *Bestimmung des reduzierten Matrixelementes des Quadrupolmoment-Tensors* wird ausgegangen vom experimentell bekannten Quadrupolmoment eines Atomkerns mit der Ladung e. Dieser Wert wird üblicherweise mit dem Erwartungswert der Nullkomponente des Quadrupoltensors mit der größtmöglichen Projektionsquantenzahl $M = I$ gleichgesetzt. Es gilt also:

$$\frac{e\,Q}{2} = \langle I\, M_I = I \,\|\, \hat{Q}_0^{(2)} \,\|\, I\, M_I = I \rangle$$

Da nunmehr eine Komponente des Quadrupolmoment-Tensors bekannt ist, kann das Wigner-Eckart-Theorem angewandt werden. Man erhält so das Reduzierte Matrixelement

$$\langle I \,\|\, \hat{Q}^{(2)} \,\|\, I \rangle = \frac{\langle I M_1 = I \,|\, \hat{Q}_0^{(2)} \,|\, I M_I = I \rangle}{\begin{pmatrix} I & 2 & I \\ -I & 0 & I \end{pmatrix}} = \frac{e\,Q}{2} \cdot \frac{1}{\begin{pmatrix} I & 2 & I \\ -I & 0 & I \end{pmatrix}} \qquad (25)$$

Das Reduzierte Matrixelement des Feldgradiententensors läßt sich mit Hilfe des Wigner-Eckart-Theorems durch das Matrixelement der Nullkomponente des Feldgradiententensors ausdrücken. Man setzt dabei in Analogie zum vorhergehenden Fall

$$M_J = M_J' = J'$$

Es gilt dann

$$\langle J\, K \,\|\, \hat{V}^{(2)} \,\|\, J'\, K' \rangle = (-1)^{J'-J} \frac{\langle J\, K\, M_J = J' \,|\, \hat{V}_0^{(2)} \,|\, J'\, K'\, M_J' = J' \rangle}{\begin{pmatrix} J & 2 & J' \\ -J' & 0 & J' \end{pmatrix}} \qquad (26a)$$

Aufgrund des Zusammenhangs der sphärischen Komponente mit den kartesischen Komponenten des Tensors, Gleichung (15), kann man dies aber auch folgendermaßen schreiben:

$$\langle J\,K \parallel \hat{V}^{(2)} \parallel J'\,K' \rangle = (-1)^{J'-J} \frac{\langle J\,K M_J = J' \mid \hat{V}_{ZZ} \mid J'\,K'\,M'_J = J' \rangle}{\begin{pmatrix} J & 2 & J' \\ -J' & 0 & J' \end{pmatrix}} \qquad (26b)$$

Dabei bedeutet $\hat{V}_{ZZ}$ die Komponente des Feldgradientenoperators in Richtung einer raumfesten Achse Z am Ort des Quadrupolkerns. Die Beziehung (26b) setzt bei der Berechnung des Reduzierten Matrixelementes $\langle J\,K \parallel \hat{V}^{(2)} \parallel J'\,K' \rangle$ voraus, daß das Matrixelement $\langle J\,K M_J = J' \mid \hat{V}_{ZZ} \mid J'\,K' M'_J = J' \rangle$ – das ja ein Integral darstellt – angebbar ist. Dies ist unmittelbar möglich für die Fälle des linearen und des symmetrischen Kreisels (siehe Abschnitt 3.2.). Für den Fall des asymmetrischen Kreisels werden für $J = J'$ in der Literatur verschiedene, einander äquivalente Ausdrücke angegeben, die eine Auswertung gestatten [23].

Für den Fall $J' \neq J$ ist zwar ebenfalls eine Auswertung möglich, jedoch erfordert sie einen erheblichen rechnerischen Aufwand. Aus diesem Grund werden die angegebenen Ausdrücke für das Reduzierte Matrixelement in der kartesischen Basis nur bei der störungstheoretischen Behandlung 1. Ordnung der Quadrupolfeinstruktur von Mikrowellenspektren benutzt (siehe Abschnitt 4).

Hier soll *ein anderer Weg* gewählt werden, der zu geschlossenen Ausdrücken für das Matrixelement

$$\langle J\,K \parallel \hat{V}_0^{(2)} \parallel J'\,K' \rangle$$

und damit auch für die Wechselwirkungsenergie führt. Zur Auswertung spaltet man die Nullkomponente des Feldgradiententensoroperators $\hat{V}_0$ noch einmal auf in ein Skalarprodukt von zwei Tensoroperatoren, indem man das schon einmal benutzte Additionstheorem der Kugelfunktionen [Gleichung (13)] anwendet. Man erhält so folgenden Ausdruck

$$\hat{V}_0^{(2)} = \sum_e \frac{e_e}{r_e^3} \hat{C}_0^{(2)}(\omega_e, \varphi_e) \doteq \sum_{q=-2}^{+2} (-1)^q \hat{C}_q^{(2)}(\theta, \phi) \sum_e \frac{e_e}{r_e^3} \hat{C}_{-q}^{(2)}(\theta_e, \phi_e) \qquad (27)$$

Hierbei bedeuten θ und ϕ die Winkel der raumfesten Z-Achse gegenüber dem körperfesten Koordinatensystem, für das im allgemeinen das Hauptträgheitsachsensystem gewählt wird, θ_e und ϕ_e die Winkel des e-ten Lagevektors der Ladung e_e, bezogen auf das körperfeste Koordinatensystem, ω_e und φ_e sind die Winkel zwischen der raumfesten Achse und dem betreffenden Lagevektor der Ladung.

Die angegebene Gleichung bedeutet damit die *Transformation des Feldgradiententensors vom körperfesten in das raumfeste Koordinatensystem.* Der Term $\hat{C}_q^{(2)}(\theta, \phi)$ enthält als wesentliche Bestandteile die Richtungs-Cosinus der beiden Koordinatensysteme.

Nun läßt sich das *Matrixelement der Nullkomponente* des Feldgradiententensors berechnen. Dabei faßt man die Summe, die sich über die Koordinaten der Ladungen im körperfesten System erstreckt, zusammen. Dann kann man schreiben:

$$\frac{1}{2}\chi'_q = \sum_e \frac{e_e}{r_e^3} C_q^{(2)}(\theta_e, \phi_e)$$

Die Größe χ'_q kann bei der Bildung des Matrixelementes als konstanter Faktor vor die Integration genommen werden, da diese sich nur über die Winkel θ und ϕ erstreckt und nur diese Winkel zwischen raumfester Achse und körperfestem Koordinatensystem bzw. die ihnen entsprechenden Eulerschen Winkel in den Eigenfunktionen für den symmetrischen Kreisel (S-Darstellung) auftreten. Zwischen den Polarkoordinaten θ und ϕ und den Eulerschen Winkeln β und γ besteht folgende Beziehung

$$\theta = \beta, \quad \phi = \pi - \gamma$$

Es sind also nur noch folgende Matrixelemente zu berechnen:

$$\langle J K M | \hat{C}_q^{(2)}(\theta, \phi) | J' K' M \rangle$$

Damit schreibt sich das gesuchte Matrixelement in Integralform:

$$\langle J K M | \hat{C}_q^{(2)}(\beta, \pi-\gamma) | J' K' M \rangle =$$

$$= \int_0^{2\pi} \int_0^{\pi} \int_0^{2\pi} \psi^{J*}_{MK}(\alpha,\beta,\gamma)\, \hat{C}_q^{(2)}(\beta,\pi-\gamma)\, \psi^{J'}_{MK'}(\alpha,\beta,\gamma) \sin\beta\, d\alpha\, d\beta\, d\gamma \qquad (28)$$

Zur Auswertung des Integrals benötigt man die im Anhang gegebene Beziehung, daß die Eigenfunktionen des symmetrischen Kreisels in der S-Darstellung proportional den irreduziblen Darstellungen der Drehgruppe sind, d.h.

$$\psi^J_{MK}(\alpha,\beta,\gamma) \sim \sqrt{2J+1}\, \mathcal{D}^J_{MK}(\alpha,\beta,\gamma) \qquad (29a)$$

Wie im Anhang gezeigt, läßt sich auch $\hat{C}_q^{(2)}(\beta, \pi-\gamma)$ als spezielle Darstellung der Drehgruppe schreiben

$$\hat{C}_q^{(2)}(\beta,\pi-\gamma) \equiv \mathcal{D}^2_{0q}(\alpha,\beta,\pi-\gamma) \qquad (29b)$$

Berücksichtigen wir noch die ebenfalls im Anhang aufgeführten Symmetriebeziehungen der irreduziblen Darstellungen der Drehgruppe, so ergibt sich folgender Ausdruck für das gesuchte Matrixelement:

$$\langle J K M | \hat{C}_q^{(2)}(\beta,\pi-\gamma) | J' K' M \rangle = (-1)^{M-K+q} \sqrt{2J+1}\, \sqrt{2J'+1}$$

$$\cdot \frac{1}{8\pi^2} \int \mathcal{D}^J_{-M-K}(\alpha,\beta,\gamma)\, \mathcal{D}^2_{0-q}(\alpha,\beta,\gamma)\, \mathcal{D}^{J'}_{MK'}(\alpha,\beta,\gamma) \sin\beta\, d\alpha\, d\beta\, d\gamma =$$

$$= (-1)^{M-K+q} \sqrt{2J+1}\sqrt{2J'+1} \begin{pmatrix} J & 2 & J' \\ -M & 0 & M \end{pmatrix} \begin{pmatrix} J & 2 & J' \\ -K & -q & K' \end{pmatrix} \qquad (30)$$

Das Integral über das Produkt der drei $\mathcal{D}$ läßt sich also wie angegeben als

Produkt zweier *3j*-Symbole ausdrücken. Aus den Eigenschaften der *3j*-Symbole kann man entnehmen, daß für gegebene K und K' immer nur ein *3j*-Symbol von Null verschieden ist (siehe Anhang D). Demzufolge wurde die Summation über q gemäß Gleichung (27) bereits weggelassen.

Bei erneuter Anwendung des Wigner-Eckart-Theorems erhält man für das gesuchte Reduzierte Matrixelement des Feldgradienten-Tensoroperators

$$\langle J\,K \parallel \hat{V} \parallel J'\,K' \rangle = (-1)^{J-K} \cdot \frac{1}{2}\sqrt{2J+1}\,\sqrt{2J'+1} \begin{pmatrix} J & 2 & J' \\ -K-q & K' \end{pmatrix} \chi'_{-q} \qquad (31)$$

Durch Einsetzen der beiden jetzt bekannten Reduzierten Matrixelemente des Quadrupolmoment-Tensoroperators [Gleichung (25)] und des Feldgradienten-Tensoroperators [Gleichung (31)] in die Gleichung für die Matrixelemente des $\hat{H}_Q$-Operators, Gleichung (24), erhalten wir folgenden Ausdruck

$$\langle J\,K\,I\,F \mid \hat{H}_Q \mid J'\,K'\,I\,F \rangle =$$

$$= (-1)^{I+J+J'-K+F+1}\,\frac{1}{4}\sqrt{2J'+1}\,\sqrt{2J+1}\,\frac{\begin{Bmatrix} F & I & J \\ 2 & J' & I \end{Bmatrix}}{\begin{pmatrix} I & 2 & I \\ -I & 0 & I \end{pmatrix}} \begin{pmatrix} J & 2 & J' \\ -K & -q & K' \end{pmatrix} \chi_{-q} \qquad (32)$$

Hierbei ist gesetzt $\chi_q = e\,Q\,\chi'_q$.

Die mit diesen Matrixelementen aufzubauende Matrix ist diagonal in den Quantenzahlen F, M_F und I. Sie ist nichtdiagonal in J und K. Von Null verschiedene Matrixelemente treten auf zwischen J und $J \pm 1$ sowie J und $J \pm 2$. Dasselbe gilt für die Quantenzahl K. Beides folgt aus der Struktur der *3j*-Symbole. Für $F = \frac{5}{2}$ und $I = \frac{3}{2}$ ist der Aufbau einer solchen Matrix gezeigt; die von Null verschiedenen Elemente sind durch ein Kreuz angedeutet (Abb. 3).

Geschlossene Ausdrücke für die Matrixelemente von $\hat{H}_Q$, bei denen die Vektorkopplungskoeffizienten bereits ausgewertet sind, findet man bei Benz, Bauder und Günthard [25].

Zur Berechnung der Energieniveaus eines rotierenden Moleküls mit einem Quadrupolkern benötigt man nun noch die Eigenwerte der Matrixelemente des Operators $\hat{H}_{\text{rot}}$ in der *Produktbasis*. Es kann leicht gezeigt werden, daß der Operator $\hat{H}_{\text{rot}}$ die gleichen Matrixelemente wie in der *S*-Darstellung besitzt, da er nur auf einen Teil des Raumes der Produktdarstellung wirkt. Es gelten also die in Abschnitt 2.1. angegebenen Matrixelemente, Gleichung (3a), (3b).

Die Eigenwerte des gesamten Hamilton-Operators $\hat{H}_g$ erhält man nun, indem man die Matrixelemente von $\hat{H}_{\text{rot}}$ und $\hat{H}_Q$ bei der Aufstellung der Gesamtmatrix addiert. Die Gesamtmatrix muß dann mit einer Digitalrechenanlage diagonalisiert werden. Die so erhaltenen Eigenwerte lassen sich nicht mehr nach J indizieren, da diese keine „guten Quantenzahlen" mehr sind, sondern man muß eine neue

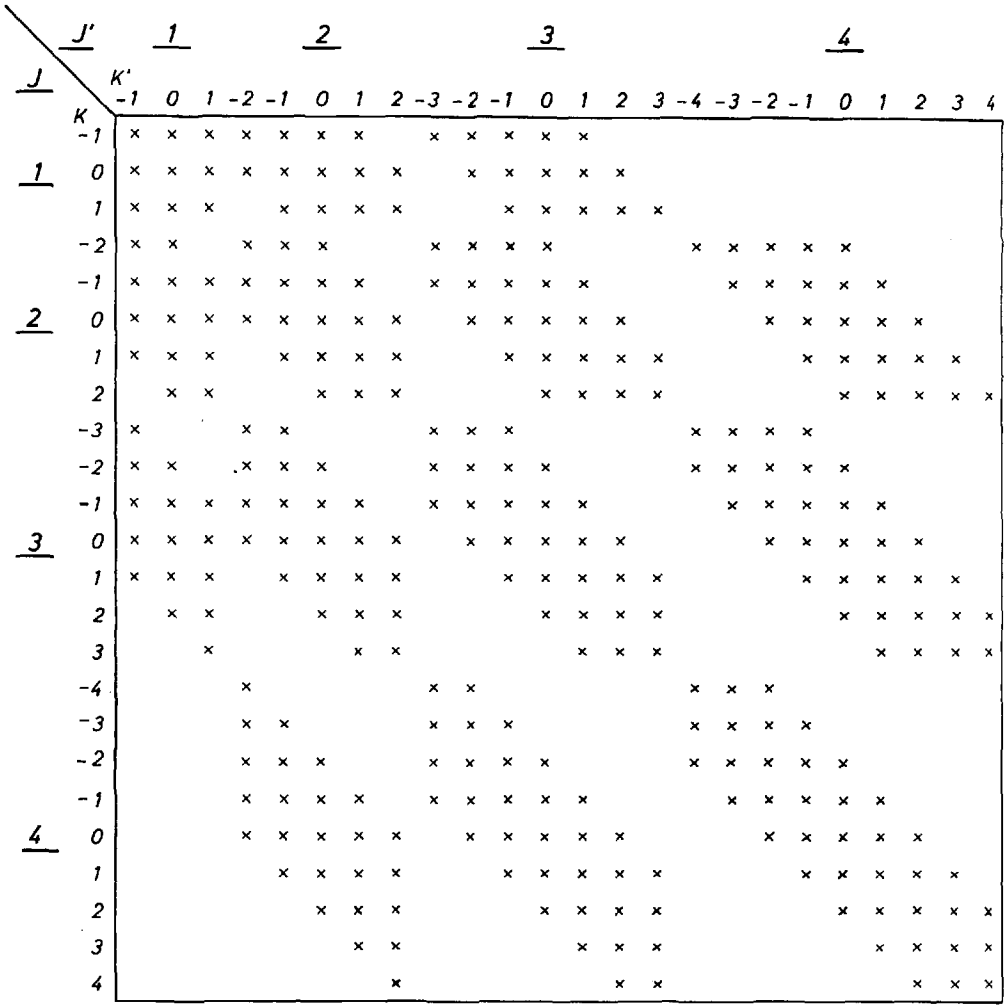

Abb. 3

Laufzahl – analog der Pseudoquantenzahl τ im Falle des asymmetrischen Kreisels ohne Quadrupolkern – einführen. Bei der Diagonalisierung erhält man automatisch als Spaltenvektoren der Transformationsmatrix die Eigenvektoren des asymmetrischen Kreiselmoleküls mit einem Quadrupolkern in der Produktbasis. Diese werden später bei der Berechnung der Intensitäten der durch die Quadrupolaufspaltung bedingten Multiplett-Linien benötigt.

3.1.4. Matrixelemente des Dipolmoment-Operators $\hat{\mu}$

Bei der vorstehend gegebenen vollständigen Behandlung eines rotierenden Moleküls mit einem Quadrupolkern, bei dem nur noch F und M_F „gute Quantenzahlen" sind, lassen sich die Auswahlregeln in den üblichen Quantenzahlen F, J und τ nicht mehr angeben [24], da durch die Nichtdiagonalglieder in J diese verändert werden. Es ist daher zur Interpretation eines entsprechenden Spektrums erforderlich, die Intensitäten aller möglichen Übergänge zu berechnen.

Es gilt, daß die Intensität einer Spektrallinie proportional dem Quadrat des entsprechenden Dipolmoment-Matrixelements ist. Für unseren Fall ist dabei wichtig, daß diese Matrixelemente in der Eigenbasis des Gesamt-Hamilton-Operators $\hat{H}_{ges}$ dargestellt werden müssen. Diese Eigenbasis liegt aber vor als Ergebnis der numerischen Diagonalisierung der Matrix des Gesamt-Hamilton-Operators.

Man bezeichnet als Dipolmoment-Operator $\hat{\mu}'$ im körperfesten Koordinatensystem den irreduziblen Tensoroperator 1. Stufe, dessen Komponenten den klassischen Dipolmoment-Vektorkomponenten in der sphärischen Basis entsprechen. Um das Problem zu behandeln, transformiert man den Operator $\hat{\mu}'$ in ein raumfestes Koordinatensystem. Es gilt dann analog Gleichung (27) für die Nullkomponente des so transformierten Operators $\hat{\mu}$:

$$\hat{\mu}_0 = \sum_l (-1)^l \hat{C}_l^{(1)}(\theta, \phi)\, \mu'_{-l} \tag{33}$$

Die Berechnung der Dipol-Matrixelemente erfolgt nun vollkommen analog der Methode, die für die Feldgradienten-Matrixelemente in Abschnitt 3.1.3 angegeben wurde, wobei allerdings noch ein Satz aus der Theorie der Matrixelemente von Tensoroperatoren hierzu benötigt wird. Wenn ein Tensoroperator $\hat{T}^{(k)}$ nur auf *einen* Teil einer Produktbasis wirkt, gilt für ein Matrixelement [26]:

$$\langle \gamma j_1 j_2 j_3 \| \hat{T}^{(k)} \| j_1' j_2 j_3' \gamma' \rangle =$$

$$= (-1)^{j_1+j_2+j_3'+k} \sqrt{2j_3+1}\sqrt{2j_3'+1} \begin{Bmatrix} j_1 & j_3 & j_2 \\ j_3' & j_1' & k \end{Bmatrix} \cdot \langle j_1 \gamma \| \hat{T}^{(k)} \| j_1' \gamma' \rangle \tag{34}$$

Damit wird das Matrixelement im gekoppelten Schema als Funktion des Reduzierten Matrixelements im ungekoppelten Schema angegeben.

Da der Operator $\hat{\mu}$ nur auf den J-Raum wirkt, erhält man damit für diesen Fall

$$\langle JKIF \| \hat{\mu} \| J'K'IF' \rangle =$$

$$= (-1)^{J+I+F'+1} \sqrt{2F+1}\sqrt{2F'+1} \begin{Bmatrix} J & F & I \\ F' & J' & 1 \end{Bmatrix} \cdot \langle JK \| \hat{\mu} \| J'K' \rangle \tag{35}$$

Nun benötigt man zur weiteren Berechnung die Kenntnis des Reduzierten Matrixelements $\langle JK \| \hat{\mu} \| J'K' \rangle$.

Die Matrixelemente von μ_0 in der S-Darstellung kann man schreiben:

$$\langle JKM \mid \hat{\mu}_0 \mid J'K'M \rangle = \sum_{l=-1}^{+1} (-1)^l \mu'_{-l} \langle JKM \mid \hat{C}_l^{(1)}(\theta, \phi) \mid J'K'M' \rangle$$

wobei man μ'_{-l} als konstanten Faktor vor die Integration genommen hat. Verfährt man weiterhin wie bei der Berechnung der Matrixelemente des Feldgradienten-Tensoroperators, so erhält man schließlich

$$\langle JKM \parallel \hat{\mu}_0 \parallel J'K'M \rangle =$$

$$= (-1)^{M-K} \sqrt{2J+1} \sqrt{2J'+1} \begin{pmatrix} J & 1 & J' \\ -M & 0 & M' \end{pmatrix} \begin{pmatrix} J & 1 & J' \\ -K & -l & K' \end{pmatrix} \mu'_{-l} \qquad (36)$$

Auch hier erübrigt sich die Summation über l, analog der Behandlung des Feldgradienten-Tensoroperators.

Die Anwendung des Wigner-Eckart-Theorems liefert dann für das gesuchte Reduzierte Matrixelement folgenden Ausdruck:

$$\langle JK \parallel \hat{\mu} \parallel J'K' \rangle = (-1)^{J-K} \sqrt{2J+1} \sqrt{2J'+1} \begin{pmatrix} J & 1 & J' \\ -K & -l & K' \end{pmatrix} \mu'_{-l} \qquad (37)$$

Wird dieser Ausdruck in die Gleichung (35) eingesetzt und wendet man erneut das Wigner-Eckart-Theorem an, so erhält man die gesuchten Matrixelemente des Dipolmoment-Operators in der Produktbasis

$$\langle JKIFM_F \mid \hat{\mu}'_q \mid J'K'IF'M'_F \rangle =$$

$$= (-1)^{F+F'-K+1+I-M_F} \sqrt{2J+1} \sqrt{2J'+1} \sqrt{2F+1} \sqrt{2F'+1} \cdot$$

$$\cdot \begin{Bmatrix} J & F & I \\ F' & J' & 1 \end{Bmatrix} \begin{pmatrix} F & 1 & F' \\ -M_F & q & M'_F \end{pmatrix} \begin{pmatrix} J & 1 & J' \\ -K & -l & K' \end{pmatrix} \mu'_{-l} \qquad (38)$$

Geschlossene Ausdrücke für die Matrixelemente in Abhängigkeit von den Quantenzahlen findet man bei Benz, Bauder und Günthard [25].

Aus der Struktur der $3j$-Symbole ist ersichtlich, daß für die von Null verschiedenen Matrixelemente die Beziehungen gelten:

$$F' = F,\ F \pm 1$$
$$J' = J,\ J \pm 1$$
$$K' = K,\ K \pm 1$$

Nun müssen die so erhaltenen Dipolmoment-Matrixelemente auf die Eigenbasis des Gesamt-Hamilton-Operators transformiert werden. Gesucht ist also

$$\bar{\mu}_q = V_F^{\dagger} \hat{\mu}_q V_{F'}$$

Hierbei sind die Spalten der Transformationsmatrix V die bei der Diagonalisierung des Gesamt-Hamilton-Operators erhaltenen Eigenvektoren. Die gesuchten Intensitäten der einzelnen Übergänge erhält man dann durch Quadrierung und Summation über alle q und alle entarteten Endzustände M'_F [27]:

$$\text{Intensität} \sim \sum_{q, M'_F} \bar{\mu}_q^2 \tag{39}$$

Die Ähnlichkeitstransformation V wirkt nur auf die (F, F')-Blöcke; dadurch kann der Faktor

$$(-1)^{F-M_F} \cdot \begin{pmatrix} F & 1 & F' \\ -M_F & q & M'_F \end{pmatrix}$$

außerhalb der Transformation geschrieben werden. Dann ist die Abhängigkeit der Matrixelemente von q, M_F, M'_F im $3j$-Symbol enthalten. Dies bedeutet, daß die Intensität proportional dem Quadrat der reduzierten Matrixelemente ist:

$$\text{Intensität} \sim \langle V^{\dagger} \parallel \hat{\mu} \parallel V \rangle^2 \sum_{M'_F, q} \begin{pmatrix} F & 1 & F' \\ -M_F & q & M'_F \end{pmatrix}^2 \tag{40}$$

Es kann leicht gezeigt werden, daß die Summe im Ausdruck (40) stets gleich 1 ist.

3.2. Störungstheoretische Behandlung der Energieniveaus von rotierenden Molekülen mit Quadrupolatomen

Nachdem im Abschnitt 3.1.3. die exakte Behandlung der Rotationsspektren eines Moleküls mit einem Quadrupolkern in der Näherung des starren Rotators durchgeführt wurde, soll in diesem Abschnitt die *störungstheoretische Behandlung desselben Problems* gegeben werden. In vielen Fällen wird eine störungstheoretische Behandlung zur Auswertung der Spektren in bezug auf den Feldgradienten-Tensor genügen. Dies wird immer dann der Fall sein, wenn die Kopplungsenergie zwischen rotierendem Molekül und Quadrupolkern klein gegenüber der Differenz der Energieniveaus ist, die an einem Rotationsübergang beteiligt sind. Dies gilt sicher für Kerne mit sehr kleinem Quadrupolmoment wie z.B. Stickstoff oder bei sehr polaren Bindungen. Man wird die Störungsrechnung vor allem deswegen bevorzugen, weil bei Rechnungen mittels Digitalrechner der Bedarf an Speicherplatz sich stark reduziert gegenüber dem Bedarf bei einer exakten Auswertung, wo er infolge des hohen Ranges der Matrizen $[4FI + 2(F+I) + 1]$ schon bei einem Quadrupolkern im Molekül sehr groß ist.

Die Störungsrechnung liefert bei einem Quadrupolkern im Molekül für die Energie

$$E = E_{\text{rot}} + E_Q^{(1)} + E_Q^{(2)} + \ldots \tag{41a}$$

E_{rot} ist die Energie des asymmetrischen Kreiselmoleküls ohne Quadrupolkopplung, $E_Q^{(1)}$ entspricht dem Diagonalmatrixelement des Störoperators $\hat{H}_Q^{(1)}$ in der Basis der ungestörten Rotationseigenfunktionen des Moleküls, $E_Q^{(2)}$ entspricht der Summe über die Quadrate der Nichtdiagonalelemente des Störoperators $\hat{H}_Q$ in derselben Basis, dividiert durch die Differenz der jeweiligen, durch die beiden ψ-Funktionen verknüpften Energieniveaus.

Wir erhalten folgende Beziehung:

$$\begin{aligned} E_Q &= E_Q^{(1)} + E_Q^{(2)} \ldots \\ &= \langle IJ\tau FM_F | \hat{H}_Q^{(1)} | IJ\tau FM_F \rangle + \sum_{J'\tau'} \frac{\langle IJ\tau FM_F | \hat{H}_Q^{(1)} | IJ'\tau' FM_F \rangle^2}{W_{J\tau} - W_{J'\tau'}} + \ldots . \end{aligned} \tag{41b}$$

Mit dieser Beziehung ist der allgemeinste Fall des asymmetrischen Kreisels angegeben. Über die Indizes I, F und M_F wird im 2. Glied nicht summiert, was bedeutet, daß die Matrix des Störoperators $\hat{H}_Q$ in I, F und M_F diagonal ist.

Für die Spezialfälle der symmetrischen und linearen Kreiselmoleküle sind dann die entsprechenden Rotationsfunktionen (ψ-Funktionen) einzusetzen. Je nach der gewünschten Genauigkeit der Ergebnisse sind unter Berücksichtigung der Größe der Kopplungsenergie gegenüber der Differenz der Rotationsenergie nur das 1. Glied oder beide bzw. auch höhere Glieder zu berechnen.

Der in den Korrekturgliedern auftretende Störoperator $\hat{H}_Q^{(1)}$ wurde von Casimir [28] für den Fall *eines* Quadrupolkerns im Molekül angegeben. Er fand folgenden Ausdruck für diesen Operator:

$$\begin{aligned} \hat{H}_Q &= \frac{3e^2 q_J Q}{8I(2I-1)J(2J-1)} \left[\frac{4(\hat{I}\hat{J})^2}{\hbar^4} + \frac{2\hat{I}\hat{J}}{\hbar^2} - \frac{4\hat{I}^2\hat{J}^2}{3\hbar^4} \right] \\ q_J &= \left\langle \left(\frac{\partial^2 V}{\partial Z^2} \right) \right\rangle_{\text{Mittel}} \end{aligned} \tag{42}$$

Dieses Ergebnis von Casimir bezog sich zunächst auf Atome. Es läßt sich jedoch auf rotierende Moleküle übertragen, wenn man – wie in Gleichung (42) geschehen – die Bahndrehimpulsquantenzahl L durch die Rotationshauptquantenzahl J und die Eigenfunktion des Bahndrehimpulses durch die Eigenfunktion des molekularen Rotators entsprechender Symmetrie ersetzt.

Als Lösung für die Diagonalelemente, die die Störenergie 1. Ordnung liefern, wird von Casimir folgender Ausdruck angegeben [28]:

$$\begin{aligned} E_Q^1 &= \frac{1}{2} \frac{e^2 Q q_J}{I(2I-1)J(2J-1)} \left[\frac{3}{4} C(C+1) - I(I+1)J(J+1) \right] \\ C &= F(F+1) - I(I+1) - J(J+1) \end{aligned} \tag{43}$$

Diese Beziehung gilt für alle Molekültypen, wobei allerdings q_J für lineare Moleküle, symmetrische Kreiselmoleküle und asymmetrische Kreiselmoleküle verschieden ist.

Zur Berechnung der Energien eines rotierenden mit *einem* Quadrupolkern behafteten Moleküls benötigen wir also in 1. Ordnung nur noch die Kenntnis von q_J. q_J ist proportional dem Feldgradienten in Richtung der raumfesten Achse Z und ist gegeben durch folgenden Ausdruck

$$q_J = \langle J \tau M_J = J' \left| \frac{\partial^2 V}{\partial Z_J^2} \right| J' \tau' M_J = J' \rangle \tag{44a}$$

für den Fall des asymmetrischen Kreisels und

$$q_J = \langle J K M \left| \frac{3\cos^2\theta - 1}{2} \right| J K M \rangle \cdot \left(\frac{\partial^2 V}{\partial z^2} \right) \tag{44b}$$

für den Fall des symmetrischen Kreisels. Dieselbe Beziehung gilt mit $K = 0$ für das lineare Molekül. Für das symmetrische und das lineare Kreiselmolekül gelten wegen der Laplace-Gleichung:

$$\frac{\partial^2 V}{\partial x^2} = \frac{\partial^2 V}{\partial y^2} = -\frac{1}{2} \frac{\partial^2 V}{\partial z^2} \tag{44c}$$

z ist Richtung der Kernverbindungslinie

$\frac{\partial^2 V}{\partial z^2} = q_m$ ist die Komponente des Feldgradienten in Richtung der Figurenachse des Moleküls.

Zunächst sollen die einfachen Fälle des *linearen und des symmetrischen Kreiselmoleküls* behandelt werden. Einsetzen der entsprechenden Eigenfunktion [Gleichung (9b)] ergibt für das lineare Kreiselmolekül

$$q_J = \langle J \left| \frac{\partial^2 V}{\partial Z^2} \right| J \rangle =$$

$$= q_m \cdot \frac{2J+1}{4\pi (2J)!} \int_0^{\pi} \int_0^{2\pi} [P_J^J(\cos\theta)]^2 \frac{3\cos^2\theta - 1}{2} \sin\theta \, d\theta \, d\phi = -\frac{J}{2J+3} q_m \tag{45}$$

Die Störenergie 1. Ordnung wurde damit für das lineare Molekül zu

$$E_Q^{(1)} = -\frac{e^2 Q q_m}{2I(2I-1)(2J-1)(2J+3)} \cdot \left[\frac{3}{4} C(C+1) - I(I+1) J(J+1) \right] \tag{46a}$$

Sie kann folgendermaßen geschrieben werden:

$$E_Q^{(1)} = -e^2 Q \left(\frac{\partial^2 V}{\partial z^2} \right) f(I,J,F) \tag{46b}$$

Dabei ist $f(I,J,F)$ die sogenannte *Casimir-Funktion;* sie liegt in tabellierter Form vor [29].

Hier wurde zur Berechnung der Störenergie der von Casimir eingeschlagene Weg gezeigt. Selbstverständlich hätten die Diagonalmatrixelemente auch mit der in Abschnitt 3.1.3 dargestellten Methode erhalten werden können. In dem dort angegebenen Rechenformalismus unter Benutzung der *6j-* und *3j*-Symbole läßt sich die Casimir-Funktion auch so darstellen:

$$f(I,J,F) = \frac{1}{4}(-1)^{F+I+J}\,\frac{J}{2J+3}\,\frac{\begin{Bmatrix} F & I & J \\ 2 & J & I \end{Bmatrix}}{\begin{pmatrix} I & 2 & I \\ -I & 0 & I \end{pmatrix}\begin{pmatrix} J & 2 & J \\ -J & 0 & J \end{pmatrix}} \tag{46c}$$

Wie man aus dem Ausdruck für die Störenergie sieht, wird hierbei J noch als „gute Quantenzahl" verwendet, was ja mit der alleinigen Verwendung der Diagonalelemente in J identisch ist. Die durch die Quadrupolkopplung bedingte Aufspaltung der Rotationslinien für ein lineares Molekül erhält man dann in 1. Näherung unter Berücksichtigung der Auswahlregeln $\Delta J = 0, \pm 1; \Delta F = 0, \pm 1; \Delta I = 0$. Die relativen Intensitäten der einzelnen Multiplett-Linien liegen ebenfalls in tabellierter Form vor [29].

Die Matrixelemente – nichtdiagonal in J – die zur Berechnung der Störenergie in 2. Ordnung benötigt werden, sind für das lineare Kreiselmolekül in seinem Schwingungsgrundzustand von Null verschieden, wenn $J' = J \pm 2$. Es werden also durch die Störung lediglich solche Niveaus miteinander verbunden, die sich um die Differenz 2 der Quantenzahl J unterscheiden. Der Ausdruck lautet [30]:

$$\langle IJFM_F | \hat{H}_Q | IJ+2FM_F \rangle =$$

$$= \frac{-3\,e^2 q\,Q}{16I(2I-1)\,(2J+3)} \cdot \Big\{ (I+J+F+3)\,(I+J+F+2)\,(I+J-F+2)(I+J-F+1)(J+F-I+2) \cdot$$

$$\cdot \frac{(J+F-I+1)\,(I+F-J)\,(I+F-J-1)}{(2J+1)\,(2J+5)} \Big\}^{\frac{1}{2}} \tag{47}$$

Bei Molekülen mit einer hohen Kernquadrupolkopplungskonstante, d.h. mit einem Atomkern mit sehr hohem Kernquadrupolmoment wie z.B. im *TlJ*, wurde in jüngster Zeit gezeigt, daß auch die Berücksichtigung höherer Terme, also der Glieder $E_Q^{(3)}$ und $E_Q^{(4)}$ erforderlich wird. In Ergänzung zu den Energiekorrekturen in 1. und 2. Ordnung, die bei Townes und Schawlow tabelliert sind [29], werden hierfür von Miller [31] für den Spezialfall des linearen Kreiselmoleküls auch die Störenergien 3. und 4. Ordnung für Kerne mit dem Spin $\frac{3}{2}, \frac{5}{2}, \frac{7}{2}$ und $\frac{9}{2}$ angegeben.

Wegen der mindestens dreizähligen Symmetrie läßt sich für den Fall des symmetrischen Kreiselmoleküls q_m wieder einfach durch $\frac{\partial^2 V}{\partial z^2}$, d.h. durch die Feldgradientenkomponente in Richtung der Symmetrieachse des Moleküls ausdrücken. Der Erwartungswert ergibt sich wieder als Matrixelement dieses Ausdrucks in der Basis des symmetrischen Kreisels:

$$q_J = \langle JKM \left| \frac{3\cos^2\theta - 1}{2} \right| JKM \rangle q_m = \left[\frac{3K^2}{J(J+1)} - 1 \right] \frac{J}{2J+3} q_m \qquad (48)$$

Die *Störenergie 1. Ordnung* für das symmetrische Kreiselmolekül mit einem Quadrupolkern wird dann unter Berücksichtigung der Casimir-Funktion wie folgt geschrieben:

$$E_Q^{(1)} = -e^2 Q \left(\frac{\partial^2 V}{\partial z^2} \right) \left(\frac{3K^2}{J(J+1)} - 1 \right) f(F, I, J) \qquad (49)$$

Dieser Ausdruck, der neben der Quantenzahl J auch die Projektionsquantenzahl K enthält, reduziert sich – wie leicht ersichtlich – auf den Ausdruck für das lineare Kreiselmolekül, wenn die Projektionsquantenzahl $K = 0$ gesetzt wird. Der Ausdruck für das symmetrische Kreiselmolekül kann auch verwendet werden für lineare Moleküle, die sich in einer angeregten entarteten Schwingungsmode befinden. In diesem Fall ist K durch l, die Drehimpulsquantenzahl für den *inneren Drehimpuls*, der bei den entarteten Knickschwingungen in linearen Molekülen auftritt [32], zu ersetzen.

Bei der Berücksichtigung der *Störenergie 2. Ordnung* zeigt sich, daß die Nichtdiagonal-Matrixelemente des Störoperators nur dann von Null verschieden sind, wenn $K' = K$ und $J' = J \pm 1$ oder $J' = J \pm 2$. Es ergeben sich folgende Ausdrücke für die von Null verschiedenen Nichtdiagonalelemente des Störoperators [30]:

$$\langle IJKFM_F | \hat{H}_Q | IJ+1\, KFM_F \rangle = -\frac{3e^2 q_m QK[F+1) - I(I+1) = -J(J+2)]}{8I(2I-1)J(J+2)}$$

$$\cdot \left\{ \frac{\left[\left(1 - \frac{K^2}{(J+1)^2} \right) (I+J+F+2)\,(J+F-I+1) \cdot (I+F-J)\,(I+J-F+1) \right]}{(2J+1)\,(2J+3)} \right\}^{\frac{1}{2}}$$

$$\langle IJKFM_F | \hat{H}_Q | IJ+2\, KFM_F \rangle =$$

$$= -\frac{3e^2 q_m Q}{16I(2I-1)\,(2J+3)} \cdot \left\{ \left[1 - \frac{K^2}{(J+1)^2} \right] \left[1 - \frac{K^2}{(J+2)^2} \right] (I+J+F+3)\,(I+J+F+2) \right.$$

$$\cdot (I+J-F+2)\,(I+J-F+1)\,(J+F-I+2)$$

$$\left. \cdot \frac{(J+F-I+1)\,(I+F-J)\,(I+F-J-1)}{(2J+1)\,(2J+5)} \right\}^{\frac{1}{2}} \qquad (50)$$

Die Werte dieser Ausdrücke liegen ebenfalls für Kerne mit Spin $\frac{3}{2}, \frac{5}{2}$ und $\frac{7}{2}$ in tabellierter Form vor [29].

Die Auswahlregeln zur Bestimmung der durch Quadrupolkopplung bedingten Feinstruktur von Rotationslinien eines symmetrischen Kreiselmoleküls lauten in 1. Ordnung $\Delta J = \pm 1$; $\Delta K = 0$; $\Delta F = 0, \pm 1$.

Da die Aufspaltung jetzt vom Wert K der Projektionsquantenzahl abhängt, ergeben sich für jeden K-Zustand verschiedene Aufspaltungen. Das bedeutet, daß die Feinstrukturaufspaltung eines symmetrischen Kreiselmoleküls wesentlich komplexer ist als die eines linearen Moleküls.

Dort, wo eine Berücksichtigung der Störenergie 2. Ordnung notwendig ist, ist es auch möglich, daß die normalerweise verbotenen Übergänge mit $\Delta J = \pm 3$. auftreten. Für den Fall $K \neq 0$ sind auch Übergänge mit $\Delta J = \pm 2$ zu erwarten.

Im Falle eines asymmetrischen Kreiselmoleküls resultieren drei verschiedene Diagonalglieder des Feldgradiententensors. Dies bedeutet, daß keine so einfachen Beziehungen wie beim linearen und symmetrischen Kreiselmolekül für den Erwartungswert der Komponenten des Feldgradiententensors in Z-Richtung mehr gegeben werden können. Man muß jetzt alle Komponenten des Feldgradiententensors berücksichtigen: Im kartesischen System sind dies 6, von denen allerdings nur 5 linear unabhängig sind, da die Spur des Feldgradiententensors wegen der Laplace-Gleichung gleich Null ist.

$$\frac{\partial^2 V}{\partial Z^2} = \alpha_{Za} \frac{\partial^2 V}{\partial a^2} + \alpha_{Zb} \frac{\partial^2 V}{\partial b^2} + \alpha_{Zc} \frac{\partial^2 V}{\partial c^2} + 2\alpha_{Za}\alpha_{Zb} \frac{\partial^2 V}{\partial a \partial b} + 2\alpha_{Za}\alpha_{Zc} \frac{\partial^2 V}{\partial a \partial c} + \\ + 2\alpha_{Zb}\alpha_{Zc} \frac{\partial^2 V}{\partial b \partial c} \tag{51}$$

a, b, c = Hauptträgheitsachsen des Moleküls

Man kann nun zeigen, daß die gemischten Ausdrücke für die Erwartungswerte verschwindende Integrale des Typs

$$\langle J K M \left| \alpha_{Za}\alpha_{Zb} \frac{\partial^2 V}{\partial a \partial b} \right| J K M \rangle$$

liefern [33]. Die gegebene Beziehung reduziert sich dadurch zu

$$q_J = \sum_{g=a,b,c} \langle J \tau M = J | \alpha_{Zg}^2 | J \tau M = J \rangle \frac{\partial^2 V}{\partial g^2} \tag{52}$$

wobei für die Erwartungswerte der Richtungscosinus folgender Ausdruck gilt:

$$\langle J \tau M = J | \alpha_{Zg}^2 | J \tau M = J \rangle = \frac{2J}{(2J+1)(2J+3)} \sum_{\tau'} {}^{g}S_{J\tau J\tau'}$$

S bedeutet die in tabellierter Form vorliegenden Linienstärken (line strengths) [8]. Unter Berücksichtigung der Richtungscosinus kann man den Erwartungswert der Z-Komponente des Feldgradiententensors im raumfesten System noch auf andere Weise durch die drei Diagonalkomponenten des Feldgradiententensors im molekülfesten System, wofür das Hauptträgheitsachsensystem gewählt wird, angeben. Hier soll nur noch der am häufigsten verwendete, von Bragg und Golden angegebene Ausdruck [34] angeführt werden. Allerdings wird dieser Ausdruck hier in einer etwas abgewandelten Form, die speziell für Iterationsrechnungen zur Bestimmung der Kernquadrupolkopplungskonstante bzw. der Komponenten des Feldgradiententensors geeignet ist, geschrieben:

$$q_J = \langle J\tau M_J = J \left| \frac{\partial^2 V}{\partial Z^2} \right| J\tau M_J = J \rangle = \frac{J}{2J+3}\left[D_1(J,\tau,\kappa)\left(\frac{\partial^2 V}{\partial a^2}\right) + D_2(J,\tau,\kappa)\left(\frac{\partial^2 V}{\partial b^2}\right)\right] \tag{53a}$$

$$D_1(J,\tau,\kappa) = \frac{2}{J(J+1)}\left[E(\kappa) - \kappa \frac{dE(\kappa)}{d\kappa} \right] \tag{53b}$$

$$D_2(J,\tau,\kappa) = \frac{1}{J(J+1)}\left[E(\kappa) + (3-\kappa) \frac{dE(\kappa)}{d\kappa} \right] - 1 \tag{53c}$$

Bei der Beziehung (53) wurde davon Gebrauch gemacht, daß die Laplace-Gleichung eine lineare Abhängigkeit der $\frac{\partial^2 V}{\partial g^2}$ liefert. Dabei bedeutet $E(\kappa)$ die in 2.1 angeführte reduzierte, nur von κ, J und τ abhängige Energie, wobei κ den Asymmetrieparameter darstellt. Die Differentialquotienten $\frac{dE(\kappa)}{d\kappa}$ lassen sich aus den $E(\kappa)$-Tabellen als Differenzenquotienten bzw. besser durch die numerischen Berechnungen von $E(\kappa)$ bei verschiedenen κ-Werten und numerischer Differentiation gewinnen. Sie liegen aber auch, da sie in der I^r-Darstellung den Erwartungswerten der Quadrate des Drehimpulses um die mittlere Hauptträgheitsachse entsprechen (es gilt also $\langle P_b^2 \rangle = \frac{dE(\kappa)}{d\kappa}$), abhängig von J, τ und κ in tabellierter Form vor [35].

Mit der Gleichung (53a) läßt sich damit durch Einsetzen in Gleichung (43) die Störenergie 1. Ordnung auch für asymmetrische Kreisel berechnen.

An dieser Stelle sei darauf hingewiesen, daß der Feldgradiententensor in dem hier verwendeten molekularen Koordinatensystem der Hauptträgheitsachsen im allgemeinen nicht diagonal ist. Die Nichtdiagonalelemente sind aber in der Gleichung (53) nicht enthalten. Dies bedeutet, daß die drei Nichtdiagonalelemente im allgemeinen Fall bzw. das eine Nichtdiagonalelement, wenn C_s-Symmetrie vorliegt, unter Benutzung der Störungstheorie 1. Ordnung zunächst nicht bestimmt werden können.

Die für die Ermittlung der Störenergie 2. Ordnung notwendigen Nichtdiagonalelemente d.h. die Erwartungswerte von Mischprodukten der Richtungscosinus sind von Schwendeman in der Wang-Darstellung angegeben worden [36].

Der zur Auswertung erforderliche Rechenaufwand dürfte allerdings in diesem Fall vergleichbar werden mit dem für die exakte Lösung – wie sie in Abschnitt 3.1 beschrieben wurde – erforderlichen, sodaß immer dort, wo die Störungsrechnung 1. Ordnung zur Beschreibung der Quadrupolfeinstruktur eines *asymmetrischen* Kreiselmoleküls nicht ausreicht, die exakte Lösung vorzuziehen ist.

Wie trotz des Gesagten auch bei Verwendung der Energieausdrücke in 1. Ordnung die Nichtdiagonalglieder des Feldgradiententensors im Trägheitsachsensystem bestimmt werden können, wird in Abschnitt 4 gezeigt werden.

3.3. Moleküle mit zwei und mehr Quadrupolatomen

Grundlegend erfolgt die Berechnung der Rotationsenergieniveaus von Molekülen, die zwei oder mehr Atome mit Quadrupolkern besitzen, in analoger Weise zu Abschnitt 3.1. Die gekoppelte Basis wird dabei wiederum als Linearkombination von Produkten der Basisfunktion der koppelnden Drehimpulse dargestellt. Dabei sind die Koeffizienten im Falle von zwei Quadrupolkernen durch *6j*-Symbole, im Falle von drei Quadrupolkernen durch *9j*-Symbole wiedergegeben. Es liegen auch rein störungstheoretische Ansätze vor, deren Ergebnisse jedoch weitgehend von der Reihenfolge der Kopplung abhängig sind [37].

Ein Verfahren zur exakten Behandlung eines Moleküls mit zwei Quadrupolatomen soll im folgenden skizziert werden [38]:

Bei einem rotierenden Molekül, das zwei Quadrupolkerne enthält, treten *drei Drehimpulse miteinander in Wechselwirkung:* der Drehimpuls des Moleküls $\vec{J}$ und die zwei Kernspins $\vec{I}_1, \vec{I}_2$. Das Problem kann auf zwei verschiedene Weisen behandelt werden entsprechend den zwei Möglichkeiten, mit denen man den resultierenden Gesamtdrehimpuls $\vec{F}$ aufbauen kann. Letzterer ist in Abwesenheit eines äußeren Feldes eine Konstante der Bewegung. Dies bedeutet, daß die diesem Drehimpuls entsprechende Quantenzahl F eine „gute Quantenzahl" ist. Die beiden Kopplungsmöglichkeiten sind:

$$\text{a)} \quad \vec{I} + \vec{J} = \vec{F}_1; \quad \vec{F}_1 + \vec{I}_2 = \vec{F} \qquad (I_1 J F_1 I_2 F\text{-Schema})$$

$$\text{b)} \quad \vec{I}_1 + \vec{I}_2 = \vec{I}\ ; \quad \vec{I} + \vec{J} = \vec{F} \qquad (I_1 I_2 I J F\text{-Schema})$$

Dabei sind $\vec{F}_1$ bzw. $\vec{I}$ die intermediären Drehimpulse, denen natürlich keine physikalische Bedeutung zukommt.

Das Schema a) eignet sich bei einer störungstheoretischen Behandlung für diejenigen Fälle, wo die Kopplungskonstanten der Quadrupolkerne stark voneinander verschieden sind, während das Schema b) zur Beschreibung für Kerne mit gleichen oder vergleichbaren Kopplungskonstanten geeigneter ist. Die hier

gemachte Aussage bedeutet, daß die jeweiligen Matrizen im einen oder anderen Fall die kleineren Nichtdiagonalelemente enthalten. Bei einer Behandlung ohne Vernachlässigung ist es ohne Bedeutung, welches Schema zur Lösung des Problems verwandt wird.

Bei der Aufstellung der vollständigen Matrix für die Quadrupolkopplungsenergie wird unter Benutzung des Schemas a) folgendermaßen verfahren:

Man baut den Hamilton-Operator aus drei Operatoren auf:

$$\hat{H}_{\text{ges}} = \hat{H}_{\text{rot}} + \hat{H}_{Q1} + \hat{H}_{Q2}$$

$\hat{H}_{\text{rot}}$ ist wiederum die Energie des ungestörten Rotators im allgemeinen Fall des asymmetrischen Rotators. $\hat{H}_{Q1}$ liefert die Kopplungsenergie, wenn der Spin eines Quadrupolkerns zum Moleküldrehimpuls koppelt und daraus der intermediäre Drehimpuls $\vec{F}_1$ resultiert. $\hat{H}_{Q2}$ liefert dann die Kopplungsenergie, wenn zum intermediären Drehimpuls $\vec{F}_1$ der Spin des zweiten Kerns zum Gesamtdrehimpuls $\vec{F}$ koppelt. Die Gesamteigenfunktion des Problems sei:

$$|I_1 J F_1 I_2 F M_F\rangle$$

Für $\hat{H}_{Q1}$ wird das Matrixelement des Skalarproduktes von zwei Tensoroperatoren benötigt. Man geht von dem allgemeinen Ansatz in Gleichung (23) aus und setzt

$$j_1 = I_1 \quad j_2 = J \quad j_3 = F_1 \quad j'_1 = I'_1 \quad j'_2 = J' \quad j'_3 = F'_1 .$$

Hierbei ist wieder vorausgesetzt, daß keine Änderung im Zustand des Atomkerns und damit von I_1 auftritt, d.h. daß $I_1 = I'_1$.

Man erhält damit als Matrixelement für den zweiten Term $\hat{H}_{Q1}$ im Gesamtoperator folgenden Ausdruck:

$$\langle I_1 J F_1 I_2 F M_F | \hat{V}^{(2)}_{(1)} \hat{Q}^{(2)}_{(1)} | I_1 J' F'_1 I_2 F M_F \rangle =$$

$$= \delta_{F_1 F'_1} (-1)^{I_1 + J + F'_1} \begin{Bmatrix} F'_1 & J & I_1 \\ 2 & I_1 & J' \end{Bmatrix} \langle J \| \hat{V}^{(2)}_{(1)} \| J' \rangle \langle I_1 \| \hat{Q}^{(2)}_{(1)} \| I_1 \rangle \qquad (54)$$

Dabei ist berücksichtigt, daß $\hat{V}_{(1)}$, der Feldgradiententensor am Ort des jetzt angekoppelten Atomkerns 1, nur auf den Drehimpuls $\vec{J}$ und damit auf $\vec{F}_1$ wirkt, jedoch nicht auf $\vec{I}_2$ und damit auch nicht auf $\vec{F}$.

Im zweiten Schritt wird der Spin des zweiten Atomkerns an das jetzt erhaltene System gekoppelt. Während die Basis des Reduzierten Matrixelements des Feldgradienten-Tensoroperators $\hat{V}_{(1)}$ und des Quadrupolmoment-Tensoroperators $\hat{Q}_{(1)}$

$$|J\rangle \quad \text{bzw.} \quad |I_1\rangle$$

waren, erhält man als Basis für das Matrixelement von $\hat{V}^{(2)}_{(2)}$ jetzt

$$|I_1 J' F_1'\rangle$$

und für $\hat{Q}^{(2)}_{(2)}$:

$$|I_2\rangle$$

und damit in Analogie zu $\hat{H}_{Q1}$ folgenden Ausdruck für die Matrixelemente von $\hat{H}_{Q2}$

$$\langle IJF_1 I_2 F M_F | \hat{V}^{(2)}_{(2)} \hat{Q}^{(2)}_{(2)} | I_1 J' F' I_2 F M_F\rangle =$$

$$= (-1)^{F_1' + I_2 + F} \begin{Bmatrix} F & I_2 & F_1 \\ 2 & F_1' & I_2 \end{Bmatrix} \langle I_1 J F_1 \| \hat{V}^{(2)}_{(2)} \| I_1 J' F_1' \rangle \langle I_2 \| \hat{Q}^{(2)}_{(2)} \| I_2 \rangle \qquad (55)$$

Das *Reduzierte Matrixelement* von $\hat{V}^{(2)}_{(2)}$ kann nun unter Benutzung eines Satzes aus der Theorie der Matrixelemente von irreduziblen Tensoroperatoren, der schon einmal angewandt wurde, siehe Gleichung (34), berechnet werden. Man erhält:

$$\langle I_1 J F_1 I_2 F M_F | \hat{V}^{(2)}_{(2)} \hat{Q}^{(2)}_{(2)} | I_1 J' F_1' I_2 F M_F\rangle =$$

$$= (-1)^{J' + F_1 + F_1' + I_1 + I_2 + F} \cdot \left[(2F_1 + 1)(2F_1' + 1)\right]^{\frac{1}{2}} \begin{Bmatrix} F & I_2 & F_1 \\ 2 & F_1' & I_2 \end{Bmatrix} \begin{Bmatrix} J & F_1 & I_1 \\ F_1' & J' & 2 \end{Bmatrix}$$

$$\cdot \langle J \| \hat{V}^{(2)}_{(2)} \| J' \rangle \langle I_2 \| \hat{Q}^{(2)}_{(2)} \| I_2 \rangle \qquad (56)$$

Die Matrixelemente der gesamten Kernquadrupolkopplungsenergie, hervorgerufen durch zwei Atomkerne, lassen sich jetzt folgendermaßen ausdrücken:

$$\langle I_1 J F_1 I_2 F M_F | \hat{H}_Q | I_1 J' F_1' I_2 F M_F\rangle =$$

$$= (-1)^{I_1 + J + F_1' + 1} \delta_{F_1 F_1'} \begin{Bmatrix} F_1' & I_1 & J' \\ 2 & J & I_1 \end{Bmatrix} \langle J \| \hat{V}^{(2)}_{(1)} \| J' \rangle \langle I_1 \| \hat{Q}^{(2)}_{(1)} \| I_1 \rangle +$$

$$+ (-1)^{J' + F_1' + F_1 + F + I_1 + I_2 + 1} \left[(2F_1' + 1)(2F_1 + 1)\right]^{1/2}$$

$$\cdot \begin{Bmatrix} F & I_2 & F_1' \\ 2 & F_1 & I_2 \end{Bmatrix} \begin{Bmatrix} I_1 & J' & F_1' \\ 2 & F_1 & J \end{Bmatrix} \langle J \| \hat{V}^{(2)}_{(2)} \| J' \rangle \langle I_2 \| \hat{Q}^{(2)}_{(2)} \| I_2 \rangle \qquad (57)$$

In diesem Ausdruck sind die Matrixelemente der Kernquadrupolkopplungsenergie für den Fall eines Rotators mit zwei Quadrupolkernen durch die entsprechenden Quantenzahlen und die Reduzierten Matrixelemente der Tensoroperatoren $V_{(1)}$, $V_{(2)}$, $Q_{(1)}$ und $Q_{(2)}$, bezogen auf die vollkommen *entkoppelte* Basis, dargestellt. Die letzteren Größen sind aber bereits aus Abschnitt 3.1 bekannt. Sie können sowohl in den sphärischen Komponenten des Feldgradienten-Tensors als auch in den kartesischen Komponenten dargestellt werden. Für die beiden Möglichkeiten gelten folgende Beziehungen:

$$\langle I_1 J K F_1 I_2 F M_F | \hat{H}_Q | I_1 \; J_1' \; K' F_1' I_2 F M_F \rangle =$$

$$= + \frac{1}{4}(-1)^{F_1'+J'+I_1+J-K+1} \delta_{F_1 F_1'} \sqrt{2J+1}\sqrt{2J'+1} \frac{\begin{pmatrix} J & 2 & J' \\ -K & -q & K' \end{pmatrix}}{\begin{pmatrix} I_1 & 2 & I_1 \\ -I_1 & 0 & I_1 \end{pmatrix}} \begin{Bmatrix} F_1' & I_1 & J' \\ 2 & J & I_1 \end{Bmatrix} \chi_{-q}^{(1)}$$

$$+ \frac{1}{4}(-1)^{F+F_1+F_1'+I_1+I_2-K+1} \sqrt{2J+1}\sqrt{2J'+1}$$

$$\cdot \sqrt{2F_1+1}\sqrt{2F_1'+1} \frac{\begin{pmatrix} J & 2 & J' \\ -K & -q & K' \end{pmatrix}}{\begin{pmatrix} I_2 & 2 & I_2 \\ -I_2 & 0 & I_2 \end{pmatrix}} \begin{Bmatrix} F & I_2 & F_1' \\ 2 & F_1 & I_2 \end{Bmatrix} \begin{Bmatrix} I_1 & J' & F_1' \\ 2 & F_1 & J \end{Bmatrix} \chi_{-q}^{(2)}$$

(58a)

$$\langle I_1 J F_1 I_2 F M_F | \hat{H}_Q | I_1 J' F_1' I_2 F M_F \rangle =$$

$$= \frac{1}{4}(-1)^{F_1'+J'+I_1+1} \delta_{F_1 F_1'} \frac{\begin{Bmatrix} F_1' & I_1 & J' \\ 2 & J & I_1 \end{Bmatrix}}{\begin{pmatrix} I_1 & 2 & I_1 \\ -I_1 & 0 & I_1 \end{pmatrix}\begin{pmatrix} J & 2 & J' \\ -J' & 0 & J' \end{pmatrix}}$$

$$\cdot e\, Q_1 \langle J, M_J = J' | \hat{V}_{ZZ(1)} | J', M_J' = J' \rangle + \frac{1}{4}(-1)^{F+F_1'+F_1-J+I_1+I_2+1}$$

$$\cdot \left[(2F_1'+1)(2F_1+1)\right]^{\frac{1}{2}} \frac{\begin{Bmatrix} F & I_2 & F_1' \\ 2 & F_1 & I_2 \end{Bmatrix}\begin{Bmatrix} I_1 & J' & F_1' \\ 2 & F_1 & J \end{Bmatrix}}{\begin{pmatrix} I_2 & 2 & I_2 \\ -I_2 & 0 & I_2 \end{pmatrix}\begin{pmatrix} J & 2 & J' \\ -J' & 0 & J' \end{pmatrix}}$$

$$\cdot e\, Q_2 \langle J, M_J = J' | \hat{V}_{ZZ(2)} | J', M_J' = J' \rangle \qquad (58b)$$

In den meisten Fällen wird man darauf verzichten, die Gesamtenergiematrix (wie in Abschnitt 3.1 für den Fall mit einem Quadrupolkern dargestellt) aufzustellen, da der Rang der dann auftretenden Matrizen schon bei relativ kleinen F-Werten sehr groß wird: $[4F \cdot (I_1 + I_2) + 2 \cdot (I_1 + I_2 + F) + 1]$. Man wird sich aus diesem Grunde häufig mit dem Störungsrechnungsansatz begnügen und lediglich die in J und τ diagonalen Elemente für den asymmetrischen Rotator als 1. Näherung benutzen. Dies ergibt dann unter Verwendung der Beziehungen (53b) und (53c) folgenden Ausdruck:

$$\langle I_1 J K F_1 I_2 F M_F | \hat{H}_Q | I_1 J K F_1' I_2 F M_F \rangle =$$

$$= \frac{1}{4}(-1)^{F_1'+J+I_1+1}\,\delta_{F_1 F_1'}\,\frac{J}{2J+3}\,\frac{\begin{Bmatrix} F_1' & I_1 & J \\ 2 & J & I_1 \end{Bmatrix}}{\begin{pmatrix} I_1 & 2 & I_1 \\ -I_1 & 0 & I_1 \end{pmatrix}\begin{pmatrix} J & 2 & J \\ -J & 0 & J \end{pmatrix}}$$

$$\cdot\left[D_1 \chi_{aa(1)} + D_2 \chi_{bb(1)}\right] + \frac{1}{4}(-1)^{F+F_1'+F_1-J+I_1+I_2+1}$$

$$\cdot\left[(2F_1'+1)(2F_1+1)\right]^{\frac{1}{2}}\,\frac{J}{2J+3}\,\frac{\begin{Bmatrix} F & I_2 & F_1' \\ 2 & F_1 & I_2 \end{Bmatrix}\begin{Bmatrix} I_1 & J & F_1' \\ 2 & F_1 & J \end{Bmatrix}}{\begin{pmatrix} I_2 & 2 & I_2 \\ -I_2 & 0 & I_2 \end{pmatrix}\begin{pmatrix} J & 2 & J \\ -J & 0 & J \end{pmatrix}}$$

$$\left[D_1 \chi_{aa(2)} + D_2 \chi_{bb(2)}\right] \tag{59}$$

Dieser Ausdruck läßt sich dann auch auf den Fall eines symmetrischen Kreiselmoleküls bzw. eines linearen Rotators reduzieren. Setzt man in Gleichung (58b) für die Matrixelemente der Operatoren $\hat{V}_{ZZ(1)}$ und $\hat{V}_{ZZ(2)}$ die entsprechenden Beziehungen für den symmetrischen Kreisel ein:

$$\langle J K M = J' | \hat{V}_{ZZ} | J' K' M' = J' \rangle =$$

$$= (-1)^{K'-J'}\,\delta_{K,K'}\left[(2J+1)(2J'+1)\right]^{\frac{1}{2}}\begin{pmatrix} J & 2 & J' \\ -J' & 0 & J' \end{pmatrix}\begin{pmatrix} J & 2 & J' \\ -K & 0 & K' \end{pmatrix} q_m \tag{60}$$

so ergeben sich die vollständigen Matrixelemente für die Energieniveaus eines symmetrischen Kreiselmoleküls mit zwei Quadrupolkernen auf der Figurenachse.

Setzt man $K = 0$ in D_1 und D_2 und beachtet, daß dann das *3j*-Symbol $\begin{pmatrix} J & 2 & J' \\ -K & 0 & K' \end{pmatrix} = 0$ wird, es sei denn daß $J + 2 + J'$ gerade ist, so folgt, daß im Falle des linearen Rotators lediglich Nichtdiagonalelemente auftreten, die die Niveaus J und $J \pm 2$ miteinander verknüpfen.

Die Berechnung der Auswahlregeln für die Rotationsübergänge d.h. für die Linienintensitäten, erfolgt wiederum völlig analog dem in Abschnitt 3.1.4 angegebenen Verfahren, wobei man auch hier in den meisten Fällen auf den störungstheoretischen Ansatz, der J noch als „gute Quantenzahl" betrachtet, zurückgreifen wird. Unter dieser Voraussetzung erhält man für das Reduzierte Matrixelement des Dipolmomentoperators in der gekoppelten Basis

$$\langle I_1 J F_1 I_2 F \| \hat{\mu}^{(1)} \| I_1 J' F_1' I_2 F' \rangle = (-1)^{J'+2F_1+F'+I_1+I_2}$$
$$\cdot \left[(2F_1'+1)(2F_1+1)(2F'+1)(2F+1)\right]^{\frac{1}{2}} \begin{Bmatrix} F_1 & F & I_2 \\ F' & F_1' & 1 \end{Bmatrix} \begin{Bmatrix} J & F_1 & I_1 \\ F_1' & J' & 1 \end{Bmatrix} \langle J \| \hat{\mu} \| J' \rangle \tag{61}$$

wobei das Reduzierte Matrixelement in der ungekoppelten Basis gegeben ist durch

$$\langle J K \| \hat{\mu} \| J' K' \rangle = (-1)^{J-K} \left[(2J+1)(2J'+1)\right]^{\frac{1}{2}} \begin{pmatrix} J & 1 & J' \\ -K & 0 & K \end{pmatrix} \mu_{-1}' \, \delta_{K,K'} \tag{62}$$

Bei Benutzung dieser Ausdrücke zur Berechnung der Intensitäten muß außerdem berücksichtigt werden, daß die Niveaus $K \neq 0$ doppelt entartet sind und infolgedessen die Intensität mit dem Faktor 2 versehen werden muß.

Ergänzend sollen noch die Matrixelemente für das Kopplungs-Schema $I_1 I_2 I J F$ gegeben werden:

$$\langle I_1 I_2 I J F M_F | \hat{H}_Q | I_1 I_2 I' J' F M_F \rangle =$$
$$= \frac{1}{4}(-1)^{1+F+J'+I'+I_1+I_2} \left[(2I+1)(2I'+1)\right]^{1/2} \frac{\begin{Bmatrix} F & I' & J' \\ 2 & J & I \end{Bmatrix}}{\begin{pmatrix} J & 2 & J' \\ -J' & 0 & J' \end{pmatrix}}$$
$$\left[(-1)^{I'} \frac{\begin{Bmatrix} I_2 & I_1 & I' \\ 2 & I & I_1 \end{Bmatrix}}{\begin{pmatrix} I_1 & 2 & I_1 \\ -I_1 & 0 & I_1 \end{pmatrix}} e\, Q_1 \langle J M_J = J' | \hat{V}_{ZZ(1)} | J' M_J' = J' \rangle + \right.$$
$$\left. + (-1)^{I} \frac{\begin{Bmatrix} I_1 & I_2 & I' \\ 2 & I & I_2 \end{Bmatrix}}{\begin{pmatrix} I_2 & 2 & I_2 \\ -I_2 & 0 & I_2 \end{pmatrix}} \cdot e\, Q_2 \langle J M_J = J' | \hat{V}_{ZZ(2)} | J' M_J' = J' \rangle \right] \tag{63}$$

Die Behandlung der Moleküle mit drei Quadrupolkernen läßt sich analog dem Bisherigen durchführen. In der Literatur sind bis heute nur Fälle mit drei äquivalenten Quadrupolatomen bearbeitet worden. Es handelt sich dabei insbesondere um Moleküle vom Typ Cl_3XY [39]. In diesem Spezialfall des symmetrischen Kreisels kann man nach Svidzinskij [40] davon ausgehen, daß, wenn äquivalente Quadrupolatome vorliegen – was in dem genannten Molekültyp der Fall ist – die Wechselwirkungsenergie in 1. Ordnung in den Termen der Wechselwirkung eines der drei Kerne angegeben werden kann. Eine ausführliche Behandlung des Drei-Quadrupolkern-Problems soll hier nicht gegeben wer-

den, da das infolge der Entartung, bedingt durch die Dreiersymmetrie, auftretende Phasenproblem die Darlegung zu umfangreich machen würde. Es sei hier auf die Literatur verwiesen [39].

4. Transformation des Feldgradienten-Tensors vom Trägheitsachsensystem auf sein Hauptachsensystem

Für viele Probleme der chemischen Bindung sind folgende Fragen von Interesse:

1. Liegt die Achse des Feldgradienten-Tensors in der Richtung der Achse der chemischen Bindung, also der Kernverbindungslinie, oder weichen die beiden Achsen voneinander ab? Im letzteren Fall würde eine sogenannte „bentbond" vorliegen.
2. Ist der Feldgradienten-Tensor asymmetrisch, d.h. ist $\eta \neq 0$? Dies muß immer dann der Fall sein, wenn ein partieller Doppelbindungsgrad in asymmetrischen Kreiselmolekülen vorliegt. Bei symmetrischen Kreiselmolekülen ist per definitionem die Ladungsverteilung, auch bei Vorliegen eines Doppelbindungsgrades, symmetrisch.

Die Beantwortung dieser Fragen setzt die Kenntnis des Feldgradienten-Tensors in seinem eigenen Achsensystem voraus. Experimentell zugänglich sind aber lediglich die Komponenten des Feldgradienten-Tensors im Hauptträgheitsachsensystem. Prinzipiell läßt sich, wenn der vollständige Feldgradienten-Tensor im Hauptträgheitsachsensystem bekannt ist, dieser gemäß folgender Beziehung auf das Feldgradienten-Achsensystem transformieren:

$$\begin{pmatrix} \chi_{aa} & \chi_{ab} & \chi_{ac} \\ \chi_{ba} & \chi_{bb} & \chi_{bc} \\ \chi_{ca} & \chi_{cb} & \chi_{cc} \end{pmatrix} = T^{\dagger} \begin{pmatrix} \chi_x & & \\ & \chi_y & \\ & & \chi_z \end{pmatrix} T \qquad (64)$$

Es gilt: $\chi_{gg'} = \chi_{g'g}$

Bei Auswertung mit den exakten Matrixelementen kann man alle Komponenten des Feldgradienten-Tensors erhalten, jedoch ist dazu notwendig, um starke Korrelationen bei der Rechnung zu vermeiden, daß eine große Anzahl von Linien gefunden wird, die sich nicht durch die Störungsrechnung 1. Ordnung beschreiben lassen. Dies wird wohl immer dann der Fall sein, wenn Brom- oder Jodatome, also Atome mit sehr hohem Kernquadrupolmoment, im Molekül auftreten. Im Falle von Chloratomen jedoch genügt in den meisten Fällen die Auswertung in 1. Ordnung. Dann ist es allerdings unmöglich, die Nichtdiagonalglieder des Feldgradienten-Tensors aus dem Spektrum direkt zu ermitteln. Damit kann aber auch eine Transformation auf das Feldgradientenachsensystem nicht mehr durchgeführt werden.

Es gibt aber auch hier einen Weg, die drei Komponenten V_{xx}, V_{yy} und V_{zz} des Feldgradienten-Tensors im eigenen Hauptachsensystem zu bestimmen. Erforderlich ist dazu, die Feinstruktur der Rotationsspektren von zwei verschieden isotopensubstituierten Molekülen – die Isotopensubstitution darf nicht am Quadrupolatom stattfinden – zu vermessen und zu analysieren. Weitere Voraussetzung ist die Kenntnis der Struktur der beiden Moleküle [41].

Als *Beispiel,* wie die Bestimmung der gewünschten Größen vor sich geht, sei der Fall eines Moleküls mit einer Symmetrieebene senkrecht zur *C*-Achse betrachtet. Hier besitzt die Transformationsmatrix folgende Form:

$$T = \begin{vmatrix} \cos\theta & \sin\theta & 0 \\ -\sin\theta & \cos\theta & 1 \\ 0 & 0 & 0 \end{vmatrix} \tag{65}$$

Die Beziehungen zwischen den Elementen von $\chi_{(abc)}$ und $\chi_{(xyz)}$ sind dann:

$$\begin{aligned} \chi_x &= \frac{\chi_{aa}\cos^2\theta - \chi_{bb}\sin^2\theta}{\cos^2\theta - \sin^2\theta} \\ \chi_y &= \frac{\chi_{bb}\cos^2\theta - \chi_{aa}\sin^2\theta}{\cos^2\theta - \sin^2\theta} \\ \chi_z &= \chi_{cc} \end{aligned} \tag{66}$$

$$\begin{aligned} \chi_{aa} &= \chi_x\cos^2\theta + \chi_y\sin^2\theta \\ \chi_{bb} &= \chi_x\sin^2\theta + \chi_y\cos^2\theta \\ \chi_{ab} &= (\chi_x - \chi_y)\sin\theta\cos\theta \\ \chi_{cc} &= \chi_z \end{aligned} \tag{67}$$

Hierbei ist θ der Winkel zwischen der *A*-Achse im Hauptträgheitsachsensystem und der *a*-Achse im Feldgradientenachsensystem. Ebenso gilt die umgekehrte Beziehung. Unbekannt ist zunächst dabei der Winkel θ.

Für die beiden untersuchten isotopensubstituierten Moleküle erhält man dann unter Voraussetzung, daß sich die Feldgradienten χ_x und χ_y am Quadrupolkern bei der Isotopensubstitution an anderen Atomen nicht ändern, folgende Beziehungen:

$$\begin{aligned} \chi_{aa}(1) &= \chi_x\cos^2\theta_1 + \chi_y\sin^2\theta_1 & \chi_{aa}(2) &= \chi_x\cos^2\theta_2 + \chi_y\sin^2\theta_2 \\ \chi_{bb}(1) &= \chi_x\sin^2\theta_1 + \chi_y\cos^2\theta_1 & \chi_{bb}(2) &= \chi_x\sin^2\theta_2 + \chi_y\cos^2\theta_2 \\ \chi_{ab}(1) &= (\chi_x - \chi_y)\sin\theta_1\cos\theta_1 & \chi_{ab}(2) &= (\chi_x - \chi_y)\sin\theta_2\cos\theta_2 \end{aligned} \tag{68}$$

θ_1 ist dabei der Winkel zwischen der größten Hauptachse des Feldgradienten-Tensors und der in der Symmetrie-Ebene liegenden Hauptträgheitsachse für das ursprüngliche Molekül. θ_2 ist der analoge Winkel für das isotopensubstituierte Molekül, siehe Abbildung 4.

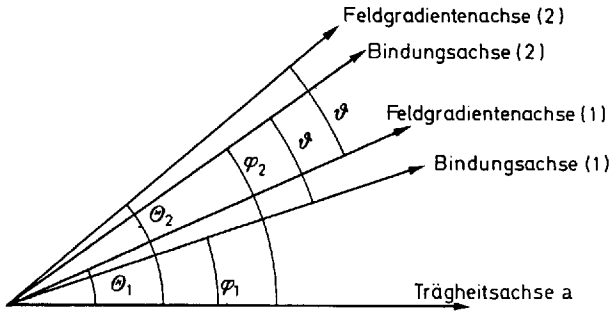

Abb. 4

Die angegebenen Beziehungen lassen sich in folgende Form bringen, die $\chi_{aa}(2)$ als Funktion der $\chi_{aa}(1)$ und $\chi_{cc}(1)$ in den Feldgradienten-Komponenten des unsubstituierten Moleküls und vom Winkel $\theta(1)$ dieses Moleküls sowie vom Winkel ϑ, d.h. der Differenz zwischen $\theta(1)$ und $\theta(2)$ angibt [42]:

$$\chi_{aa}(2) = \frac{\alpha x^2 - \beta x \cdot \sqrt{1-x^2} + \gamma}{1 - 2x^2} \tag{69}$$

$\alpha = c - (c+2a)(u^2 - v^2)$ $\quad x = \sin\theta(1)$ $\quad u = \cos\vartheta$
$\beta = 2(c+2a)\,u\,v$ $\quad a = \chi_{aa}(1)$ $\quad v = \sin\vartheta$
$\gamma = a - v^2(c+2a)$ $\quad c = \chi_{cc}(1)$ $\quad \vartheta = \theta(2) - \theta(1) = \varphi(2) - \varphi(1)$

Die Werte χ_{aa} χ_{cc} sind aus den Messungen bekannt.

Die Werte $\vartheta = \theta(2) - \theta(1)$ lassen sich jetzt graphisch nach $x = \sin\theta(1)$ auflösen. Damit ist dann der Winkel zwischen der Hauptachse des Feldgradiententensors und der Hauptträgheitsachse bestimmt. Auf diese Weise läßt sich ermitteln, ob die Hauptachse des Feldgradienten-Tensors mit einer Kernverbindungslinie d.h. mit der Richtung der chemischen Bindung, übereinstimmt. Weiterhin können damit die drei Komponenten des Feldgradienten-Tensors, da jetzt der Transformationswinkel bekannt ist, im eigenen Hauptachsensystem ermittelt werden. Damit läßt sich aber auch die Größe η, d.h. der Asymmetrieparameter des Feldgradienten-Tensors, festlegen. Das bisher unbekannte Nichtdiagonalglied des Feldgradienten-Tensors im Trägheitsachsensystem fällt ebenfalls bei diesen Rechnungen an.

Mit diesem Verfahren konnte gezeigt werden, daß in den Verbindungen

$$CH_3SiH_2Cl \text{ und } (CH_3)_2SiHCl$$

nur ein verschwindender Asymmetrieparameter vorliegt, was für die Diskussion der Frage, ob bei diesen Verbindungen ein gewisser Grad von *pd*-π-Bindungen auftritt, von Bedeutung ist [43].

5. Beispiele

Im letzten Abschnitt sollen einige Beispiele für die in den vorhergehenden Kapiteln behandelten Verfahren gebracht werden.

Einen Vergleich zwischen gemessenen Werten und Werten, die nach der Störungsrechnung 1. Ordnung (53) und nach der exakten Methode (32) berechnet wurden, zeigt Tabelle 1 für ein Molekül mit *einem* Quadrupolkern.

Tabelle 1. *Rotationslinien von* $CH_3SiH_2{}^{35}Cl$

A = 16 077,892 MHz, B = 3 904,384 MHz, C = 3 325,581 MHz
$\chi_{xx} = -37{,}65$ MHz, $\chi_{yy} = 18{,}63$ MHz, $\chi_{zz} = 19{,}02$ MHz

		Beob (MHz)	Berechnet	
			Exakt (MHz)	1. Ordnung (MHz)
$1_{11} \rightarrow 2_{12}$	5/2 – 7/2	13882,94	13882,923	13882,921
	5/2 – 5/2	13878,20	13878,169	13878,170
$2_{11} \rightarrow 3_{12}$	7/2 – 9/2	22545,95	22545,965	22545,968
	5/2 – 7/2	22544,18	22544,213	22544,218
	7/2 – 7/2	22541,97	22542,036	22542,039
$3_{03} \rightarrow 4_{04}$	9/2 – 11/2	28720,04	28720,044	28720,050
	5/2 – 7/2	28719,23	28719,155	28719,161
	7/2 – 7/2	28722,54	28722,455	28722,459
	9/2 – 9/2	28713,06	28712,871	28712,876
$3_{13} \rightarrow 4_{14}$	9/2 – 11/2	27723,32	27723,691	27723,696
	7/2 – 9/2	27722,57	27722,973	27722,978
	5/2 – 7/2	27722,08	27722,470	27722,476

Man sieht, daß hier die Berechnung nach der Störungsrechnung 1. Ordnung vollauf befriedigende Resultate liefert, weil die Kopplungskonstante – bedingt durch das Quadrupolmoment des Atoms ^{35}Cl – klein ist.

Tabelle 2 gibt für ein hypothetisches Molekül [25] den Vergleich zwischen den mit der Störungsrechnung 1. Ordnung und den mit der Störungsrechnung 2. Ordnung erhaltenen Ergebnissen und den Werten, die nach der exakten Methode berechnet wurden.

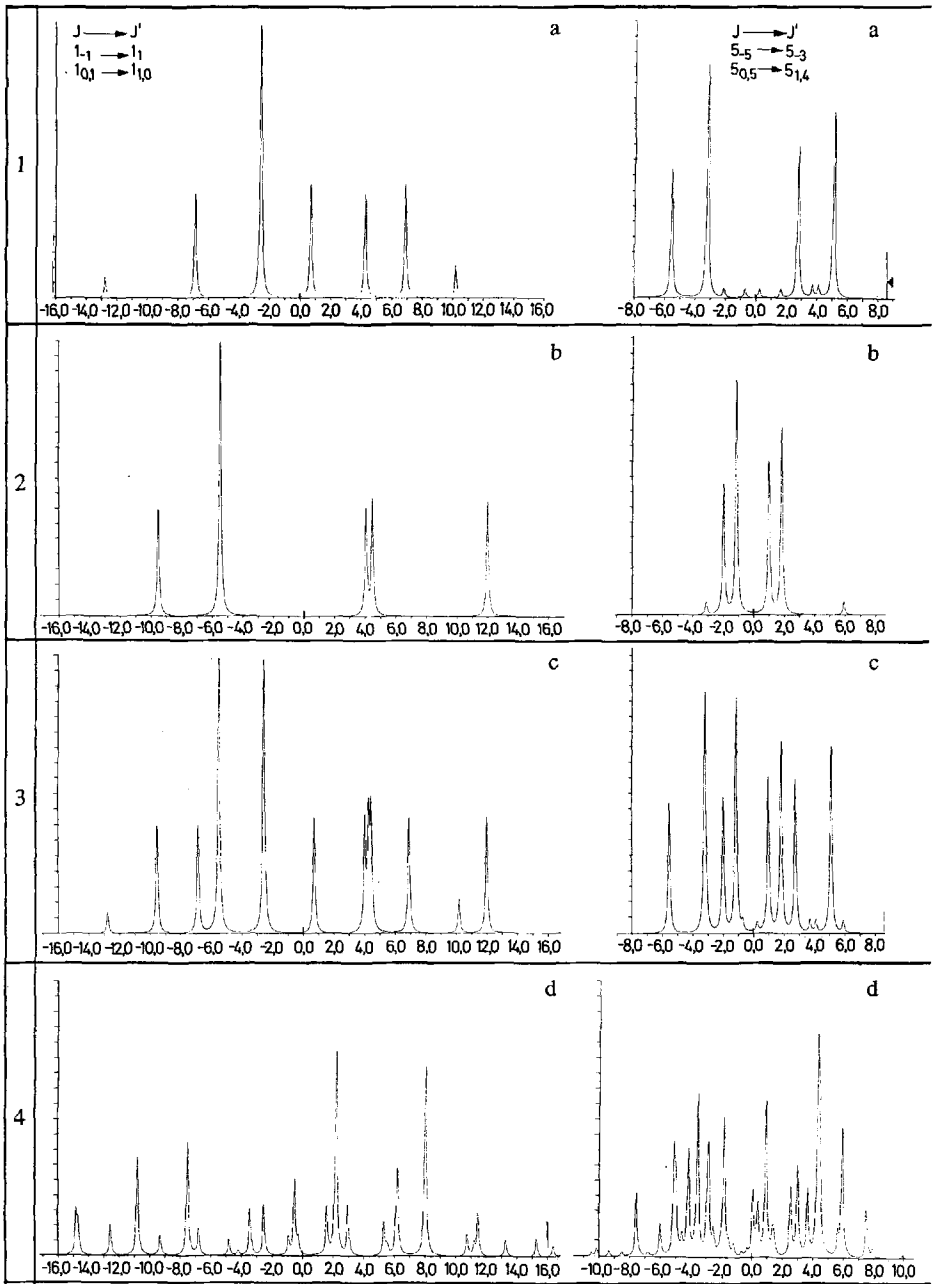

Abb. 5a–d

Abb. 6a–d

Reihe 1: Aufspaltung, hervorgerufen durch das Cl-Atom der Gruppe Cl–C≡

Reihe 2: Aufspaltung, hervorgerufen vom Cl-Atom der Gruppe $ClCH_2-$

Abszissen: Frequenzen in MHz

Koordinaten: Relative Intensitäten in willkürlichen Einheiten

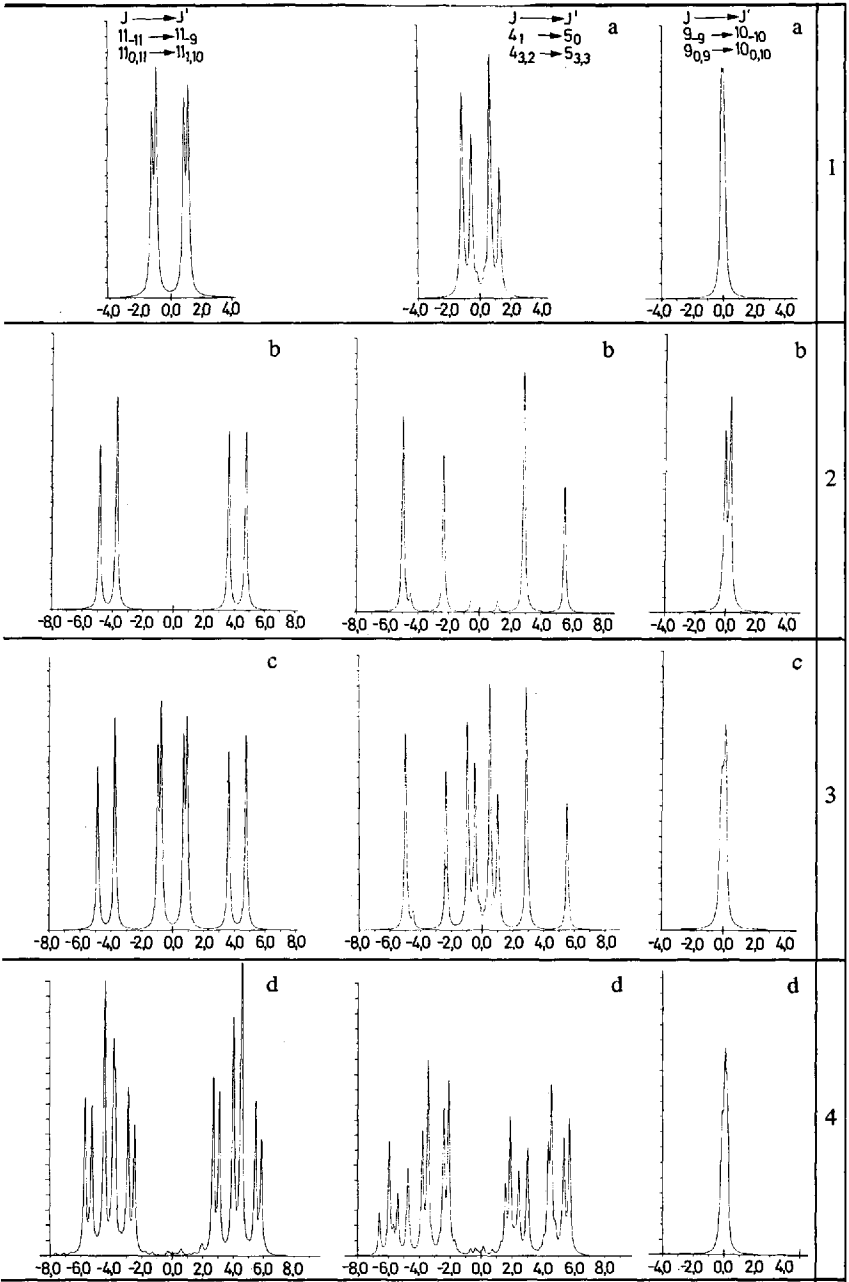

Abb. 7a–d Abb. 8a–d Abb. 9a–d

Reihe 3: Aufspaltung, wenn Fall 1 und Fall 2 einfach überlagern
Reihe 4: Aufspaltung, berechnet durch Diagonalisierung der exakten Störmatrix
Abszissen: Frequenzen in MHz
Koordinaten: Relative Intensitäten in willkürlichen Einheiten

Tabelle 2. *Rotationsfrequenzen (in MHz) eines hypothetischen symmetrischen Kreiselmoleküls ($B = 6$ GHz, $I = 5/2$, $\chi_{zz} = 2$ GHz) berechnet nach verschiedenen Methoden*

$J - J'$	K	$F - F'$	Exakt	Exakt - 2. Ordnung	Exakt - 1. Ordnung
$1 \rightarrow 2$	± 1	7/2 - 9/2	23880,578	- 0,277	1,907
		5/2 - 7/2	24285,612	- 0,032	4,184
		3/2 - 5/2	23936,964	0,001	5,535
		7/2 - 7/2	24077,304	- 0,192	5,876
		5/2 - 5/2	24233,837	- 0,062	2,408
		3/2 - 3/2	23797,916	0,055	9,345
		7/2 - 5/2	24025,530	- 0,221	4,101
		5/2 - 3/2	24094,790	- 0,007	6,219
		3/2 - 1/2	23664,967	0,033	4,967

Als Beispiel für ein Molekül mit *zwei* gleichen Quadrupolkernen, aber verschiedenen Feldgradienten und damit verschiedenen Kopplungskonstanten seien die Abb. 5 bis 9 angeführt. Hier sind für vier verschiedene Fälle die Ausdrucke eines Digitalrechners wiedergegeben, die für einige ausgewählte Übergänge für das Molekül $ClCH_2{-}C{\equiv}C{-}Cl$, ausgehend von folgenden Konstanten:

$$A = 16407{,}075 \text{ MHz}$$
$$B = 964{,}410 \text{ MHz}$$
$$C = 915{,}481 \text{ MHz}$$

$$\chi_{aa}(1) = -69{,}98 \text{ MHz} \qquad \chi_{aa}(2) = -13{,}13 \text{ MHz}$$
$$\chi_{bb}(1) = 30{,}18 \text{ MHz} \qquad \chi_{bb}(2) = -24{,}77 \text{ MHz}$$
$$\chi_{cc}(1) = 39{,}80 \text{ MHz} \qquad \chi_{cc}(2) = 37{,}90 \text{ MHz}$$

berechnet wurden.

Die verschiedenen Aufspaltungsbilder der Reihen 1 und 2 sind bedingt durch den unterschiedlichen Feldgradienten und die entsprechenden Richtungen des Feldgradiententensors gegenüber dem Hauptträgheitsachsensystem. Ein Vergleich der Reihen 3 und 4 zeigt deutlich den Unterschied zwischen einer Überlagerung der beiden Kopplungsschemata gegenüber der exakten Berechnung, deren Ergebnisse vollkommen mit dem Experiment übereinstimmen.

Die sehr spezifische Struktur der Aufspaltungsbilder erwies sich gerade bei diesem Molekül als eine außergewöhnliche Hilfe für die Zuordnung der Rotationsübergänge [44].

Eine vollkommen exakte Berechnung unter Einbeziehung der Glieder „nicht diagonal in J" war uns wegen der Größe der dabei auftretenden Matrizen nicht möglich. Jedoch zeigt die gute Übereinstimmung der dargestellten Feinstrukturen mit den experimentell erhaltenen Spektren, daß die angewandte Näherung – zumindest für die Chlor-Kerne – genügt.

Ich danke Herrn Diplom-Physiker Horst Günther für viele Diskussionen. Für kritische Durchsicht des Manuskriptes sei dem Genannten und Herrn Professor Dr. H. Dreizler, Universität Kiel, gedankt.

Anhang

A. Eigenfunktionen des symmetrischen Kreisels und Jacobi-Polynome

In der Eigenfunktion des symmetrischen Kreisels tritt nach Reiche und Rademacher [A1] die Funktion $w(d, s, p)$ auf, die als Argument t enthält und im folgenden $w(d, s, p; t)$ geschrieben wird. Nach den genannten Autoren ist

$$w(d, s, p; t) = \sum_{r=0}^{p} (-1)^r \binom{p}{r} \frac{(d+s+p+r)!\,d!}{(d+s+p)!\,(d+r)!}\, t^r \tag{A1}$$

Dabei entspricht

$$t = \frac{1-\cos\vartheta}{2} = \sin^2\frac{\vartheta}{2}.$$

Die Jacobi-Polynome $P_n^{(\alpha,\beta)}(x)$ sind durch folgende Reihe definiert [A2]:

$$P_n^{(\alpha,\beta)}(x) = \frac{\Gamma(\alpha+n+1)}{n!\,\Gamma(\alpha+\beta+n+1)} \sum_{m=0}^{n} \binom{n}{m} \frac{\Gamma(\alpha+\beta+n+m+1)}{2^m\,\Gamma(\alpha+m+1)} (x-1)^m \tag{A2}$$

Ersetzt man $\alpha \to d$, $\beta \to s$, $\frac{1-x}{2} \to t$ bzw. $x \to 1-2t$, so ergibt sich wegen $x = \cos\vartheta - t = \sin^2\frac{\vartheta}{2}$ und nach Ersetzen der Γ-Funktion durch den Fakultätsausdruck:

$$P_n^{(d,s)} = \frac{(d+n)!}{n!\,(d+s+n)!} \sum_{m=0}^{n} (-1)^r \binom{n}{r} \frac{(d+s+n+r)!}{(d+r)!} (\sin^2\frac{\vartheta}{2})^r \tag{A3}$$

Vergleich von (A1) und (A3) liefert dann

$$w(d, s, n; \sin^2\frac{\vartheta}{2}) = \frac{n!\,d!}{(d+n)!} \cdot P_n^{(d,s)}(\cos\vartheta) \tag{A4}$$

Damit ist gezeigt, daß die Eigenfunktionen des symmetrischen Kreisels den Jacobi-Polynomen proportional sind.

B. Die Matrixelemente des Operators der endlichen Drehungen

Die Matrixelemente des Operators der endlichen Drehungen [A3a] werden geschrieben:

$$\mathcal{D}^{(j)}_{mm'} \equiv \langle j\,m\,|\,\hat{D}(\alpha\beta\gamma)\,|j\,m'\rangle \tag{A5}$$

Dabei gilt für den unitären Operator

$$\hat{D}(\alpha\beta\gamma) = \exp(i\alpha J_z)\exp(i\beta J_y)\exp(i\gamma J_z) \tag{A6}$$

Man definiert

$$\mathcal{D}^{(j)}_{mm'}(0\beta 0) \equiv d^{(j)}_{mm'}(\beta).$$

In einer Darstellung, in der $\hat{J}_z$ diagonal ist, gilt:

$$\mathcal{D}^{(j)}_{mm'}(\alpha\beta\gamma) = \exp(i m \alpha)\, d^{(j)}_{mm'}(\beta) \exp(i m' \gamma) \tag{A7}$$

Weiter gilt

$$d^{(j)}_{mm'}(\beta) = \langle j m \,|\exp \frac{i\beta}{\hbar} J_y \,| j m' \rangle \tag{A8}$$

Die Exponentialfunktion kann folgendermaßen dargestellt werden [A3b]:

$$\exp\left(\frac{i\beta}{\hbar} J_y\right) = \begin{array}{c|cc} m' & +1/2 & -1/2 \\ \hline m & & \\ +1/2 & \cos\frac{\beta}{2} & \sin\frac{\beta}{2} \\ -1/2 & -\sin\frac{\beta}{2} & \cos\frac{\beta}{2} \end{array}$$

Damit wird

$$d^{(j)}_{mm'}(\beta) = \left[\frac{(j+m)!(j-m)!}{(j+m')!(j-m')!}\right]^{\frac{1}{2}} \sum_{\sigma} \binom{j+m'}{j-m-\sigma}\binom{j-m'}{\sigma} \cdot (-1)^{j-m-\sigma} \cdot \left(\cos\frac{\beta}{2}\right)^{2\sigma+m'+m} \left(\sin\frac{\beta}{2}\right)^{2j-2\sigma-m'-m} \tag{A9}$$

Dies läßt sich durch Jacobi-Polynome ausdrücken:

$$d^{(j)}_{mm'}(\beta) = \left[\frac{(j+m)!(j-m)!}{(j+m')!(j-m')!}\right]^{\frac{1}{2}} \left(\cos\frac{\beta}{2}\right)^{m+m'} \left(\sin\frac{\beta}{2}\right)^{m-m'} \cdot P_{j-m}^{(m-m')(m+m')}(\cos\beta) \tag{A10}$$

Damit wird $d^{(j)}_{mm'}(\beta)$ und damit wird auch $\mathcal{D}^{(J)}_{MK}(\alpha\beta)$ proportional zu den Eigenfunktionen des symmetrischen Kreisels. Unter anderem folgt daraus die wichtige Beziehung:

$$\mathcal{D}^{(l)}_{0M}(\alpha\beta\gamma) = \left(\frac{4\pi}{2l+1}\right)^{1/2} Y_{lm}(\beta\gamma) = C^{(l)}_m \tag{A11}$$

C. Die Symmetrie-Eigenschaften von $\mathcal{D}^{(j)}_{mm'}$

Es gelten folgende Beziehungen [A4]:

$$d^{(j)}_{mm'}(-\beta) = d^{(j)}_{m'm}(\beta) \tag{A12a}$$

$$d^{(j)}_{mm'}(\beta) = (-1)^{m-m'} \cdot d^{(j)}_{-m-m'}(\beta) \tag{A12b}$$

$$d^{(j)}_{mm'}(\beta) = (-1)^{m-m'} \cdot d^{(j)}_{m'm}(\beta) \tag{A12c}$$

Für die Integrale über das Produkt von 3 $\mathcal{D}$ ergibt sich [A5]:

$$\frac{1}{8\pi^2} \int_0^{2\pi} \int_0^{\pi} \int_0^{2\pi} \mathcal{D}^{(j_1)}_{m'_1 m_1}(\alpha\beta\gamma)\, \mathcal{D}^{(j_2)}_{m'_2 m_2}(\alpha\beta\gamma) \cdot \mathcal{D}^{(j_3)}_{m'_3 m_3}(\alpha\beta\gamma)\, d\alpha \sin\beta\, d\beta\, d\gamma =$$

$$= \begin{pmatrix} j_1 & j_2 & j_3 \\ m'_1 & m'_2 & m'_3 \end{pmatrix} \begin{pmatrix} j_1 & j_2 & j_3 \\ m_1 & m_2 & m_3 \end{pmatrix} \tag{A13}$$

D. Die 3j-Symbole und ihre Eigenschaften

Die *3j*-Symbole werden nach Wigner [A6] geschrieben $\begin{pmatrix} j_1 & j_2 & j_3 \\ m_1 & m_2 & m_3 \end{pmatrix}$ und sind verknüpft mit den Clebsch-Gordan-Koeffizienten [A7]:

$$\begin{pmatrix} j_1 & j_2 & j_3 \\ m_1 & m_2 & m_3 \end{pmatrix} = \frac{(-1)^{j_1 - j_2 - m_3}}{(2j_3+1)^{1/2}} \cdot (j_1 m_1 j_2 m_2 | j_1 j_2 j_3 - m_3) \tag{A14}$$

Für andere Phasenfaktoren siehe Rotenberg *et al.* [A8].

Die *3j*-Symbole sind folgendermaßen definiert:

$$\begin{pmatrix} j_1 & j_2 & j_3 \\ m_1 & m_2 & m_3 \end{pmatrix} = (-1)^{j_1 - j_2 - m_3} \cdot$$

$$\left(\frac{(j_1+j_2-j_3)!(j_1-j_2+j_3)!(-j_1+j_2+j_3)!(j_1+m_1)!(j_1-m_1)!(j_2+m_2)!(j_2-m_2)!(j_3+m_3)!(j_3-m_3)!}{(j_1+j_2+j_3+1)!} \right)^{\frac{1}{2}}$$

$$\sum_k \frac{(-1)^k}{k!(j_1+j_2-j_3-k)!(j_1-m_1-k)!(j_2+m_2-k)!(j_3-j_2+m_1+k)!(j_3-j_1-m_2+k)!} \tag{A15}$$

Es gelten folgende Symmetriebeziehungen, wenn (k, l, n) eine gerade Permutation von (1,2,3) ist:

$$\begin{pmatrix} j_1 & j_2 & j_3 \\ m_1 & m_2 & m_3 \end{pmatrix} = \begin{pmatrix} j_k & j_l & j_n \\ m_k & m_l & m_n \end{pmatrix} \tag{A16}$$

und wenn (k, l, n) eine ungerade Permutation von (1, 2, 3) ist:

$$\begin{pmatrix} j_1 & j_2 & j_3 \\ m_1 & m_2 & m_3 \end{pmatrix} = (-1)^{j_1+j_2+j_3} \begin{pmatrix} j_k & j_l & j_n \\ m_k & m_l & m_n \end{pmatrix} \tag{A17}$$

Die *3j*-Symbole sind nur dann von Null verschieden, wenn folgende Beziehungen gelten:

$$m_1+m_2+m_3=0 \quad \text{und} \quad \vec{j}_1+\vec{j}_2+\vec{j}_3=0. \tag{A18}$$

Damit gilt die „Dreiecksbeziehung"

$$\begin{aligned} j_1+j_2-j_3 &\geqslant 0 \\ j_1-j_2+j_3 &\geqslant 0 \\ -j_1+j_2+j_3 &\geqslant 0 \end{aligned} \tag{A19}$$

wobei $j_1+j_2+j_3$ ganzzahlig sein muß.

E. Die 6j-Symbole und einige ihrer Eigenschaften

Die *6j*-Symbole werden geschrieben [A9] $\begin{Bmatrix} j_1 & j_2 & j_3 \\ l_1 & l_2 & l_3 \end{Bmatrix}$ und sind definiert

$$\begin{Bmatrix} j_1 & j_2 & j_3 \\ l_1 & l_2 & l_3 \end{Bmatrix} = (-1)^{j_1+j_2+l_1+l_2}\,\Delta(j_1j_2j_3)\,\Delta(l_1l_2j_3)\,\Delta(l_1j_2l_3)\,\Delta(j_1l_2l_3)$$

$$\sum_k \frac{(-1)^k(j_1+j_2+l_1+l_2+1-k)!}{k!\,(j_1+j_2-j_3-k)!\,(l_1+l_2-j_3-k)!\,(j_1+l_2-l_3-k)!\,(l_1+j_2-l_3-k)!\,(-j_1-l_1+j_3+l_3+k)!\,(-j_2-l_2+j_3+l_3+k)!} \tag{A20}$$

wobei gilt:

$$\Delta(a,b,c)=\frac{(a+b-c)!(a-b+c)!(-a+b+c)!}{(a+b+c+1)!}^{\frac{1}{2}} \tag{A21}$$

Die *6j*-Symbole sind invariant gegen eine Vertauschung der Spalten und sind nur dann von Null verschieden, wenn jedes Tripel $(j_1j_2j_3)$, $(l_1l_2l_3)$, $(j_1l_2l_3)$ und $(l_1j_2l_3)$ ein Dreieck gemäß der Beziehung (A19) bildet. Außerdem muß die Summe der Elemente von jedem Tripel ganzzahlig sein.

F. Die 9j-Symbole und einige ihrer Eigenschaften

Die *9j*-Symbole sind definiert durch [A10]

$$\begin{Bmatrix} j_{11} & j_{12} & j_{13} \\ j_{21} & j_{22} & j_{23} \\ j_{31} & j_{32} & j_{33} \end{Bmatrix} = \sum_j (-1)^{2j}(2j+1) \begin{Bmatrix} j_{11} & j_{21} & j_{31} \\ j_{32} & j_{33} & j \end{Bmatrix} \begin{Bmatrix} j_{12} & j_{22} & j_{32} \\ j_{21} & j & j_{23} \end{Bmatrix} \begin{Bmatrix} j_{13} & j_{23} & j_{33} \\ j & j_{11} & j_{12} \end{Bmatrix}$$

$$= \sum_{\text{alle } m} \begin{pmatrix} j_{11} & j_{12} & j_{13} \\ m_{11} & m_{12} & m_{13} \end{pmatrix} \begin{pmatrix} j_{21} & j_{22} & j_{23} \\ m_{21} & m_{22} & m_{23} \end{pmatrix} \begin{pmatrix} j_{31} & j_{32} & j_{33} \\ m_{31} & m_{32} & m_{33} \end{pmatrix}$$

$$\begin{pmatrix} j_{11} & j_{21} & j_{31} \\ m_{11} & m_{21} & m_{31} \end{pmatrix} \begin{pmatrix} j_{12} & j_{22} & j_{32} \\ m_{12} & m_{22} & m_{32} \end{pmatrix} \begin{pmatrix} j_{13} & j_{23} & j_{33} \\ m_{13} & m_{23} & m_{33} \end{pmatrix} \tag{A22}$$

Wenn in einem *9j*-Symbol einige Parameter doppelt vorkommen und eine Null auftritt, dann ist das *9j*-Symbol proportional einem *6j*-Symbol [A11]:

$$\begin{Bmatrix} a & b & e \\ c & d & e \\ f & f & 0 \end{Bmatrix} = (-1)^{b+c+e+f}\left[(2e+1)(2f+1)\right]^{\frac{1}{2}} \begin{Bmatrix} a & b & e \\ d & c & f \end{Bmatrix} \tag{A23}$$

und

$$\begin{Bmatrix} 0 & b & c \\ d & e & f \\ d & e & f \end{Bmatrix} = (-1)^{b+d+e+f}\left[2(2b+1)\right]^{\frac{1}{2}} \begin{Bmatrix} b & f & f \\ d & e & e \end{Bmatrix} \delta(b,c) \tag{A24}$$

Die *9j*-Symbole spielen eine wichtige Rolle bei der Berechnung der Matrixelemente von Produkten von Tensoroperatoren. Wenn $\hat{T}^{(j_1)}_{m_1}$ und $\hat{T}^{(j_2)}_{m_2}$ Tensoroperatoren sind, dann ist das *Tensor*produkt, das einen irreduziblen Tensor der Stufe *j* bildet, gegeben durch

$$T^{(j)}_{m}(j_1 j_2) \equiv (2j_3+1)^{1/2} \sum_{m_1 m_2} (-1)^{-j_1+j_2-m} \begin{pmatrix} j_1 & j_2 & j_3 \\ m_1 & m_2 & -m \end{pmatrix} T^{(j_1)}_{m_1} T^{(j_2)}_{m_2} \tag{A25}$$

Wenn die Tensoroperatoren $\hat{T}^{(k_1)}_{n_1}$ und $\hat{U}^{(k_2)}_{n_2}$ sich auf verschiedene, d.h. kommutierende dynamische Variablen beziehen, dann ist das Matrixelement des Produktes $X^{(k)}_{n}(k_1, k_2)$ gegeben durch

$$\langle \gamma j_1 j_2 j m \mid \hat{X}^{(k)}_{n}(k_1 k_2 \mid \gamma' j'_1 j'_2 j' m' \rangle =$$

$$= (-1)^{j-m} \langle \gamma j_1 j_2 j \parallel \hat{X}^{(k)}(k_1 k_2) \parallel \gamma' j'_1 j'_2 j' \rangle \begin{pmatrix} j & k & j' \\ -m & n & m' \end{pmatrix} \tag{A26}$$

wobei

$$\langle \gamma j_1 j_2 j \parallel \hat{X}^{(k)}(k_1 k_2) \parallel \gamma' j'_1 j'_2 j' \rangle =$$

$$= \left[(2j+1)(2j'+1)(2k+1)\right]^{\frac{1}{2}} \begin{Bmatrix} j_1 & j_2 & j \\ j'_1 & j'_2 & j' \\ k_1 & k_2 & k \end{Bmatrix} \sum_{\gamma''} \langle \gamma j_1 \parallel \hat{T}^{(k_1)} \parallel \gamma'' j'_1 \rangle \langle \gamma'' j_2 \parallel \hat{U}^{(k_1)} \parallel \gamma'' j'_2 \rangle \tag{A27}$$

Das Matrixelement des Skalarproduktes zweier kommutierender Tensoroperatoren ist

$$\langle \gamma j_1 j_2 j m \mid \hat{X}(l) \mid \gamma' j'_1 j'_2 j' m' \rangle =$$

$$= \delta(j,j')\delta(m,m')(-1)^{j'_1+j_2+j'} \begin{Bmatrix} j' & j_2 & j_1 \\ l & j'_1 & j'_2 \end{Bmatrix} \sum_{\gamma''} \langle \gamma j_1 \parallel \hat{T}^{(l)} \parallel \gamma'' j'_1 \rangle \langle \gamma'' j_2 \parallel \hat{D}^{(l)} \parallel \gamma' j'_2 \rangle \tag{A28}$$

Literatur

1) Watson, J. K. G.: J. Chem. Phys. *45,* 1360 (1966).
2a) Casimir, H. B. G.: Rotation of a Rigid Body in Quantum Mechanics. Acad. Proefschrift. Groningen: J. B. Wolters Uitg. Maatsch. 1931.
2b) Allen, H. C., Jr., Cross, P. C.: Molecular Vib-Rotors, S. 7. New York: J. Wiley & Sons 1963.
3) – – Molecular Vib-Rotors, S. 15. New York: J. Wiley & Sons 1963.
4) – – Molecular Vib-Rotors, S. 16. New York: J. Wiley & Sons 1963.
5) Wang, C. S.: Phys. Rev. *34,* 243 (1929).
6) loc. cit. 2b), S. 19.
7a) Rotational Energy Levels of Asymmetric Top Molecules. Bethpage, N.Y.: Gruman Aircraft Engg. Corp. 1962.
7b) Dreizler, H., Peter, R.: Tabellen zur Analyse von Rotationsspektren mit Zentrifugalaufweitung und Torsionsfeinstruktur. Phys. Inst. Univ. Freiburg (1963).
7c) Townes, C. H., Schawlow, A. L.: Microwave Spectroscopy. New York: McGraw-Hill Book Co. Inc. 1955.
8) Wacker, P. F., Pratto, M. R.: Microwave Spectral Tables. Line Strengths of Asymmetric Rotors. N.B.S. Monogr. 70, Bd. II. Washington 1964.
9) Wollrab, J. E.: Rotational Spectra and Molecular Structure, Kap. 7. New York: Academic Press 1967.
10) Reiche, F., Rademacher, H.: Z. Physik *39,* 444 (1926).
11) loc. cit. 9), Kap. 9.
12) Zeil, W.: Naturwissenschaften *57,* 274 (1970).
13) Margenau, H., Murphy, G. M.: The Mathematics of Physics and Chemistry, Ed. II, S. 100. Princeton: D. van Nostrand Co. Inc. 1956.
14) Edmonds, A. R.: Drehimpulse in der Quantenmechanik. Mannheim: B. I. 1964.
15a) Racah, G.: Phys. Rev. *61,* 186 (1942); *62,* 438 (1942).
15b) Rotenberg, M., Bivins, R., Metropolis, N., Wooten, J. K.,Jr.: The 3j and 6j symbols. Cambridge, Mass.: Technology Press MIT 1959.
16) Rose, M. E.: Elementary Theory of Angular Momentum, Kap. 5. New York: J. Wiley & Sons 1957.
17) – Elementary Theory of Angular Momentum, Kap. 3. New York: J. Wiley & Sons 1957.
18) loc. cit. 15b), Kap. 1.
19) Wigner, E. P.: Gruppentheorie. Braunschweig: F. R. Vieweg 1931. – Eckart, C.: Rev. Mod. Phys. *2,* 305 (1930). – loc. cit. 14), Kap. 5.3.
20) loc. cit. 14), Kap. 7.1.
21) loc. cit. 15b), Kap. 3.
22) loc. cit. 15b), Kap. 2.
23) loc. cit. 9), Kap. 5.
24) loc. cit. 9), Kap. 2.
25) Benz, H. P., Bauder, A., Günthard, Hs. H.: J. Mol. Spectr. *21,* 156 (1966).
26) loc. cit. 14), Kap. 7.1.
27) Condon, E. H., Shortley, G. H.: Theory of Atomic Spectra. Cambridge, Mass.: University Press 1935.
28a) Casimir, H. B. G.: On the Interaction between Atomic Nuclei and Electrons. Prize Essay. Haarlem: "Teyler's Tweede Gen." De Erven F. Bohn, N. V. 1936.
28b) Ramsay, N. F.: Nuclear Moments. New York: J. Wiley & Sons 1953.
28c) Heine, V.: Group Theory in Quantum Mechanics, Kap. 21. New York: Pergamon Press 1964.
29) loc. cit. 7c), Anhang I.

30) Bragg, J. K.: Phys. Rev. *74*, 533 (1948).
31) Miller, C. E.: J. Mol. Spectr. *35*, 170 (1970).
32) loc. cit. 30).
33) loc. cit. 30).
34) Bragg, J. K., Golden, S.: Phys. Rev. *75*, 1453 (1949).
35) loc. cit. 7b).
36) Schwendeman, R. H.: J. Mol. Spectr. *15*, 451 (1965).
37a) Bardeen, J., Townes, C. H.: Phys. Rev. *73*, 627 (1948); Erratum Phys. Rev. *73*, 1204 (1948).
37b) loc. cit. 9).
37c) Myers, R. J., Gwinn, W. D.: J. Chem. Phys. *20*, 1420 (1952).
37d) Flygare, W. H., Gwinn, W. D.: J. Chem. Phys. *36*, 787 (1962).
38) Krusic, P. J.: Mitt. aus dem Laboratorium W. D. Gwinn, University of California, Berkeley 1968.
39a) Wolf, A. A.: Quadrupole Hyperfine Structure in the Rotational Spectrum of $CFCl_3$ and $CHCl_3$. Thesis. Georgia Inst. Technology, Atlanta 1966.
39b) – Williams, Q., Weatherly, T. L.: J. Chem. *47*, 5101 (1967).
39c) Nave, C. R., Weatherly, T. L., Williams, Q.: J. Chem. Phys. *49*, 1413 (1968).
40) Svidzinskij, K. K.: Theorie der Hyperfeinstruktur der molekularen Rotationsspektren. Trudi fiziceskogo instituta im. Lebeda ANSSSR *21*, 107 (1963).
41) loc. cit. 9), Kap. 5.4.
42) Ronchi, R., Zeil, W.: Unveröffentlicht.
43) Jetter, H., Ronchi, R., Gegenheimer, R., Zeil, W.: Unveröffentlicht.
44) Günther, H., Zeil, W.: Unveröffentlicht.

Literatur zum Anhang

A1) Reiche, F., Rademacher, H.: Z. Physik *39*, 444 (1926).
A2) Handbook of Mathematical Functions with Formulas, Graphs, and Mathematical Tables. N.B.S. Appl. Math. Ser. 55 (Hrsg. M. Abramowitz und I. A. Stegun). Washington 1965.
A3) Edmonds, A. R.: Drehimpulse in der Quantenmechanik, S. 71. Mannheim: B.I. 1964.
A3a) – Drehimpulse in der Quantenmechanik, S. 72. Mannheim: B.I. 1964.
A4) – Drehimpulse in der Quantenmechanik, S. 76. Mannheim: B.I. 1964.
A5) – Drehimpulse in der Quantenmechanik, S. 79. Mannheim: B.I. 1964.
A6) Wigner, E. P.: Gruppentheorie. Braunschweig: F. R. Vieweg 1931.
A7) Rose, M. E.: Elementary Theory of Angular Momentum, Kap. 3. New York: J. Wiley & Sons 1957.
A8) Rotenberg, M., Bivins, R., Metropolis, N., Wooten, J. W., Jr.: The 3j and 6j symbols, S. 1, Gleichung 1.1. Cambridge, Mass.: Technology Press MIT 1959.
A9) – – – – The 3j and 6j symbols, S. 13. Cambridge, Mass.: Technology Press MIT 1959.
A10) – – – – The 3j and 6j symbols, S. 19. Cambridge, Mass.: Technology Press MIT 1959.
A11) – – – – The 3j and 6j symbols, S. 22. Cambridge, Mass.: Technology Press MIT 1959.

Eingegangen am 26. Oktober 1970

Nuclear Quadrupole Resonance

Theoretical Interpretation

Prof. Dr. Edwin A. C. Lucken
Département de chimie physique, Université de Genève, Suisse

Contents

A. Introduction

The components of the field-gradient tensor, q_{ij} produced by a distribution of point charges are given by the expression

$$q_{\alpha\beta} = \sum_r \rho_r \frac{(3x_{\alpha r}x_{\beta r} - R_r^2\delta\alpha\beta)}{R_r^5} \equiv \sum_r q_{\alpha\beta}^r \tag{1}$$

where x_α, x_β are the generalised Cartesians coordinates of the particle whose charge is ρ_r, and R_r $(= (x_\alpha^2 + x_\beta^2 + x_\gamma^2)^{\frac{1}{2}})$ is the distance of that charge from the origin of the coordinate system (i.e., the point at which the field-gradient components are defined). Since Eq. (1) contains only the position coordinates of the r particles the quantum mechanical operator equivalent of $q_{\alpha\beta}$, is identical with (1) and if the wave function describing the system under study is Φ, the observable $q_{\alpha\beta}$ is given by the usual equation

$$q_{\alpha\beta} = \int \Phi^* q_{\alpha\beta} \Phi d\tau = \sum_r \int \Phi^* q_{\alpha\beta}^r \Phi \, d\tau \tag{2}$$

The usual Born-Oppenheimer approximation for molecular wave functions gives rise to the separation of the wave function Φ into the nuclear and electronic components

$$\Phi = \Phi_{\text{nuc}} \cdot \Phi_{\text{elec}}$$

The function Φ_{nuc} is further sub-divided into the translational, rotational and vibrational components

$$\Phi_{\text{nuc}} = \Phi_{\text{trans}} \cdot \Phi_{\text{rot}} \cdot \Phi_{\text{vib}}$$

The field gradient is measured at a fixed point within the molecule, the translational part of the wave-function is thus of no consequence for $(q_{\alpha\beta})$. The effect of molecular rotation does, however, modify $(q_{\alpha\beta})$ but the relationship between the rotating and stationary $(q_{\alpha\beta})$'s has already been treated in the chapter dealing with microwave spectroscopy. In the present context, we are interested in the field gradients in a vibrating molecule in a fixed coordinate system. The Born-Oppenheimer approximation for molecular wave-functions enables us to separate the nuclear and electronic motions, the electronic wave functions being calculated for the nuclei in various fixed positions. The observed $\langle q_{\alpha\beta} \rangle$'s will then be average values over the vibrational motion. If $\langle q_{\alpha\beta} \rangle$ is expressed as a polynomial in terms of the displacement of the nuclei from their equilibrium positions then, for simple harmonic oscillations of amplitude sufficiently low that only the linear term in the displacement need be

Table 1. *The effect of vibrational state on quadrupole coupling constants*

Molecule	Vibrational state	Nucleus	e^2Qq (MH_z)	Ref.
CH_3Cl	$v = 0$	35 Cl	-74:77 ± 0.10	
	$v_3 = 1$	35 Cl	-74.87 ± 0.10	1
	$v_6 = 1$	35 Cl	-74.89 ± 0.20	
HCN	$v = 0$	14_N	- 4.58 ± 0.05	2
	$v_2 = 1$	14_N	- 4.81 ± 0.02	
Tl Br	$v = 0$	^{79}Br	125.2 ± 2.1	
	$v = 1$	^{79}Br	123.8 ± 2.1	
	$v = 2$	^{79}Br	125.8 ± 2.1	3
	$v = 3$	^{79}Br	123.8 ± 2.1	
	$v = 4$	^{79}Br	125.8 ± 2.5	
K F	$v = 0$	^{39}K	- 7.933878	
	$v = 1$	^{39}K	- 7.837739	
	$v = 2$	^{39}K	- 7.742809	4
	$v = 3$	^{39}K	- 7.649539	
	$v = 4$	^{39}K	- 7.556619	
K Cl	$v = 0$	^{35}Cl	- 0.0585	
	$v = 1$	^{35}Cl	- 0.1003	
	$v = 2$	^{35}Cl	- 0.2588	4
	$v = 3$	^{35}Cl	- 0.4137	
	$v = 4$	^{35}Cl	- 0.5544	
ReO_3F	$v = 0$	^{187}Re	-48.4 ± 1.3	
	$v_3 = 1$	^{187}Re	-27.0 ± 1.5	
	$v_5 = 1$	^{187}Re	-34.9 ± 2.9	
	$v_6 = 1$	^{187}Re	-58.2 ± 1.3	5
	$v_3 = 1, v_6 = 1$	^{187}Re	-37.8 ± 3.6	
	$v_3 = 2$	^{187}Re	-17.0 ± 2.2	
	$v_3 = 2, v_6 = 1$	^{187}Re	-25.7 ± 4.3	

considered, the average value $\langle q_{\alpha\beta} \rangle$ is just calculated for the stationary molecule in its equilibrium configuration. For higher vibrational amplitudes and anharmonic oscillation, however, this is no longer the case and one must therefore expect a dependence of observed coupling constants on the vibrational state. This is indeed observed, as the results in Table 1 show.

Except for the alkali halides, however, there have been few attempts at investigating this effect theoretically. Nevertheless, it is usually small except when the field gradients themselves are small (the reasons for this will become apparent shortly) and in most cases field gradients have been estimated theoretically only for the molecule in its stationary equilibrium configuration.

For the ^{14}N coupling in H–C ≡ N, Bonaccorsi, Scrocco and Tomasi [6] calculated the coupling constant both in the rigid equilibrium internuclear distance configuration and as an average over the linear stretching vibration using the wave functions calculated by Mclean and Yoshimine [7] for various linear configurations. The two coupling constants agreed within 1%. In most cases the agreement between the theoretically predicted and the experimental field gradients is rarely as good as 99% so that the rigid molecule approximation will, except in the circumstances to be discussed below, introduce no appreciable error.

The above considerations lead us to a wave function of the form

$$\Phi = \Phi_{\text{nuc.fix.}}\, \Phi_{\text{elec.}}$$

where the function $\Phi_{\text{nuc.fix}}$ is a product of δ functions located at the various equilibrium nuclear positions.

The expression for the field gradient (Eq. (1)) thus becomes a difference of two terms (the nuclear and electronic terms are of opposite sign)

$$q_{\alpha\beta} = \sum_s \int \Phi^*_{\text{nuc.fix}}\, q^s_{\alpha\beta}\, \Phi_{\text{nuc.fix}}\, d\tau + \sum_t \int \Phi^*_{\text{elec}}\, q^t_{\alpha\beta}\, \Phi_{\text{elec}} \cdot d\tau$$

where the sums are over the s nuclei and the t electrons. With the fixed nuclei approximation the first sum can be calculated exactly, irrespective of the electronic wave function. This fact is the origin of one of the greatest difficulties in calculations of field gradients from approximate wave functions, since the individual nuclear and electronic terms are in general many times greater than the resultant $q_{\alpha\beta}$. The theoretical field gradient is thus the difference between two large quantities one of which is known exactly. Thus a wave function which gives an electronic contribution to the field gradient which only differs by 5% from that given by the true wave function, may give rise to a total field gradient differing by a factor of two from the experimental field gradient. An illustration of this point is given by the data in Table 2.

Table 2. *Values of nuclear and electronic contributions to the field gradient in simple molecules*

Molecule	Nucleus	q electronic	q nuclear	q total	Ref.
H – F	^{2}H	– 2.1988	3.4596	0.5408	8
H – Cl	^{2}H	– 2.1192	2.4329	0.3137	8
N ≡ N	^{14}N	– 2.669	1.583	– 1.086	9
HC ≡ N	^{14}N	– 2.138	1.190	– 0.948	9

This brings us at once to the fact that most atomic and molecular wave functions are approximate, and we must consider the effect of the various approximations usually made on the resultant field gradient. Essentially all

calculations on poly-electronic systems make use of the variation method and thus as a starting point a set of trial functions containing certain parameters is established. For closed-shell atomic N-electron systems the most usual procedure has been to set the trial functions in the form

$$\Phi_{\text{elec}} = \frac{1}{\sqrt{N!}} \mid \Psi_1^1 \; \Psi_2^2 \; \Psi_3^3 \ldots \Psi_N^N \mid$$

where the vertical bars indicate a Slater determinant and the functions Ψ_i are atomic spin-orbitals. For open-shell systems a sum of such slater determinants is usually necessary. The atomic spin-orbitals are assumed to be products of radial $R_{(r)}^{nlms}$, angular (the spherical harmonics $Y^{l,m}(\Theta, \Phi)$) and spin (X^s) functions n, l, m, s

$$\Psi = A \, R_{(r)}^{nlms} \, Y^{l,m}(\Theta, \Phi) \, X^s$$

where A is a normaliser. Since the X^s functions are just the two usual $s = +\frac{1}{2}$ functions only $R_{(r)}^{nlms}$ is unknown and contains any desired parameters. The functions Ψ_i are thus solutions to the central field problem. The parameters in $R_{(r)}^{nlms}$ are then selected according to the variation procedure to give a minimum to the energy associated with the function. In almost all cases the interelectron repulsion is taken care of by the Hartree-Fock method where each electron is supposed to move in the average potential field produced by all the others. In the unrestricted Hartree-Fock method $R_{(r)}^{nlms}$ is assumed as the symbols indicate, to be a function of n, l, m and s, the principal, azimuthal, magnetic and spin quantum numbers; most calculations however assume that the radial function is a function of n and l only. This is the restricted Hartree-Fock method and in the present context it gives rise to a very significant error in the field gradient calculated from the resultant wave function. This error is one of the phenomena known under the collective name of Sternheimer shielding [10]. Briefly the restricted Hartree-Fock method has the consequence that all filled shells have spherical symmetry, and contribute nothing to the field-gradient which thus, in atoms, arises solely from the electrons in the (incomplete) valence shell. One may formally relate the true field gradient, q, to that produced by the valence-electrons alone, q_{valence}, by the equation

$$q = (1 - R) q_{\text{valence}}$$

Values of R for free atoms have been calculated in Table 3 from the restricted Hartree-Fock functions by perturbation theory and are usually in the range 0.0–0.5. For molecules, however, the only satisfactory procedure is to introduce the dependence on m right from the start and indeed to include the m dependence as one of the parameters to be minimised in the variation method. In H – Cl the inner shell polarisation accounts for 17% of the electronic field-gradient [12]

Table 3. *Sternheimer shielding in atoms electronic configurations labelled a and b correspond to two slightly different Hartree-Fock functions used as basis functions*

Atom	Electronic configuration	R	$1/1-R$	Ref.
Li	He 2p	0.1156	1.131	10
Be	He $1s^2 2s2p$	0.0395	1.042	10
B	He $1s^2 2s^2 2p$	0.143	1.17	11
Na	Ne 3p	−0.243	0.805	11
Cl	Ne $3s^2 3p^5$	−0.112	1.13	11
K	Ar $4p^a$	−0.188	0.842	11
K	Ar $5p^a$	−0.142	0.876	11
K	Ar $4p^b$	−0.009	0.991	11
K	Ar $5p^b$	−0.003	0.997	11
Rb	Kr $5p^a$	−0.271	0.787	11
Rb	Kr $6p^a$	−0.209	0.827	11
Rb	Kr $6p^b$	−0.141	0.876	11
Rb	Kr $6p^b$	−0.120	0.893	11
Cs	Xe $6p^a$	−0.332	0.751	11
Cs	Xe $7p^a$	−0.275	0.784	11
Cs	Xe $6p^b$	−0.204	0.831	11
Cs	Xe $7p^b$	−0.178	0.849	11

Table 4. *Molecules for which field-gradients from ab initio wave-functions are available. This list is by no means exhaustive but is intended to illustrate the precision at present available*

Molecule	Nucleus	Theoretical field gradient (a.u.)	Experimental field gradient (a.u.)	Ref.
Hydrogen fluoride	^{2}H	−0.541	−0.52	8
Formaldehyde	^{2}H	−0.207	−0.261	13
Hydrogen sulphide	^{2}H	−0.265, $\eta = 0.167$	−0.229 $\eta = 0.205$	14
Hydrogen cyanide	^{2}H	−0.317	−0.310	9
	^{14}N	−1.204	−1.131	
Nitrogen	^{14}N	−1.35	−1.323	15
Hydrogen chloride	^{35}Cl	3.923	3.639	12
		3.612	3.639	8
Aziridine	^{14}N	−1.008, $\eta = 0.683$	−1.038, $\eta = 0.629$	16
Pyrole	^{14}N	−1.480, $\eta = 0.109$	−0.752, $\eta = 0.071$	16
Isoxazole	^{14}N	−1.695, $\eta = 0.704$	0.3	16
Oxazole	^{14}N	−1.405, $\eta = 0.314$	−1.123, $\eta = 0.21$	16
Pyridine	^{14}N	−1.778, $\eta = 0.115$	−1.374, $\eta = 0.405$	16
Pyrazine	^{14}N	−1.868, $\eta = 0.048$	−1.291, $\eta = 0.536$	16

Table 5. *Steinheimer shielding in ions in a field gradient arising from distant charges (γ_∞)*

Ion	Electronic configuration	γ_∞	Ref.
H^-	He	1.051	17
Li^+	He	0.257	17
F^-	Ne	- 23.03	17
Na^+	Ne	- 3.835	17
Cl^-	Ar	- 66.56	17
K^+	Ar	- 12.17	17
Br^-	Kr	- 123.0	18
Rb^+	Kr	- 47.2	18
I^-	Xe	- 138.4	18
Cs^+	Xe	- 102.5	18

Table 4 shows a collection of field gradients calculated from wave-functions which, from the point of view of their energy, must be considered quite satisfactory. It is clear that as far as field gradients are concerned the results, at least as far as the more complex molecules are concerned, leave much to be desired. The reason is essentially that whereas the energy of an atomic orbital depends on $\langle \frac{1}{r} \rangle$, the field gradient depends on $\langle \frac{1}{r^3} \rangle$ and converges much more slowly.

While on the subject of Sternheimer shielding and calculations of exact field gradients, mention must be made of the problem of calculating field gradients in *ionic crystals.* In a pure ionic crystal the field gradient is non-vanishing in sites of less than cubic symmetry while the ion itself, if it has a closed shell structure, has spherical symmetry. At first sight it would seem that the field gradient could then be calculated exactly from the distribution of point charges. The problem is similar to that of calculating the Madelung energy for an ionic crystal although the summation converges more slowly Sternheimer has shown that in this case the polarisation terms can become extremely large, as the values for γ_∞ shown in Table 5 certify.
The reason for the considerable difference between the shielding in Atoms (R) and the shielding when the field gradient arises from distant charges (γ_∞) is briefly as follows. A distant negative charge – which of course gives rise to a positive field gradient nucleus – repels the electrons of the closed shell, and the originally spherical charge distribution takes on the form of an oblate spheroid whose symmetry axis lies along the line forming the distant charge and the nucleus. Such a charge distribution produces a positive filed-gradient at the nucleus and since those electrons are close to the nucleus it is usually much greater than the field gradient produced by the distant charge. When, however, the source of the field gradient is a valence electron this electron

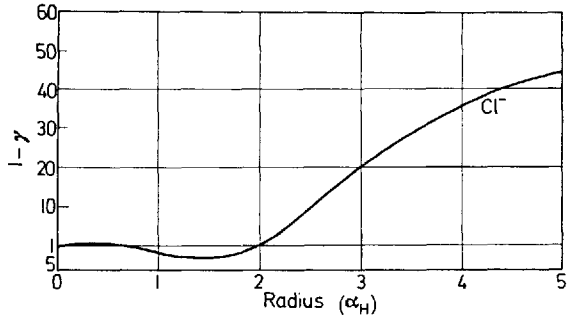

spends part of its time within the inner shell and here its effect is to expand the inner shell and give a negative polarisation field gradient. The total perturbation is then the sum of two opposite effects and the shielding is small. Fig. 1 shows a calculation of the shielding for a charge at different distances from the nucleus of the chloride anion.

It is clear from the foregoing that in principle it is a straight-forward but lengthy matter to calculate a field-gradient from a molecular wave function. However, agreement between this theoretical field-gradient and the experimental one will only be satisfactory if as few restrictions as possible are imposed on the form of the trial wave function and in particular that the polarization of inner shells is not neglected. Such calculations at the present state are only satisfactory for small molecules although undoubtly much progress towards more complex systems is to be expected in the future. The molecules for which quadrupole coupling data are available cover a field for which we cannot expect reasonably exact wave functions for many years to come,and indeed one of the main reasons behind the determination of these constants is the need to obtain information about electronic structure at a time when it cannot be done by calculation. We are thus interested in seeing to what extent the reverse process of relating nuclear quadrupole coupling constants to electron distributions is either a unique or a reliable one.

The N-electron wave-function of a polyatomic molecule containing the atoms $A, B \ldots, n$ is usually most conveniently expressed as a Slater product of molecular spin orbitals each of which is a linear combination of atomic orbitals multiplied by a spin function

$$\Phi = \frac{1}{\sqrt{N!}} \left| (\Psi_{1\alpha})^1 \, (\Psi_{1\beta})^2 \, (\Psi_{2\alpha})^3 \ldots (\Psi_{N/2\beta})^N \right.$$

$$\Psi_i = \sum_j a_{ij} \, X_{Aj} + \sum_k b_{ik} \, X_{Bk} + \ldots\ldots .$$

where X_{Aj} are atomic orbitals of atom A, etc. Since the field gradient at the nucleus A, $q^A_{\alpha\beta}$ is a sum of one-particle operators independant of spin, its expectation value is simply the sum of one-electron terms. (The factor two arises from the two different spin functions.)

$$q^A_{\alpha\beta} = 2 \sum_i^N \int \Psi_i^* \, q^A_{\alpha\beta} \, \Psi_i \, d\tau$$

Each of these integrals may now be expanded as a sum of integrals over atomic orbitals. It will be convenient to separate the terms in this expansion involving the atomic orbitals of atom A from those of the other atoms

$$\begin{aligned} \int \Psi_i^* \, q^A_{\alpha\beta} \, \Psi_i \, d\tau = {} & 2 \sum_j \sum_k a_{ij} \, a_{ik} \int X^*_{Aj} \, q^A_{\alpha\beta} \, X_{Ak} \, d\tau \\ & + 2 \sum_j \sum_k a_{ij} \, b_{ik} \int X_{Aj} \, q^A_{\alpha\beta} \, X_{Bk} \, d\tau \\ & + 2 \sum_j \sum_k b_{ij} \, b_{ik} \int X^*_{Bj} \, q^A_{\alpha\beta} \, X_{Bk} \, d\tau \\ & + 2 \sum_j \sum_k b_{ij} \, c_{ik} \int X^*_{Bj} \, q^A_{\alpha\beta} \, X_{Ck} \, d\tau \end{aligned}$$

For distant atoms in electrically neutral molecules the sum of all the terms of the last three types over all the electrons will be approximately numerically equal but of opposite sign to the field gradients produced by the nuclei B, C, etc. This cancellation is fairly good when the nuclei in question are not directly bonded to A, the field gradient being of course proportional to $\langle \frac{1}{r^3} \rangle$. From directly bonded atoms the cancellation is far from perfect, however, as the data in Table 6 indicates.

The total electron population of each inner shell orbital will of course be two, and if the radial function were independent of the magnetic quantum number, the total contribution of such inner shell electrons to the field gradient would be zero because of the spherical symmetry of the resultant closed shell. We know from Steinheimer's work that this will not be the case and that an inner shell field gradient will indeed be present.

The Townes and Dailey [19] method for analyzing nuclear quadrupole resonance data is based on wave function involving only the valence electrons. All inner shell electrons are presumed to be spherically symmetric and contribute nothing to the field-gradient, and all the two and three-center integrals in the above expression presumed to cancel exactly the field-gradient produced by the residual nuclear charges of the atoms B, C..., etc. Thus

$$q^A_{\alpha\beta} = 2 \sum_i \sum_j a_{ij}^2 \int X^*_{Aj} \, q^A_{\alpha\beta} \, X_{Aj} \, d\tau + 4 \sum_i \sum_{j \neq} \sum_k a_{ji} \, a_{ik} \int X^*_{Aj} \, q^A_{\alpha\beta} \, X_{Ak} \, d\tau$$

For atomic wave functions of the usual kind where the angular dependence

Table 6. *Cancellation of nuclear and off-diagonal (two and three-center) electronic contributions to the field gradient*

Molecule	Nucleus	$q_{valence}$	$q_{nuclear}{}^{*} - q_{non\text{-}diagonal}$	Ref.
H CN	^{14}N	- 1.0932	- 0.0409	1
H CN	^{14}N	- 1.132	- 0.1850	9
F CN	^{14}N	- 0.7100	+ 0.0167	1
Cl CN	^{14}N	- 0.8973	- 0.057	1
NC CN	^{14}N	- 1.1196	- 0.060	1
HC_2CN	^{14}N	- 1.1355	+ 0.026	1
H_3N	^{14}N	- 1.974	0.238	9
H Cl	^{35}Cl	3.845	0.116	12

is expressed by a spherical harmonic $Y^{lm}(\theta, \Phi)$, the integrals of the second kind are zero unless $l_j = l_k \pm 2$ and are in any case small. The Townes and Dailey method moreover has mostly been applied to molecules where the valence orbitals are essentially only s and p so that the final expression becomes

$$q^A_{\alpha\beta} = 2 \sum_i \sum_j a^2_{ij} \int X^*_{Ai}\, q^A_{\alpha\beta}\, X_{Aj}\, d\tau$$

This equation has been used with considerable success in explaining the trends observed in coupling constants. It can be expected to be reasonably valid when the integrals in it are in fact the dominant terms of the equation, and when they can be determined experimentally by measurements on either extremely simple molecules or, preferably, on atoms. Table 6 shows the results of exact calculations of the field-gradient yielded by SCF approximate wave-function for several molecules containing either ^{14}N or ^{35}Cl which indicate the extent to which the approximations of the Townes-Dailey theory are valid. It is clear that for ^{14}N nuclei the approximation is generally poor but much more satisfactory for ^{35}Cl and indeed, since the one-center terms increase with atomic number it can be expected to be equally satisfactory for most heavy elements. It is significant that the Townes and Dailey method has been most extensively used for halogen (^{35}Cl, ^{79}Br, ^{127}I) nuclei and achieved a deserved success in correlating a considerable body of data.

The precise form of the Townes and Dailey equation depends of course on the details of the molecular environment. If we restrict our attention to systems in which the only one-center integrals arise from the valence p orbitals we have three unknowns and the gradients are given by the equations:

$$\frac{q_{xx}}{q_0} = \rho_x - \frac{1}{2}(\rho_y + \rho_z)$$

$$\frac{q_{yy}}{q_0} = \rho_y - \frac{1}{2}(\rho_x + \rho_z)$$

$$\frac{q_{zz}}{q_0} = \rho_z - \frac{1}{2}(\rho_x + \rho_y)$$

Hence

$$\eta \frac{q_{zz}}{q_0} = \frac{3}{2}(\rho_x - \rho_y)$$

where ρ_x, ρ_y and ρ_z are the populations of the p_x, p_y and p_z orbitals respectively and q_0 is the field gradient along the axis of the valence p orbital by a single electron in that p orbital, i.e.

$$q_0 = \int X_z^* q_{zz} X_z \, d\tau$$

where X_z is a valence p_z orbital. It is assumed that the coordinate system has been correctly chosen to be the principal axis of the field gradient tensor, in which the off-diagonal elements are zero. The field gradients, however, provide

Table 7. *Values of $e^2Q_{q_0}$. For ^{14}N the value is derived from a variety of theoretical studies on simple molecules, the remainder come from direct measurements of atomic hyperfine coupling constants*

Nucleus	Electron	$e^2Q_{q_0}$(MHz)	Ref
N^{14}	2p	−8 to −10	20
Na^{23}	3p	−5.16	21
K^{39}	4p	+5.6	22
Rb^{85}	5p	−48.8	23
Rb^{87}	5p	−23.6	23
B^{11}	2p	−5.390	24
Al^{27}	3p	−37.52	25
Ga^{69}	4p	−125.044940	26
Ga^{71}	4p	−78.79808	26
In^{115}	5p	−899.1048	27
Cl^{35}	3p	+109.746	28
Cl^{37}	3p	+86.510	28
Br^{79}	4p	−769.756	29
Br^{81}	4p	−643.032	29
I^{127}	5p	+2292.712	30

at most only two experimental parameters. When the field gradient has cylindrical symmetry, and thus may be expressed as just one experimental quantity, this cylindrical symmetry will result in two of the valence p orbitals having the same population. Thus in all cases the Townes and Dailey method leads to a population determination only if one of the populations can be determined or assigned in some other way. In the following paragraphs a few particular cases are treated and the general Townes and Dailey formulae are given for the field gradient at the A nucleus [20]. Table 7 gives appropriate values for e^2Qq_0 for various nuclei.

B. Linear Diatomic Molecules AB

The A atom uses a valence p orbital for the formation of a σ bond, population a. The two $p\pi$ orbitals have identical populations, b. The cylindrically symmetrical field gradient lies along the A–B axis

$$\frac{q_{zz}}{q_0} = (a - b)$$

For singly bonded atoms it can often be assumed that $b = 2$

$$\frac{q_{zz}}{q_0} = -(2 - a)$$

The fractional ionic character, i, of such a bond is given by $\pm(1 - a)$ according to whether A is the least or most electro-negative partner. Thus

$$\frac{q_{zz}}{q_0} = -(1 \pm i)$$

B is planar group rather than an atom interaction between one of the $p\pi$ orbitals of A and the π-system of the planar group can take place. The population of this orbital is then $2\text{-}\pi$ and the field gradient is no longer cylindrically symmetric

$$\frac{q_{zz}}{q_0} = -(2 - \frac{\pi}{2} - a)$$

$$\frac{q_x - q_y}{q_0} = \eta \frac{q_z}{q_0} = \frac{3\pi}{2}$$

C. Two Coordinate Molecule AB_2

If the interbond angle is 2θ the fractional s character of the A – B hybrid σ bond, population a, is $\frac{1}{2}(1 - \cot^2\theta)$. If the third σ orbital is occupied by

c electrons and the $p\pi$ orbital perpendicular to the molecular plane by b electrons, the field gradients along the molecular two-fold axis, it is given by

$$\frac{q_u}{q_0} = (1 - \cot^2\theta)(c - a) + \frac{a - b}{2}$$

while along the axes perpendicular to this, in and perpendicular to the molecular plane, (v and w respectively)

$$\frac{q_v}{q_0} = (1 - \cot^2\theta)\frac{(a - c)}{2} + \frac{a - b}{2}$$

$$\frac{q_w}{q_0} = (1 - \cot^2\theta)\frac{(a - c)}{2} + b - a$$

Any further development depends on the possibility of assigning one of these orbital populations and of knowing which of the directions corresponds to the field-gradient x, y and z axes. For example, for the nitrogen atom in pyridine it could be assumed that the third σ orbital contained two electrons and the field gradient axes were experimentally determined as $u = z$, $v = y$ and $w = x$.

These assignments then lead to the equations

$$a - b = \frac{2}{3}\eta\frac{q_{zz}}{q_0}$$

$$2 - a = \frac{1}{1 - \cot^2\theta}\left(1 - \frac{\eta}{3}\frac{q_{zz}}{q_0}\right)$$

An interesting situation arises when the B atoms or groups are incapable of forming π bonds so that both b and c can be set equal to 2. In this case the field-gradient lies along the axis perpendicular to the molecular plane and one may directly obtain the relationships

$$\frac{q_{zz}}{q_0} = \frac{2 - a}{1 + \frac{\eta}{3}}$$

$$\eta = -3\cos 2\theta$$

Thus the asymmetry parameter is entirely determined by the hybridisation of the σ bonds.

D. Pyramidal Molecules AB_3 or XAB_3

These molecules have a 3-fold axis going through A and hence have cylindrically symmetric field gradients. In a manner similar to that used for the planar molecules the field gradient is given by

$$\frac{q_{zz}}{q_0} = -\frac{3\cos\alpha}{1-\cos\alpha}(b-a)$$

where a is the population of the $s-p$ hybrid orbitals used in the formation of the $A-B$ σ bonds and b the population of the fourth orbital. α is the BAB bond angle. For compounds such as ammonia b may be set equal to 2. Note that for $\alpha = \pi/2$ the field gradient is zero, whereas the angular term increases to 1.5 when α takes on the limiting value of 120°. The field gradient is thus extremely sensitive to the angular term and in these circumstances will be very sensitive to the vibrational state. This is undoubtedly the reason for the data given in Table 1 for ReO_3F.

E. Limitations of the Townes and Dailey Type Method

As the data in Table 6 show, the sum of the terms neglected in the Townes and Dailey method is by no means small. Cotton and Harris [31] have attempted to re-vamp the method and after a series of approximations which at first sight appear more reasonable than the original ones, arrive at a series of equations in which the valence orbital populations of the Townes and Dailey method are replaced by the corresponding Mulliken gross atomic orbital populations.

In both of these methods the inner shell polarization is neglected. It may be argued that in a given molecular environment this term remains fairly constant, for example at a chlorine atom singly bonded to a carbon atom, and hence the Townes and Dailey method gives good values for the *changes* in orbital population as more remote features of the environment are altered, for example the variation of R in a series RCH_2Cl. Perhaps more serious is the fact that no account is taken of the m dependence of the field gradients produced by the valence orbitals themselves. In this case the field gradients are given by equations such as

$$q_{zz} = \rho_z\, q_{z0} - \frac{1}{2}(\rho_x\, q_{x0} + \rho_y\, q_{y0})$$

where q_{x0}, etc., is the field gradient produced along the x axis by an electron in a valence p_x orbital. An equation of this sort may well be useful over a narrow range of orbital populations but of course cannot be extended over the whole of population space since when the three populations are equal $q_z = 0$ and hence $q_{z0} = q_{y0} = q_{z0}$. Once more for an atom in a particular environment, again for example the chlorine atom in RCH_2Cl, this hypothesis, together with the hypothesis of constant inner shell polarization, gives the equation

$$q_{zz} = \rho_z q_{z0} - \frac{1}{2}(\rho_x q_{x0} + \rho_y q_{y0}) + q_{\text{Steinheimer}}$$

If the field gradient is cylindrically symmetric or approximately so and it is assumed that the only parameter which changes from one molecule to another is p_z then we have

$$q_{zz} = \rho_z q_{z0} - \rho_x q_{x0} + q_{\text{Steinheimer}}$$

$$= \rho_z q_{z0} - \text{constant}$$

or in terms of the resonance frequencies

$$\nu = \rho_z \nu_1 - \nu_2$$

Dewar *et al.* [32] have used with some success an equation of this sort to relate the quadrupole coupling constants of the polychlorobenzenes to orbital populations calculated by the semi-empirical M.I.N.D.O. method. In this case

$$\nu_1 = -39.818 \text{ MHz and } \nu_2 = 92.051 \text{ MHz}$$

For a small degree of asymmetry it may be reasonably assumed that

$$q_{x0} \approx q_{y0} \equiv q_\pi$$

and we have

$$\eta \frac{q_{zz}}{q_\pi} = \frac{3}{2}(\rho_x - \rho_y)$$

As far as the author knows, no attempt at using an equation of this type has been made so far. Clearly however, whether a universal q_0 or a specific q_π is used, this equation, first proposed by Bersohn, will give satisfactory *relative* values of the extent of π bonding, for *e.g.* chlorine attached to a carbon conjugable residue though the *absolute* values remain in some doubt. White and Drago [33] have developed equations along these lines for ^2H and ^{14}N coupling constants.

From the foregoing it is clear that the more the environment of the nucleus is changed the less we may rely on the results given by the Townes and Dailey analysis. Thus it is better to compare a chlorine atom attached to an aliphatic carbon atom with another chlorine attached to an aliphatic carbon atom, than to a chlorine attached to an unsaturated carbon atom. Much more care should be exercised in, say, comparing a nitrogen atom in a tertiary amine with a nitrogen atom in the nitrile group. It is even more hazardous to compare the field gradient at a chlorine atom in, say, carbon tetrachloride, with the field gradient at a chlorine atom in silicon tetrachloride. Finally the most unreliable comparison would be between the chlorine in carbon tetrachloride and another halogen in the corresponding tetrahalide.

Despite all these censures there is no doubt that Townes and Dailey type equations account for the gross features of quadrupole coupling constants.

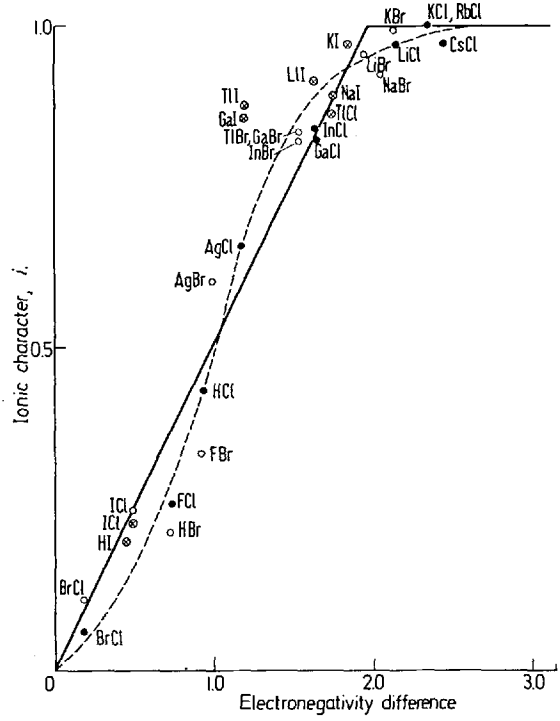

Fig. 2

This last and concluding remark is illustrated by the data for the diatomic halides in Fig. 2. Provided that it is not pushed too far and that time is not wasted in useless polemic, the Townes and Dailey method can be made to yield reliable information of value to the chemist along the lines which have been sketched above, and of which many examples are given in this monograph.

F. References

1) Kraitchman, J., Dailey, B. P.: J. Chem. Phys. *22*, 1477 (1954).
2) White, R. L.: J. Chem. Phys. *23*, 249 (1955).
3) Fritzky, U. G.: Z. Physik. *151*, 351 (1958).
4) Van Wachem, R., Dymanus, A.: J. Chem. Phys. *46*, 3749 (1967).
5) Lotspeich, J. F., Javan, A., Engelbrecht, A.: J. Chem. Phys. *31*, 633 (1959).
6) Bonnacorsi, R., Scrocco, E., Tomasi, J.: J. Chem. Phys. *50*, 2940 (1969).
7) McLean, A., Yoshimine, M.: J. Chem. Phys. *46*, 1812 (1967).
8) McLean, A., Yoshimine, M.: J. Chem. Phys. *47*, 3256 (1967).

9) O'Konski, C. F., Tae-Kyu Ha: J. Chem. Phys. *49,* 5354 (1968).
10) Sternheimer, R.: Phys. Rev. *164,* 10 (1967) and references therein.
11) Scrocco, E., Tomasi, J.: Theoret. Chem. Acta. *2,* 386 (1964).
12) Sternheimer, R. M.: Phys. Rev. *105,* 158 (1957).
13) Thaddeus, P., Krisher, L. C.: J. Chem. Phys. *40,* 257 (1964).
14) Rottenberg, S., Young, R. H., Schaefer III, H. F.: J. Am. Chem. Soc. *92,* 3243 (1970).
15) Cade, P. E., Sales, K. D., Wahl, A. C.: J. Chem. Phys. *44,* 1973 (1966).
16) Kochanski, E., Lehn, J. M., Levy, B.: Chem. Phys. Lett. *4,* 75 (1969); Theoret. Chim Acta. *22,* 111 (1971).
17) Langhoff, F. W., Hurst, R. P.: Phys. Rev. *139A,* 1415 (1965).
18) Sternheimer, R. M.: Phys. Rev. *146,* 140 (1966).
19) Townes, C. H., Dailey, B. P.: J. Chem. Phys. *17,* 782 (1949).
20) Lucken, E. A. C.: Nuclear quadrupole coupling constants. London: Academic Press 1969.
21) Perl, M., Rabi, I. I., Senitzky, B.: Phys. Rev. *98,* 611 (1955).
22) Buck, P., Rabi, I. I., Senitzky, B.: Phys. Rev. *104,* 553 (1956).
23) Senitzky, B., Rabi, I. I.: Phys. Rev. *103,* 315 (1956).
24) Węssel, G.: Phys. Rev. *92,* 1582 (1953).
25) Lew, H., Wessel, G.: Phys. Rev. *90,* 1 (1953).
26) Daly, R. T., Jr., Holloway, J. H.: Phys. Rev. *96,* 539 (1954).
27) Kusch, P., Eck, T. G.: Phys. Rev. *94,* 1799 (1954).
28) Jaccarino, V., King, J. G.: Phys. Rev. *63,* 471 (1951).
29) King, J. G., Jaccarino, V.: Phys. Rev. *94,* 1610 (1954).
30) Jaccarino, V., King, J. G., Satten, R. H., Stroke, H. H.: Phys. Rev. *94,* 1798 (1954).
31) Cotton, F. A., Harris, C. B.: Proc. Nat. Acad. Sci. *56,* 12 (1966).
32) Dewar, M. J. S., Lo, D. H., Patterson, D. B., Trinajstić, Peterson, G. E : Chem. Commun. *1971,* 238.
33) White, W. D., Drago, R. S.: J. Chem. Phys. *52,* 4717 (1970). See also Olympia, P. J.: J. Chem. Phys. *55,* 2609 (1971) and White, W. D., Drago, R. S.: J. Chem. Phys. *55,* 2611 (1971).

Received December 20, 1971.

Nuclear Magnetic Resonance

Isotope	NMR frequency MHz at 14,092G	NMR frequency MHz at 23,487G	Natural abundance %	Relative sensitivity for equal number of nuclei at constant field	Spin* I in multiples of $h/2\pi$	Electric quadrupole moment Q in multiples of $10^{-24}cm^2$
H^1	60.000	100.00	99.985	1.00	1/2	—
H^2	9.2104	15.351	1.5×10^{-2}	9.65×10^{-3}	1	2.73×10^{-3}
Li^7	23.317	38.862	92.58	0.293	3/2	$-3 \times .10^{-2}$
Be^9	8.4321	14.054	100.	1.39×10^{-2}	(-)3/2	5.2×10^{-2}
B^{10}	6.4479	10.746	19.58	1.99×10^{-2}	3	7.4×10^{-2}
B^{11}	19.250	32.084	80.42	0.165	3/2	3.55×10^{-2}
C^{13}	15.087	25.144	1.108	1.59×10^{-2}	1/2	—
N^{14}	4.3343	7.2238	99.63	1.01×10^{-3}	1	7.1×10^{-2}
N^{15}	6.0798	10.133	0.37	1.04×10^{-3}	(-)1/2	—
O^{17}	8.134	13.56	3.7×10^{-2}	2.91×10^{-2}	(-)5/2	-2.6×10^{-2}
F^{19}	56.446	94.077	100.	0.833	1/2	—
Na^{23}	15.871	26.452	100.	9.25×10^{-2}	3/2	0.14-0.15
Al^{27}	15.634	26.057	100.	0.206	5/2	0.149
Si^{29}	11.919	19.865	4.70	7.84×10^{-3}	(-)1/2	—
P^{31}	24.288	40.481	100.	6.63×10^{-2}	1/2	—
S^{33}	4.6018	7.6696	0.76	2.26×10^{-3}	3/2	-6.4×10^{-2}
Cl^{35}	5.8790	9.7983	75.53	4.70×10^{-3}	3/2	-7.89×10^{-2}
Cl^{37}	4.893	8.155	24.47	2.71×10^{-3}	3/2	-6.21×10^{-2}
V^{51}	15.77	26.28	99.76	0.382	7/2	-4×10^{-2}
Mn^{55}	14.798	24.664	100.	0.175	5/2	0.55

Co^{59}	14.168	23.614	100.	0.277	7/2	0.40
Cu^{63}	15.903	26.506	69.09	9.31×10^{-2}	3/2	-0.16
Cu^{65}	17.036	28.394	30.91	0.114	3/2	-0.15
As^{75}	10.276	17.127	100.	2.51×10^{-2}	3/2	0.3
Se^{77}	11.44	19.07	7.58	6.93×10^{-3}	1/2	—
Br^{79}	15.032	25.054	50.54	7.86×10^{-2}	3/2	0.33
Br^{81}	16.204	27.006	49.46	9.85×10^{-2}	3/2	0.28
Rb^{87}	19.632	32.720	27.85	0.175	3/2	0.13
Nb^{93}	14.666	24.443	100.	0.482	9/2	-0.2
Sn^{117}	21.376	35.626	7.61	4.52×10^{-2}	(-) 1/2	—
Sn^{119}	22.363	37.272	8.58	5.18×10^{-2}	(-) 1/2	—
Sb^{121}	14.359	23.931	57.25	0.160	5/2	-0.5
I^{127}	12.004	20.007	100.	9.34×10^{-2}	5/2	-0.69
Cs^{133}	7.8702	13.117	100.	4.74×10^{-2}	7/2	3×10^{-3}
Pt^{195}	12.90	21.50	33.8	9.94×10^{-3}	1/2	—
Hg^{199}	10.696	17.827	16.84	5.67×10^{-3}	1/2	—
Hg^{201}	3.9598	6.5998	13.22	1.44×10^{-3}	(-) 3/2	0.50
Tl^{203}	34.290	57.150	29.50	0.187	1/2	—
Tl^{205}	34.625	57.709	70.50	0.192	1/2	—
Pb^{207}	12.553	20.922	22.6	9.16×10^{-3}	1/2	—
Bi^{209}	9.6418	16.070	100.	0.137	9/2	-0.4

* A minus sign in parantheses (-) beside an entry in the Spin I column signifies that the magnetogyric ratio and hence magnetic moment, is negative. To calculate the magnetic moment of an isotope, in multiples of the nuclear magneton, multiply the product of columns 2 and 6 by 0.093089; or multiply the product of columns 3 and 6 by 0.055854. (Reproduced by courtesy from Varian Associates)